SUBMISSION OF FINAL REPORT OF THE WORK DONE ON UGC - MAJOR RESEARCH PROJECT

Submitted to

UNIVERSITY GRANTS COMMISSION
Bahadurshah Zafar Marg
New Delhi - 110 002.

By

Dr. Mrs. M. ARULMOZHI
Associate Professor, Department of Physics
Principal Investigator - UGC-MRP

(No. F. 42-836/2013 (SR) dated 22.03.2013)

INVESTIGATIONS ON EXCITONS IN NANOSTRUCTURES

Jayaraj Annapackiam College for Women (Autonomous)
(A unit of the Sisters of St. Anne of Tiruchirapalli)
Re-accredited with 'A' Grade (Cycle – 3) by NAAC
DST-FIST supported College
Affiliated to Mother Teresa Women's University, Kodaikanal.
Periyakulam - 625 601.
Theni District, Tamil Nadu.

March 2017

JAYARAJ ANNAPACKIAM COLLEGE FOR WOMEN (AUTONOMOUS)

PERIYAKULAM-625 601, THENI DT.

Reaccredited with 'A' Grade by NAAC

Affiliated to Mother Teresa Women's University

SERVE WITH LOVE
JAYARAJ ANNAPACKIAM COLLEGE FOR WOMEN
JAC
PERIYAKULAM

Dr. Sr. T. Nirmala, M.Sc., B.Ed., Ph.D., D.HRD.
Principal

Res. : 04546 - 231382
Off : 04546 - 231482
Fax : 04546 - 231482
Website : www.annejac.com
E-mail : principal@annejac.com

Ref: JAC/UGC-MRP/Physics/2016-17 Date: 27.03.2017

To

The Under Secretary, (FD III)
University Grants Commission,
Bahadurshah Zafar Marg,
New Delhi – 110 002.

COLLEGE CODE NO. TNMK022

Dear Sir.

Sub: JAC – Submission of Final Report of the work done – forwarded – Reg.

Ref: UGC – MRP No. F.42-836/2013 (SR), Dated: 22.03.2013.

* *** *

Greetings from JAC!

I am glad to forward herewith the Final Report of the work done on the Project in Physical Sciences of **Dr. Mrs. M. ARULMOZHI,** Associate Professor of Physics on the Major Research Project (as referred above) entitled **Investigations on Excitons in Nanostructures'.**

The amount allocated by UGC for the Project is **Rs. 12,82,480/-** which is fully utilized for the Project and the amount sanctioned by UGC (in 2 instalments) is **Rs. 11,96,512/-.** Audited Utilization Certificate and Statement of Expenditure are enclosed. I request you to kindly sanction the balance amount of **Rs. 85,968/-** at your earliest.

We thank UGC for the financial assistance to complete the Project. Thank you.

Yours faithfully,

Principal
Jayaraj Annapackiam College
for Women (Autonomous)
Periyakulam - 625 601.
Theni District.

Enclosures:

1. Copy of UGC-MRP sanction letter
2. Copy of intimation letter for extension of MRP
3. Copy of letter for sanction of 2nd instalment grant
4. Annexure - III. Audited Statement of Expenditure in respect of Major Research Project
5. Annexure - V. Audited Utilization Certificate
6. Details of the amount allocated and expenditure incurred under various heads
7. Audited statement of expenditure for Books and Journals
8. Accession Certificate from Librarian (Books handed over to General library)
9. Audited Statement of Expenditure for Equipments
10. Asset Certificate from Head of the Department (Equipments handed over to the Department)
11. Audited Statement of Expenditure for Honorarium to Project Fellow
12. Audited Statement of Expenditure for HRA to Project Fellow
13. Audited Statement of Expenditure for Chemicals/Glassware/Consumables
14. Audited Statement of Expenditure for Contingency
15. Audited Statement of Expenditure for Travel/Field Work
16. Audited Statement of Expenditure for Overhead charges
17. Annexure -IX. Final report of the work done on the MRP
18. Appendix - I. Objectives of the Project
19. Appendix - II. Achievements from the project
20. Appendix - III. Summary of the findings
21. Appendix - IV. Contribution to the Society
22. Appendix - V. Ph.D Enrolled
23. Appendix - VI. List of publications
24. Copies of the research papers published in Journals and Proceedings
25. Copies of the certificates for presentations in the Seminars/Conferences/Workshops
26. Copy of the Mandate Form

PRINCIPAL

Jayaraj Annapackiam College
for women [Autonomous]
Periyakulam - 625 601.
Theni District.

23236351, 23232701, 23237721, 23234116
23235733, 23232317, 23236735, 23239437

विश्वविद्यालय अनुदान आयोग
बहादुरशाह जफर मार्ग
नई दिल्ली-110 002

UNIVERSITY GRANTS COMMISSION
BAHADURSHAH ZAFAR MARG
NEW DELHI-110 002

F. No. **42-836/2013 (SR)**

The Under Secretary (FD-III)
University Grants Commission
New Delhi-110002

22 MAR 2013

Sub:- UGC support for the Major Research Project in Physical Sciences, Bio-Sciences, Maths , Medical, Agricultural Sciences and Engineering & Chemistry to University/College Teachers – Project entitled,

"Investigations on excitions in Nanostrucutures"

Sir,

I am to refer to your letter forwarding the application of **Dr. Mrs. M. Arulmozhi** of your institution for financial assistance under the above scheme and to convey the Commission's approval & sanction an on account grant of **Rs. 8,36,800/- (Rupees: eight lakh thirty six thousand eight hundred only)** to the Principal, **Jayaraj Annapackiam College for Women, periyakulam-625601,. TN** in r/o Major Research Project of **Dr. Mrs. M. Arulmozhi,** Department of **Physics** for the period of 3 years w.e.f. **1.4.2013** as detailed below:-

S.No	ITEMS	AMOUNT APPROVED	GRANT RELEASED AS Ist INSTALMENT	Category
A.	**Non - Recurring**		**3,50,000/-**	**GEN**
1.	Books & Journals	1,00,000/-		
2.	Equipment (Work station, software)	2,50,000/-		
B.	**Recurring**		**4,86,800/-**	
1.	Honorarium to Retd. Teacher @ Rs. 12, 000/- p.m.	nil		
2.	Project Fellow @14,000/- p.m. for initial 2 years and Rs. 16,000/- p.m. from the third year onwards.	5,28,000/-		
3.	Chemical/ Glassware / Consumable	1,00,000/-		
4.	Hiring Services	nil		
5.	Contingency	1,00,000/-		
6.	Travel/Field Work	1,00,000/-		
7.	Special Need	nil		
8.	Overhead Charges @ Rs. 10% approved recurring Grant (Except Travel & Field Work)	72,800/-		
	Total (A +B)	**12,50,800/-**	**8,36,800/-**	

The acceptance Certificate in prescribed format (Annexure-1 available on the UGC web-site) may be sent to the undersigned within one month from the issue of the award letter failing which the project may be treated as cancelled.

If the terms & conditions are acceptable, as per guideline which are available on UGC web-site www.ugc.ac.in the Demand Draft/ Cheque being sent may be retained. Otherwise the same may be returned in original to the UGC by Registered Post in variably with in 15 days from the receipt of the Demand Draft/Cheque in favour of Secretary, UGC, New Delhi.

Principal Investigators should ensure that the statement of expenditure & utilization Certificate to the effect that the grant has been utilized for the purpose for which it has been sanctioned shall be furnished to the University Grants Commission in time.

The first instalment of the grant shall comprise of 100% of the Non –Recurring including Over Head Charges, and 50% of the total Recurring grant.

1. The sanctioned amount is debitable to the Major Head **4. (i) .a (31) Rs. 4,86,800/- & 4. (i) .a (35) Rs. 3,50,000/-** and is valid for payment during financial year **2012-13**.
2. The amount of the Grant shall be drawn by the Under Secretary (drawing and Disbursing Office), University Grants Commission on the Grants-in-aid Bill and shall be disbursed to and credited to the Principal, **Jayaraj Annapackiam College for Women, periyakulam-625601,. TN** through Cheque/Demand Draft/ Mail Transfer.
3. The Grants is subject to the adjustment of the basis of Utilization Certificate in the prescribed performa submitted by the University/Colleges/institution.
4. The University/College shall maintain proper accounts of the expenditure out of the grants which shall be utilized only on approved items of expenditure.
5. The Utilization Certificate of the effect that the grant has been utilized for the purpose for which it has been sanctioned shall be furnished to the University Grants Commission as early as possible after the close of the current financial year.
6. The assets acquired wholly or substantially out of University Grant Commission's grant shall not be disposed or encumbered of utilized for the purposes other that those for which the grant was given, without proper sanctioned of the University Grants Commission and should, at any time the College/University ceased in function such assets shall revert to the University Grant Commission.
7. A Register of assets acquired wholly or substantially out of the grant shall be maintained by the University/College in the prescribed form.
8. The grantee institution shall ensure the utilization of grant-in-aid for which it is being sanction/paid. In case non-utilization/part utilization, the simple interest @ 10% per annum as amended from time to time on unutilized amount from the date of drawl to the date of refund as per provisions contained in General Financial Rules of Govt. of India will be charged.
9. The interest earned by the University/College/Institute on this grants in aid shall be treated as additional grant and may be shown in the Utilization Certificate/Statement of expenditure to be furnished by grantee institution.
10. The University/College/Institute shall follow strictly all the instructions issued by the Government of India from time to time with regard to reservation of posts for Scheduled Castes/Scheduled Tribes/OBC/PH etc.
11. The University/College shall fully implement to Official Language Policy of Union Govt. and comply with the Official Language Act, 1963 and Official Languages (Use for Official purposes of the Union) Rules, 1978 etc.
12. The sanction issues in exercise of the delegation of powers vide Commission Office Order No. 25/92 dated May 01, 1992.
13. An amount of **Rs.** ----------- out the grant of **Rs.** ------------- sanctioned vide letter No. F. **42-836/2013 (SR)** dated has been utilized by University/College/Institution for he purpose for which it was sanctioned. Utilization Certificate for **Rs.** ------------- has already been entered at S. No. ------- now we may enter Utilization Certificate for **Rs.** --------------- S. No ------ and in the U. C. Registrar at page No. -----.
14. It is also certified from the B.C.R. that the funds are available under the scheme. Entered in BCR at S.No 31$8/55
The above grant is sanctioned against the budget provision of **Rs.** .... during the current financial year leaving a balance of **Rs.** -- under the head of Account **4. (i) .a (31) Rs. 4,86,800/- & 4. (i) .a (35) Rs. 3,50,000/-**
15. The funds to the extent are available under the Scheme.
16. The University/Institution/College is strictly following the UGC regulations on curbing the menace of ragging in Higher Educational Institutions, 2009.

(Dr. (Mrs.) Urmila Devi)
Joint Secretary

Copy forwarded for information and necessary action for:-

1. The Principal, **Jayaraj Annapackiam College for Women, periyakulam-625601,. TN,** Acknowledgement for the receipt of DD / Cheque / Mail Transfer for **Rs. 8,36,800/-** may be sent to the Under Secretary, Finance Division III, UGC,
2. **Dr. Mrs. M. Arulmozhi,** Principal Investigator, Department of **Physics** **Jayaraj Annapackiam College for Women, periyakulam, 625601,. TN**
3. office of the Director General of Audit, Central Revenues, A. G. C. R. Building, I. P. Estate, New Delhi.
4. The Registrar, **Mother teresa Women's University, Kodaikanal, Tn**

(Pramod Sharma)
Section Officer

विश्वविद्यालय अनुदान आयोग
University Grants Commission
मानव संसाधन विकास मंत्रालय, भारत सरकार
(Ministry of Human Resource Development, Govt. of India)
बहादुरशाह जफर मार्ग नई दिल्ली –110002
Bahadurshah Zafar Marg, New Delhi-110002

सत्यमेव जयते

ज्ञान-विज्ञान विमुक्तये

No. F. 42-836/2013 (SR)

March, 2016 26 MAR 2016

The Principal,
Jayaraj Annapackiam college
For Women, Periyakulam, Tamil Nadu-625601.

Subject:- **Extension** of Major Research Project awarded **Dr. Mrs. M. Arulmozhi, Department of Physics** by UGC during 2013.

Sir,/ Madam,

I am directed to say that the tenure of the Major Research Project awarded to you has been extended by the UGC upto 31.03.2017 without any financial assistance for the extended period.

Yours faithfully,

(**G. S. Aulakh**)
Under Secretary

Copy to:-
Dr. Mrs. M. Arulmozhi,
Department of Physics,
Jayaraj Annapackiam college
For Women, Periyakulam, Tamil Nadu-625601.

(**Arun Kumar Sinha**)
Section Officer

10

UNIVERSITY GRANTS COMMISSION
BAHADUR SHAH ZAFAR MARG
NEW DELHI 110002

FD Diary No. 5043

Dated : 21-06-2016

4 JUL 2016

GEN

F .No.42-836/2013 (SR)

June 2016

The Under Secretary (FD-III)
University Grants Commission
Bahadur Shah Zafar Marg
New Delhi – 110002

Sub: Release of Grant-in aid to **Jayaraja Annapackiam College of Women, Periyakulam - 625 601, Tamil Nadu** for the year 2016-17 under plan in respect of Major Research Project entitled **Investigations…………………………Nanostrucutures"** awarded to **Dr. (Mrs.) M. Arulmozhi, Department of Physics** , tenure of project from **01.04.2013 to 31.03.2017.**

Sir,

I am directed to convey the sanction of the University Grants Commission for payment of grant of **Rs. 3,59,712/- (Rupees Three Lakh Fifty Nine Thousand Seven Hundred Twelve Only)** as **2nd installment** for the year 2016-17 towards Major Research Project to **The Principal, Jayaraja Annapackiam College of Women, Periyakulam - 625 601, Tamil Nadu** for the plan expenditure to be incurred during 2016-17.

I am also directed to say that the tenure of the above project has been extended by the UGC upto 31.03.2017 without any additional financial assistance for the extended period.

Name of the Item	Amount Allocated	Head of Account	Grant now Being Sanctioned	Grant already Released	Total Grant
Books & Journal	1,00,000/-	3.A(56).35	....	1,00,000/-	1,00,000/-
Equipment	2,50,000/-		....	2,50,000/-	2,50,000/-
Honorarium			....		
Project fellow	5,28,000/-	3.A(56).31	2,11,200/-	2,64,000/-	4,75,200/-
HRA	31,680/-		28,512/-		28,512/-
Chemicals	1,00,000/-		40,000/-	50,000/-	90,000/-
Contingency	1,00,000/-		40,000/-	50,000/-	90,000/-
Hiring Services					
Travel/field work	1,00,000/-		40,000/-	50,000/-	90,000/-
Overhead Charges	72,800/-		....	72,800/-	72,800/-
Additional Grant	....		....	............,	....
Total	12,82,480/-		3,59,712/-	8,36,800/-	11,96,512/-

1. The sanctioned amount is debit able to **Major Research Project head Sector 3.A(56).31** and is valid for payment during the financial year **2016-17** only.

2. The amount of the Grant shall be drawn by the Under Secretary (Drawing and Disbursing Officer) UGC on the Grants-in-aid bill and shall be disbursed to and credited to **The Principal, Jayaraja Annapackiam College of Women, Periyakulam - 625 601, Tamil Nadu** through Electronic mode as per the following details:-

(a)	Bank Name & Address of Branch	**Indian Overseas Bank, Tamaraikulam, Jayaraj Annapackiam College for Women, (Autonomous), Thamaraikulam, Periyakulam (P.O) Theni – 625 601**
(b)	Account No	**178901000002717**
(c)	Type of Account : SB /Current /Cash Credit	**SB**
(d)	**IFSC Code**	**IOBA0001789**
(e)	MICR Code	**625020107**
(f)	Whether Bank Branch is RTGS or NEFT enabled : RTGS / NEFT /Both	**YES**
(g)	Name & Address of Account Holder	**The Principal, Jayaraja Annapackiam College of Women, Periyakulam - 625 601, Tamil Nadu.**

3. The Grant is Subject to the adjustment on the basis of Utilization Certificate in the prescribed proforma submitted by the University / Institution.

4. The University / Institution shall maintain proper accounts of the expenditure out of the Grants, which shall be utilized, only on the approved items of expenditure.

5. The University / Institution may follow the General Financial Rules, 2005 and take urgent necessary action to amend their manuals of financial procedures to bring them in conformity with GFRs, 2005 and those don't have their own approved manuals on financial procedures may adopt the provisions of GFRs, 2005 and instructions / guidelines there under from time to time.

6. The Utilization Certificate to the effect that the grant has been utilized for the purpose for which it has been sanctioned shall be furnished to UGC as early as possible after the close of current financial year.

7. The assets acquired wholly for substantially out of University Grants Commission's Grant shall not be disposed or encumbered or utilized for the purposes other than those for which the grants waayanands given without proper sanction of the UGC and should at any time the University ceased to function, such assets shall revert to the University Grants Commission.

8. A Register of Assets acquired wholly or substantially out of the grant shall be maintained by the University in the prescribed proforma.

9. The grantee institution shall ensure the utilization of grants-in-aid for which it is being sanctioned / paid. In case of non-utilization / part utilization thereof, simple interest @ 10% per annum, as amended from time to time on the unutilized amount from the date of drawal to the date of refund as per provisions contained in General Financial Rules of Govt. of India, will be charged.

10. The University / Institutions shall follow strictly the Government of India / UGC guidelines regarding implementation of the reservation policy [both vertical (for SC, ST & OBC) and horizontal (for persons with disability etc.)] in teaching and non-teaching posts.

11. The University / Institution shall fully implement the Official Language Policy of Union Government and comply with the Official Language Act, 1963 and Official Languages (Use for Official Purposes of the Union) Rules, 1976 etc.

12. The sanction is issued in exercise of the delegation of powers vide UGC Order No. 69/2014 [F.No.10-11/12 (Admn. IA & B)] dated 26/3/2014.

13. The University / Institution shall strictly follow the UGC Regulations on curbing the menace of Ragging in Higher Education Institutions, 2009.

14. The University / Institution shall take immediate action for its accreditation by National Assessment & Accreditation Council (NAAC).

15. The accounts of the University / Institution will be open for audit by the Comptroller & Auditor General of India in accordance with the provisions of General Financial Rules, 2005.

16. The annual accounts i.e. balance sheet, income and expenditure statement and statement of receipts and payments are to be prepared strictly in accordance with the Uniform Format of Accounting prescribed by Government.

17. The grantee institution shall remit the amount the grants-in-aid and/or interest through e-mode (RTGS/NEFT) directly to UGC account as per following bank details:-

Account Holder	Secretary, UGC, New Delhi-110 002
Name of Bank & Address	Canara Bank, UGC Office, New Delhi-110 002
A/C No.	**8627101002122**
Type of A/C	Savings
IFSC Code	CNRB0008627
MICR Code	110015170

18. An amount of **Rs. 8,44,612/-** out the grant of **Rs. 8,36,800/-**..... Sanctioned vide letter No. **F. No. 42-836/2013 (SR)** dated **22-03-2013** has been utilized by University/College/Institution for the purpose for which it was sanctioned. Utilization Certificate for **Rs ......** ...NIL...... has been entered at S. No.......... now we may enter Utilization Certificate for **Rs**...**8,44,612/-** ....S. No.U36. and in the U.C. Register at page No..102

19. Funds to the extent of Rs are available under the scheme or BE / RBE of the year 2016-17.

20. These issues with the concurrence of IFD vide **Diary No 1020 (IFD) dated 24/05/2016.**

21. This issues with the approval of Joint Secretary (MRP) vide **Diary No. 59352 dated 01/06/2016.**

Your faithfully,

(G.S. AULAKH)
UNDER SECRETARY

Copy forwarded for information and necessary action for :-

1. **The Principal, Jayaraja Annapackiam College of Women, Periyakulam - 625 601, Tamil Nadu.**
2. Office of The Finance Officer, General of Audit, Central Revenues, AGCR Building, I.P. Estate, New Delhi.
3. Accountant General, State Govt. of **Jayaraja Annapackiam College of Women, Periyakulam - 625 601, Tamil Nadu.**
4. **Dr. (Mrs.) M. Arulmozhi, Department of Physics Jayaraja Annapackiam College of Women, Periyakulam - 625 601, Tamil Nadu.**
5. **The Registrar, Mother Teresa Women's University, Kodaikanal, Tamil Nadu.**
6. Guard file.

(ARUN KUMAR SINHA)
(SECTION OFFICER)

S. No	Contents	Page No
1.	Annexure - III. Audited Statement of Expenditure in Respect of Major Research Project	**1**
2.	Annexure - V. Audited Utilization Certificate	**3**
3.	Details of Amount Allocated and Expenditure Incurred under Various Heads	**4**
4.	Audited Statement of Expenditure for Books and Journals	**5**
5.	Accession Certificate from Librarian (Books Handed Over to General Library)	**7**
6.	Audited Statement of Expenditure for Equipments	**8**
7.	Asset Certificate from Head of the Department (Equipments handed over to the Department)	**9**
8.	Audited Statement of Expenditure for Honorarium to Project Fellow	**10**
9.	Audited Statement of Expenditure for HRA to Project Fellow	**12**
10.	Audited Statement of Expenditure for Chemicals/Glassware/Consumables	**14**
11.	Audited Statement of Expenditure for Contingency	**16**
12.	Audited Statement of Expenditure for Travel/Field Work	**21**
13.	Audited Statement of Expenditure for Overhead Charges	**24**
14.	Annexure -IX. Final Report of the Work Done on the MRP	**25**
15.	Appendix - I. Objectives of the Project	**27**
16.	Appendix - II. Achievements from the Project	**29**
17.	Appendix - III. Summary of the Findings	**32**

18.	Appendix - IV. Contribution to the Society	**39**
19.	Appendix - V. Ph.D Enrolled	**41**
20.	Appendix - VI. List of Publications	**43**
21.	Copies of the Research Papers Published in Journals and Proceedings	**45**
22.	Copies of the Certificates for Presentations in the Seminars/Conferences/Workshops	**123**
23.	Copy of the Mandate Form	**137**

Annexure - III

ज्ञान-विज्ञान विमुक्तये

UNIVERSITY GRANTS COMMISSION

BAHADUR SHAH ZAFAR MARG

NEW DELHI – 110 002.

STATEMENT OF EXPENDITURE IN RESPECT OF MAJOR RESEARCH PROJECT

1. Name of the Principal Investigator : **Dr. Mrs. M. Arulmozhi**
2. Name of the Principal Investigator : **Associate Professor**
   Department of Physics
   Jayaraj Annapackiam College for Women
   (Autonomous)
   Periyakulam - 625601
   Theni District, Tamil Nadu, India
3. UGC approval letter No. and date : **No. F. 42-836/2013 (SR) dated 22.03.2013**
4. Title of the Research Project : **Investigations on excitons in nanostructures**
5. Effective Date of starting the project : **01.04.2013**
6. a. Period of Expenditure : **From 01.04.2013 to 31.03.2017**

   b. Details of Expenditure

S. No	Item	Amount Approved Rs.	Expenditure Incurred Rs.
i.	Books & Journals	1,00,000/-	1,00,046/-
ii.	Equipment	2,50,000/-	2,50,029/-
iii.	Contingency	1,00,000/-	1,00,240/-
iv.	Field work/Travel	1,00,000/-	1,00,973/-
v.	Hiring Services	---	---

Annexure - III

vi.	Chemicals & Glassware	1,00,000/-	1,00,273/-
vii.	Overhead	72,800/-	72,800/-
viii.	Any other items	---	---

c. Staff

Date of Appointment: **03.05.2013**

S.No	**Items**	**From**	**To**	**Amount Approved**	**Expenditure incurred**
1.	Honorarium to PI (Retired Teachers)	---	---	---	---
2.	Project Fellow	03.05.2013	30.04.2016	5,28,000/-	5,28,000/-
3.	HRA	03.05.2013	30.04.2016	31,680/-	31,680/-

1. It is certified that the appointment have been made in accordance with the terms and conditions laid down by the commission.

2. If as a result of check or audit objection some irregularly is noticed at later date, action will be taken to refund, adjust or regularize the objected amounts.

3. Payment @ revised rates shall be made with arrears on the availability of additional funds.

4. It is certified that the grant of **Rs.12,82,480/- (Rupees Twelve Lakhs Eighty Two Thousand Four Hundred and Eighty only**) received from the University Grants Commission under the scheme of support for Major Research Project entitled **Investigations on excitons in nanostructures** vide UGC letter **No. F. 42-836/2013 (SR) dated 22.03.2013** has been fully utilized for the purpose for which it was sanctioned and in accordance with the terms and conditions laid down by the University Grants Commission.

M. Arulmozhi

PRINCIPAL INVESTIGATOR

Dr.Mrs. M. ARULMOZHI
Principal Investigator-UGC MRP
Associate Professor in Physics
Jayaraj Annapackiam College-for Women (Autonomous)
Periyakulam - 625 601, Theni (Dt)

R. Nirmala

PRINCIPAL

Jayaraj Annapackiam College for women [Autonomous]
Periyakulam - 625 601.
Theni District.

STATUTORY AUDITOR

P. RAMALINGAM, B.Sc., F.C.A., CHARTERED ACCOUNTANT, M.No: 19516, PH: 2430391, 57, PANDIAN NAGAR, DINDIGUL-1.

P. RAMALINGAM
CHARTERED ACCOUNTANT.

3

Annexure - V

ज्ञान-विज्ञान विमुक्तये

UNIVERSITY GRANTS COMMISSION
BAHADHUR SHAH ZAFAR MARG
NEW DELHI - 110 002.

Utilization Certificate

Certified that the grant of **Rs.12,82,480/- (Rupees Twelve Lakhs Eighty Two Thousand Four Hundred and Eighty only)** received from the University Grants Commission under the scheme of support for Major Research project entitled **Investigations on excitons in nanostuctures** vide UGC Letter **No. F. 42-836/2013 (SR) dated 22.03.2013** has been fully utilized for the purpose for which it was sanctioned and in accordance with the terms and conditions laid down by the University Grants Commission.

M. Arulmozhi

PRINCIPAL INVESTIGATOR

Dr.Mrs. M. ARULMOZHI
Principal Investigator-UGC MRP
Associate Professor in Physics
Jayaraj Annapackiam College-
for Women (Autonomous)
Periyakulam - 625 601, Theni (Dt)

PRINCIPAL

Jayaraj Annapackiam College
for women [Autonomous]
Periyakulam - 625 601.
Theni District.

STATUTORY AUDITOR

P. RAMALINGAM, B.Sc., F.C.A., CHARTERED ACCOUNTANT
M.No: 19516
PH: 2430391
57, PANDIAN -NAGAR,
DINDIGUL - 1.

P. RAMALINGAM
CHARTERED ACCOUNTANT,

4

UGC- MAJOR RESEARCH PROJECT

"Investigations on excitons in nanostructures"

No. F. 42-836/2013(SR) dated 22.03.2013

Principal Investigator: Dr. Mrs. M. Arulmozhi
Associate Professor in Physics
Jayaraj Annapackiam College for Women (Autonomous)
Periyakulam - 625601. Theni District. Tamil Nadu.

DETAILS OF AMOUNT ALLOCATED AND EXPENDITURE INCURRED

S.No.	Items	Amount Allocated (Rs.)	Amount sanctioned in 1st and 2nd instalments (Rs.)	Expenditure incurred (Rs.)
1.	Books & Journals	1,00,000/-	1,00,000/-	1,00,046/-
2.	Equipments	2,50,000/-	2,50,000/-	2,50,029/-
3.	Honorarium to Project Fellow **(from 03.05.2013 to 31.04.2016)**	5,28,000/-	4,75,200/-	5,28,000/-
4.	HRA for the Project Fellow **(from 03.05.2013 to 31.04.2016)**	31,680/-	28,512/-	31,680/-
5.	Chemicals/ Glasswares/ Consumables	1,00,000/-	90,000/-	1,00,273/-
6.	Contingency	1,00,000/-	90,000/-	1,00,240/-
7.	Travel/Field work	1,00,000/-	90,000/-	1,00,973/-
8.	Overhead Charges	72,800/-	72,800/-	72,800/-
	Total	**Rs. 12,82,480/-**	**Rs. 11,96,512/-**	**Rs. 12,84,041/-**

Balance amount to be sanctioned by UGC: **Rs. 85,968/-**

M. Arulmozhi

PRINCIPAL INVESTIGATOR

Dr.Mrs. M. ARULMOZHI
Principal Investigator-UGC MRP
Associate Professor in Physics
Jayaraj Annapackiam College-
for Women (Autonomous)
Periyakulam - 625 601, Theni (Dt)

PRINCIPAL

Jayaraj Annapackiam College
for women [Autonomous]
Periyakulam - 625 601.
Theni District.

STATUTORY AUDITOR

P. RAMALINGAM, B.Sc., F.C.A., CHARTERED ACCOUNTANT
M.No: 19516
PH: 2430391
57, PANDIAN -NAGAR,
DINDIGUL - 1.

P. RAMALINGAM
CHARTERED ACCOUNTANT.

UGC- MAJOR RESEARCH PROJECT

"Investigations on excitons in nanostructures"

No. F. 42-836/2013(SR) dated 22.03.2013

Principal Investigator: Dr. Mrs. M. Arulmozhi
Associate Professor in Physics
Jayaraj Annapackiam College for Women (Autonomous)
Periyakulam - 625601. Theni District. Tamil Nadu.

STATEMENT OF EXPENDITURE FOR BOOKS AND JOURNALS

Amount allocated by UGC : Rs. 1,00,000/-

Amount sanctioned by UGC : Rs. 1,00,000/-

Expenditure incurred: Rs. 1,00,046/-

S.No.	Bill Date	Bill No	Name of the Book Dealer	Amount (Rs)
1.	01.07.2014	58	Selvi Book Shop	2,175/-
2.	13.07.2014	OD40713111279	Flipkart.com	1,509/-
3.	21.08.2014	OD40821183399	Flipkart.com	1,535/-
4.	22.08.2014	402-6293111-5465952	amazon.in	2,855/-
5.	22.08.2014	402-3848512-6666761	amazon.in	1,050/-
6.	22.08.2014	402-3480599-7993925	amazon.in	1,632/-
7.	22.08.2014	402-0916013-2173961	amazon.in	1,605/-
8.	22.08.2014	402-1214744-0397908	amazon.in	1,493/-
9.	22.08.2014	402-0430484-3623532	amazon.in	3,408/-
10.	02.09.2014	OD40902191404	Flipkart.com	16,181/-
11.	06.09.2014	402-2630463-4963521	amazon.in	1,080/-
12.	06.09.2014	402-7844607-7309113	amazon.in	1,272/-
13.	06.09.2014	402-4559319-3755540	amazon.in	4,299/-
14.	06.09.2014	402-4561494-7129124	amazon.in	1,560/-
15.	06.09.2014	402-3975472-1741908	amazon.in	4,011/-
16.	26.09.2014	402-9215173-5223560	amazon.in	22,754/-
17.	26.09.2014	402-4089079-0009909	amazon.in	9,464/-
18.	10.10.2014	479	Power Book House	3,433.50/-
19.	10.10.2014	481	Power Book House	625.50/-
20.	16.12.2014	402-6080949-1525104	amazon.in	3,336/-

21.	16.12.2014	402-3050528-2032346	amazon.in	1,312/-
22.	16.12.2014	402-6381794-5607543	amazon.in	8,073/-
23.	16.12.2014	402-4723555-5229947	amazon.in	478/-
24.	16.12.2014	402-5971560-6197110	amazon.in	550/-
25.	16.12.2014	402-5199640-4330741	amazon.in	499/-
26.	18.12.2014	402-7134916-8340321	amazon.in	1,170/-
27.	18.12.2014	402-1563762-3076368	amazon.in	777/-
28.	18.12.2014	402-2150421-6071520	amazon.in	915/-
29.	29.03.2017	---	Maaya Book Centre	994/-
Total				**Rs. 1,00,046/-**

M. Arulmozhi

PRINCIPAL INVESTIGATOR

Dr.Mrs. M. ARULMOZHI
Principal Investigator-UGC MRP
Associate Professor in Physics
Jayaraj Annapackiam College-
for Women (Autonomous)
Periyakulam - 625 601, Theni (Dt)

PRINCIPAL

Jayaraj Annapackiam College
for Women (Autonomous)
Thamaraikulam, Periyakulam-625 601.
Theni District Tamilnadu.

STATUTORY AUDITOR

P. RAMALINGAM, B.Sc., F.C.A., CHARTERED ACCOUNTANT
M.No: 19516
PH: 2430391
57, PANDIAN NAGAR,
DINDIGUL-1.

P. RAMALINGAM
CHARTERED ACCOUNTANT.

JAYARAJ ANNAPACKIAM COLLEGE FOR WOMEN (AUTONOMOUS)
(A unit of the Sisters of St. Anne of Tiruchirapalli)
Re-accredited with 'A' Grade (Cycle – 3) by NAAC
Affiliated to Mother Teresa Women's University, Kodaikanal.
PERIYAKULAM – 625 601, THENI DISTRICT.

Phone : 04546-231482
Fax : 04546231482
Website : www.annejac.com
e-mail : principal@annejac.com

ACCESSION CERTIFICATE

Certified that the books and journals purchased for **Rs.1,00,046/-** (**Rupees One Lakh and Forty Six only**) out of the grant from the University Grants Commission under the scheme of support for Major research Project entitled **Investigations on excitons in nanostructures** vide UGC Letter **No. F. 42-836/2013(SR) dated 22.03.2013** have been transferred to the General Library by **Dr. Mrs. M. Arulmozhi**, Associate Professor in Physics, Jayaraj Annapackiam College for Women (Autonomous), Periyakulam.

M. Arulmozhi

PRINCIPAL INVESTIGATOR

Dr.Mrs. M. ARULMOZHI
Principal Investigator-UGC MRP
Associate Professor in Physics
Jayaraj Annapackiam College-
for Women (Autonomous)
Periyakulam - 625 601, Theni (Dt)

Sr Sylvia

LIBRARIAN

LIBRARIAN
Jayaraj Annapackiam College
for Women (Autonomous)
PERIYAKULAM.

R Nirmala

PRINCIPAL

Jayaraj Annapackiam College
for women [Autonomous]
Periyakulam - 625 601.
Theni District.

UGC- MAJOR RESEARCH PROJECT

"Investigations on excitons in nanostructures"

No. F. 42-836/2013(SR) dated 22.03.2013

Principal Investigator: Dr. Mrs. M. Arulmozhi
Associate Professor in Physics
Jayaraj Annapackiam College for Women (Autonomous)
Periyakulam - 625601. Theni District. Tamil Nadu.

STATEMENT OF EXPENDITURE FOR EQUIPMENTS

Amount allocated by UGC : Rs. 2,50,000/-

Amount sanctioned by UGC : Rs. 2,50,000 /-

Expenditure incurred: Rs. 2,50,029/-

S.No.	Bill Date	Bill No	Name of the Equipments	Amount (Rs)
1.	19.03.2014	406	HP- Workstation	1,10,000/-
2.	23.05.2014	453	Dell- Computer	60,000/-
3.	01.10.2014	DOT-0003278	Sony-Mini Laptop	40,000/-
4.	27.11.2014	AO-262/INV	Mathematica Software	38,729/-
5.	22.12.2014	507	Toner & Pendrive	1,300/-
Total				**2,50,029/-**

M. Arulmozhi

PRINCIPAL INVESTIGATOR

Dr.Mrs. M. ARULMOZHI
Principal Investigator-UGC MRP
Associate Professor in Physics
Jayaraj Annapackiam College-
for Women (Autonomous)
Periyakulam - 625 601, Theni (Dt)

PRINCIPAL

Jayaraj Annapackiam College
for women [Autonomous]
Periyakulam - 625 601.
Theni District.

STATUTORY AUDITOR

P. RAMALINGAM, B.Sc., F.C.A.,
M.No : 19516
PH : 2430391
57, PANDIAN -NAGAR,
DINDIGUL - 1.
CHARTERED ACCOUNTANT

P. RAMALINGAM
CHARTERED ACCOUNTANT.

JAYARAJ ANNAPACKIAM COLLEGE FOR WOMEN (AUTONOMOUS)
(A unit of the Sisters of St. Anne of Tiruchirapalli)
Re-accredited with 'A' Grade (Cycle – 3) by NAAC
Affiliated to Mother Teresa Women's University, Kodaikanal.
PERIYAKULAM – 625 601, THENI DISTRICT.

Phone : 04546-231482 Website : www.annejac.com
Fax : 04546231482 e-mail : principal@annejac.com

ASSET CERTIFICATE

Certified that the Equipments purchased for **Rs.2,50,029/- (Rupees Two lakh fifty thousand and Twenty Nine only)** out of the grant from the University Grants Commission under the scheme of support for Major research Project entitled **Investigations on excitons in nanostructures** vide UGC Letter **No. F. 42-836/2013(SR) dated 22.03.2013** have been handed over to the Department of Physics by **Dr. Mrs. M. Arulmozhi**, Associate Professor in Physics, Jayaraj Annapackiam College for Women (Autonomous), Periyakulam.

M. Arulmozhi

PRINCIPAL INVESTIGATOR
Dr.Mrs. M. ARULMOZHI
Principal Investigator-UGC MRP
Associate Professor in Physics
Jayaraj Annapackiam College-
for Women (Autonomous)
Periyakulam - 625 601, Theni (Dt)

R. Mary Mathelan

HEAD OF THE DEPARTMENT
Head of the Department of Physics
Jayaraj Annapackiam College
for Woman (Autonomous)
Periyakulam - 625 601

R. Nirmala

PRINCIPAL
Jayaraj Annapackiam College
for women [Autonomous]
Periyakulam - 625 601.
Theni District.

UGC- MAJOR RESEARCH PROJECT

"Investigations on excitons in nanostructures"

No. F. 42-836/2013(SR) dated 22.03.2013

Principal Investigator: Dr. Mrs. M. Arulmozhi
Associate Professor in Physics
Jayaraj Annapackiam College for Women (Autonomous)
Periyakulam - 625601. Theni District. Tamil Nadu.

STATEMENT OF EXPENDITURE FOR HONORARIUM TO PROJECT FELLOW

Amount allocated by UGC : Rs. 5, 28, 000/-

Amount sanctioned by UGC: Rs. 4,75,200/-

Expenditure incurred: Rs. 5,28,000/-

Amount to be sanctioned by UGC: Rs. 52,800/-

S. No.	Name	Date	Honorarium per month
1.	A. Anitha	03.06.2013	Rs.14,000/-
2.	A. Anitha	01.07.2013	Rs.14,000/-
3.	A. Anitha	01.08.2013	Rs.14,000/-
4.	A. Anitha	02.09.2013	Rs.14,000/-
5.	A. Anitha	03.10.2013	Rs.14,000/-
6.	A. Anitha	01.11.2013	Rs.14,000/-
7.	A. Anitha	02.12.2013	Rs.14,000/-
8.	A. Anitha	02.01.2014	Rs.14,000/-
9.	A. Anitha	03.02.2014	Rs.14,000/-
10.	A. Anitha	03.03.2014	Rs.14,000/-
11.	A. Anitha	03.04.2014	Rs.14,000/-
12.	A. Anitha	02.05.2014	Rs.14,000/-
13.	A. Anitha	02.06.2014	Rs.14,000/-
14.	A. Anitha	01.07.2014	Rs.14,000/-
15.	A. Anitha	01.08.2014	Rs.14,000/-
16.	A. Anitha	01.09.2014	Rs.14,000/-

17.	A. Anitha	01.10.2014	Rs.14,000/-
18.	A. Anitha	01.11.2014	Rs.14,000/-
19.	A. Anitha	01.12.2014	Rs.14,000/-
20.	A. Anitha	02.01.2015	Rs.14,000/-
21.	A. Anitha	02.02.2015	Rs.14,000/-
22.	A. Anitha	02.03.2015	Rs.14,000/-
23.	A. Anitha	01.04.2015	Rs.14,000/-
24.	A. Anitha	01.05.2015	Rs.14,000/-
25.	A. Anitha	01.06.2015	Rs.16,000/-
26.	A. Anitha	01.07.2015	Rs.16,000/-
27.	A. Anitha	03.08.2015	Rs.16,000/-
28.	A. Anitha	01.09.2015	Rs.16,000/-
29.	A. Anitha	01.10.2015	Rs.16,000/-
30.	A. Anitha	02.11.2015	Rs.16,000/-
31.	A. Anitha	01.12.2015	Rs.16,000/-
32.	A. Anitha	01.01.2016	Rs.16,000/-
33.	A. Anitha	01.02.2016	Rs.16,000/-
34.	A. Anitha	01.03.2016	Rs.16,000/-
35.	A. Anitha	01.04.2016	Rs.16,000/-
36.	A. Anitha	31.04.2016	Rs.16,000/-
Total			**Rs. 5,28,000/-**

M. Arulmozhi

PRINCIPAL INVESTIGATOR

Dr.Mrs. M. ARULMOZHI
Principal Investigator-UGC MRP
Associate Professor in Physics
Jayaraj Annapackiam College-
for Women (Autonomous)
Periyakulam - 625 601, Theni (Dt)

PRINCIPAL

Jayaraj Annapackiam College
for women [Autonomous]
Periyakulam - 625 601.
Theni District.

STATUTORY AUDITOR

P. RAMALINGAM, B.Sc., F.C.A., CHARTERED ACCOUNTANT
M.No : 19516
PH : 2430391
57, PANDIAN -NAGAR,
DINDIGUL - 1.

P. RAMALINGAM
CHARTERED ACCOUNTANT.

UGC- MAJOR RESEARCH PROJECT

"Investigations on excitons in nanostructures"

No. F. 42-836/2013(SR) dated 22.03.2013

Principal Investigator: Dr. Mrs. M. Arulmozhi
Associate Professor in Physics
Jayaraj Annapackiam College for Women (Autonomous)
Periyakulam - 625601. Theni District. Tamil Nadu.

STATEMENT OF EXPENDITURE FOR HOUSE RENT ALLOWANCE TO PROJECT FELLOW

Amount allocated by UGC: Rs. 31,680/-

Amount sanctioned by UGC: Rs. 28,512/-

Expenditure incurred: Rs. 31,680/-

Amount to be sanctioned by UGC: Rs. 3,168/-

S. No.	Name	Date	HRA per month
1.	A. Anitha	03.06.2013	Rs.880/-
2.	A. Anitha	01.07.2013	Rs.880/-
3.	A. Anitha	01.08.2013	Rs.880/-
4.	A. Anitha	02.09.2013	Rs.880/-
5.	A. Anitha	03.10.2013	Rs.880/-
6.	A. Anitha	01.11.2013	Rs.880/-
7.	A. Anitha	02.12.2013	Rs.880/-
8.	A. Anitha	02.01.2014	Rs.880/-
9.	A. Anitha	03.02.2014	Rs.880/-
10.	A. Anitha	03.03.2014	Rs.880/-
11.	A. Anitha	03.04.2014	Rs.880/-
12.	A. Anitha	02.05.2014	Rs.880/-
13.	A. Anitha	02.06.2014	Rs.880/-
14.	A. Anitha	01.07.2014	Rs.880/-
15.	A. Anitha	01.08.2014	Rs.880/-
16.	A. Anitha	01.09.2014	Rs.880/-

17.	A. Anitha	01.10.2014	Rs.880/-
18.	A. Anitha	01.11.2014	Rs.880/-
19.	A. Anitha	01.12.2014	Rs.880/-
20.	A. Anitha	02.01.2015	Rs.880/-
21.	A. Anitha	02.02.2015	Rs.880/-
22.	A. Anitha	02.03.2015	Rs.880/-
23.	A. Anitha	01.04.2015	Rs.880/-
24.	A. Anitha	01.05.2015	Rs.880/-
25.	A. Anitha	01.06.2015	Rs.880/-
26.	A. Anitha	01.07.2015	Rs.880/-
27.	A. Anitha	03.08.2015	Rs.880/-
28.	A. Anitha	01.09.2015	Rs.880/-
29.	A. Anitha	01.10.2015	Rs.880/-
30.	A. Anitha	02.11.2015	Rs.880/-
31.	A. Anitha	01.12.2015	Rs.880/-
32.	A. Anitha	01.01.2016	Rs.880/-
33.	A. Anitha	01.02.2016	Rs.880/-
34.	A. Anitha	01.03.2016	Rs.880/-
35.	A. Anitha	01.04.2016	Rs.880/-
36.	A. Anitha	31.04.2016	Rs.880/-
Total			**Rs. 31,680/-**

M. Arulmozhi

PRINCIPAL INVESTIGATOR

Dr.Mrs. M. ARULMOZHI
Principal Investigator-UGC MRP
Associate Professor in Physics
Jayaraj Annapackiam College-
for Women (Autonomous)
Periyakulam - 625 601, Theni (Dt)

PRINCIPAL

Jayaraj Annapackiam College
for women [Autonomous]
Periyakulam - 625 601.
Theni District.

STATUTORY AUDITOR

P. RAMALINGAM, B.Sc., F.C.A.,
M.No: 19518
PH: 2430391
57, PANDIAN NAGAR,
DINDIGUL - 1.
CHARTERED ACCOUNTANT

P. RAMALINGAM
CHARTERED ACCOUNTANT

UGC- MAJOR RESEARCH PROJECT

"Investigations on excitons in nanostructures"

No. F. 42-836/2013(SR) dated 22.03.2013

Principal Investigator: Dr. Mrs. M. Arulmozhi
Associate Professor in Physics
Jayaraj Annapackiam College for Women (Autonomous)
Periyakulam - 625601. Theni District. Tamil Nadu.

STATEMENT OF EXPENDITURE FOR CHEMICALS / GLASSWARE / CONSUMABLES

Amount allocated by UGC: Rs. 1,00,000 /-

Amount sanctioned by UGC: Rs. 90,000 /-

Expenditure incurred: Rs. 1,00,273/-

Amount to be sanctioned by UGC: Rs. 10,000/-

S.No.	Date	Bill No.	Items	Amount (Rs)
1.	24.01.2014	A 0176	Toner and Network switch	4,650/-
2.	13.03.2014	8506	Chemicals and Glassware	7,076/-
3.	25.03.2014	8507	Chemicals and Glassware	2,019/-
4.	17.07.2014	A 0442	Toner and CD pack	10,300/-
5.	16.08.2014	---	Consumables	11,600/-
6.	26.08.2014	8281	Chemicals and Glassware	2,731/-
7.	10.09.2014	8602	Chemicals and Glassware	3,405/-
8.	24.10.2014	487	Consumables	7,200/-
9.	26.11.2014	8567	Chemicals	905/-
10.	11.12.2014	8610	Chemicals	462/-
11.	19.12.2014	019	Conductivity - Characterization studies	18,743/-
12.	20.12.2014	1938	Consumables	150/-
13.	20.12.2014	---	A4 sheets	1,570/-
14.	11.01.2015	334	Consumables	1,290/-
15.	04.02.2015	579	Toner Refill	1,600/-
16.	27.06.2015	1016	UPS Battery Service	1,800/-
17.	21.08.2015	1033	Toner Refill	800/-

18.	07.03.2016	1099	Toner Refill	800/-
19.	13.07.2016	B 0391	2 TB hard disk	8,000/-
20.	03.12.2016	7655	Chemicals and Glassware	2342/-
21.	11.12.2016	A 0442	Toner and 32 GB Pendrive	6,100/-
22.	16.12.2016	---	A4 Sheets	1,020/-
23.	04.02.2017	C 0218	Toner	3,900/-
24.	16.02.2017	PKM/B164	Consumables	1,300/-
25.	15.03.2017	---	A4 Sheets	510/-
Total				**Rs. 1,00,273/-**

M. Arulmozhi

PRINCIPAL INVESTIGATOR

Dr.Mrs. M. ARULMOZHI
Principal Investigator-UGC MRP
Associate Professor in Physics
Jayaraj Annapackiam College-
for Women (Autonomous)
Periyakulam - 625 601, Theni (Dt)

PRINCIPAL

Jayaraj Annapackiam College
for women [Autonomous]
Periyakulam - 625 601.
Theni District.

STATUTORY AUDITOR

P. RAMALINGAM, B.Sc., F.C.A., CHARTERED ACCOUNTANT
M.No: 19516
PH: 2430391
57, PANDIAN NAGAR,
DINDIGUL-1.

P. RAMALINGAM
CHARTERED ACCOUNTANT.

UGC- MAJOR RESEARCH PROJECT

"Investigations on excitons in nanostructures"

No. F. 42-836/2013(SR) dated 22.03.2013

Principal Investigator: Dr. Mrs. M. Arulmozhi
Associate Professor in Physics
Jayaraj Annapackiam College for Women (Autonomous)
Periyakulam - 625601. Theni District. Tamil Nadu.

STATEMENT OF EXPENDITURE FOR CONTINGENCY

Amount allocated by UGC: Rs. 1, 00,000/-

Amount sanctioned by UGC: Rs. 90,000 /-

Expenditure incurred: Rs. 1, 00,240/-

Amount to be sanctioned by UGC: Rs. 10, 000/-

S.No	Bill No.	Date	Particulars	Amount Rs.
1.	---	06.04.2013	A4 paper and Xerox	1,706/-
2.	---	10.04.2013	Postal charge	22/-
3.	---	10.04.2013	Postal charge	22/-
4.	---	09.04.2013	Xerox	24/-
5.	---	08.04.2013	Xerox	44/-
6.	145	01.05.2013	Stationery	400/-
7.	---	19.04.2013	Xerox	64/-
8.	---	25.04.2013	Honorarium to External Subject Expert-UGC-MRP-Selection of Research Fellow	1,500/-
9.	154454/MDU	07.04.2013	Advertisement for UGC-MRP-Selection of Research Fellow	5,088/-
10.	55	25.04.2013	Other expenses for interview on UGC-MRP-Selection of Research Fellow	4,610/-
11.	---	16.08.2013	Postal charge	52/-
12.	---	29.04.2014	Xerox	310/-
13.	1207	07.05.2013	OHP Binding	75/-
14.	---	09.05.2013	Files	105/-
15.	---	12.05.2013	Stationery	190/-
16.	5236013	21.05.2014	Courier	40/-
17.	4106869	28.09.2013	Courier	30/-
18.	B14/33	29.08.2014	Stationery	680/-
19.	04544753	02.02.2014	Courier	15/-
20.	5395620	06.12.2014	Courier	25/-

21.	28	25.09.2014	Rubber Stamp	450/-
22.	85	24.01.2014	Flex printing	336/-
23.	8	28.01.2014	To attend the International Conference on "Nano Electronic Science & Technology" organized by Sri Vasavi College, Erode. Registration fee.	2,500/-
24.	---	17.07.2014	To attend the National Conference on "Optics, Photonics and Lasers" organized by Arul Anandar College, Karumathur. Registration fee	200/-
25.	454	04.05.2014	CD pouch and Pen drives	2,200/-
26.	1806	16.09.2014	Spiral Binding	60/-
27.	---	19.03.2014	Membership in ISCA	2,050/-
28.	---	21.08.2014	Stationery	1,979/-
29.	---	19.09.2014	To attend the National Seminar on "Recent Trends in Novel Materials for Technical Applications" organized by K.L.N. College of Engineering, Sivagangai. Registration fee.	150/-
30.	741401	13.08.2014	To attend the workshop on "Research Methodology for Ph.D. Scholars" organized by M. T. W. University, Kodaikanal. Registration fee.	1,500/-
31.	5345538	30.09.2014	Courier	25/-
32.	1872	24.11.2014	OHP binding	180/-
33.	437	24.03.2014	Printer	12,500/-
34.	438	10.04.2014	Computer Maintenance	7,500/-
35.	473	06.05.2014	Accessories	5,540/-
36.	1863	29.10.2014	Letter pad	790/-
37.	1867	31.10.2014	OHP binding	90/-
38.	---	24.11.2014	Color Printing	282/-
39.	---	25.11.2014	Stationery	245/-
40.	---	24.01.2015	Xerox	50/-
41.	---	10.01.2015	Colour Printout	60/-
42.	---	10.01.2015	Colour Printout	80/-
43.	05463211	03.02.2015	Courier	25/-
44.	05463210	03.02.2015	Courier	25/-
45.	066	03.02.2015	To attend the International Conference on "Nanoscience and Nanotechnology" organized by SRM University. Registration fee for Principal Investigator	4,000/-
46.	067	03.02.2015	To attend the International Conference	3,000/-

			on "Nanoscience and Nanotechnology" organized by SRM University. Registration fee for Project Fellow.	
47.	---	13.02.2015	To attend the National Level Workshop on "Computational Physics Using Gaussian" organized by N.M.S.S.V.N. College, Madurai. Registration fee.	200/-
48.	---	20.02.2015	Pl Spectra	1,500/-
49.	94	25.02.2015	To attend the Workshop on "Materials Characterization Techniques"organized by Kalasalingam University, Krishnakoil. Registration fee.	2,100/-
50.	---	07.03.2015	SEM and EDAX	3,000/-
51.	194	25.03.2015	To attend the National Seminar on "Semiconductor Materials and Device processing for Energy Applications" organized by A.P.A College for Women, Palani. Registration fee.	200/-
52.	149	10.07.2015	OHP binding	150/-
53.	---	03.08.2015	To attend the National Workshop on "Research Practices in Mathematics and Computer Science" organized by J. A. College for Women, Periyakulam. Registration fee for Principal Investigator.	500/-
54.	---	03.08.2015	To attend the National Workshop on Research Practices in Mathematics and Computer Science organized by J. A. College for Women, Periyakulam. Registration fee for Project Fellow.	400/-
55.	230	03.09.2015	Spiral and OHP binding	60/-
56.	5596095	11.09.2015	Courier	30/-
57.	255	09.10.2015	OHP binding	30/-
58.	5606492	27.10.2015	Courier	30/-
59.	616478	26.10.2015	To attend the Workshop on "Physics in Engineering" organized by Thiagarajar College of Engineering, Madurai. Registration fee	1,850/-
60.	M14093530a15	30.10.2015	Internet recharge	299/-
61.	M59802023b15	23.11.2015	Internet recharge	299/-
62.	3925	05.12.2015	XRD Pattern	4,850/-
63.	---	15.12.2015	To attend the State Level Seminar on "Expanding Frontiers in Material	200/-

			Science on Physics in Engineering" organized by Arul Anandar College, Karumathur. Registration fee for Principal Investigator.	
64.	---	15.12.2015	To attend the State Level Seminar on Expanding Frontiers in Material Science on Physics in Engineering organized by Arul Anandar College, Karumathur. Registration fee for Project Fellow.	100/-
65.	362	18.12.2015	Chart binding	1,140/-
66.	MT03366719c5	19.12.2015	Internet recharge	299/-
67.	MT0371791416	23.11.2015	Internet recharge	299/-
68.	---	04.02.2016	To attend the National Conference on "Recent Trends in Physics & Materials Research" organized by J. A. College for Women, Periyakulam. Registration fee.	150/-
69.	1520208572	08.02.2016	Internet recharge	299/-
70.	---	20.02.2016	Postal charge	40/-
71.	440	25.02.2016	OHP binding	60/-
72.	---	29.02.2016	To attend the International Conference on "Recent Trends in Materials science and Applications" organized by Jamal Mohamed College, Tiruchirappalli. Registration fee.	3,150/-
73.	5674811	03.03.2016	Courier	30/-
74.	MT0095600436	04.03.2016	Internet recharge	399/-
75.	---	14.03.2016	Paper publication charge for a Paper on ñA Comparative study on the properties of ZnO and Zns nanoparticlesò in International Journal of Chemtech Research.	2,770/-
76.	106	31.03.2016	To attend the International Conference on "Innovations in science and Technology" organized by Sriguru Institute of Technology, Coimbatore. Registration fee.	2,000/-
77.	MT0120020246	02.04.2016	Internet recharge	399/-
78.	1793615883	07.06.2016	Internet recharge	299/-
79.	1845175885	28.06.2016	Internet recharge	299/-
80.	5768062	12.07.2016	Courier	30/-
81.	622	21.07.2016	OHP binding	210/-

82.	005793783	04.08.2016	Courier	30/-
83.	005793798	08.08.2016	Courier	50/-
84.	---	08.08.2016	Paper publication charge for a Paper on "Effect of temperature on exciton binding energy in Znse/ZnMgSe quantum well with Poschl-Teller Potential" in International Journal of Chemtech Research	2,100/-
85.	---	24.08.2016	Paper publication charge for a Paper on "A Comparative analysis of the properties of ZnO nanoparticles Synthesised by hydrothermal and sol-gel methods" in Indian Journal of Science and Technology.	8,550/-
86.	---	26.09.2016	To attend the International Workshop on "Physics in Engineering" organized by Thiagarajar College of Engineering, Madurai. Registration fee for Principal Investigator.	250/-
87.	---	26.09.2016	To attend the International Workshop on "Physics in Engineering" organized by Thiagarajar College of Engineering, Madurai. Registration fee for Project Fellow.	250/-
88.	5866343	18.10.2016	Courier	30/-
89.	833	03.01.2017	Chart binding	490/-
Total				**Rs. 1,00,240/-**

M. Arulmozhi

PRINCIPAL INVESTIGATOR

Dr.Mrs. M. ARULMOZHI
Principal Investigator-UGC MRP
Associate Professor in Physics
Jayaraj Annapackiam College-
for Women (Autonomous)
Periyakulam 625 601, Theni (Dt)

PRINCIPAL

Jayaraj Annapackiam College
for Women (Autonomous)
Thamaraikulam. Periyakulam-625 601.
Theni District Tamilnadu.

STATUTORY AUDITOR

P. RAMALINGAM, B.Sc., F.C.A. CHARTERED ACCOUNTANT
M.No : 18516
PH : 2430391
57, PANDIAN NAGAR,
DINDIGUL - 1.

P. RAMALINGAM
CHARTERED ACCOUNTANT.

UGC- MAJOR RESEARCH PROJECT

"Investigations on excitons in nanostructures"

No. F. 42-836/2013(SR) dated 22.03.2013

Principal Investigator: Dr. Mrs. M. Arulmozhi
Associate Professor in Physics
Jayaraj Annapackiam College for Women (Autonomous)
Periyakulam - 625601. Theni District. Tamil Nadu.

STATEMENT OF EXPENDITURE FOR TRAVEL/FIELD WORK

Amount allocated by UGC: Rs. 1, 00,000/-

Amount sanctioned by UGC: Rs. 90,000 /-

Expenditure incurred: Rs. 1,00,973/-

Amount to be sanctioned by UGC: Rs. 10, 000/-

S.No	Bill No.	Bill Date	Particulars	Mode of Journey	Amount Rs
1.	5621	14.04.2013	The American College, Madurai.	Taxi	1,800/-
2.	5622	28.05.2013	SFR College for Women, Sivakasi.	Taxi	2,800/-
3.	22848	29.10.2013	Thiagarajar College (Autonomous), Madurai.	Taxi	1,800/-
4.	22851	05.12.2013	Arul Anandar College (Autonomous), Madurai.	Taxi	1,800/-
5.	SF291707 856635	14.12.2013	Loyola College, Chennai	Bus & Taxi	2,500/-
6.	---	15.02.2014	Sri Vasavi College, Erode.	Bus & Auto	1,000/-
7.	---	12.04.2014	Fatima College (Autonomous), Madurai.	Taxi	1,800/-
8.	---	21.04.2014	Arul Anandar College (Autonomous), Madurai.	Taxi	1,800/-
9.	---	17.07.2014	Mother Teresa Women's University, Kodaikanal.	Taxi	2,500/-

10.	---	18.07.2014	Meenakshi Govt. Arts College (Autonomous), Madurai.	Taxi	2,000/-
11.	---	04.09.2014	Govt. Arts College, Melur.	Taxi	2,000/-
12.	---	14.09.2014	Arul Anandar College (Autonomous), Madurai.	Taxi	1,800/-
13.	---	18.09.2014	K.L.N. College of Engineering, Sivagangai.	Taxi	3,800/-
14.	---	21.09.2014	SFR College for Women, Sivakasi.	Taxi	2,800/-
15.	KCKTIA & KCKVPZ	01.10.2014 & 04.10.2014	IMSc, Chennai.	Bus & Taxi	4,500/-
16.	22832	03.11.2014	The American College, Madurai.	Taxi	2,000/-
17.	22900	19.11.2014	NMSSVN College, Madurai.	Taxi	2,000/-
18.	---	20.11.2014	The American College, Madurai.	Taxi	2,000/-
19.	---	05.12.2014	Alagappa University, Karaikudi.	Taxi	4,500/-
20.	TATECG 967281 & TS-MMT1174 9685UKQ	26.12.2014 & 28.10.2014	IMSc, Chennai.	Bus & Auto	3,000/-
21.	28	02.01.2015	The American College, Madurai.	Taxi	2,000/-
22.	---	14.01.2015	UGC, New Delhi.	Flight & Taxi	26,059/-
23.	TH2E569 99567 & TH2E383 95865	03.02.2015 & 06.02.2015	SRM University, Chennai.	Bus & Taxi	5,880/-
24.	---	13.02.2015	N.M.S.S.V.N College, Madurai.	Taxi	1,500/-
25.	---	25.02.2015	Kalasalingam University, Krishnankoil	Taxi	3,500/-

26.	---	28.07.2015	Mangayarkarasi College of Arts and Science, Madurai.	Taxi	2,000/-
27.	THAR797 24846 & THAR426 46874	01.10.2015 & 04.10.2015	Sathyabama University, Chennai	Bus & Taxi	5,334/-
28.	010576 & TATFAK LT3755	20.10.2015 & 22.10.2015	Loyola College, Chennai	Bus & Taxi	4,500/-
29.	72471	05.11.2015	Thiagarajar Engineering College, Madurai	Taxi	2,000/-
Total					**Rs. 1,00,973/-**

M. Arulmozhi

PRINCIPAL INVESTIGATOR

Dr.Mrs. M. ARULMOZHI
Principal Investigator-UGC MRP
Associate Professor in Physics
Jayaraj Annapackiam College-
for Women (Autonomous)
Periyakulam - 625 601, Theni (Dt)

PRINCIPAL

Jayaraj Annapackiam College
for women [Autonomous]
Periyakulam - 625 601.
Theni District.

STATUTORY AUDITOR

P. RAMALINGAM, B.Sc., F.C.A., CHARTERED ACCOUNTANT
M.No: 19516
PH: 2430391
57, PANDIAN -NAGAR,
DINDIGUL - 1.

P. RAMALINGAM
CHARTERED ACCOUNTANT.

UGC- MAJOR RESEARCH PROJECT

"Investigations on excitons in nanostructures"

No. F. 42-836/2013(SR) dated 22.03.2013

Principal Investigator: Dr. Mrs. M. Arulmozhi
Associate Professor in Physics
Jayaraj Annapackiam College for Women (Autonomous)
Periyakulam - 625601. Theni District. Tamil Nadu.

STATEMENT OF EXPENDITURE FOR OVERHEAD CHARGES

Amount allocated by UGC: Rs.72,800/-

Amount sanctioned by UGC: Rs.72,800/-

Expenditure incurred: Rs.72,800/-

S.No.	Date	Head of the Institution	Amount (Rs.)
1.	29.04.2013	The Principal, Jayaraj Annapackiam College for Women (Autonomous), Periyakulam - 625601. Theni District. Tamil Nadu.	**Rs. 72, 800/-**

M. Arulmozhi

PRINCIPAL INVESTIGATOR

Dr.Mrs. M. ARULMOZHI
Principal Investigator-UGC MRP
Associate Professor in Physics
Jayaraj Annapackiam College-
for Women (Autonomous)
Periyakulam - 625 601, Theni (Dt)

PRINCIPAL

Jayaraj Annapackiam College
for women [Autonomous]
Periyakulam - 625 601.
Theni District.

STATUTORY AUDITOR

P. RAMALINGAM, B.Sc., F.C.A., CHARTERED ACCOUNTANT
M.No : 19516
PH : 2430391
57, PANDIAN -NAGAR,
DINDIGUL - 1.

P. RAMALINGAM
CHARTERED ACCOUNTANT.

Annexure - IX

ज्ञान-विज्ञान विमुक्तये

UNIVERSITY GRANTS COMMISSION

BAHADUR SHAH ZAFAR MARG

NEW DELHI – 110 002.

FINAL REPORT OF THE WORK DONE ON UGC - MAJOR RESEARCH PROJECT

1.	Name and address of the Principal Investigator	: **Dr. Mrs. M. Arulmozhi** **Associate Professor** **Department of Physics** **Jayaraj Annapackiam College for Women (Autonomous)** **Periyakulam - 625601** **Theni District, Tamil Nadu, India**
2.	Name and address of the Institution	: **Jayaraj Annapackiam College for Women (Autonomous)** **Periyakulam - 625601** **Theni District, Tamil Nadu, India**
3.	UGC approval letter No. and date	: **No. F. 42-836/2013 (SR) dated 22.03.2013**
4.	Date of implementation	: **03.05.2013**
5.	Tenure of the project	: **3 years + 1 year Extension (01.04.2013 to 31.03.2017)**
6.	Total grant allocated	: **₹ 12,82,480**

Annexure - IX

7. Total grant received : **₹ 11,96,512**

8. Final expenditure : **₹ 12,84,041**

9. Title of the project : **Investigations on excitons in nanostructures**

10. Objectives of the project : **Kindly refer Appendix - I**

11. Whether the objectives were achieved : **Yes**

12. Achievements from the project : **Kindly refer Appendix - II**

13. Summary of the findings : **Kindly refer Appendix - III**

14. Contribution to the society : **Kindly refer Appendix - IV**

15. Whether any Ph.D enrolled/produced : **Yes, Kindly refer Appendix - V**

16. No. of publications out of the project : **Kindly refer Appendix - VI**

M. Arulmozhi

PRINCIPAL INVESTIGATOR

Dr.Mrs. M. ARULMOZHI
Principal Investigator-UGC MRP
Associate Professor in Physics
Jayaraj Annapackiam College-
for Women (Autonomous)
Periyakulam - 625 601, Theni (Dt)

PRINCIPAL

Jayaraj Annapackiam College
for women [Autonomous]
Periyakulam - 625 601.
Theni District.

APPENDIX-I

Appendix-I

OBJECTIVES OF THE PROJECT

General Objectives

The main of this project is to investigate the behaviour of excitons in nanostructures of materials with potential applications under the influence of external fields in close interaction with experiments in this field of research and to develop and study the structural and optical properties of nanomaterials, experimentally.

Specific Objectives

The proposed project would focus its attention on the following objectives.

- To calculate the energy levels of a free electron, light hole and heavy hole at the bottom of the conduction band of the nanostructures.
- To determine the ground state energy of an exciton in the nanostructures.
- To study the light hole and heavy hole exciton binding energies in the nanostructures as a function of the size of the nanostructures.
- To analyse the behaviour of the binding energy of an exciton in nanostructures made of different materials.
- To study the behaviour of excitons under the influence of external perturbations in all the above nanostructures.
- To investigate the possibility of incorporating some of the theoretical results into experimental situations.
- To develop nanostructures experimentally and study their structural and optical properties.

Methodology

- The ground quantized energy level for the electron, light hole and heavy hole in the nanostructures will be determined variationally.

Appendix-I

- The ground state of a light hole and heavy hole excitons in nanostructures will be determined variationally by minimizing the appropriate Hamiltonian using the appropriate trial function.
- Ground state exciton binding energy in nanostructures will be calculated from the above, for various sizes of the nanostructures and the results will be analysed.
- Effect of eternal perturbations on the behaviour of the excitons will be studied by incorporating relevant terms in the expressions.
- Behaviour of excitons will be studied for various nanomaterials.
- All numerical calculations and required iterations will be made by numerical methods and by using the computer symbolic software (Mathematica) to be installed in the computer
- Structural and optical properties of the nanomaterials will be studied experimentally by XRD, UV and FTIR studies.

APPENDIX-II

Appendix-II

ACHIEVEMENTS FROM THE PROJECT

Ph.D enrolment

- The Project Fellow working under the major research project has registered for Ph.D.

Publication

- Eight research articles have been published in reputed peer-reviewed journals, one research article is in review and one research articles is submitted and the list of research papers are given in Appendix-VI.
- Three research articles have been published in proceedings of National Conferences and the list is also given in Appendix-VI.

Paper Presentations in Conference/Seminar/Workshop

- "**Theoretical investigations on the properties of quantum nanostructures dependent on density of states**" at the International Conference on 'Nano Electronic Science and Technology (ICNEST-2014)', organised by Post Graduate & Research Department of Electronics, Sri Vasavi College (Self finance wing), Erode on 14th - 15th February 2014.
- "**Magnetic field effects on the exciton binding energy in a near triangular quantum well**" in 3rd International Conference on 'Nanoscience and Nanotechnology (ICONN 2015)' organised by Department of Physics and Nanotechnology, SRM University during 4th - 6th February 2015 in association with Shizuoka University, Japan and Institute of Geological and Nuclear Sciences, New Zealand.
- "**Mathematical modelling of novel potential profile and associated energy levels by variational method**" in UGC sponsored National workshop on 'Research Practices in Mathematics and Computer Science' organised by the Research Center of Mathematics, Jayaraj Annapackiam College for Women (Autonomous), Periyakulam - 625 601, Tamil Nadu, on 3rd & 4th August, 2015.

Appendix-II

- "**Simultaneous effect of temperature, pressure and magnetic field on subband energy on NTQW** " in State Level Seminar on 'Expanding Frontiers in Material Science' held on 15th December 2015 at Arul Anandar College (Autonomous), Karumathur - 625 512, Madurai District, Tamil Nadu.
- "**Sub-band energies of electron, heavy hole and light hole in surface quantum well with applied electric field**" in UGC sponsored National conference on 'Recent Trends in Physics & Material Research' on 4th & 5th February 2016 at Jayaraj Annapackiam College for Women (Autonomous), Periyakulam - 625 601, Tamil Nadu.
- "**Exciton binding energy in surface quantum well under magnetic field**" in International conference on 'Recent Trends Material Science and Applications (ICRTMSA-2016)' held on 29th February 2016 Organized by the PG and Research Department of Physics, Jamal Mohamed College (Autonomous), Tiruchirappalli - 620 020, Tamil Nadu.
- "**Effect of temperature on exciton binding energy in $ZnSe/Zn_{1-x}Mg_xSe$ quantum well with Poschl-Teller potential**" in International Conference on 'Innovations in Science and Technology (ICIST' 2016)' during 31st March and 1st April 2016 at Sriguru Institute of Technology, Coimbatore - 641110, Tamil Nadu.

Appendix-II

Manpower trained

- The Following Four M.Sc students have done their project work under this Major Research Project

S.No	Name	Title of the Project	Year
1.	K. Santhiya	Theoretical investigations on properties of quantum nanostructures dependent on density of states	2014
2.	S. Preethi	Theoretical Studies on properties of nanostructured material dependent on grain size	2014
3.	A. Menaka	Synthesis and characterization of ZnS semiconducting nanoparticles	2015
4.	D. Panchavarnam	Synthesis, characterization and optical properties of Zinc Oxide nanoparticles	2015

- Three M.Phil Scholars have done their dissertation work under this Major Research Project as follows.

S.No	Name	Title of the M.Phil dissertation	Year
1.	S. Preethi	A comparative analysis of structural and optical properties of ZnO nanparticles prepared by hydrothermal and sol-gel method	2015
2.	K. Santhiya	Effect of dielectric constant mismatch on exciton binding energies in a corner of CdTe/CdMnTe	2016
3.	P. Sathiyajothi	Effect of temperature on exciton binding energy in ZnSe/ $Zn_{1-x}Mg_xSe$ quantum well with Poschl-Teller Potential	2016

APPENDIX-III

Appendix-III

SUMMARY OF THE FINDINGS

1. The properties of quantum nanostructures dependent on density of states

The project started with basic studies and literature survey of quantum nanostructures. First, we have performed the calculations on density of states (DOS) in bulk (3D), quantum wire (2D) and quantum well (1D) with different confinement length. Then the properties of quantum nanostructures such as Specific heat capacity, Susceptibility, Carrier concentration and Energy gap have been investigated theoretically as a function of DOS. The results show that the DOS in all quantum nanostructures increases with confinement length. The DOS in bulk material is more than that of quantum well, and it is more than that of quantum wire, which implies that the DOS strongly depends on the dimension of the material. Further investigations on the properties of quantum nanostructures confirm that, both specific heat capacity and susceptibility of a nanostructured material increases with the DOS of the material, but the variation is small between bulk, quantum well and quantum wire. The energy gap and carrier concentration of a nanostructure decreases with DOS for all dimensions and they are sensitive to the dimension of the nanostructure. Theoretical results agree well with the experimental data available in the literature and confirm the influence of DOS on various important properties of materials.

2. The properties of quantum nanostructures dependent on grain size

In this work, mechanical properties like yield strength and strain rate, thermal property like melting point and optical property like refractive index of nanostructured materials are calculated as a function of grain size for various dimensions. When the grain size decreases, yield strength increases due to the increase in grain boundaries, blocking dislocation movement. There is a significant decrease in the slope for small grain sizes. The yield strength plateaus below a critical grain size (å 60nm). The yield strength of quantum wire is more than that of quantum well, and less than that of quantum dot. The strain rate of the nanostructured material increases, when the grain size decreases. The strain rate, at which the grain-boundary diffusion processes become important (0.001s-1), corresponds to grain sizes less than 20nm. As the grain size decreases, the melting point of the material also decreases. Changes in melting point occur because nanoscale materials have a much larger surface-to-volume than bulk materials, drastically altering their thermodynamic and thermal properties. There is a sudden decrease in the melting point at a critical grain size å 40nm. Beyond the grain size of 60 nm, the melting point is nearly a constant. The refractive index is directly proportional to the grain size. Hence light propagation becomes faster as the grain size decreases. Optical properties change at nanoscale level because the nanoparticles are so small that electrons in them are not as much free to move as in the case of bulk material. Due to this restricted movement of electrons, nanoparticles react differently with light as compared to bulk material.

3. Excitons in a Surface quantum well

Exciton binding energies in a Surface Quantum Well (SQW) composed of vacuum/GaAs/$Al_xGa_{1-x}As$ as a function of wellwidth are calculated with and without the effect of mass anisotropy and the effect of image charges which arises due to the large dielectric discontinuity at the vacuum/GaAs interface. The effect of non-parabolicity is considered by using an energy dependent effective mass.

The effect of image charges in a SQW is different from that in a symmetrical rectangular QW where the carriers experience repulsion by the image charges arising due to the polarization at both the interfaces and is compelled to be at the center of the QW. But in the SQW, they are repelled by the image charge at the single vacuum/GaAs interface only. Calculation of the average distances of the electron $\langle ?_{?} \rangle$ and the hole $\langle ?_{?} \rangle$ from the vacuum/GaAs interface, with and without image charges and the integrated probability of finding an electron and a hole inside the well show that the deadlayer in a SQW is smaller compared to semi-infinite solids.

4. Polarizability of exciton in Surface Quantum Well

Effect of electric field on binding energies of light hole and heavy hole exciton in Surface Quantum Well composed of vacuum/GaAs/$Ga_{1-x}Al_xAs$ are theoretically calculated as a function of wellwidth and Al composition. Effect of image charges arising due to the mismatch of the dielectric constant at the vacuum/GaAs interface is considered. Stark shift and Polarizability of exciton in this Surface Quantum well are also calculated for various strengths of electric field with different wellwidth confinement as well as Al concentration. The obtained results show that i) Exciton binding energy increases with increased applied electric field along the growth axis ii) Stark shift in exciton energy increases with increased electric field and Al composition, but decreases with increased wellwidth iii) Polarizability of exciton decreases when the electric field increased, but increases with increased wellwidth. Most of our results are contrary to those for other symmetrical wells and hence will provide a choice of the parameters of the well for electric field applications.

5. Excitonic susceptibity in near triangular quantum wells (NTQW)

Diamagnetic susceptibility and binding energy of lh exciton and hh-exciton in NTQW formed by GaAs/GaAlAs and ZnO/ZnMgO as a function of wellwidth and Al/Mg composition have been studied with different magnetic fields. The diamagnetic susceptibility and the binding energy increases when the applied magnetic field increases. Excitons in ZnO/ZnMgO quantum well have larger binding energy than in GaAs/GaAlAs quantum well which leads to higher stability of the exciton in this quantum well and enhancement of the performance of ZnO based excitonic devices. Diamagnetic susceptibility is larger in ZnO/ZnMgO quantum well than in GaAs/GaAlAs quantum well, which implies ZnO to be more promising for magnetic field applications.

Appendix-III

6. Temperature effect on exciton binding energy in a QW with Pöschl-Teller potential

Binding energies of hh-exciton and lh-exciton in the presence of temperature in a $ZnSe/Zn_{1-x}Mg_xSe$ quantum well with P̣ schl-Teller (PT) potential are calculated variationally. Using the temperature dependent value of the effective mass and barrier height, the sub-band energies of the electron, heavy hole and light hole are calculated by variational method. Binding Energy of light hole exciton and heavy hole exciton are calculated as a function of the wellwidth for different temperatures. A maximum value of binding energy occurs at a critical well width (12 nm for hh-exciton and 10 nm for lh exciton), same for all values of temperature. For a fixed wellwidth, the binding energy decreases as temperature increases. For same wellwidth and temperature, the binding energy of hh-exciton is more than that of lh-exciton.

7. Simultaneous effects of pressure and temperature on excitons in a QW with Pöschl-Teller potential

The binding energy of hh and lh-exciton under the effects of pressure, temperature and asymmetry pattern of the PT quantum well composed of GaAs as a function of wellwidth have been studied by variational method. The following points are noted. i) Increase in the degree of asymmetry of the PT quantum well increases the binding energy of both excitons. ii) Both in symmetric and asymmetric cases, for $L \leq 20$ nm, lh-exciton binding energy increases with pressure upto 30 kbar and decreases for further increase in pressure. But for $L > 20$ nm, it increases with pressure continuously. iii) hh-exciton binding energy increases with pressure for all wellwidths (noted upto 80 kbar). iv) In the asymmetric case, for $L \leq (>)$ 20 nm, lh-exciton binding energy increases (decreases) with temperature. But in the symmetric case, the same behavior is observed for $L \leq 8$ nm. v) Similar behavior is observed for hh-exciton binding energy also, in asymmetric case for $L \leq 10$ nm and in symmetric case for $L \leq 8$ nm vi) Simultaneous effects of pressure, temperature and asymmetry pattern of PT quantum well lead to increased binding of both excitons. The values of pressure and temperature in semiconductor materials for the potential device applications must be properly chosen and our calculations give an idea of the choice of these values which will be surely useful in the preparation of semiconductor devices.

8. Properties of ZnO and ZnS nanoparticles synthesized by simple precipitation method

Zinc Oxide (ZnO) and Zinc Sulphide (ZnS) nanoparticles are successfully synthesized by simple precipitation method with various growth temperatures. The XRD patterns clearly indicate that ZnO and ZnS nanoparticles prepared with various growth temperatures have hexagonal structure, but the size of the particles vary with growth temperature. The band gaps are calculated from the UV-Visible absorption spectra for each sample. The functional groups are analysed by FTIR spectra. SEM images show that the ZnO nanoparticles have the morphology of spherical for 100^{o}C and 200^{o}C, sheets for 150^{o}C. The morphology of ZnS nanoparticles is cluster structure for the growth temperatures 100^{o}C and 150^{o}C, cluster of sheets for 200^{o}C. The conductivity of both ZnO and ZnS nanoparticles increases with the growth temperatures as well as concentration. Comparing the characterization studies, it is found that ZnO nanoparticles are more application oriented (i.e. more suitable for optoelectronic devices) than ZnS nanoparticles.

9. Properties of ZnO nanoparticles synthesized by Hydrothermal and Sol-Gel methods

ZnO nanopowders are synthesized by hydrothermal and sol-gel methods at different temperatures such as 100^{o}C, 150^{o}C and 200^{o}C for 2hrs. In both the methods, the mean crystal size, calculated from XRD pattern, is found to be in the range 20-30 nm. The pattern confirmed the composition, crystallinity and the synthesized products are ZnO with high purity and the hexagonal phase. Crystallite size decreases as temperature increases. The peak in absorption spectra of the prepared ZnO nanoparticles shows a blue-shift comparatively larger than the bulk. When the temperature increases, the absorbance also increases and the band gap decreases. In hydrothermal method, the band gap is large (i.e) from 4.4-4.9 eV and hence it has large applications in solar field. ZnO nanoparticles synthesized by both the methods exhibit similar luminescence. SEM pictures reveal the morphology as near-spherical prismatic nanoparticles for hydrothermal method and as nanoflakes for sol-gel method. The EDAX analysis confirms the presence of ZnO only and no other elements is present. The maximum peak is obtained for Zinc. In both hydrothermal as well as sol-gel methods, a pure ZnO occurrence is obtained. The conductivity decreases with the growth temperature as well as the concentration of the ZnO samples by sol gel method. In contrast the conductivity of the sample prepared by hydrothermal method increases as the growth temperature increases, but decreases as the concentration increases.

10. Exciton binding energy in Pyramidal Quantum dot

The light hole and heavy hole exciton binding energies in an infinite pyramid quantum dot of GaAs have been investigated with even mirror boundary conditions with and without nonparabolicity of conduction band. The results implies that the exciton binding energy with nonparabolicity is larger than that of with parabolicity, hence crafting the conduction band of the quantum dot material as non-parabolic leads to enhanced binding energy. The individual and combined effects of Dielectric Screening Function (DSF) and Spatially Dependent Effective Mass (SDEM) on exciton binding energy in pyramid quantum dot are also studied and the results are as follows: (i) when the DSF is included, the binding energy of exciton increases (ii) when the SDEM is included, the binding energy of exciton decreases (iii) When DSF and SDEM are included, the binding energy becomes smaller than that with DSF and larger than that with SDEM. The variation of binding energy of exciton with respect to DSF and SDEM occurs only for strong confinement and it remains unchanged for large confinement i.e. above 5 nm. Hence the SDEM for exciton binding energies in a infinite pyramid quantum dot with suitable DSF will be more fascinating in the probe of inter-band quantum dot laser that employ optical transitions between valence and conduction bands.

APPENDIX-IV

Appendix-IV

CONTRIBUTION TO THE SOCIETY

Origin of the research problem

There has been an enormous interest in the study of the structural, electronic and optical properties of nanostructures, which has been motivated by desire to understand their fundamental properties as well as by the prospectus of their potential applications in opto-electronic devices. A variety of nanostructures like quantum wells, quantum wires and quantum dots with various cross-sections viz., Finite and infinite, surface, symmetric and asymmetric, Rectangular, Parabolic, Triangular and |z|2/3 have been fabricated at the nanoscale, using epitaxial growth techniques such Molecular beam epitaxy (MBE) and Metal-Organic Vapor Deposition (MOCVD) and their electronic properties are being investigated using several optical characterization techniques.

Unlike an excitation in a single atom or molecule, an exciton (electron-hole pair) can in general move through the solid like a particle. Excitonic recombination plays an important role in lasing emission processes even at room temperature. Excitons are the main mechanism for light emission in semiconductors at low temperature (when the characteristic thermal energy kT is less than the exciton binding energy), replacing the free electron-hole recombination at higher temperatures. Knowledge of the exciton binding energy is crucial to the interpretation of the photoluminescence spectra and photoluminescence excitation spectra, which are used to determine the electronic properties of heterostructures. An increase in the binding energy could be exploited to make efficient room temperature luminescent devices in the visible range.

The present work, in view of all these applications aimed at investigating the behaviour of excitons in different nanostructures made by materials of potential applications like $GaAs/Ga_{1-x}Al_xAs$, $GaN/Al_{0.3}Ga_{0.7}N$, $ZnS/Be_xZn_{1-x}S$, GaInNAs/GaAs etc, including the effect of various external perturbations like pressure, temperature, electric field, magnetic field etc, which bring out appreciable changes in their electrical and optical properties in close association with the ongoing experimental research.

Interdisciplinary relevance

- The size of nanomaterials is similar to that of most biological molecules and structures: therefore, nanomaterials can be useful for both in vivo and in vitro biomedical research and applications.

Appendix-IV

- All chemical synthesis can be understood in terms of nanotechnology, because of its ability to manufacture certain molecules.
- The most advanced nanotechnology projects related to energy are: storage, conversion, manufacturing improvements by reducing materials and process rates, energy saving and enhanced renewable energy sources.
- Current high-technology production processes are based on traditional top down strategies, where nanotechnology has already been introduced silently.
- An inevitable use of nanotechnology will be in heavy industry which helps to reduce the size of equipments used.
- Nanotechnology is already impacting the field of consumer goods, providing products with novel functions ranging from easy-to-clean to scratch-resistant.

Hence, this project work made an attempt to study the novel properties, phenomena and processes in nanomaterials, which find applications in different fields and hence significant in terms of interdisciplinary research.

Significance of the study

Studies of this kind will certainly be helpful in the understanding of Physics of nanostructures and the electronic and structural properties of semiconductor compounds which have given rise to very important technological advances in high speed electronic devices. This study will also provide a motivation for pure scientific interest for the study of nanostructures as well as potential device applications such as photodetectors, phototransistor and solar cells.

Its potential contribution to knowledge in the field of social relevance or national importance

With nanotechnology, a large set of materials and improved products rely on a change in the physical properties when the feature sizes are shrunk. Nanoparticles take advantage of their dramatically increased surface area to volume ratio. Their optical properties, e.g. fluorescence, become a function of the particle diameter.

When brought into a bulk material, nanoparticles can strongly influence the mechanical properties of the material, like stiffness or elasticity. For example, traditional polymers can be reinforced by nanoparticles resulting in novel materials which can be used as lightweight replacements for metals. Therefore, an increasing societal benefit of such nanoparticles can be expected. Such nanotechnologically enhanced material will enable a weight reduction accompanied by an increase in stability and an improved functionality.

APPENDIX-V

Appendix-V

Ph.D ENROLLED

Name of the candidate	**: A. Anitha**
Topic	**: Studies on Excitons in Low Dimensional Nanostructures with Varied Profiles**
Registration No. and Date	**: PHDPHY2014F312**
University where the candidate registered for Ph.D	**: Mother Teresa Women's University, Kodaikanal-624601, Tamil Nadu, India.**
Institution where the Candidate carried out the research	**: Research Center of Physics, Jayaraj Annapackiam College for Women (Autonomous), Periyakulam- 625 601, Tamil Nadu, India.**

Ph: 04542-245671

MOTHER TERESA WOMEN'S UNIVERSITY, KODAIKANAL

Dr.K.Rethi Devi
Dean Research
E-mail: deanresearchmtwu@gmail.com

Reg.No.PHDPHY2014F312/ WU/Dean/Ph.D/2014/dated 09.07.2014

Sub: Application of **Ms.A.Anitha,** registration for **Ph.D (Full – Time) scholar in Physics** and Provisional Registration – intimation– sent – reg.

*****

Ms. A.Anitha, M.Phil, has been provisionally registered for Ph.D degree in Physics **(Full -Time)** under Dr.Mrs.Arulmozhi, Associate Professor in Physics, Jayaraj Annapackiam College for Women (Autonomous), Periyakulam, Theni.

Duration	:	The candidate is required to work for a **minimum period of 2 years and maximum period of 5 years** from the date of registration.
Date of Provisional Registration	:	09.07.2014
Topic	:	**" Studies on Excitons in Low Dimensional Nanostructures with Varied Profiles ".**

K. Rethi Devi
9/7/14
DEAN-RESEARCH

DEAN - RESEARCH
Mother Terasa Women's University
Kodaikanal-624 101.

To
Ms.A.Anitha,
D/o.V.Ayyappan,
3-9-29, Perumal Koil Street,
Lakshmipuram,
Theni – 625 523
M: 9843661212

Copy to
The Supervisor,
File
HOD

APPENDIX-VI

Appendix-VI

LIST OF PUBLICATIONS

Papers published in journals

1. A. Anitha and M. Arulmozhi, Theoretical Investigations on the properties of quantum nanostructures dependent on density of states, Journal of NanoScience and NanoTechnology, **2**(1), February 2014, Pp 83-86, ISSN: 2279-0381.
2. M. Arulmozhi and A. Anitha, Excitons in a surface quantum well, Superlattices and Microstructures, **75**, 2014, Pp 222-232, ISSN: 0749-6036.
3. A. Anitha and M. Arulmozhi, Magnetic field effects on the exciton binding energy in a near triangular quantum well, International Journal of ChemTech Research, **7(**3), 2015, Pp 1438-1444, ISSN: 0974-4290.
4. A. Anitha and M. Arulmozhi, Excitonic susceptibility in near triangular quantum wells, Indian Journal of Physics, **91**(3), 2017, Pp.287-292, DOI:10.1007/s12648-016-0924-8, ISSN: 0973-1458.
5. D. Panchavarnam, S. Menaka, A. Anitha and M. Arulmozhi, A comparative study on the properties of ZnO and ZnS nanoparticles, International Journal of ChemTech Research, **9(**3), 2016, Pp 308-315, ISSN: 0974-4290.
6. P. Sathiyajothi, A. Anitha and M. Arulmozhi, Effect of temperature on exciton binding energy in $ZnSe/Zn_{1-x}Mg_xSe$ quantum well with P schl-Teller potential, International Journal of ChemTech Research, **9(**8), 2016, Pp 298-304, ISSN: 0974-4290.
7. S. Preethi, A. Anitha and M. Arulmozhi, A comparative analysis of the properties of Zinc Oxide (ZnO) nanoparticles synthesized by hydrothermal and sol-gel methods, Indian Journal of Science and Technology, **9**(40), October 2016, Pp. 1-6, DOI: 10.17485/ijst/2016/v9i40/92696, ISSN: 0974-6846.
8. A. Anitha and M. Arulmozhi, Simultaneous effects of pressure and temperature on excitons in Pöschl-Teller quantum well, International Journal of Modern Physics B, 31(8),

2017, Pp. 1750050(1)-1750050(13), DOI: 10.1142/S0217979217500503, ISSN: 1793-6578.

9. A. Anitha and M. Arulmozhi, Polarizability of exciton in surface quantum well, Indian Journal of Pure and Applied Physics (In review).
10. A. Anitha and M. Arulmozhi, Exciton binding energy in Pyramidal Quantum dot, Indian Journal of Science and technology (Submitted).

Paper published in conference proceedings

1. S. Preethi, A. Anitha and M. Arulmozhi, Mechanical and thermal properties of nanostructured materials - A theoretical study, Proceedings of the UGC sponsored National Conference on "Latest Trends in Physics for interdisciplinary advancements" at Jayaraj Annapackiam College for Women (Autonomous), Periyakulam, 6th & 7th February 2014, Pp 39-42, ISBN: 978-81-923038-4-0.
2. A. Anitha and M. Arulmozhi, Mathematical modeling of novel potential profiles and associated energy levels by variational method, Proceedings of the UGC sponsored National Workshop on "Research Practices in Mathematics and Computer Science" at Jayaraj Annapackiam College for Women (Autonomous), Periyakulam, 3rd & 4th August 2015, Pp 40-42, ISBN: 978-81-923038-8-8.
3. A. Anitha and M. Arulmozhi, Sub-band energies of electron, heavy hole and light hole in surface quantum well with applied electric field, Proceedings of the UGC sponsored National Conference on "Recent Trends in Physics and Materials Research" at Jayaraj Annapackiam College for Women (Autonomous), Periyakulam, 4th & 5th February 2016, Pp 28-34, ISBN: 978-81-923038-9-5.

Copies of the Research Papers Published in Journals and Proceedings

Vol 2 | Issue 1 | Spring Edition | DOI : February 2014 | Pp 83-86 | ISSN 2279 – 0381

Knowledge is power
India Science Tech

Available at http://www.indiasciencetech.com

Journal of NanoScience and NanoTechnology

Theoretical Investigations on the Properties of Quantum Nanostructures dependent on Density of States

A. Anitha * [a] , M. Arulmozhi [b]

[a] Research Scholar, Jayaraj Annapackiam College for Women (Autonomous),Periyakulam, Tamil Nadu, India.

[b] Associate Professor in Physics, Jayaraj Annapackiam College for Women (Autonomous), Periyakulam, Tamil Nadu, India.

* e-mail id: anitha.jayarani@gmail.com

Keywords: Quantum well, quantum wire, Bulk material, density of states, specific heat, carrier concentration, paramagnetic susceptibility, energy gap.

Abstract: In solid-state and condensed matter physics, the density of states (DOS) of a system describes the number of states per interval of energy at each energy level that are available to be occupied by electrons. DOS $D(E_F)$ of conduction electrons are affected by the dimensionality of a material which influences some properties of the material. At low temperatures, there is a contribution to the specific heat of a conductor 'C_{el}' arising from the conduction electrons, and it depends on the electronic DOS at Fermi level as $C_{el}=(\pi^2 D(E_F)k_B^2T)/3$. Susceptibility of a magnetic material arising from the conduction electrons is given by $\chi_{el}=\mu_B^2 D(E_F)$. The carrier concentration in a semiconductor also depends on the DOS of electrons and holes respectively. The energy gap of a superconductor also depends on the D(E). Thus properties of almost all kinds of quantum nanostructured materials are affected by the DOS $D(E_F)$. The above properties are theoretically studied and discussed in this paper. The studies show new results which calls for further research and are in close agreement with the available experimental data.

Introduction

The subject of quantum nanostructures has emerged as a very fascinating area in condensed matter physics. The quantum nanostructures have a great potential for application in infrared detectors, quantum dot lasers, superconductivity, solar cells, single electron transistors and quantum computers. The conduction electron in nanostructures can be partially delocalized, depending on the shape and the dimensions of the structure. One limiting case is a quantum dot in which they are totally confined, and the other limiting case is a bulk material, in which they are all delocalized. The intermediate case are a quantum wire, which is long in one dimension and very small in its transverse direction; and a quantum well, which is a flat plate nanosized in thickness and much more larger in length and width. The quantum wire exhibits electron confinement in two dimensions and delocalization in one dimension, and the quantum well reverse these characteristics. Because of the dimensionality changes, DOS are strongly affected [1]. Some properties of nanostructured material like specific heat of solid, susceptibility of magnetic material, energy gap of superconductors, carrier concentration in semiconductor, are influenced by the changes in DOS.

The purpose of the present paper is to report the results on the properties of quantum nanostructures dependent on DOS for different dimensions.The above properties of nanostructured material are theoretically calculated for bulk (3D), quantum well (2D) and quantum wire (1D). Finally we compare the results between bulk, quantum wire and quantum well.

Model and Formulation

Density of States. The DOS for various dimensions of nanostructured materials are expressed as follows

$$D(E_F)_{3D} = \frac{2\sqrt{3}mL^2}{\pi\hbar} \quad (1)$$

$$D(E_F)_{2D} = \frac{mL^2}{\pi\hbar} \quad (2)$$

$$D(E_F)_{1D} = \frac{mL^2}{\pi^2\hbar^2} \quad (3)$$

Where, 'm' is the mass of the free-electron and 'L' is confinement length [1].

Journal of NanoScience and NanoTechnology | Vol 2 | Issue 1 | Spring Edition | ISSN 2279 – 0381

Specific Heat Capacity. When the temperature of a specimen is increased, the energy of the system is increased by ΔU [2]. Then the specific heat of the specimen is given by

$$C_{el} = D(E_F)\int_0^{\infty} dE\,(E - E_F)\frac{df(E)}{dT} \quad (4)$$

where, '$D(E_F)$' is DOS at Fermi energy level and 'T' is the temperature of the specimen. 'f (E') is Fermi-Dirac distribution is given as

$$f(E) = \frac{1}{e^{\frac{(E-E_F)}{k_BT}} + 1} \quad (5)$$

Eq. 5 is substituted in Eq. 4 and then the integration is evaluated, which gives the expression for electronic contribution to the Specific Heat of Solid as

$$C_{el} = \frac{\pi^2 D(E_F) k_B{}^2 T}{3} \quad (6)$$

Susceptibility. At absolute zero, the concentration of electrons with magnetic moment parallel to the magnetic field is

$$N_+ = \frac{1}{2}\int_{-\mu_B}^{E_F} dE\; D(E + \mu_B) \quad (7)$$

Similarly the concentration of electrons with magnetic moments antiparallel to the magnetic field is

$$N_- = \frac{1}{2}\int_{\mu_B}^{E_F} dE\; D(E - \mu_B) \quad (8)$$

The magnetization is given by

$$M = \mu\,(N_+ - N_-) \quad (9)$$

$$M = \mu^2 B D(E_F) \quad (10)$$

The paramagnetic susceptibility is expressed as $\chi_{el} = \frac{M}{B}$ [2].

$$\chi_{el} = \mu^2 D(E_F) \quad (11)$$

Carrier Concentration. The concentration of electrons in conduction band [2] is given by

$$n = \int_{E_c}^{\infty} D_e(E_F)\, f_e(E_F)\, dE_F \quad (12)$$

The Eq.12 is used to derive the expression for the concentration of electron in various dimensions as follows

$$n_{3D} = \frac{1}{4\pi^{\frac{3}{2}}}\left(\frac{2m_e}{\hbar^2}\right)^{\frac{3}{2}} e^{\left(\frac{E_F - E_c}{k_BT}\right)}(k_BT)^{\frac{3}{2}} \quad (13)$$

$$n_{2D} = \frac{m_e}{\pi\hbar^2} k_B T e^{\left(\frac{E_F - E_c}{k_BT}\right)} \quad (14)$$

$$n_{1D} = \frac{1}{\pi^{\frac{1}{2}}}\left(\frac{2m_e}{\hbar^2}\right)^{\frac{1}{2}} e^{\left(\frac{E_F - E_c}{k_BT}\right)}(k_BT)^{\frac{1}{2}} \quad (15)$$

Energy gap. Let us comparethe plane wave ψ(x)= e^{ikx} with modulated wave function $\varphi(x) = 2^{\frac{-1}{2}}\left[e^{i(k+q)x} + e^{ikx}\right]$.

The kinetic energy of the plane wave is $\frac{\hbar^2 k^2}{2m}$.Then the kinetic energy of the modulated wave is $\frac{\hbar^2 k^2}{2m} + \frac{\hbar^2 kq}{2m}$.where q is modulation wave vector. So the energy required to modulate the wave is $\frac{\hbar^2 kq}{2m}$. If $\frac{\hbar^2 kq}{2m} >$ E_g, the superconductivity will be destroyed [2].

$$E_g = \frac{\hbar^2 k_F q_0}{2m} \quad (16)$$

where, q_0 is the critical value of modulation wave vector. By substituting the value of k_F in Eq. 20 we get the expression of energy gap of superconductor for various dimensions as follows

$$E_{g1D} = \frac{\hbar^2 \pi E}{2mL} D(E_F) q_0 \quad (17)$$

$$E_{g2D} = \frac{\hbar^2\left(\pi^2 E D(E_F)\right)^{\frac{1}{2}}}{2mL} q_0 \quad (18)$$

$$E_{g3D} = \frac{\hbar^2 \pi^2 E}{2m^2 L^3} D(E_F) q_0 \quad (19)$$

Results and Discussion

First we have performed the calculation of Density of States $D(E_F)$ of bulk, quantum wire and quantum well with different values of confinement length 'L'. And then specific heat, susceptibility, carrier concentration and energy gap are calculated for various dimensions as a function of DOS.

Fig. 1 shows the DOS of bulk, quantum wire, quantum well as a function of 'L'. When the confinement length is increased, the DOS is also increased. The DOS of bulk material is more than that of quantum well, and it is more than that of quantum wire. So we can say the DOS which depends on the dimension of the material.

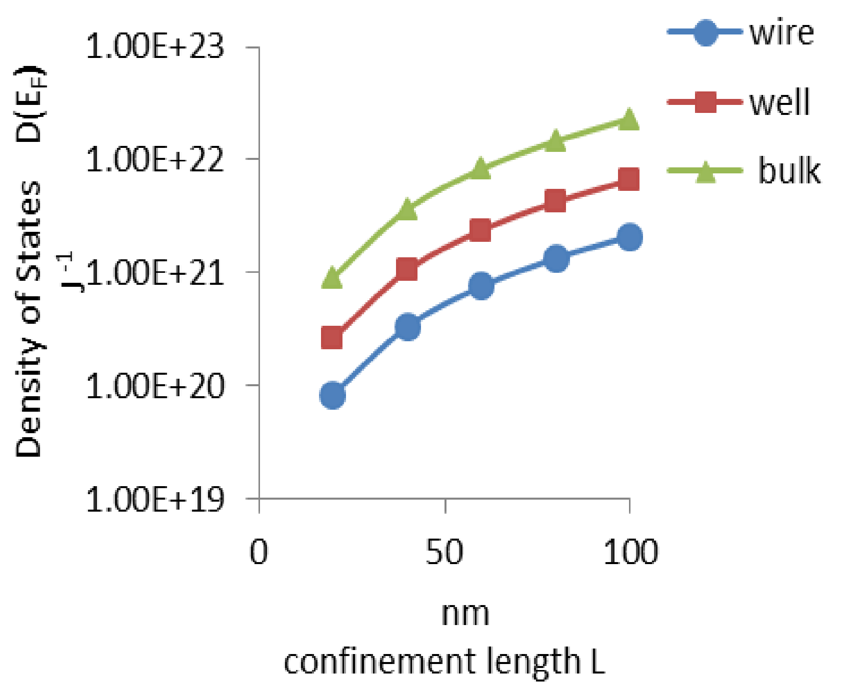

Fig.1 Variation of DOS with confinement length 'L'

Fig. 2 shows the specific heat C_{el} of nanostructured material for various dimensions as a function of DOS at 300K. If the DOS is increased, as expected the specific heat of the nanostructured material also increases with the

DOS of the material at the fixed value of the temperature.

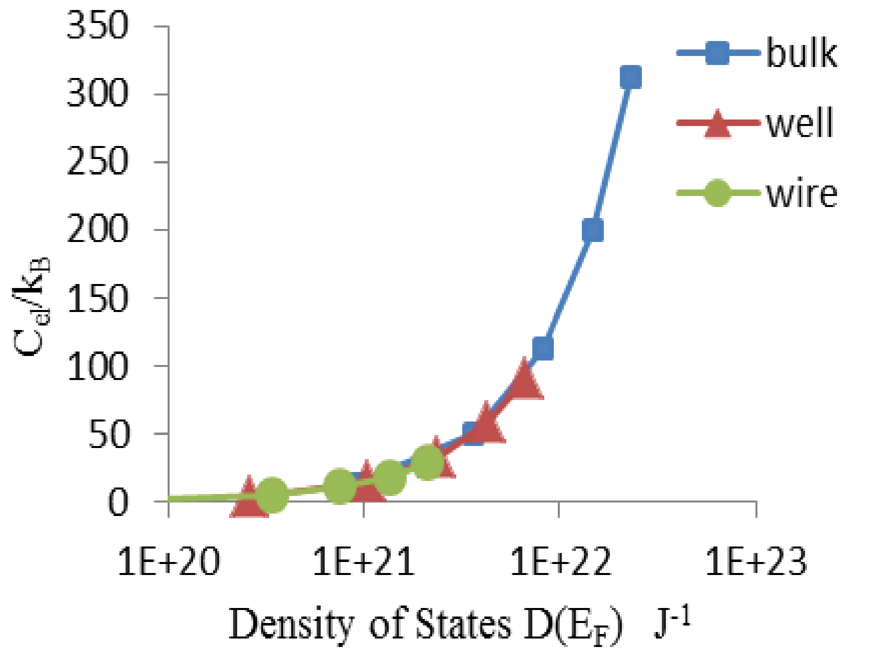

Fig.2 Variation of specific heat as a function of DOS at 300K

Fig. 3 shows the behavior of susceptibility of magnetic material as a function of DOS. Like the behavior of specific heat with DOS, the susceptibility of the magnetic material is increased, when the DOS is increased. But the variation is negligible between bulk, quantum well and quantum wire.

The specific heat and paramagnetic susceptibility are found to be less dependent on dimensionality effects, but more dependent on DOS.

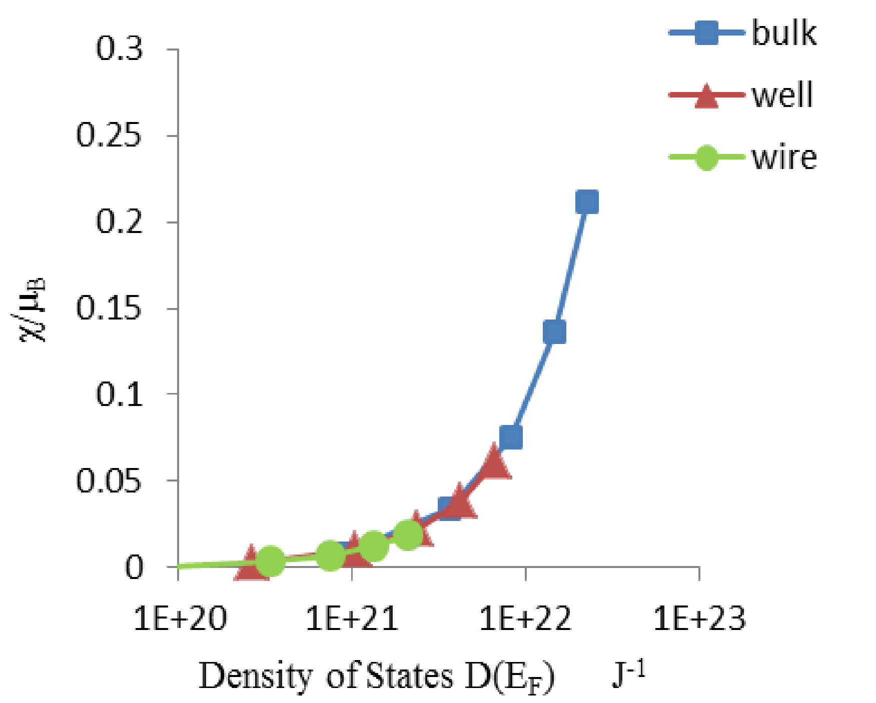

Fig. 3 Susceptibility Vs DOS

Fig. 4 shows the variation of energy gap of the superconductor as a function of DOS. If the DOS is increased, the energy gap is decreased for all dimensions.

The energy gap of bulk materials are more than that of quantum well and it is more than that of quantum wire. Here, q_0 is critical value of modulation wave vector which depends on the material, at this value the superconductivity will be destroyed.

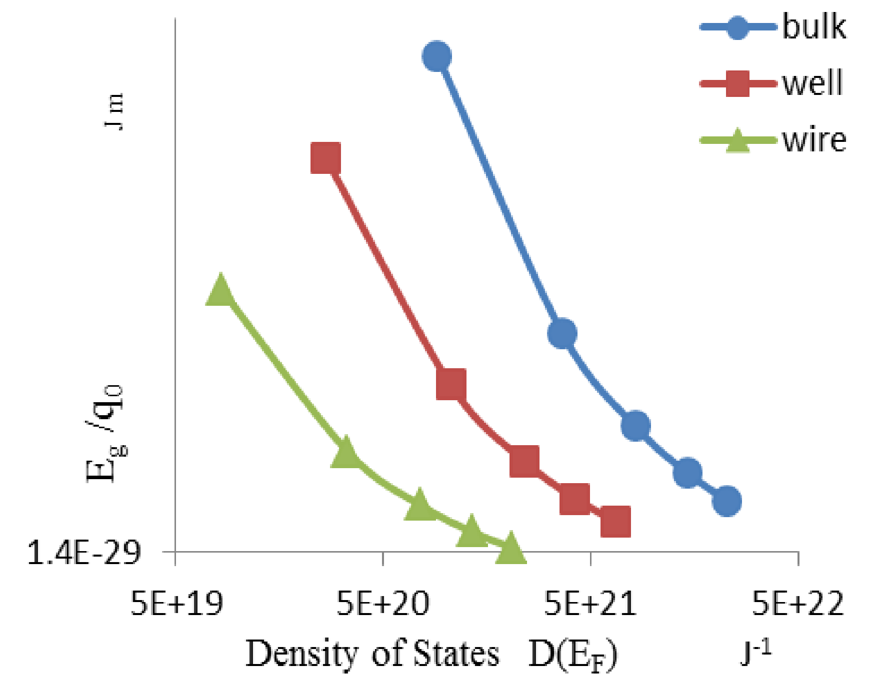

Fig.4 Behavior of energy gap as a function of DOS

Fig. 5 shows the variation of carrier concentration in intrinsic semiconductor. For all dimension the concentration of electron in semiconductor is decreased when the DOS is increased.

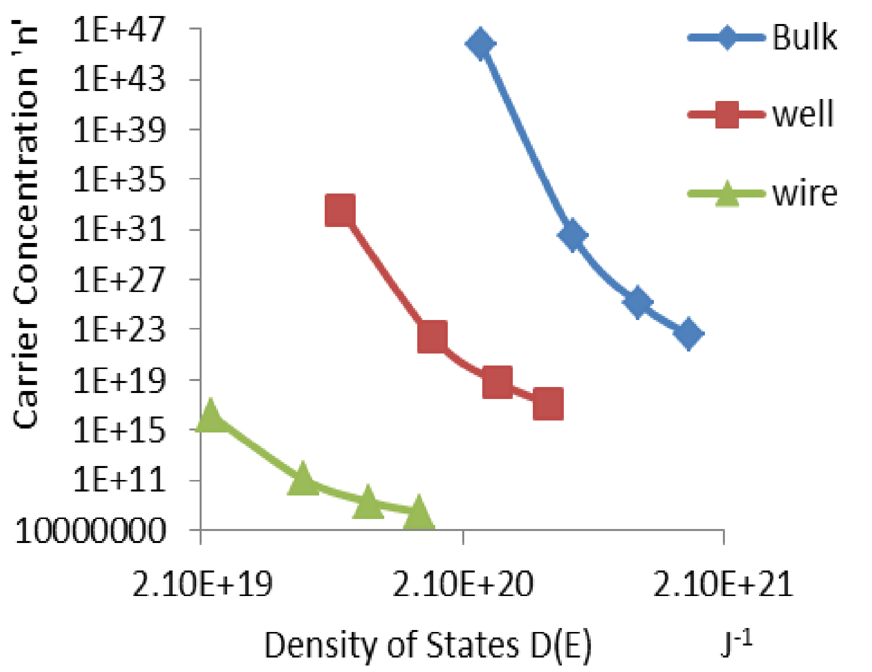

Fig. 5 Variation of electron concentration with DOS

Summary

Variation of Density of States with dimension of a material is studied. We have presented the behavior of specific heat of solid, susceptibility of magnetic material, energy gap of superconductivity and concentration electrons at conduction band in intrinsic semiconductors as a function of the DOS for bulk material, quantum well and quantum wire. The theoretical results agree well with the experimental data available in the literature and confirm the influence of DOS on various important properties of materials.

References

[1] Charles P. Poole, Jr., Frank J. Owens, Introduction to Nanotechnology, John Wiley & Sons, NewDelhi, 2006.

[2] Charles Kittel, Introduction to Solid State Physics, Seventh Edition, John Wiley & Sons, NewDelhi, 2007.

[3] Information on http://ecee.colorado.edu/~bart/book/chapter2/pdf/ch2_3_7.pdf

[4] Safa Kasap, Thermoelectric effects in metals, Special Custom published e-booklet (2001)

[5] Pallab Bhattacharya, Roberto Fornari, Hiroshi Kamimura, Comprehensive Semiconductor Science and Technology, Elsevier publications, (2011) pp.336-340.

[6] B. Boyacioglu, A. Chatterjee, Heat capacity and Entropy of GaAs quantum dot with gaussian confinement, J. Appl Phys., 8 (2012) pp. 112.

Superlattices and Microstructures 75 (2014) 222–232

Contents lists available at ScienceDirect

Superlattices and Microstructures

journal homepage: www.elsevier.com/locate/superlattices

Excitons in a surface quantum well

M. Arulmozhi *, A. Anitha

Department of Physics, Jayaraj Annapackiam College for Women (Autonomous), Periyakulam 625 601, Theni District, Tamilnadu, India

A R T I C L E I N F O

Article history:
Received 2 December 2013
Received in revised form 20 July 2014
Accepted 21 July 2014
Available online 1 August 2014

Keywords:
III–V Semiconductors
Quantum wells
Excitons and related phenomena

A B S T R A C T

Binding energies of excitons in a Surface Quantum Well (SQW) composed of vacuum/GaAs/$Al_xGa_{1-x}As$ as a function of wellwidth are calculated. The effect of non-parabolicity is considered by using an energy dependent effective mass. The effect of mass anisotropy and the effect of image charges which arise due to the large dielectric discontinuity at the vacuum/GaAs interface are also considered. The average distances of the electron $\langle z_e \rangle$ and the hole $\langle z_h \rangle$ from the vacuum/GaAs interface, with and without image charges and the integrated probability of finding an electron and a hole inside the well are also calculated. The results agree well with the available experimental data.

1. Introduction

Studies on thin crystalline films, surfaces and ultrathin multilayer heterostructures are of considerable interest for the past many years because of their technological importance [1] and also due to the possibility of many new effects [2–4] shown by these systems. Quantum wells (QW) with varied potential profiles have become possible with experimental techniques [5]. Many interesting features are noted in the behavior of excitons in such QW when compared to that in a bulk semiconductor [6].

Cen et al. [7] obtained appreciable correction to the binding of excitons in a symmetrical rectangular quantum well (RQW) formed by GaAs–AlAs and GaAs–ZnSe with and without an applied magnetic field along the growth axis. Mosko et al. [8] reported exciton binding energy in a vacuum barrier QW, <vacuum/GaAs/vacuum>. They showed that interface polarization is expected to repel the charge carriers causing a deadlayer near the interface. Photoluminescence at room temperature and

* Corresponding author.
E-mail addresses: arulpkm@yahoo.co.in (M. Arulmozhi), anitha.jayarani@gmail.com (A. Anitha).

http://dx.doi.org/10.1016/j.spmi.2014.07.027

cathodoluminescence studies of Muth et al. [9] showed a strong emission peak corresponding to the lowest bound state of the GaN surface quantum well and a correlation was made to the shift in surface quantum-well emission energy and the thickness of the GaN capping layer, which was varied from ~15 to 40 Å. Wang and Yang [10] studied the quantum dynamics of electrons in a surface quantum well in the time domain with autocorrelation of wave packet.

Quang et al. [11] presented the theory of an ad hoc mechanism for electron scattering in heavily-doped zinc oxide surface quantum wells and showed that the carriers must be extra scattered in the in-plane from roughness-induced fluctuations in the donor density. Niculescu and Eseanu [12] studied the exciton effects on the interband absorption spectra in near-surface square and semiparabolic quantum wells under intense laser field taking into account the correct dressing effect for the confinement potential and electrostatic self-energy due to the repulsive interaction between carriers and their image charges. Silkin et al. [13] studied low-energy plasmons in ultrathin films of silver in the thickness regimes where the surface states as well as quantum-well states must play significant roles. Gippius et al. [14] investigated the exciton transition and binding energies in near-surface InGaAs/GaAs quantum wells (NSQW) theoretically and experimentally by photoluminescence and photoluminescence excitation spectroscopy.

Diarra et al. [15] calculated the electronic states of donor and acceptor impurities in nanowires and showed that the ionization energy of the impurities is strongly enhanced with respect to the bulk, above all when the wires are embedded in a material with a low dielectric constant. Corfdir and Lefebvre [16] studied the influence of the surface and of the dielectric mismatch on the binding energy of donor atoms in GaN, ZnO and GaAs nanostructures and showed that due to the combination of these two effects, the binding energy does not monotonically decrease from the center to the surface. Tran Thoai et al. [17] calculated the binding energies of excitons in a finite barrier QW including the effects of image charges. Pierre et al. [18] measured a strong enhancement in the ionization energy of the dopant by the close proximity of materials with a different dielectric constant than the host semiconductor. Bjork et al. [19] demonstrated the deactivation of doping atoms in silicon nanostructures caused by a dielectric mismatch between the wire and its surroundings.

Experimental work of Parks et al. [20] in a SQW with structure vacuum/GaAs/$Al_xGa_{1-x}As$ showed the presence of states localized above the single quantum barrier in the $Al_xGa_{1-x}As$ layer. Their results showed a difference between the theoretical values and the experimentally measured transition energies obtained from the electromodulation spectra and this difference was attributed to the exciton binding energy. In this paper, an attempt is made to calculate the exciton binding energies in such a SQW using a variational approach. The effect of non-parabolicity on the transition energies, mass anisotropy and the role of image charges which arise due to the large difference in the dielectric constants on either side of the interface between vacuum and GaAs, in such a SQW are considered. A comparison is made with the experimental data and available results for potential wells of different shapes.

2. Theory

One-band effective mass and envelope function approximation is employed in the description of electrons and holes in semiconductor heterostructures.

2.1. Well states

The potential profiles for the electron and the hole in a SQW is taken to be of the form

$$V_i(z_i) = \begin{cases} \infty & z_i < 0 \\ 0 & 0 < z_i < L \\ V_{oi} & z_i > L \end{cases} \tag{1}$$

where V_{oi} is the barrier height (i stands for e or h for electron or hole, as the case may be). The values of the potential well heights V_{oe} and V_{oh} are determined as $0.65\Delta E_g$ and $0.35\Delta E_g$ [21] respectively, where the bandgap difference ΔE_g is related to the Al composition x [22] by

$$\Delta E_g = 1.155x + 0.37x^2 eV$$

L is the wellwidth and $z_i = z_e$ or z_h for the electron and the hole respectively. The wavefunctions for the electron and the hole states are of the form

$$\psi_i(z_i) = \begin{cases} 0 & z_i < 0 \\ A \sin \alpha_i z_i & 0 < z_i < L \\ Be^{-\beta_i z_i} & z_i > L \end{cases} \tag{2}$$

where A is a normalization constant and B is related to A through the continuity of ψ at $z_i = L$ as $B = Ae^{\beta_i L} \sin \alpha_i L$. The α's and β's are given by

$$\alpha_i = \sqrt{\frac{2m^* E_i}{\hbar^2}} \quad \text{and} \quad \beta_i = \sqrt{\frac{2m^*(V_{oi} - E_i)}{\hbar^2}} \tag{3}$$

where E_i is the well state energy ($i = e$ or h for electron or hole respectively), $m^* = m_e^*$ for the electron and $m_\pm^*$ for the holes. m_e^* is the effective mass of the conduction electron and $m_\pm^*$ is the heavy (+) or light (−) hole mass for motion along the z-direction.

The transcendental equation to be solved for the quantum well states is obtained by matching the wavefunction given in Eq. (2) and its first derivative at $z_i = L$, which is true when the effective mass mismatch between GaAs and $Ga_{1-x}Al_xAs$ is neglected. One gets after simplification and substitution for α_i and β_i,

$$\pm\left(\frac{E_i}{V_{oi}}\right)^{1/2} = \sin(\sqrt{E_i}L) \tag{4}$$

The transcendental equation for the electron states is obtained by including the non-parabolicity for the conduction band [23,24] by an expression for the energy dependent effective mass as

$$\pm\left(\frac{E_e}{V_{oe}}\right)^{1/2} = \sin\left[\left(\sqrt{\frac{m_e^*(E_e)E_e}{m_e^*}}\right)L\right] \tag{5}$$

The $m_e^*(E_e)$ is taken to be $m_e^*(E_e) = 0.0665\left(1 + \frac{0.0436E_e + 0.236E_e^2 - 0.147E_e^3}{0.0665}\right)$ where E_e is in eV.

2.2. Ground state of excitons

The Hamiltonian for an exciton in a SQW is given by

$$H = -\left[\frac{1}{\rho}\frac{\partial}{\partial \rho}\rho\frac{\partial}{\partial \rho} + \frac{1}{\rho^2}\frac{\partial^2}{\partial \phi^2}\right] - \frac{\mu_\pm^*}{m_e^*}\frac{\partial^2}{\partial z_e^2} - \frac{\mu_\pm^*}{m_\pm^*}\frac{\partial^2}{\partial z_h^2} + V_e(z_e) + V_h(z_h) - \frac{2}{r} \tag{6}$$

where $r = \sqrt{\rho^2 + |z_e - z_h|^2}$. The unit of energy is the effective Rydberg $R_\pm^* = \frac{\mu_\pm^* e^4}{2\hbar^2 \varepsilon_1^2}$ and the unit of length is the effective Bohr radius $a_\pm^* = \frac{\hbar^2 \varepsilon_1}{\mu_\pm^* e^2}$, where ε_1 is the dielectric constant of GaAs.

$\mu_\pm^*$ is the reduced effective mass of the hh exciton and the lh exciton. It is calculated, in the isotropic case, as $\frac{1}{\mu_\pm^*} = \frac{1}{m_e^*} + \frac{1}{m_\pm^*}$ and in the anisotropic case, using Kohn-Luttinger parameters [25], $\gamma_1 = 7.36$ and $\gamma_2 = 2.57$, as $\frac{1}{\mu_\pm^*} = \frac{1}{m_e^*} + \frac{1}{m_o}(\gamma_1 \pm \gamma_2)$ and $\frac{1}{m_\pm^*} = \frac{1}{m_o}(\gamma_1 \mp 2\gamma_2)$ where m_o is the free electron mass.

The potential profile is as given in Eq. (1). The trial wavefunction for the Wannier exciton (associated with the lowest electron and hole states) in the SQW is taken to be of the form

$$\psi = \begin{cases} 0 & z_e, z_h < 0 \\ A_2 \sin \alpha_e z_e \sin \alpha_h z_h e^{-ar} & 0 < z_e, z_h < L \\ B_2 e^{-\beta_e z_e} e^{-\beta_h z_h} e^{-ar} & z_e, z_h > L \end{cases} \tag{7}$$

where 'a' is a variational parameter and the α's and β's are as in Eq. (3). The continuity conditions at $z_e = L$ and $z_h = L$ give

$$B_2 = A_2 e^{\beta_e L} e^{\beta_h L} \sin \alpha_e L \sin \alpha_h L \tag{8}$$

leaving A_2 to be fixed by the normalization condition.

2.3. Effect of image charges

At the GaAs/Al_xGa_{1-x}As interface, we have neglected the effects due to the effective mass mismatch [14,26–28] and the dielectric constant mismatch [26–28] which are expected to be small, when we consider the binding energies. But image charges arises due to the large mismatch of the dielectric constant at the interface between vacuum and GaAs. Now the electron sees not only the hole but also its own image charge and that of the hole; similar is the case or the hole. Hence the Coulomb interaction between an electron and a hole is no longer isotropic. The image charge of an electron or a hole is expressed as [29]

$$q_i' = \frac{\varepsilon_1 - \varepsilon_2}{\varepsilon_1 + \varepsilon_2} q_i \tag{9}$$

where the dielectric constant in the GaAs well is ε_1 and that in vacuum is ε_2. $i = e$ for electron and h for hole. $q_e = -e$ and $q_h = e$.

Unlike the symmetrical wells, the dielectric constant mismatch is considered only at the single vacuum/GaAs interface in the SQW (the small mismatch at the GaAs/Al_xGa_{1-x}As interface is neglected). This leads to the formation of only one image each for the electron and the hole. The image potential hence has the simple form when compared to the image potentials used in other cases. For example in Ref. [8], a symmetrical vacuum barrier quantum well (vacuum/GaAs/vacuum) has been considered and for this case, there will be an infinite number of images and the image potential involves an infinite sum. In a similar fashion, Ref. [7] deals with the dielectric constant mismatch at the two interfaces in a rectangular quantum well. The image potential reduces to the expression used in our work when we consider a single interface. The additional potential in the Hamiltonian, when the image charge is considered, is given by

$$V_a = \frac{q_e q_h'}{\varepsilon_1 \sqrt{\rho^2 + (z_e + z_h)^2}} + \frac{q_e' q_h}{\varepsilon_1 \sqrt{\rho^2 + (z_e + z_h)^2}} + \frac{q_e q_e'}{\varepsilon_1 2 z_e} + \frac{q_h q_h'}{\varepsilon_1 2 z_h} \tag{10}$$

Taking the unit of energy as the effective Rydberg and the unit of length as the effective Bohr radius, the image potential now becomes

$$V_a = K \left[\frac{-4}{\sqrt{\rho^2 + (z_e + z_h)^2}} + \frac{1}{z_e} + \frac{1}{z_h} \right] \tag{11}$$

where $K = \frac{\varepsilon_1 - \varepsilon_2}{\varepsilon_1 + \varepsilon_2}$. The new Hamiltonian for the exciton is now given by

$$H_{image} = H + V_a \tag{12}$$

The exciton binding energy is determined by evaluating $\langle H_{image} \rangle$ and minimizing it w.r.t the variational parameter 'a' using the trial wavefunction given in Eq. (7). It is verified that the dielectric enhancement of electron and hole energy levels is very less for SQW (i.e., only the exciton energy levels are affected by the image charges and not the electron and hole energy levels). So only the value of the variational parameter 'a' will be different with and without the image charges. The binding energy of the exciton is now given by

$$B.E = E_e + E_h - \langle H_{image} \rangle_{\min} \tag{13}$$

The average distances of the electron $\langle z_e \rangle$ and the hole $\langle z_h \rangle$ from the vacuum/GaAs interface, with and without image charges, are also calculated, using the value of the variational parameter 'a' corresponding to $\langle H_{image} \rangle_{\min}$ and $\langle H \rangle_{\min}$ respectively as

$$\langle z_e \rangle = \frac{\int\int\int\int \psi^* z_e \psi dz_e dz_h \rho d\rho d\phi}{\int\int\int\int \psi^* \psi dz_e dz_h \rho d\rho d\phi}$$
$$\langle z_h \rangle = \frac{\int\int\int\int \psi^* z_h \psi dz_e dz_h \rho d\rho d\phi}{\int\int\int\int \psi^* \psi dz_e dz_h \rho d\rho d\phi} \tag{14}$$

where ψ is as given in Eq. (7). The integrated probability of finding an electron and a hole inside the well is calculated as

$$P = \int_0^{2\pi} \int_0^{L} \int_0^{\infty} \psi^* \psi \rho d\rho dz d\phi \tag{19}$$

The effect due to the effective mass mismatch is neglected, an effect which is expected to be small.

3. Results and discussion

Effective masses of electron (m_e^*), heavy hole (m_+^*) and electron (m_-^*); reduced masses of heavy hole exciton (μ_+^*) and light hole exciton (μ_-^*) calculated in the isotropic and anisotropic cases mentioned in Section 2.2; dielectric constants of GaAs (ε_1) and vacuum (ε_2) used in the calculations are given in Table 1.

The experimental samples used in Ref. [20] have the Al composition $x = 0.3$ and the wellwidth $L = 150$ Å, 400 Å and 1650 Å. The quantum well states for the electron and the hole are determined for various wellwidths by solving the transcendental Eq. (4). Taking $E_g(\text{GaAs}) = 1.5192$ eV, the transition energies between the hole levels in the valence band and the electron levels on the conduction band are calculated. It is found that there is a good agreement between our results and the experimental results reported by Parks et al. [20] for electron-*hh* transition energies. These values corresponding to the experimental samples are given in Table 2.

In Fig. 1, the variation of the binding energy of the ground state of a *hh* exciton and a *lh* exciton as a function of the wellwidth L, is displayed. The binding energy initially increases with the decrease of wellwidth until it reaches a maximum and then decreases quite rapidly. This behavior is similar for both the *hh* exciton and the *lh* exciton. The reason for this is that as L is reduced, the exciton wavefunction is compressed in the QW, leading to increased binding. However, beyond a certain value of L, the spread of the exciton wavefunction into the surrounding $Al_xGa_{1-x}As$ layer becomes more important. This makes the binding energy decrease as L is reduced further. Therefore, a turnover is observed in the binding energy of the exciton as the wellwidth is decreased. This behavior is similar to the case of finite QW of all shapes.

The correction for exciton binding energy applied by Parks et al. [20] for an agreement between their theoretical and experimental values of transition energies in SQW, as estimated by Nelson et al. [32], is very large compared to our results. But the wellwidth range is not the same in Parks et al. [20] and Nelson et al. [32]. The maximum value of the binding energy is also comparable with that in QWs of other shapes. Table 3 gives the comparative values in different QWs.

From Table 3, it is seen that the turnover in the binding energy in the case of SQW happens at a value of L greater than that in the case of RQW [31] and smaller than that in a $|z|^{2/3}$ [28] QW. This

Table 1
Material parameters used in the calculations.

Parameters	Isotropic [30]	Anisotropic [25]
m_e^*	$0.0665m_o$	$0.067m_o$
m_+^*	$0.34m_o$	$0.45m_o$
m_-^*	$0.094m_o$	$0.08m_o$
μ_+^*	$0.05562m_o$	$0.04m_o$
μ_-^*	$0.03895m_o$	$0.05m_o$
ε_1	13.2	13.2
ε_2	1	1

Where m_o is the free electron mass.

Table 2
Ground state energies and transition energies for experimental sample wellwidths [20].

L (Å)	Ground state energies (meV)			Transition energies (eV)	
	Electron	hh	lh	Electron-hh	Electron-lh
150	20.52	3.12	16.39	1.5428	1.5561
400	3.26	0.50	2.68	1.5223	1.5251
1650	0.20	0.03	0.17	1.5194	1.5196

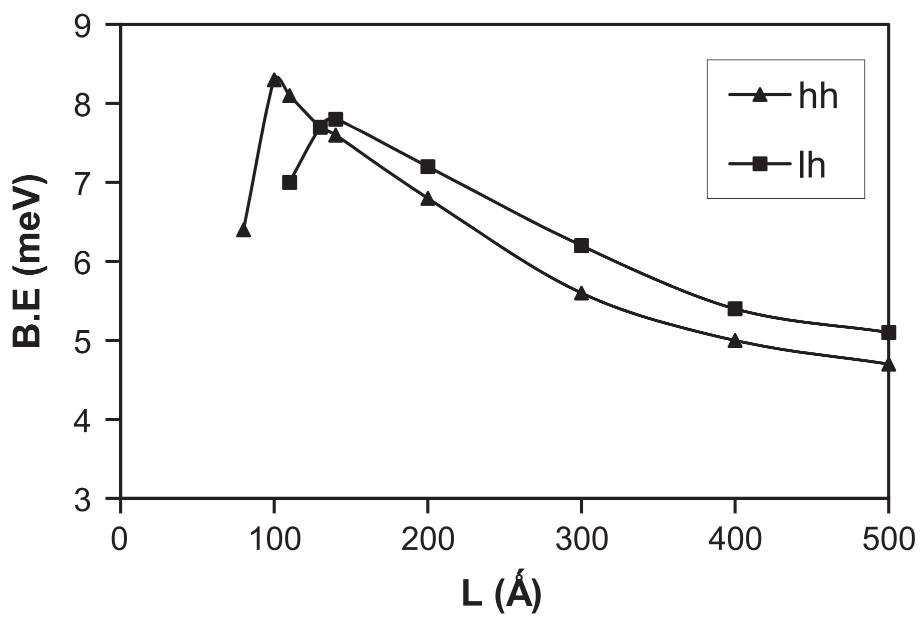

Fig. 1. Variation of the binding energy of the ground state of a heavy hole exciton (hh) and a light hole exciton (lh) without the image charges as a function of wellwidth (L) with anisotropic masses.

Table 3
Binding energies of excitons in QWs of different shapes.

Well type	$(E_{hh})_{max}$ (meV)	$(E_{lh})_{max}$ (meV)	Turnover value at L (Å)		Crossover at L (Å)
			L_{hh}	L_{lh}	
RQW [31]	9.4	9.2	25	50	50
$\|z\|^{2/3}$ [28]	7.4	5.3	225	260	250
SQW	8.3	7.8	100	140	130

shows that the exciton wavefunction penetrates into the barrier of a SQW much more than in the case of RQW and much less than the $|z|^{2/3}$ QW, as L is reduced.

It is also seen that the binding energy of the lh exciton $E_B(lh)$ is larger than that of the hh exciton $E_B(hh)$ for L greater than a certain critical value L_c at which they become equal. This shows that the lh exciton is more bound than the hh exciton until the crossover wellwidth is reached. For values below L_c, $E_B(lh)$ is smaller than $E_B(hh)$. This crossover is essentially due to the mass anisotropy involved. i.e., $m^*_+ > m^*_-$ while $\mu^*_+ < \mu^*_-$. Also $E_B(lh)$ increases less rapidly than $E_B(hh)$ since more of the lh exciton wavefunction tends to spillover into the surrounding $Al_xGa_{1-x}As$ layer, than the hh exciton wavefunction.

Fig. 2 shows the variation of the binding energy of the ground state of a hh exciton and a lh exciton as a function of the wellwidth L using an exciton Hamiltonian with isotropic masses where $m^*_+ > m^*_-$ and $\mu^*_+ > \mu^*_-$ (for anisotropic case $\mu^*_+ < \mu^*_-$). Here the hh exciton is more bound than the lh exciton for all wellwidths and hence there is no crossover as expected.

The variation of the integrated probability of finding the hh and lh exciton inside the SQW as a function of the wellwidth L is shown in Fig. 3. It is found that the probability shows a rapid decrease at nearly the wellwidth at which the binding energy shows a turnover. This is because the turnover is mainly due to the spilling over of the exciton wavefunction into the surrounding $Al_xGa_{1-x}As$ layer. No crossover is found in the hh and lh exciton probabilities because the crossover seen in the binding

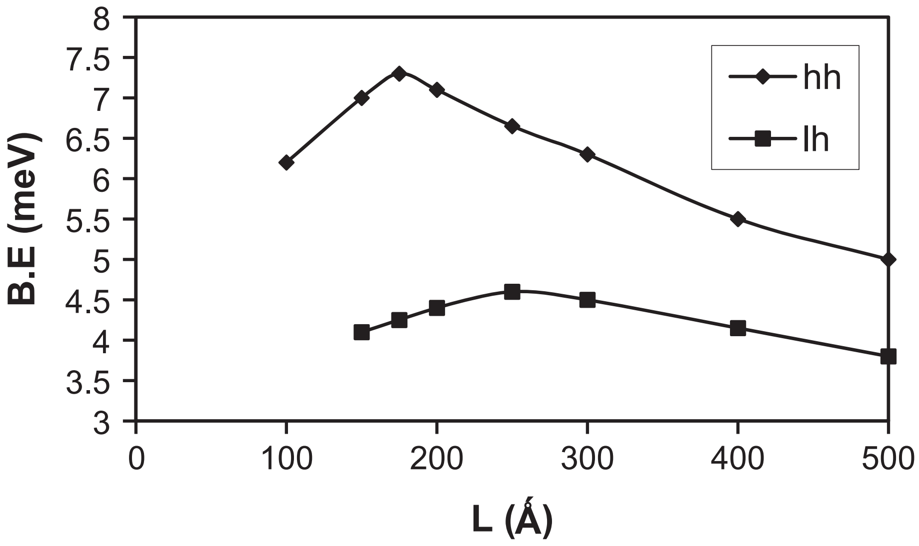

Fig. 2. Variation of the binding energy of the ground state of a heavy hole exciton (*hh*) and a light hole exciton (*lh*) without the image charges as a function of wellwidth (L) with isotropic masses.

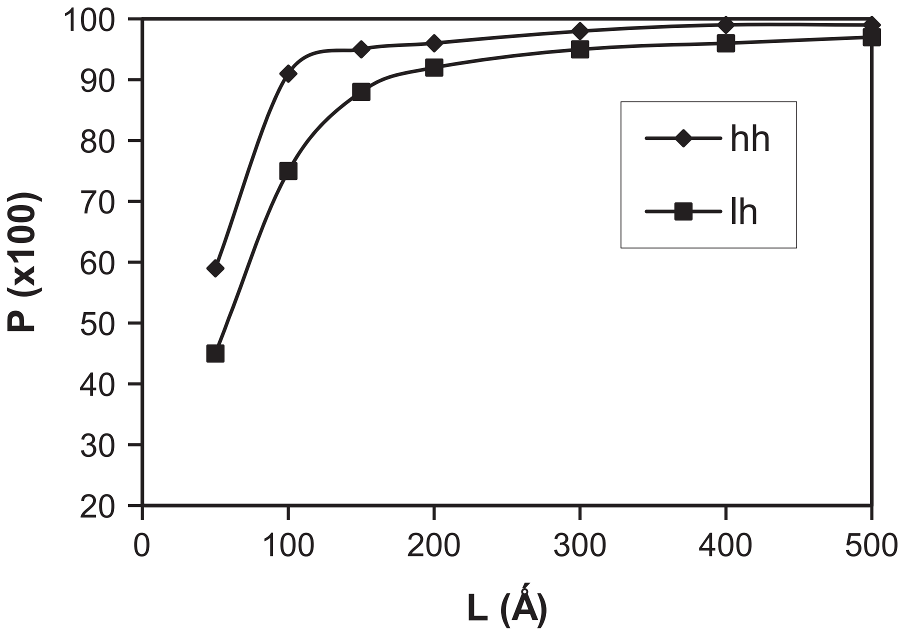

Fig. 3. Variation of the integrated probability of finding a heavy hole exciton (*hh*) and a light hole exciton (*lh*) inside a SQW as a function of wellwidth L without the image charges.

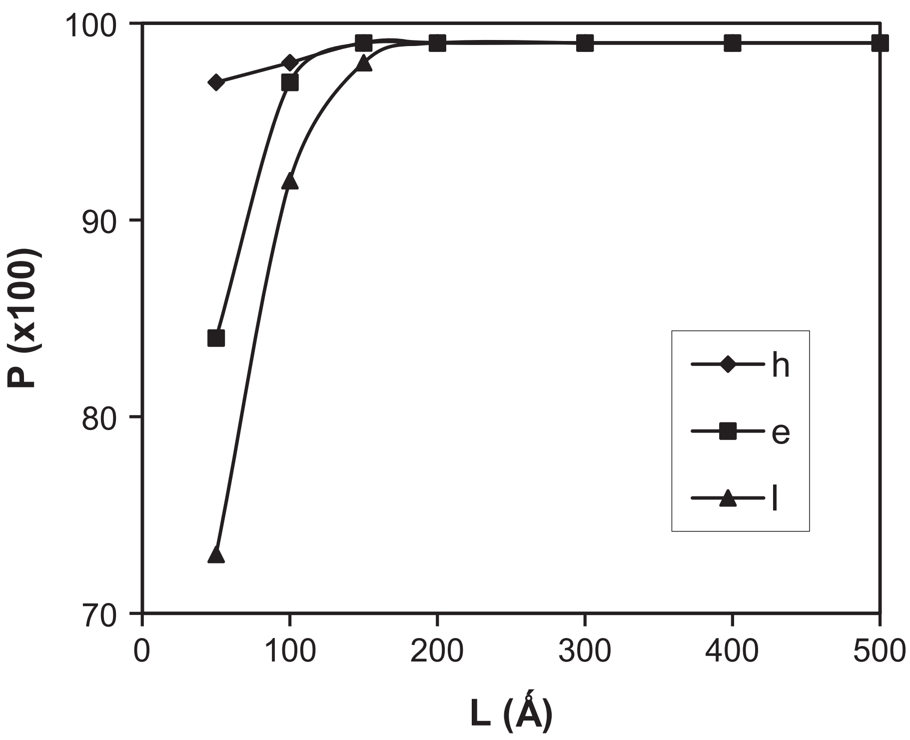

Fig. 4. Variation of the probability of finding an electron (e), a heavy hole (h) and a light hole (l) inside a SQW as a function of wellwidth L without the image charges.

energies shown in Fig. 1, is mainly due to the mass anisotropy and the fact that $m_+^* > m_-^*$ while $\mu_+^* < \mu_-^*$.

In Fig. 4, the variation of the probability of finding an electron, a *hh* and a *lh* inside the SQW as a function of the wellwidth *L*, is shown. The *hh* is found to have the highest probability, then comes the electron and finally the *lh* for a particular value of *L*. The barrier height for the electron (conduction band) is V_{oe} = 246.87 meV and for the holes (valence band), it is V_{oh} = 132.93 meV. Considering the valence band, since the effective mass of the *hh* is larger than that of the *lh*, the probability of finding the *hh* inside the well is greater than that of the *lh*, for a particular value of *L*. Though the effective mass of the electron is smaller than that of the *lh*, its probability inside the well is greater because of the larger barrier height.

The variation of the binding energies of the *hh* and *lh* excitons including the image charges as a function of the wellwidth is shown in Fig. 5. It is seen that the binding energies are significantly reduced, when image charges are included. In contrary, Gippius et al. [14] have reported that image charge effects in NSQW lead to an increase in exciton binding energy. The difference in the behavior may be due to the following variations in the calculations. (i) Non-inclusion of the layer next to InGaAs QW by Gippius et al. [14] (ii) choice of the potential levels for the QW and (iii) use of anisotropic masses of the excitons by the present authors.

We also find that the turnover in the binding energy of the excitons, as the wellwidth is reduced, is at a larger value of the wellwidth, when the effect of image charges is included. The reason again is due to the fact that the penetration of the exciton wavefunction into the surrounding $Al_xGa_{1-x}As$ layer becomes more. The repulsion of electron and hole by the polarization at the vacuum/GaAs interface assists the above penetration. The binding energies of the excitons with and without the image charges, the turnover and crossover wellwidths are presented in Table 4.

The difference in the binding energy (ΔE) of the excitons with and without the image charges is calculated and its variation with the wellwidth *L* is shown in Fig. 6. When these results are compared with those reported by various authors [7,8,15–19], the following differences are noted. The reasons for these differences are also given.

1. In the references mentioned, symmetric semiconductor nanostructures are considered where the electron and hole suffer repulsion due to the image charges arising due to the polarization at both the interfaces, which increases the confinement and hence the binding energy. But for the asymmetric SQW studied by the present authors, repulsion is experienced only at the single vacuum/well interface having dielectric discontinuity, which decreases the confinement and hence the binding energy.
2. There is no turnover in the difference in binding energy with and without the image charge as the wellwidth decreases, for a symmetrical rectangular QW [7] as well as for the vacuum barrier QW [8] up to $L \sim$50 Å. But for a SQW, a turnover is observed in the difference in binding energy of the excitons with and without the image charges as the wellwidth decreases. This difference can again be attributed to the asymmetrical nature of the polarized interfaces.

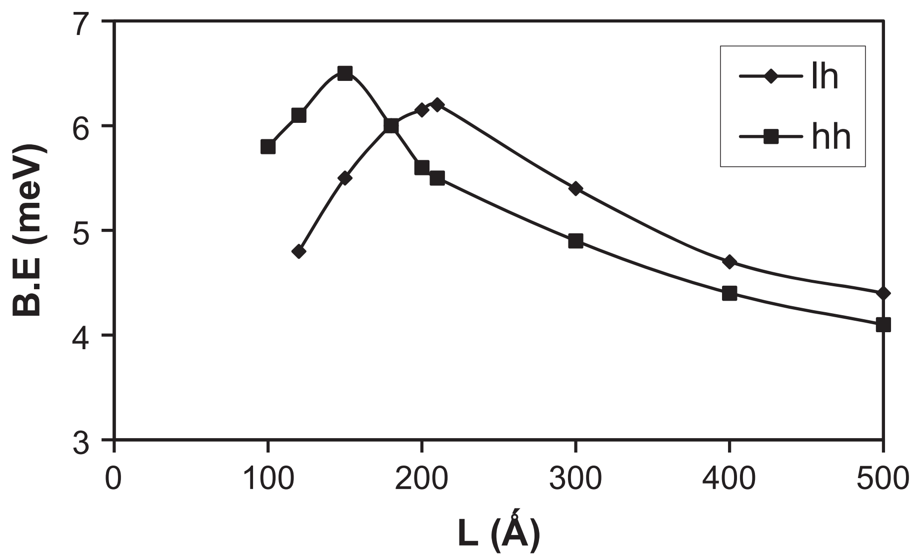

Fig. 5. Variation of the binding energy of the ground state of a heavy hole exciton (*hh*) and a light hole exciton (*lh*) with the image charges as a function of wellwidth (*L*) with anisotropic masses.

Table 4
Maximum binding energies of excitons with and without the image charges, turnover and crossover wellwidths for SQW.

Image charges	$(E_{hh})_{max}$ (meV)	$(E_{lh})_{max}$ (meV)	Turnover value at L (Å)		Crossover at L (Å)
			L_{hh}	L_{lh}	
Absent	8.3	7.8	100	140	130
Present	6.5	6.2	150	210	180

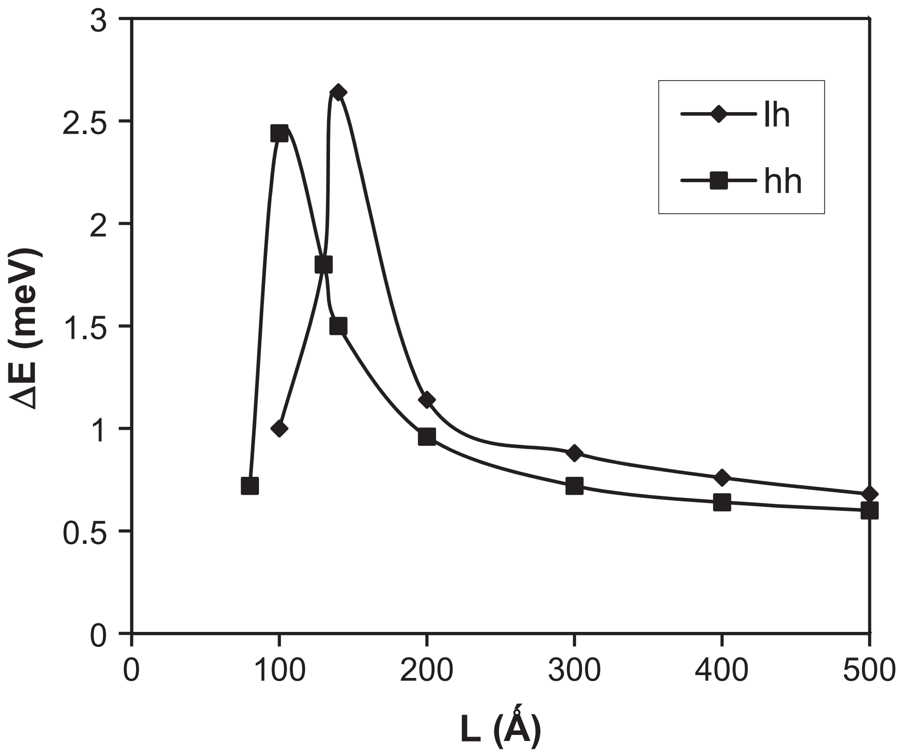

Fig. 6. Variation of the binding energy of the ground state of a heavy hole exciton (*hh*) and a light hole exciton (*lh*) with the image charges as a function of wellwidth (L) with isotropic masses.

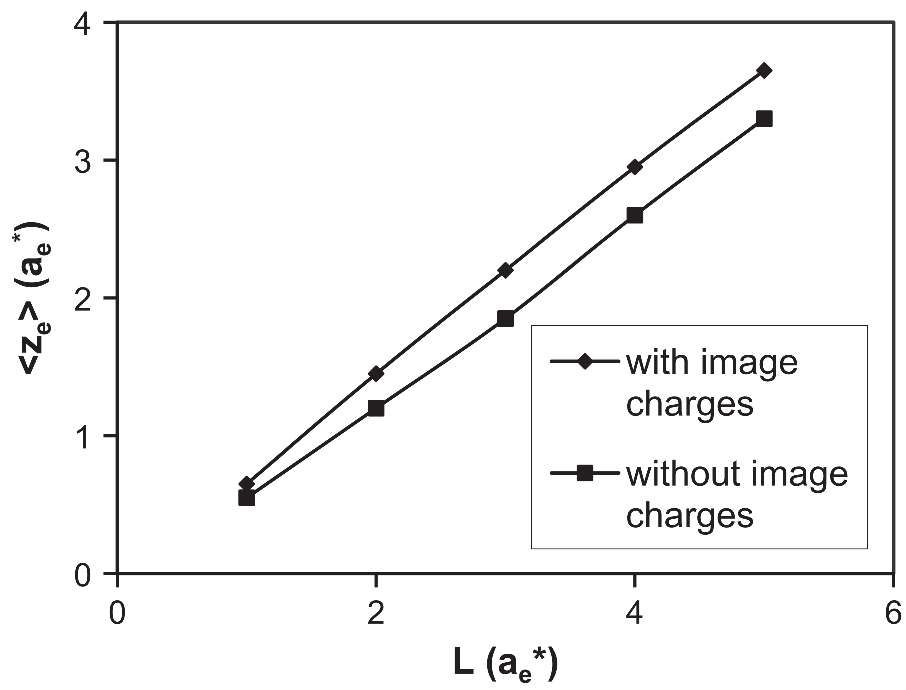

Fig. 7. Variation of the average distance of the electron $\langle z_e \rangle$ from the vacuum/GaAs interface with and without the image charges as a function of wellwidth L. Effective Bohr radius of electron, $a_e^* = 98.7$ Å.

Fig. 7 shows the variation of the average distance of an electron $\langle z_e \rangle$ calculated with the *hh* exciton wavefunction, from the vacuum/GaAs interface, with and without the image charges as a function of the wellwidth, L. It is found that as the wellwidth increases, the electron moves away from the vacuum/GaAs interface. When the effect of image charges is included, the electron is initially attracted, when the wellwidth is less than that corresponding to maximum binding energy. Thereafter, the electron is repelled and the force of repulsion increases as the wellwidth increases.

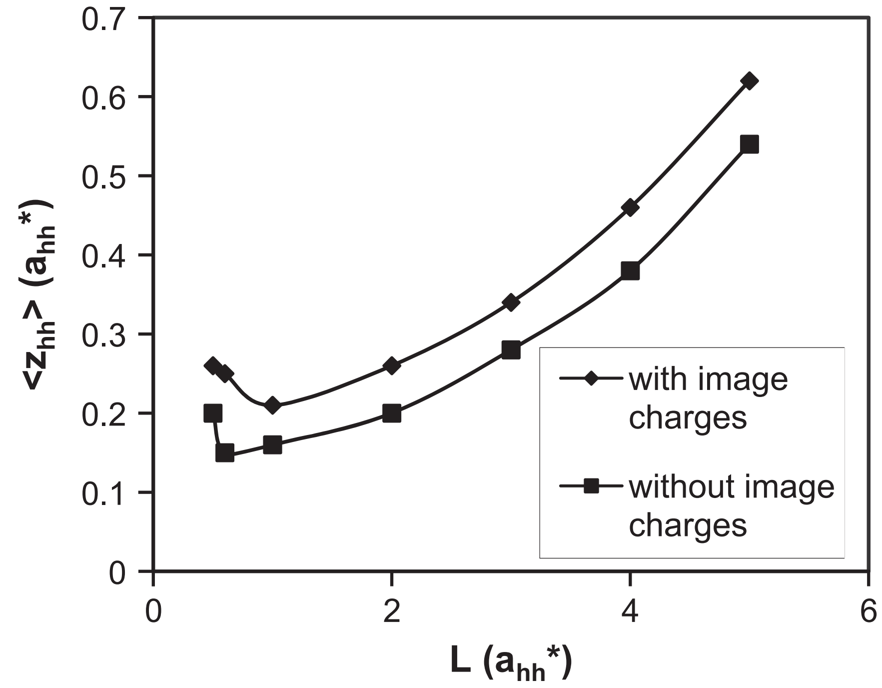

Fig. 8. Variation of the average distance of the heavy hole $\langle z_{hh} \rangle$ from the vacuum/GaAs interface with and without the image charges as a function of wellwidth L. Effective Bohr radius of heavy hole, a_{hh}^{*} = 14.7 Å.

The variation of the average distance of the heavy hole $\langle z_{hh} \rangle$ from the vacuum/GaAs interface with and without the image charges, as a function of the wellwidth L is shown in Fig. 8. Unlike the electron, the heavy hole is repelled for all wellwidths, when the effect of image charges is included. It is also found that the force of repulsion initially decreases when the wellwidth is less than that corresponding to maximum binding energy. It is noted that the *hh* is always close to the vacuum/GaAs interface, when compared to the average electron distance.

In Fig. 9, the variation of the average distance of the light hole $\langle z_{lh} \rangle$ from the vacuum/GaAs interface with and without the image charges as a function of the wellwidth L, is displayed. The variation is similar to that of the electron.

On comparison, it is seen that, for a particular value of L, the effect of image charges is the highest in the case of a *lh*, then comes the electron and then the h. This is consistent with the integrated probability shown in Fig. 4. When the probability of finding a charge carrier inside the well is larger, it is less affected by the image charges. The interface polarization is expected to repel the charge carriers causing deadlayer near the interface, which will be free of excitons.

The notion of deadlayer, discussed in the literature [6], in the context of semi-infinite solids, can be considered for the SQW. The latter differs from single interface in having a confining potential also. Hence the repulsion due to the polarization charge on the interface giving rise to an electric field does not push the charge carriers to large distance, as in the semi-infinite solids. The deadlayer in a SQW is thus expected to be small. Our calculations of $\langle z_e \rangle$ and $\langle z_{hh} \rangle$ give a qualitative idea of the dead layer in a SQW. For example, for the wellwidth of 5 a_+^*, $\langle z_e \rangle$ and $\langle z_{hh} \rangle$ are increased respectively by about 0.3 a_+^*

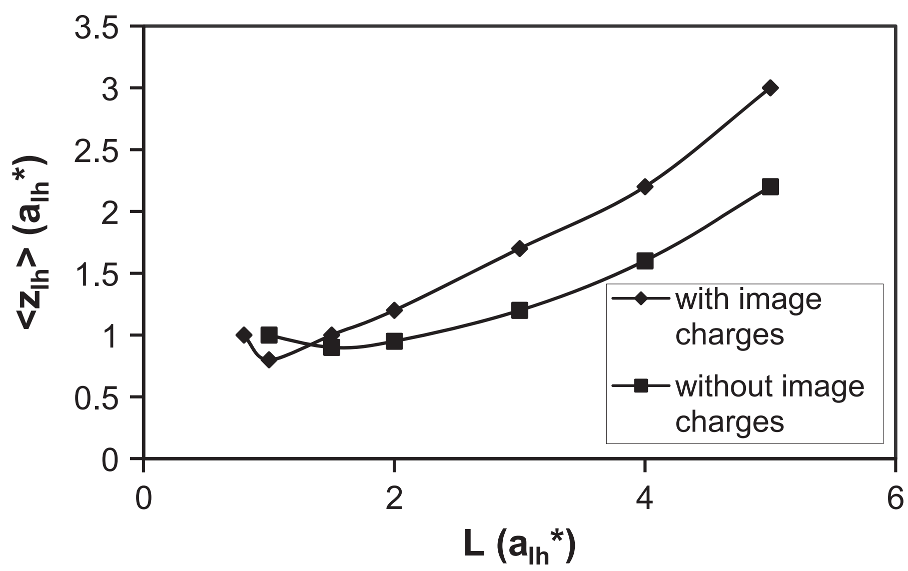

Fig. 9. Variation of the average distance of the light hole $\langle z_{lh} \rangle$ from the vacuum/GaAs interface with and without the image charges as a function of wellwidth L. Effective Bohr radius of light hole, a_{lh}^{*} = 82.7 Å.

and 0.1 a_+^*, when the image charges are included. These are about 10% of $\langle z_e \rangle$ and $\langle z_{hh} \rangle$, without the image charges.

4. Conclusion

Exciton binding energies in a SQW composed of vacuum/GaAs/$Al_xGa_{1-x}As$ as a function of wellwidth are calculated including the effect of non-parabolicity and image charges. The effect of image charges in a SQW is different from that in a symmetrical rectangular QW where the carriers experience repulsion by the image charges arising due to the polarization at both the interfaces and is compelled to be at the center of the QW. But in the SQW, they are repelled by the image charge at the single vacuum/GaAs interface only. Calculation of the average distances of the electron $\langle z_e \rangle$ and the hole $\langle z_h \rangle$ from the vacuum/GaAs interface, with and without image charges and the integrated probability of finding an electron and a hole inside the well show that the deadlayer in a SQW is smaller compared to semi-infinite solids.

Acknowledgements

The authors thank the University Grants Commission, New Delhi, India for the financial support through Major Research Project (No. F. 42-836/2013 (SR) dated 22.03.2013) and the authorities of Jayaraj Annapackiam College for Women (Autonomous), Periyakulam, Theni District, Tamil Nadu, India for the encouragements.

References

[1] Handbook of Surfaces and Interfaces of Materials, H.S. Nalwa (Ed.), vol. 4, Solid Thin Films and Layers, Copyright©2001 by Academic Press.
[2] R. Dingle, Festkorper-Probleme (Advances in Solid State Physics), vol. XV, 21, Pergamon Vieweg, Braunschweig, 1975.
[3] T. Ando, A.B. Fowler, F. Stern, Rev. Mod. Phys. 54 (1982) 437.
[4] R.R. Prange, S.M. Gorvin (Eds.), The Quantum Hall Effect, Springer Verlag, New York, 1987.
[5] Claude Weisbuch, Borge Vinter, Quantum Semiconductor Structures (Fundamentals and Applications), Academic Press Inc. (Harcourt Brace Jovanovich Publishers), Boston, 1991.
[6] R. Del Sole, A. D'Andrea, A. Lapiccirella (Eds.), Excitons in Confined Systems, in: Proceedings of the International Meeting, Rome, Italy, 1987. (Springer Verlag, Berlin, 1987).
[7] J. Cen, R. Chen, K.K. Bajaj, Phys. Rev. B 50 (1994) 10947.
[8] M. Mosko, D. Munzar, P. Vagner, Phys. Rev. B 55 (1997) 15416 (A misprint has to be corrected: x^k should read $x^{|k|}$ in Eqs. (3) and (4)).
[9] J.F. Muth, X. Zhang, A. Cai, D. Fothergill, J.C. Roberts, P. Rajagopal, J.W. Cook, Appl. Phys. Lett. 87 (19) (2005) 192117 (3 pages).
[10] Li.-Fei. Wang, Guang.-Can. Yang, Chin. Phys. B 18 (6) (2009) 2523–2528.
[11] Doan Nhat Quang, Le Tuan, Nguyen Thanh Tien, J. Appl. Phys. 107 (12) (2010) (123709-123709-8).
[12] E.C. Niculescu, N. Eseanu, Eur. Phys. J. B 79 (3) (2011) 313–319.
[13] V.M. Silkin, T. Nagao, V. Despoja, J.P. Echeverry, S.V. Eremeev, E.V. Chulkov, P.V. Echenique, Phys. Rev. B 84 (16) (2011) 165416.
[14] N.A. Gippius, A.L. Yablonskii, A.B. Dzyubenko, S.G. Tikhodeev, L.V. Kulik, V.D. Kulakovskii, A. Forchel, J. Appl. Phys. 83 (10) (1998) 5410–5417.
[15] M. Diarra, Y.-M. Niquet, C. Delerue, G. Allan, Phys. Rev. B 75 (2007) 045301.
[16] P. Corfdir, P. Lefebvre, J. Appl. Phys. 112 (2012) 106104.
[17] D.B. Tran Thoai, R. Zimmermann, M. Grundmann, D. Bimberg, Phys. Rev. B 42 (9) (1990) 5906–5909.
[18] M. Pierre, R. Wacquez, X. Jehl, M. Sanquer, M. Vinet, O. Cueto, Nat. Nanotechnol. 5 (2010) 133.
[19] M.T. Bjork, H. Schmid, J. Knoch, H. Riel, W. Riess, Nat. Nanotechnol. 4 (2009) 103.
[20] C. Parks, A.K. Ramdas, M.R. Melloch, G. Steblovsky, L.R. Ram Mohan, H. Luo, Solid State Commun. 92 (1994) 563.
[21] G. Duggan, H.I. Ralph, K.J. Moore, Phys. Rev. B 32 (1985) 8395.
[22] H.J. Lee, L.Y. Juravel, J.C. Wooley, A.J. Springthorpe, Phys. Rev. B 21 (1980) 659.
[23] K. Jayakumar, S. Balasubramanian, M. Tomak, Phys. Rev. B 33 (1986) 4002.
[24] S. Chaudhuri, K.K. Bajaj, Phys. Rev. B 29 (1984) 1803.
[25] J.M. Luttinger, W. Kohn, Phys. Rev. 97 (1955) 869.
[26] S. Chaudhuri, K.K. Bajaj, Solid State Commun. 52 (12) (1984) 967–970.
[27] A.M. Elabsy, Phys. Rev. B 46 (4) (1992) 2621–2624.
[28] M. Arulmozhi, S. Balasubramanian, Phys. Rev. B 51 (4) (1995) 2592–2595.
[29] J.D. Jackson, Classical Electrodynamics, second ed., John Wiley & Sons, Singapore, 1974. p. 147–148.
[30] D.F. Nelson, R.C. Miller, C.W. Tu, S.K. Sputz, Phys. Rev. B 21 (1980) 659.
[31] R.L. Greene, K.K. Bajaj, D.E. Phelps, Phys. Rev. B 29 (1984) 1807.
[32] D.F. Nelson, R.C. Miller, C.W. Tu, S.K. Sputz, Phys. Rev. B 36 (1987) 8063.

ChemTech

International Journal of ChemTech Research

CODEN (USA): IJCRGG ISSN: 0974-4290
Vol.7, No.3, pp 1438-1444, 2014-2015

ICONN 2015 [4th - 6th Feb 2015]
International Conference on Nanoscience and Nanotechnology-2015
SRM University, Chennai, India

Magnetic field effects on the exciton binding energy in a near triangular quantum well

A. Anitha[1] and M. Arulmozhi[1]*

Department of Physics, Jayaraj Annapackiam College for Women (Autonomous) Periyakulam-625601, Theni District, Tamil Nadu, India.

Abstract : The Binding Energy of an exciton in a Near Triangular Quantum Well (NTQW) composed of $Ga_{1-x}Al_xAs/GaAs/Ga_{1-x}Al_xAs$ with potential profile proportional to $|z|^{2/3}$ is calculated as a function of the quantum wellwidth (L) and barrier height(V_0) with uniform magnetic field applied along growth direction (i.e z-axis). In-plane electron-hole distance $<\rho^2>^{1/2}$, distance of the electron and hole respectively from the well center $<z_e^2>^{1/2}$ and $<z_h^2>^{1/2}$ are also calculated. The results are compared with those of quantum wells with other potential profiles and available experimental data.

Keywords: Quantum well, Exciton, Binding energy, Magnetic field, Barrier height.

Introduction

In recent years, due to significant improvements in micro-fabrication techniques like Molecular Beam Epitaxy and Metal Organic Chemical Vapor Deposition, it is possible to fabricate quantum wells with varied potential profiles. Miniaturization of quantum structures into nano-scale is being applied in the fabrication of nano-scale devices.

Quantum wells with parabolic potential shape (PQW) have been studied quantitatively by several workers. Kyrychenko et al[1] calculated the exciton binding energy in PQW using two different trial wave functions and compared the results with those of rectangular quantum wells (RQW). Tomasz M. Rusin[2] calculated the exciton energy in PQWs using the effective variational Hamiltonian method. They also determined the exciton binding energy in excited quantum well levels. Zang and Rustgi[3] found the effect of magnetic field normal to the plane of the well on the energy levels of a hydrogenic impurity in PQW. Tabata et al.[4] investigated the electronic structure of undoped AlGaAs/GaAs wide PQW as a function of well width, estimating the binding energies of excitons by photoluminescence measurement. The donor binding energy in PQW formed by $GaAs\text{-}Al_xGa_{1-x}As$ is determined by El-Meshad et al.[5] variationally.

The binding energy of the ground state hydrogenic donor in RQW has been calculated by Greene and Bajaj[6]. They have also reported the donor binding energies in RQW with applied magnetic field[7]. Brum and Bastard[8] studied the effect of a constant electric field on the energy position of the ground state exciton in RQW. Elabsy[9] reported the temperature dependence of the binding energy of shallow donors in RQW. Jayakumar et al.[10] determined the effect of non-parabolicity on hydrogenic donor binding energy in RQW without and with an applied magnetic field.

The ground state of a donor and light and heavy hole exciton in triangular quantum wells (TQW) have been calculated by Jiang and Wen[11]. Yu et al.[12] studied the exciton transition energy and oscillator strength under the electric field perpendicular to the heterointerface in TQW by photocurrent spectroscopy.

Vanitha and John Peter[13] reported the effect of applied magnetic field on the ground and excited states binding energy in a corrugated quantum well. Lopes et al.[14] studied the influence of the height and width of the well barrier on the binding energy of exciton in coupled double quantum wells formed by GaAs/AlGaAs. Pavel Redlinski[15] presented the results of numerical calculations of electronic states of an exciton and a trion in quantum well formed by CdTe at magnetic field upto 150T.

Andronikov et al.[16] studied the effect of temperature on excitons and trions in CdTe/CdMgTe quantum well structures and compared the results with the experimental data. The hydrogenic donor binding energy in cylindrical quantum wire with two quantum well formed by GaAs/GaAlAs has been calculated with applied magnetic field by Gonzalez et al.[17]. Arulmozhi[18] studied the effect of temperature on binding energy of hydrogenic donor in PQW. Zhao et al.[19] determined the influence of hydrostatic pressure on the exciton binding energy in quantum well formed by GaAs/AlGaAs and GaN/AlGaN. Raigoza et al.[20] studied the effects of both hydrostatic pressure and electric fields on the exciton energies in single GaAs-(Ga,Al)As quantum wells.

Arulmozhi and Balasubramanian[21] investigated the exciton and hydrogenic donor binding energy in a quantum well with potential profile proportional to $|z|^{2/3}$ (Near Triangular Quantum Well - NTQW) for different well width and barrier height. They have also calculated the binding energy of hydrogenic donor in $/z/^{2/3}$ quantum well as a function of well width and barrier height under an applied magnetic field along the growth direction[22].

The present authors[23] have studied the binding energy of light hole and heavy hole exciton in a surface quantum well (SQW) as a function of the well width including the effect of non-parabolicity. In this paper, a theoretical study is made to calculate the binding energy of light hole and heavy hole exciton in the NTQW formed by GaAlAs/GaAs/GaAlAs for different well width and barrier height with uniform magnetic field applied along growth direction including the effect of nonparabolicity and mass anisotropy. We also calculate the in-plane electron-hole distance and distance of the electron and hole from the well center. The integrated probability of finding the light exciton and heavy hole exciton inside the well is also found in the presence of magnetic field. Finally we compare our results of NTQW with available experimental data and those of quantum wells with other potential profiles.

Theory

The Hamiltonian for exciton in NTQW formed by $Ga_{1-x}Al_xAs/GaAs/Ga_{1-x}Al_xAs$ with an applied magnetic field B along the growth direction is given in the effective mass approximation as,

$$\mathcal{H} = \frac{1}{2m_e^*}\left(p - \frac{eA}{c}\right)^2 - \frac{e^2}{\varepsilon_0 r} + V(z_e) + V(z_h) \qquad (1)$$

where c is the velocity of light, e is the electric charge, ε_0 is the dielectric constant of bulk GaAs and m_e^* is the electron effective mass in GaAs. Using the cylindrical gauge, the vector potential A can be written as

$$A = \frac{1}{2} B \times r \qquad (2)$$

with **B** along the growth axis. We have considered the growth axis of the quantum well structure to be the z-axis. $r = \sqrt{\rho^2 + |z_e - z_h|^2}$, ρ is the distance in x-y plane.

Using the cylindrical co-ordinate system, the Hamiltonian for an exciton can be written as

$$\mathcal{H} = -\left[\frac{1}{\rho}\frac{\partial}{\partial\rho}\rho\frac{\partial}{\partial\rho} + \frac{1}{\rho^2}\frac{\partial^2}{\partial\varphi^2}\right] - \frac{\mu_{hi}^*}{m_e^*}\frac{\partial^2}{\partial z_e^2} - \frac{\mu_{hi}^*}{m_{hi}^*}\frac{\partial^2}{\partial z_h^2} + V(z_e) + V(z_h) - \frac{2}{r} + \gamma L_z + \frac{1}{4}\gamma^2\rho^2 \qquad (3)$$

The effective Rydberg R^* is used as the unit of energy ($R^* = \mu_{hi}^* e^4/2\hbar^2\varepsilon_0^2$) and the effective Bohr radius a^* as the unit of length ($a^* = \hbar^2\varepsilon_0/\mu_{hi}^* e^2$). In equation (3), L_z is the z-component of the angular momentum and γ is the dimensionless measure of the magnetic field, defined as $\gamma = \frac{e\hbar B}{2\mu_{hi}^* c R^*}$. The subscripts h and e stand for the hole and electron respectively. μ_{hi}^* is the reduced effective mass of the heavy hole *(i = h)* or light hole *(i = l)* and the electron. We have considered isotropic masses of light hole exciton and heavy hole exciton as

$$\frac{1}{\mu^*_{hi}} = \frac{1}{m^*_e} + \frac{1}{m^*_{hi}} \qquad (4)$$

The potential profile for the electron and hole in NTQW are given by

$$V(z) = \begin{cases} V_0 \left|\frac{z}{\frac{L}{2}}\right|^{\frac{2}{3}} & |z| < \frac{L}{2} \\ V_0 & |z| > \frac{L}{2} \end{cases} \qquad (5)$$

where V_0 is the barrier height, which depends on the composition x of Al and z = z_e (electron) or z_h (hole). The trial wave function of the exciton in the NTQW is taken to be of the form

$$\Psi = \begin{cases} N\, e^{-\alpha_e^2 z_e^2}\, e^{-\alpha_h^2 z_h^2}\, e^{-ar}\, e^{-\lambda\rho^2} & |z| < \frac{L}{2} \\ N_1\, e^{-\beta_e |z_e|}\, e^{-\beta_h |z_h|}\, e^{-ar}\, e^{-\lambda\rho^2} & |z| > \frac{L}{2} \end{cases} \qquad (6)$$

Here, α_e, α_h, β_e, β_h, a and λ are variational parameters. N is the normalization constant. The continuity conditions at z_e = L/2 and z_h = L/2 relates the normalization constant N and N_1. We have evaluated $\langle \mathcal{H} \rangle$ as a function of the variational parameters using the Hamiltonian in Eq.(3) and the trial wave function in Eq.(6).

The binding energy of exciton is then given by

$$E_B = E_e + E_h + \gamma - \langle \mathcal{H} \rangle_{\min} \qquad (7)$$

where, E_e and E_h are the ground state energies of electron and hole in bare quantum well respectively obtained variationally. $\langle \mathcal{H} \rangle_{\min}$ is the minimized value of $\langle \mathcal{H} \rangle$ with respect to the variational parameters.

The integrated probability of finding an exciton inside the well is obtained as

$$P = \int_0^{2\pi} \int_{-\frac{L}{2}}^{\frac{L}{2}} \int_{-\frac{L}{2}}^{\frac{L}{2}} \int_0^{\infty} \Psi^* \Psi\, \rho\, d\rho\, dz_e\, dz_h\, d\varphi \qquad (8)$$

The in-plane electron-hole distance $<\rho^2>^{1/2}$, distance of the electron and hole respectively from the well center $<z_e^2>^{1/2}$ and $<z_h^2>^{1/2}$ are also calculated.

Results and Discussion

For GaAs, we have taken $m_e^* = 0.0065 m_0$, $m_{hh}^* = 0.34 m_0$, $m_{lh}^* = 0.094 m_0$ and $\varepsilon_0 = 13.2$, where m_0 is the free electron mass. The difference of total bandgap between $Ga_{1-x}Al_xAs$ and GaAs is determined by the equation

$$\Delta E_g = 1.155x + 0.37x^2 \ eV \qquad (9)$$

The conduction band and valance band discontinuity is taken to be 65% and 35% of this bandgap difference respectively. We have not considered the effect due to the dielectric constant mismatch, effective mass mismatch and non-parabolicity effect of conduction band for GaAs because these effects are expected to be too small when the exciton binding energy is considered.

Fig.1 shows that the variation of binding energy of heavy hole exciton as a function of well width L for different magnetic field γ applied along the growth direction, for a barrier heights corresponding to the Al composition x = 0.3. For comparison, the variation binding energy of heavy hole exciton with L in the absence of magnetic field[21] is also shown in the figure. When L is reduced, the binding energy increases. If the L is reduced further, they reach a maximum value and then start to decrease rapidly. The peak value of binding energy is observed at L = 25 nm, for all values of γ. The presence of magnetic field leads to more binding. But as the magnetic field increases, the quantity of increase in binding energy decreases. This behavior is the similar to the cases of a hydrogenic donor in potential wells of varied profiles[3, 7, 11, 21] and for the exciton for γ = 0.

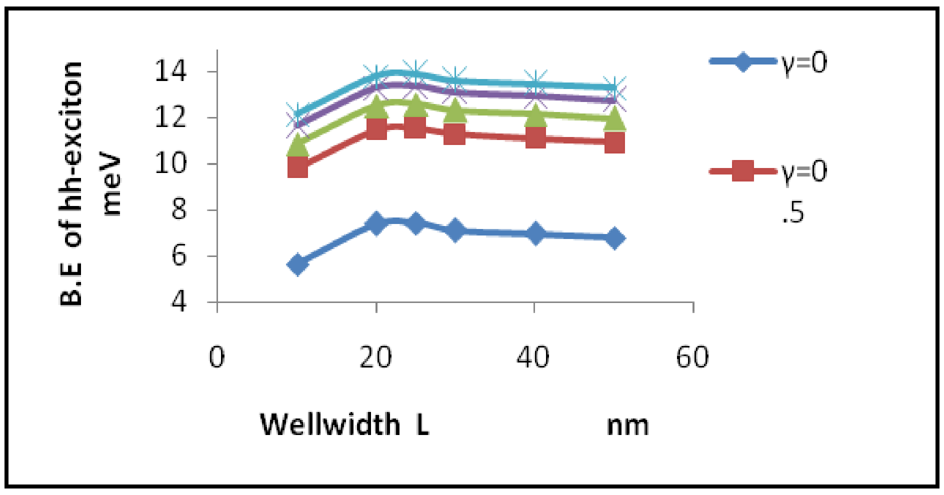

Fig.1. Variation of the binding energy of hh-exciton in $|z|^{2/3}$ quantum well as a function of well width L for different values of the magnetic field parameter γ.

The behavior of binding energy of light hole exciton as a function wellwidth L for different magnetic field parameter **γ** is displayed in Fig. 2.

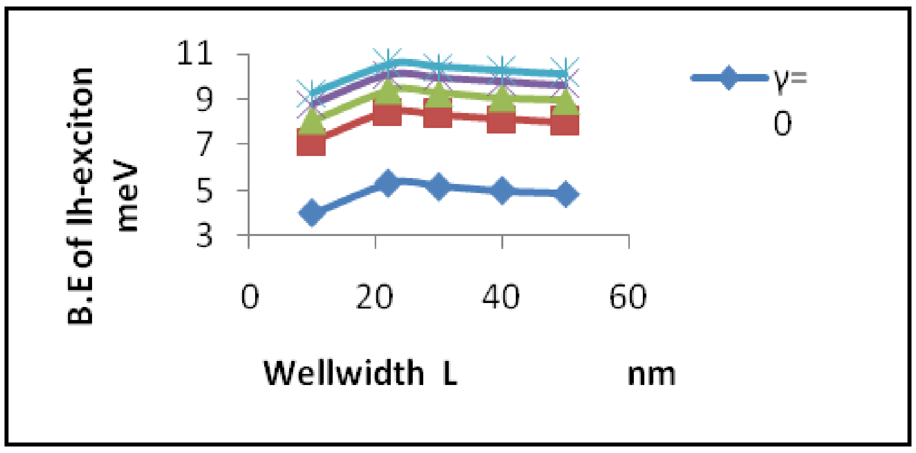

Fig.2. Variation of the binding energy of lh-exciton in $|z|^{2/3}$ quantum well as a function of well width L for different values of the magnetic field parameter γ.

Similar to the case of heavy hole exciton, the binding energy of the light hole exciton also increases and reaches its maximum and then decreases rapidly, when the well width L reduced. The peak value of binding energy is observed at L = 22 nm, for all values of **γ.** It is also noted that the binding energy of heavy hole exciton is more than that of the light hole exciton. This shows that the hh-exciton is more bound than the lh-exciton, which is due to $m_{hh}^* > m_{lh}^*$.

Figures 3 and 4 show the variation of binding energy of hh-exciton and lh-exciton as a function of barrier height V_0 respectively for the well width L = 10 nm, for different magnetic fields. In both cases, the binding energy decreases linearly with $1/\sqrt{V_0}$ for all values of magnetic field parameters.

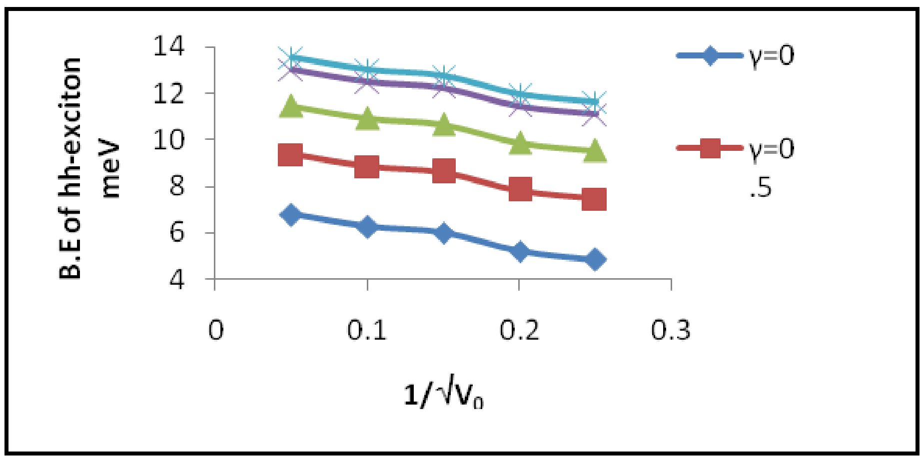

Fig.3. Variation of the binding energy of hh-exciton in $|z|^{2/3}$ quantum well as a function of barrier height V_0 for different values of the magnetic field parameter γ. V_0 is given in effective Rydberg (R*).

As the barrier height increases, the exciton is more and more bound inside the well. The results are qualitatively similar to those corresponding to quantum wells with other shapes.

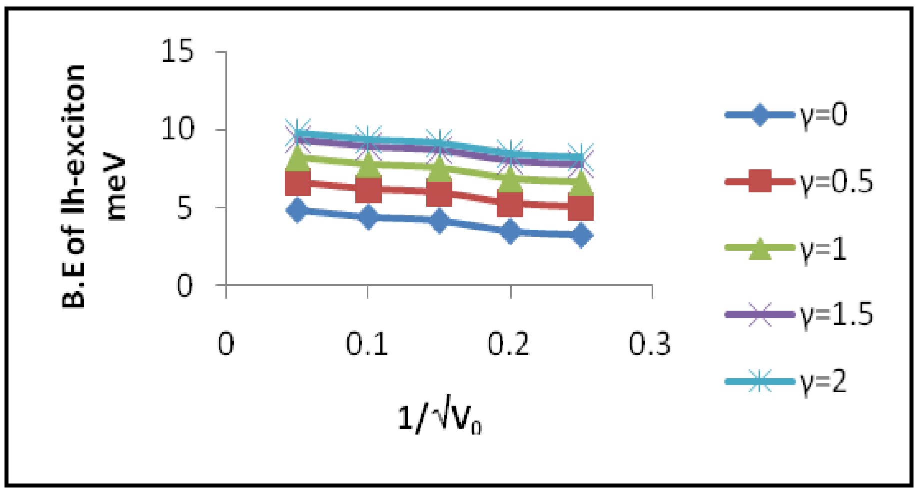

Fig.4. Variation of the binding energy of lh-exciton in $|z|^{2/3}$ quantum well as a function of barrier height V_0 for different values of the magnetic field parameter γ. V_0 is given in effective Rydberg (R*).

It can also be noted here that the binding energy of heavy hole exciton is more than that of the light hole exciton and as the magnetic field increases, the quantity of increase in binding energy decreases.

The variation of in-plane electron-hole distance $<\rho^2>^{1/2}$ as a function of wellwidth for heavy hole and light hole exciton is given in Fig. 5.

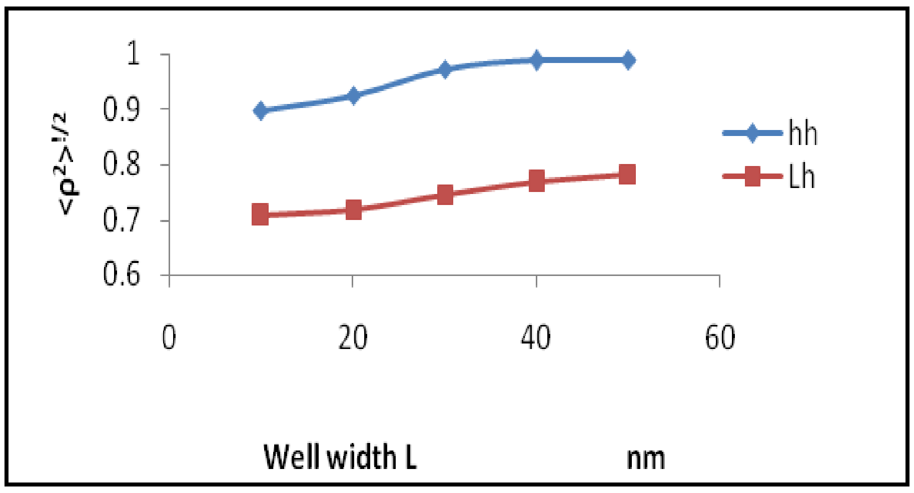

Fig.5. Variation of $<\rho^2>^{1/2}$ with the well width L for hh-exciton and lh-exciton

The values of $<\rho^2>^{1/2}$ are nearly independent of magnetic field and less dependent on L. This is expected because magnetic field is applied along z-axis and $<\rho^2>^{1/2}$ is calculated along the xy plane.

Figures 6 and 7 show the variation of $<z_e^2>^{1/2}$ and $<z_h^2>^{1/2}$ of hh-exciton and lh-exciton as a function of well width L. Both values of $<z_e^2>^{1/2}$ and $<z_h^2>^{1/2}$ for a hh-exciton increase with wellwidth and reaches a constant value (0.6 for $<z_e^2>^{1/2}$ and 0.4 for $<z_h^2>^{1/2}$) at exactly the same wellwidth at which the binding energy attains the peak value.

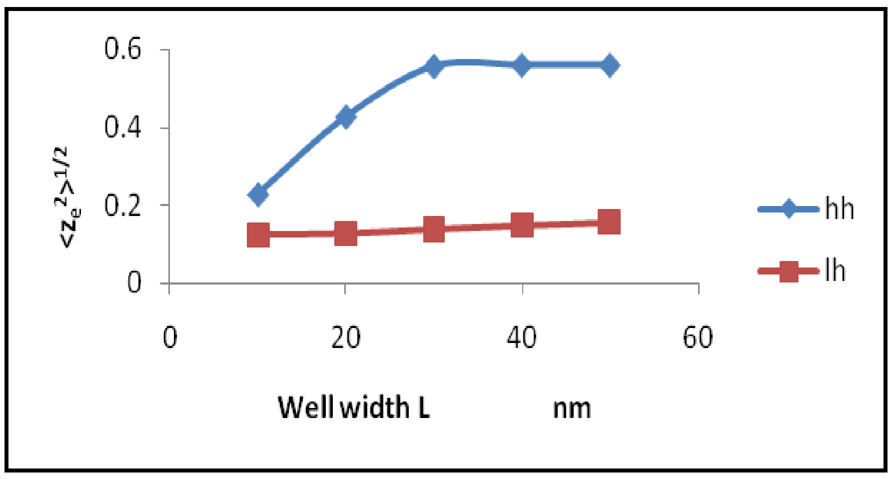

Fig.6. Variation of $<z_e^2>^{1/2}$ with the well width L for hh-exciton and lh-exciton

For the case of lh exciton, these values are nearly independent of the wellwidth.

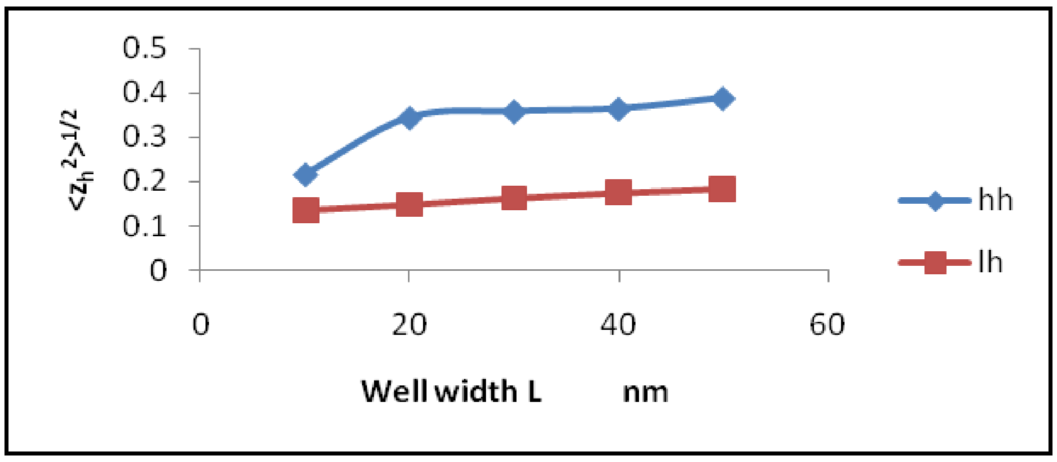

Fig.7. Variation of $<z_h^2>^{1/2}$ with the well width L for hh-exciton and lh-exciton

Conclusions

Binding energy of hh-exciton and lh-exciton in the presence of magnetic field in a Near Triangular Quantum Well (NTQW) are calculated variationally. A turnover occurs at a critical well width (25 nm for hh-exciton and 22 nm for lh-exciton), same for all values of magnetic field parameter γ. Applied magnetic field leads to more binding and the increased binding decreases as the magnetic field increases. Also the exciton binding energy decreases almost linearly with $1/\sqrt{V_0}$. $<\rho^2>^{1/2}$, is less dependent on magnetic field and wellwidth. $<z_e^2>^{1/2}$ and $<z_h^2>^{1/2}$ increases till the critical wellwidth and remains constant thereafter for hh-exciton and less dependent on wellwidth for lh-exciton.

Acknowledgements

The authors thank the University Grants Commission (UGC), New Delhi, India for the financial support through Major Research Project (No. F. 42-836/2013 (SR) dated 22.03.2013) and the authorities of Jayaraj Annapackiam College for Women (Autonomous), Periyakulam, Theni District, Tamilnadu, India for the encouragements.

References

1. Kyrychenko. F. and Kossut. J., Excitons in parabolic quantum wells, Semicond. Sci. Technol. 1998, 13, 1076.
2. Tomasz M. Rusin, The energy of excitons in parabolic quantum wells investigated by the effective variational Hamiltonian method, J. Phys.: Condens. Matter, 2000, 12, 575.
3. Zang. J. X. and Rustgi. M. L., Energy levels of hydrogenic impurity in parabolic quantum well with magnetic field, Phys. Rev. B, 1993, 48, 2465.
4. Tabata. A., Oliveira. J. B. B., da silva. E. C. F., Lamas. T. E., Duarte. C. A. and Gusev. G. M., Excitons in undoped AlGaAs/GaAs wide parabolic quantum wells, J. Physics: Conference series, 2010, 210, 012052.
5. El-Meshad. N., Hassanien. H. M. and Hassan. H. H., Donor binding energy in a parabolic quantum well, FIZIKA A (Zagreb), 2001, 1, 13.
6. Greene. R. L and Bajaj. K. K., Energy levels of hydrogenic impurity states in GaAs-$Ga_{1x}Al_xAs$ Quantum well Structures, Solid State Commun., 1985, 45, 825.
7. Greene. R. L and Bajaj. K. K., Shallow impurity centers in semiconductor quantum well structures, Solid State Commun., 1985, 53, 1103.
8. Brum. J. A. and Bastard. G., Electric field induced dissociation of excitons in semiconductor quantum wells, Phy. Rev. B, 1985, 31, 3893.
9. Elabsy. A. M., Temperature dependence of shallow donor states in GsAs-$Al_xGa_{1-x}As$ compositional superlattice, Physica Scripta, 1992, 46, 473.
10. Jayakumar. K., Balasubramanian. S and Tomak. M., Effect of non-parabolicity on the binding energy of a hydrogenic donor in a quantum well with a magnetic field, Phy. Rev. B, 1986, 33, 4002.
11. Jiang. G. Z and Wen. C. Z., Donor and excitons in triangular GaAs-$Ga_{1-x}Al_xAs$ Quantum wells, Phy. Rev. B., 1994, 50, 2689.

12. Yu, P. W., Reynolds. D. C., Sanders. G. D., Bajaj. K. K., Stutz. C. E. and Evans. K. R., Electric field effect of the excitons in asymmetric triangular $Al_xGa_{1-x}As$-GaAs quantum well, Phy. Rev. B, 1991, 43, 4344.
13. Vanitha. A. and John Peter. A., Effect of applied magnetic field on the infrared transitions between hydrogenic states in a corrugated quantum well, Eur. Phys. J. B, 2010, 73, 547.
14. Lopes. E. M., Cesar. D. F., Franchello. F., Duarte. J. L., Dias. I. F. L., Laureto. E., Elias. D.C., Pereira. M. V. M., Guimaraes. P. S. S. and Quivy. A. A., Theoretical and experimental study of the excitonic binding energy in GaAs/AlGaAs single and coupled double quantum wells, Journal of Luminescence, 2013, 144, 98.
15. Pawel Redlinski, Binding energy of negative trions at high magnetic fields in a CdTe Quantum well, Cond-mat.mtrl-sci., 2013, 0507446v1.
16. Andronikov. D. A., Fehr. M., Kochereshko. V. P., Crooker, S. A. and Karczewski. G., Behavior of Excitons and Trions in CdTe/CdMgTe Quantum-Well Structures with Variations in Temperature, Physics of the Solid State, 2007, 49 (8), 1567.
17. Gonzalez. J. D., Rondano. F. J. and Gonzalez-cujia. J. E., Donor binding energy under magnetic field in cylindrical nanotube with two GaAs/GaAlAs quantum wells, Journal of Physics: Conference series, 2014, 490, 012098.
18. Arulmozhi. M., Effect of temperature on hydrogenic donor binding energies in a nanoquantum well of Parabolic confinement, ICMSRN, 2008, 423.
19. Zhao. G. J, Liang. X. X and Ban. S. L., Effect of Hydrostatic Pressure on the binding energies of excitons in quantum wells, International Journal of Modern Physics B, 2007, 21, 2735.
20. Raigoza. N., Duque. C. A., Reyes-Gomez. E. and Oliveira. L. F., Effect of hydrostatic pressure and applied electric fields on the exciton states in GaAs(Ga,Al)As quantum wells, Physica B: Physics of Condensed Matter, 2005, 367, 267.
21. Arulmozhi. M. and Balasubramanian. S., Binding energy of hydrogenic donor and of a Wannier exciton in the $|z|^{2/3}$ quantum well, Phy. Rev. B., 1995, 51, 2592.
22. Arulmozhi. M. and Balasubramanian. S., Effect of magnetic field on the binding energy of a hydrogenic donor in a $/z/^{2/3}$ quantum well, Phy. Rev. B., 1996, 54, 651.
23. Anitha. A. and Arulmozhi. M., Excitons in a Surface quantum well, Superlattices and Microstructures, 2014, 75, 222.

*****

Indian J Phys (March 2017) 91(3):287–292
DOI 10.1007/s12648-016-0924-8

ORIGINAL PAPER

Excitonic susceptibility in near triangular quantum wells

A Anitha and M Arulmozhi*

Department of Physics, Jayaraj Annapackiam College for Women (Autonomous), Periyakulam, Theni District, Tamil Nadu 625601, India

Received: 05 February 2016 / Accepted: 17 August 2016 / Published online: 5 October 2016

Abstract: Diamagnetic susceptibility and binding energy of an exciton in a near triangular quantum well, with potential profile proportional to $|z|^{2/3}$ composed of $GaAs/Ga_{1-x}Al_xAs$ and $ZnO/Zn_{1-x}Mg_xO$ are calculated as a function of the wellwidth and concentration of Al and Mg respectively varying the magnetic field applied along growth direction (i.e. z-axis). Diamagnetic susceptibility of light hole exciton and heavy hole exciton, shows inverse behaviors in the two materials below 20 nm wellwidth and the binding energy of both excitons increases, as the magnetic field increases. The results obtained, are compared with those of quantum wells with varied potential profiles and the experimental results reported in the literature.

Keywords: Quantum wells; Exciton; Binding energy; Diamagnetic susceptibility; Magnetic field

PACS Nos.: 73.21.Fg; 71.35.-y; 71.35.Ji

1. Introduction

Advanced semiconductor growth techniques such as molecular beam epitaxy, chemical lithography and etching have made it possible to fabricate quantum wells with varied potential profiles [1]. Owing to the numerous advantages for device applications, quantum wells are fabricated with different materials such as $GaAs/Ga_{1-x}Al_xAs$ [2–13] and $ZnO/Zn_{1-x}Mg_xO$ [14–17] and investigated extensively. Studies on excitons play an important role in the development of optoelectronic devices. Excitons in rectangular quantum wells (RQW) [2–6], parabolic quantum wells (PQW) [7–9], triangular quantum wells (TQW) [10], surface quantum wells (SQW) [11], near triangular quantum wells (NTQW) with potential profile proportional to $|z|^{2/3}$ [12, 13] have been studied theoretically and experimentally by many authors.

Effect of magnetic field on a material is widely used in Nuclear Magnetic Resonance to identify the chemical and geometrical structure. Diamagnetic susceptibility is one of the important parameters to analyze the magnetic response of a material. Binding energy and diamagnetic susceptibility of a hydrogenic donor in $GaAs/Ga_{1-x}Al_xAs$ low dimensional semiconducting systems with rectangular profile have been reported by Nithiananthi and Jayakumar [18]. Effect of the nitrogen concentration and magnetic field on diamagnetic susceptibility and the binding energy of a hydrogenic donor in $Ga_xIn_{1-x}N_yAs_{1-y}/GaAs$ RQW have been studied by Kilicarslan et al. [19]. Edelshtein has theoretically proved that the diamagnetic susceptibility of an exciton molecule does not differ greatly from double the susceptibility of a single exciton [20]. Studies on the diamagnetic susceptibility of an exciton in quantum wells especially in $ZnO/Zn_{1-x}Mg_xO$ quantum wells are reported less in literature.

In this paper, the binding energy and diamagnetic susceptibility of light hole exciton (lh-exciton) and heavy hole exciton (hh-exciton) in NTQW formed by $GaAs/Ga_{1-x}Al_xAs$ and $ZnO/Zn_{1-x}Mg_xO$ are calculated as a function of width of the well as well as Al and Mg concentrations respectively. The results are compared with the available experimental data and also with the results for various potential profiles.

2. Theory

The Hamiltonian for an exciton in a quantum well with an applied magnetic field $\boldsymbol{B}$ along the growth direction (z-axis) is given in the effective mass approximation as [21],

*Corresponding author, E-mail: arulpkm@yahoo.co.in

$$\mathcal{H} = \frac{1}{2m_e^*}\left(p + \frac{eA}{c}\right)^2 + \frac{1}{2m_{ih}^*}\left(p - \frac{eA}{c}\right)^2 - \frac{e^2}{\varepsilon_o r} + V_e(z_e) + V_h(z_h) \quad (1)$$

where e is the electronic charge, c is the velocity of light and ε_o is the dielectric constant. m_{ih}^* is the effective mass of the hole, i = h for heavy hole or i = l for light hole and m_e^* is the effective mass of the electron.

The vector potential ***A*** can be written in the cylindrical gauge [22] as

$$\boldsymbol{A} = \frac{1}{2}\boldsymbol{B} \times \boldsymbol{r} \quad (2)$$

where $r = \sqrt{\rho^2 + |z_e - z_h|^2}$ and ρ is the distance in x–y plane [21].

Using the cylindrical co-ordinate system, the Hamiltonian for an exciton can be written as [13, 22]

$$\mathcal{H} = -\left[\frac{1}{\rho}\frac{\partial}{\partial\rho}\rho\frac{\partial}{\partial\rho} + \frac{1}{\rho^2}\frac{\partial^2}{\partial\varphi^2}\right] - \frac{\mu_{ih}^*}{m_e^*}\frac{\partial^2}{\partial z_e^2} - \frac{\mu_{ih}^*}{m_{ih}^*}\frac{\partial^2}{\partial z_h^2} + V_e(z_e) + V_{ih}(z_{ih}) - \frac{2}{r} + \gamma\left(\frac{m_{ih}^* - m_e^*}{m_e^* + m_{ih}^*}\right)L_z + \frac{1}{4}\gamma^2\rho^2 \quad (3)$$

μ_{ih}^* is the reduced effective mass of the exciton given by [13],

$$\frac{1}{\mu_{ih}^*} = \frac{1}{m_e^*} + \frac{1}{m_{ih}^*} \quad (4)$$

The effective Bohr radius ($a^* = \hbar^2\varepsilon_o/\mu_{ih}^* e^2$) and the effective Rydberg ($R^* = \mu_{ih}^* e^4/2\hbar^2\varepsilon_o^2$) are used as the units of length and energy respectively. In Eq. (3), L_z is the z-component of the angular momentum and γ is the dimensionless measure of the magnetic field, defined as $\gamma = \frac{e\hbar B}{2\mu_{ih}^* cR^*}$.

The potential profile for the electron and hole in NTQW [12] is given by

$$V_j(z_j) = \begin{cases} V_{oj}\left|\frac{z_j}{L/2}\right|^{\frac{2}{3}} & |z_j| < L/2 \\ V_{oj} & |z_j| > L/2 \end{cases} \quad (5)$$

where V_{oj} is the barrier height, which depends on the composition x of Al or Mg and j = e for electron or lh for light hole or hh for heavy hole.

The trial wavefunction for the exciton in the NTQW with applied magnetic field is taken to be of the form [13, 22]

$$\Psi = \begin{cases} Ne^{-\alpha_e^2 z_e^2} e^{-\alpha_h^2 z_h^2} e^{-ar} e^{-\lambda\rho^2} & |z| < L/2 \\ N_1 e^{-\beta_e|z_e|} e^{-\beta_h|z_h|} e^{-ar} e^{-\lambda\rho^2} & |z| > L/2 \end{cases} \quad (6)$$

where $\alpha_e, \alpha_h, \beta_e, \beta_h, a$ and λ are variational parameters. The wavefunction for the NTQW is chosen to be that of a PQW with $\alpha_e, \alpha_h, \beta_e$ and β_h as variational parameters, which are constants in PQW [8, 9]. e^{-ar} and $e^{-\lambda\rho^2}$ are the parts of the wavefunction for the electron–hole interaction with $r = \sqrt{\rho^2 + |z_e - z_h|^2}$ and for the applied magnetic field respectively. N is the normalization constant. The continuity conditions for wavefunction and its derivative at $z_e = L/2$ and $z_h = L/2$ relate the normalization constants N and N_1. $\langle\mathcal{H}\rangle$ is evaluated as a function of the variational parameters using the Hamiltonian in Eq. (3) and the trial wavefunction in Eq. (6) as,

$$\langle\mathcal{H}\rangle = \frac{\int \Psi^*\mathcal{H}\Psi d\tau}{\int \Psi^*\Psi d\tau} \quad (7)$$

The binding energy (E_B) of the exciton is then given by

$$E_B = E_e + E_h + \gamma - \langle\mathcal{H}\rangle_{min} \quad (8)$$

where E_e and E_h are the ground state energies of electron and hole respectively in bare NTQW given in Eq. (5) obtained variationally. $\langle\mathcal{H}\rangle_{min}$ is the minimized value of $\langle\mathcal{H}\rangle$ with respect to the variational parameters.

Diamagnetic susceptibility of an exciton in a quantum well is given by [19]

$$\chi_{dia} = \frac{-e^2}{6\mu_{ih}^*\varepsilon_0 c^2}\langle\rho^2\rangle \quad (9)$$

where c = 137, e = 1 and m_o = 1 in a.u. and $\langle\rho^2\rangle$ is the mean square distance between electron and hole.

3. Results and discussion

All the material parameters used in our calculations such as effective masses of heavy hole, light hole and electron; reduced masses of lh-exciton and hh-exciton; dielectric constants of GaAs and ZnO are given in Table 1.

The total bandgap difference ΔE_g between GaAs and $Ga_{1-x}Al_xAs$ is calculated from the equation [22],

$$\Delta E_g = 1.155x + 0.37x^2 \text{ eV} \quad (10)$$

ΔE_g between ZnO and $Zn_{1-x}Mg_xO$ is determined by the following expression [17],

Table 1 Material parameters used in the calculations

Parameters	GaAs	ZnO
m_e^*	0.0665 m_0 [13]	0.21 m_0 [17]
m_{hh}^*	0.34 m_0 [13]	0.78 m_0 [16]
m_{lh}^*	0.094 m_0 [13]	0.59 m_0 [17]
μ_{hh}^*	0.05562 m_0	0.165 m_0
μ_{lh}^*	0.03895 m_0	0.155 m_0
ε_0	13.2 [13]	8.1 [16]

Where m_0 is the free electron mass

$$\Delta E_g = 1.93x + 1.57x^2 \text{ eV} \tag{11}$$

The barrier height V_{oe} or the conduction band discontinuity is taken to be 0.65 ΔE_g for GaAs/$Ga_{1-x}Al_xAs$ [22] and 0.60 ΔE_g for ZnO/$Zn_{1-x}Mg_xO$ [16] quantum well. The effects due to the effective mass mismatch, conduction band nonparabolicity and dielectric constant mismatch are not considered, since they are expected to be small in the E_B calculations [13], which is the difference between the eigenvalues of two Hamiltonians each having to have the above features.

Figure 1 shows the variation of E_B of lh-exciton in NTQW formed by GaAs/$Ga_{0.7}Al_{0.3}As$ as a function of wellwidth L for various values of γ. The barrier heights of conduction band and valence band are calculated as 246.87 and 132.93 meV respectively. For lh-exciton in GaAs, the magnetic field $\gamma = 1$ corresponds to a magnetic field of about 20.45 kG. For comparison, we have also displayed the variation of E_B as a function of wellwidth without magnetic field i.e. $\gamma = 0$ [13]. Increase in magnetic field leads to more binding between electron and light hole. But as the magnetic field increases, the increase in E_B decreases.

As the wellwidth L is reduced, E_B slowly increases until it reaches a maximum at certain value of L. As L is reduced further, E_B decreases rapidly due to the tunnelling of trial wavefunction through the barrier and the unbounding of electron and hole. For all magnetic fields, the maximum E_B of lh-exciton is observed at L = 20 nm.

In Fig. 2 we display the variation of E_B of hh-exciton in NTQW composed of GaAs/$Ga_{0.7}Al_{0.3}As$ as a function of wellwidth L for different magnetic field parameters γ. As in the case of lh-exciton, the presence of magnetic field increases the electron–hole binding. For hh-exciton in GaAs, the magnetic field parameter $\gamma = 1$ corresponds to the magnetic field of about 41.76 kG. The behaviour of E_B of hh-exciton is similar to the case of lh-exciton. The maximum E_B occurs at 16 nm for all magnetic field parameters. E_B of hh-exciton is greater than that of lh-exciton. The behaviour of E_B is qualitatively similar to those of exciton in RQW [2–6], PQW [8, 9], TQW [10] and SQW [11]. But the values of E_B in NTQW are quantitatively larger compared to those in quantum wells of other profiles. Hence the use of NTQW will be better in optical devices than the use of quantum wells of other shapes.

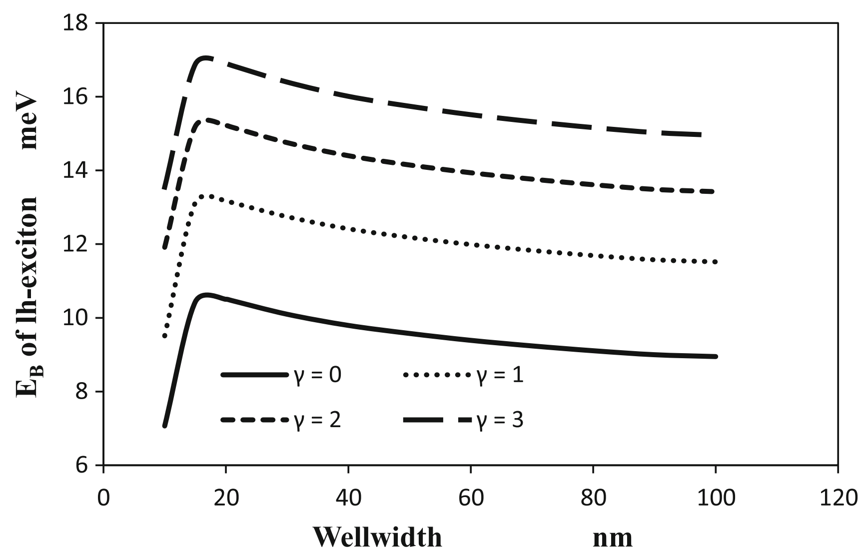

Fig. 1 Variation of the binding energy of lh-exciton in NTQW formed by GaAs/$Ga_{0.7}Al_{0.3}As$ as a function of wellwidth L for different magnetic fields

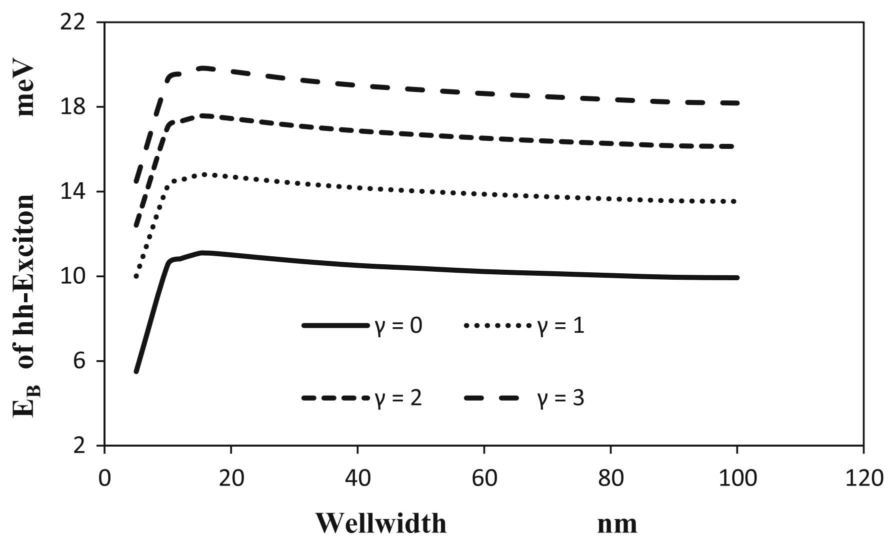

Fig. 2 Variation of the binding energy of hh-exciton in NTQW formed by GaAs/$Ga_{0.7}Al_{0.3}As$ as a function of wellwidth L for different magnetic fields

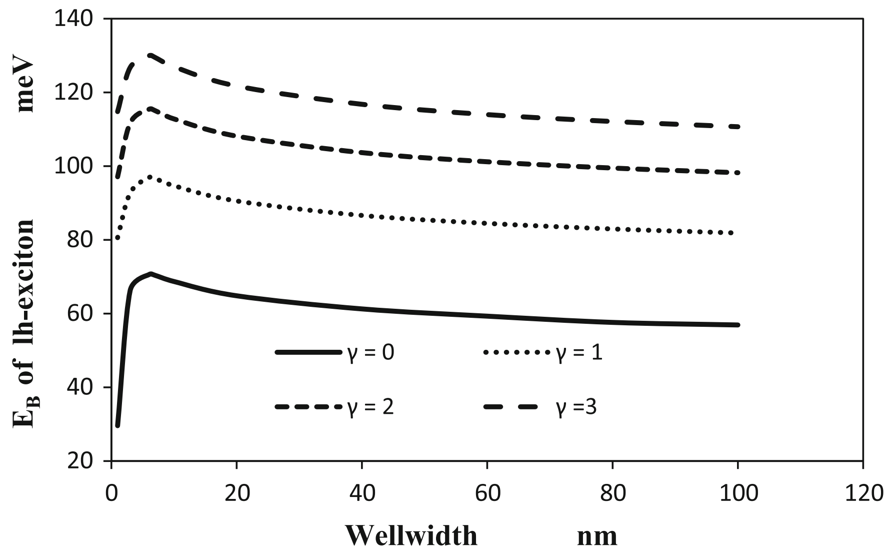

Fig. 3 Variation of the binding energy of lh-exciton in NTQW formed by ZnO/$Zn_{0.7}Mg_{0.3}O$ as a function of wellwidth L for different magnetic fields

In Figs. 1 and 2, the plots for $\gamma = 0$ are similar to those presented in Fig. 3 of Arulmozhi and Balasubramanian [13] after conversion of units (from effective Rydberg to meV and from effective Bohr radius to nm). The small variations are due to the difference in the values of the parameters used (Experimental values from Ref. [12] are used in Ref. [13]). The effect of magnetic field on the exciton binding energy in NTQW is previously reported by the authors [23] with the Zeeman term in the Hamiltonian inversely proportional to the reduced effective mass of the exciton i.e. $\left(\propto \frac{1}{\mu_{ih}}\right)$. But in the present work, due to the opposite charge sign of electron and hole, this Zeeman term in the Hamiltonian is taken to be proportional to the difference between the inverted mass of hole and inverted mass of electron $\left(\propto \frac{1}{m_e} - \frac{1}{m_{ih}}\right)$. The variations found in the results of the present work and Ref. [23] may be due to the inclusion of this effect.

Figure 3 describes the behaviour of E_B of lh-exciton in NTQW composed of ZnO/$Zn_{0.7}Mg_{0.3}O$ as a function of wellwidth L for different magnetic fields. For ZnO, 432.18 and 288.12 meV are the barrier heights of conduction band and valence band respectively. For lh-exciton in ZnO, the magnetic field parameter $\gamma = 1$ corresponds to the magnetic field of about 861.3 kG. In the presence of magnetic field, lh-exciton is more bounded than that in the absence of magnetic field. The variation of E_B with wellwidth in ZnO is similar to the case of GaAs. The maximum E_B is observed at L = 6 nm for all magnetic fields. E_B is much larger, but the turnover wellwidth is smaller in ZnO quantum well than that in GaAs quantum well.

In Fig. 4, we present the variation of E_B of hh-exciton in NTQW formed by ZnO/$Zn_{0.7}Mg_{0.3}O$ as a function of wellwidth for different magnetic fields. From this plot, it is observed that the hh-excitons are more bounded than the lh-excitons for all magnetic fields. The magnetic field parameter $\gamma = 1$ is about 976 kG. When the wellwidth increases, E_B initially increases rapidly, reaches its maximum and then starts to decrease gradually. For all magnetic fields, the maximum value of E_B occurs at 4 nm. As mentioned earlier, the reason for the decrease of E_B for L < 4 nm is the penetrating of the trial wavefunction into the barrier, so that the excitons are less bounded. The peak values of E_B of both excitons without magnetic field in ZnO/$Zn_{0.7}Mg_{0.3}O$ are larger than the experimental data reported for Mg concentration x = 0.27 and for other potential profiles [14, 16]. This again confirms that excitons are more stable in NTQW than other profiles which leads to the realization of excitonic opto-electronic devices.

Figure 5 shows the behaviour of E_B of lh-exciton and hh-exciton in NTQW composed of GaAs/$Ga_{1-x}Al_xAs$ as a function of Aluminium composition x with the magnetic field parameter $\gamma = 1$ and L = 20 nm. It is observed that the increase in Al composition leads to increased binding, because the barrier height increases as Al composition increases [3–5]. In this case, E_B of hh-exciton is more than that of lh-exciton.

In Fig. 6, we display the variation of E_B of lh-exciton and hh-exciton in ZnO/$Zn_{1-x}Mg_xO$ NTQW for various Mg compositions x with $\gamma = 1$ and L = 20 nm. As in the case of GaAs/GaAlAs quantum well, E_B increases with the increase of barrier height or Mg composition. Comparison of E_B of lh-exciton and hh-exciton shows that hh-exciton is more bounded than lh-exciton.

In Fig. 7 and 8, we present the variation of diamagnetic susceptibility of lh-exciton and hh-exciton in NTQW formed by GaAs/$Ga_{0.7}Al_{0.3}As$ as a function of wellwidth for different magnetic fields. For lh-exciton, it is observed that the diamagnetic susceptibility increases with decrease of the wellwidth, reaches a maximum and then decreases. But for $\gamma > 3$, it continuously increases as wellwidth decreases. For hh-exciton, it increases as the wellwidth

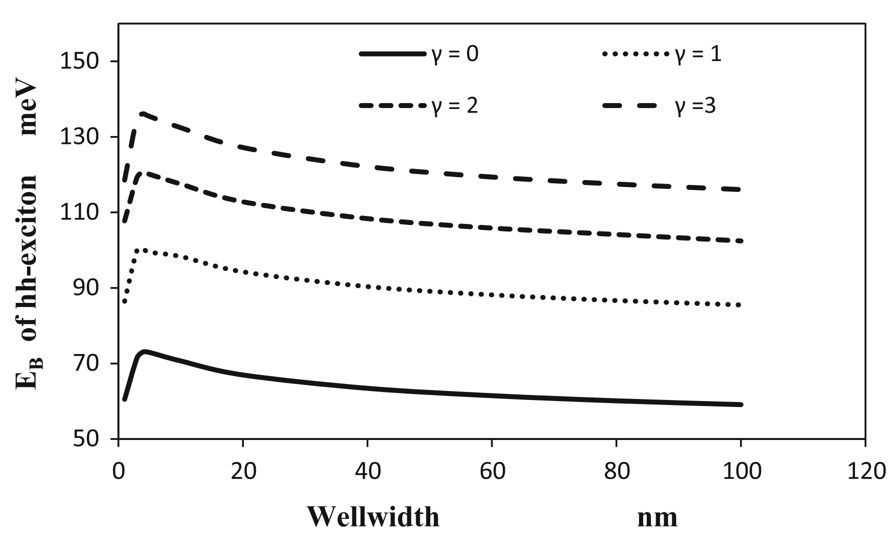

Fig. 4 Variation of the binding energy of hh-exciton in NTQW formed by ZnO/$Zn_{0.7}Mg_{0.3}O$ as a function of wellwidth L for different magnetic fields

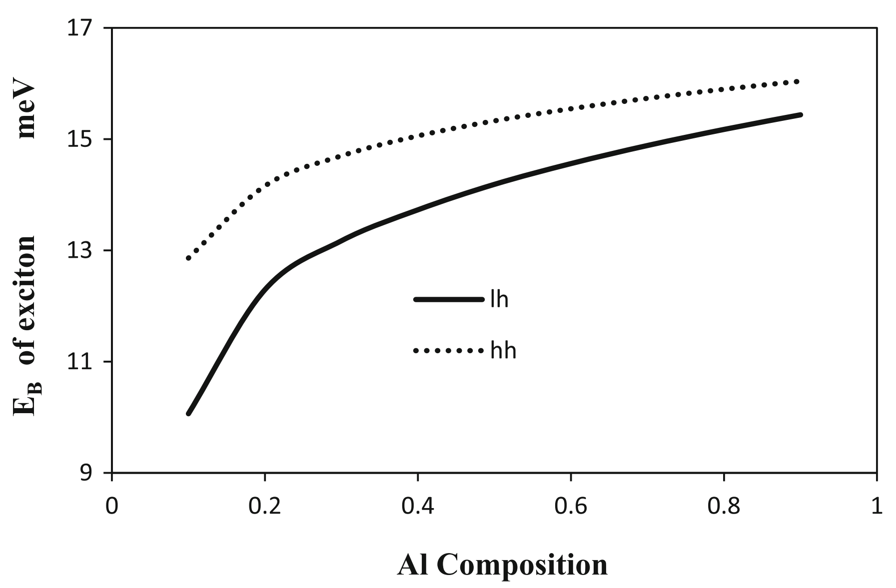

Fig. 5 Variation of the binding energy of lh-exciton and hh-exciton in NTQW formed by GaAs/$Ga_{1-x}Al_xAs$ as a function of x for $\gamma = 1$

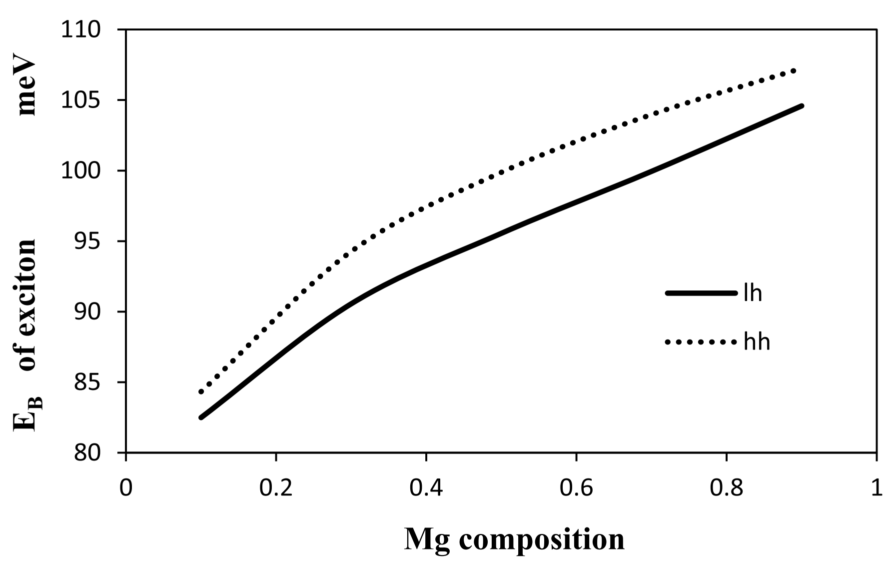

Fig. 6 Variation of the binding energy of lh-exciton and hh-exciton in NTQW formed by ZnO/$Zn_{1-x}Mg_xO$ as a function of x for $\gamma = 1$

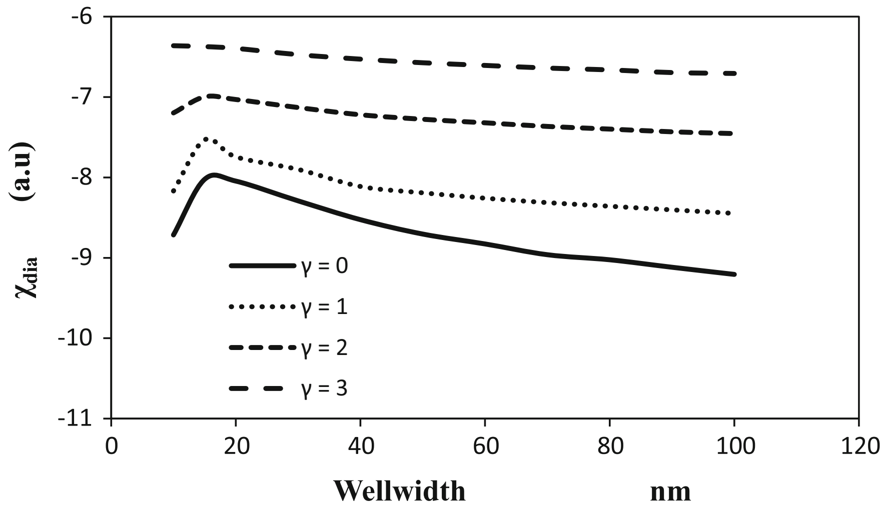

Fig. 7 Variation of the diamagnetic susceptibility of lh-exciton in NTQW formed by GaAs/$Ga_{0.7}Al_{0.3}As$ as a function of wellwidth L for different magnetic fields

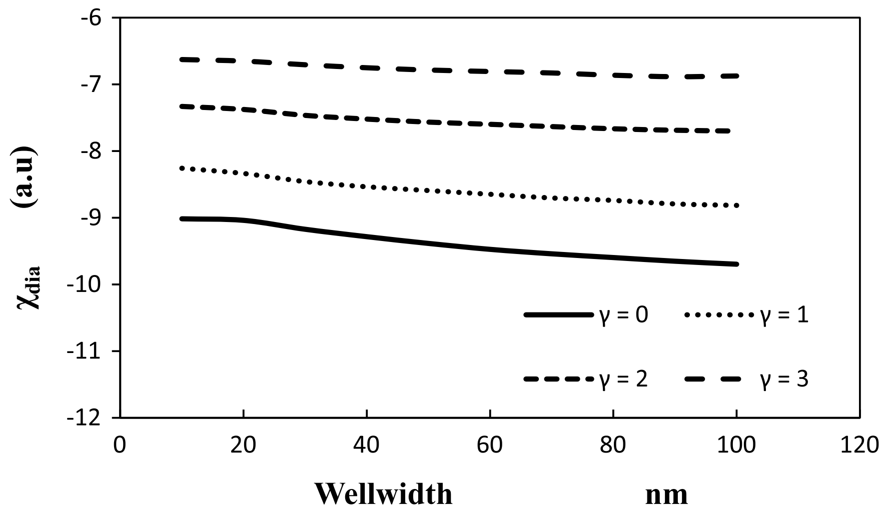

Fig. 8 Variation of the diamagnetic susceptibility of hh-exciton in NTQW formed by GaAs/$Ga_{0.7}Al_{0.3}As$ as a function of wellwidth L for different magnetic fields

decreases for all magnetic fields. This behaviour is similar to diamagnetic susceptibility of hydrogenic donor in RQW [19, 20]. The diamagnetic susceptibility of hh-exciton is greater than that of lh-exciton.

We present the variation of diamagnetic susceptibility of lh-exciton and hh exciton in NTQW composed of ZnO/$Zn_{0.7}Mg_{0.3}O$ as a function of wellwidth for various magnetic fields in Figs. 9 and 10 respectively. From both graphs, it is observed that the diamagnetic susceptibility of lh-exciton and hh-exciton decreases as wellwidth increases. Diamagnetic susceptibility has greater value in ZnO/ZnMgO quantum well than in GaAs/GaAlAs quantum well.

Figure 11 shows the variation of diamagnetic susceptibility of lh-exciton and hh-exciton in NTQW formed by GaAs/$Ga_{1-x}Al_xAs$ and ZnO/$Zn_{1-x}Mg_xO$ as a function of x for $\gamma = 1$ and L = 20 nm. When the Al/Mg composition or barrier height increases, the diamagnetic susceptibility increases in all the cases. At present, there are no theoretical or experimental data to compare our results for the

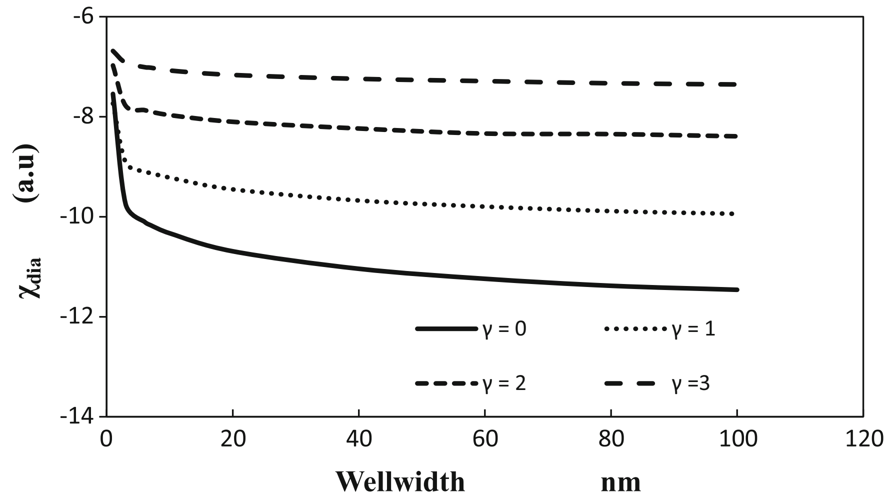

Fig. 9 Variation of the diamagnetic susceptibility of lh-exciton in NTQW formed by ZnO/$Zn_{0.7}Mg_{0.3}O$ as a function of wellwidth L for different magnetic fields

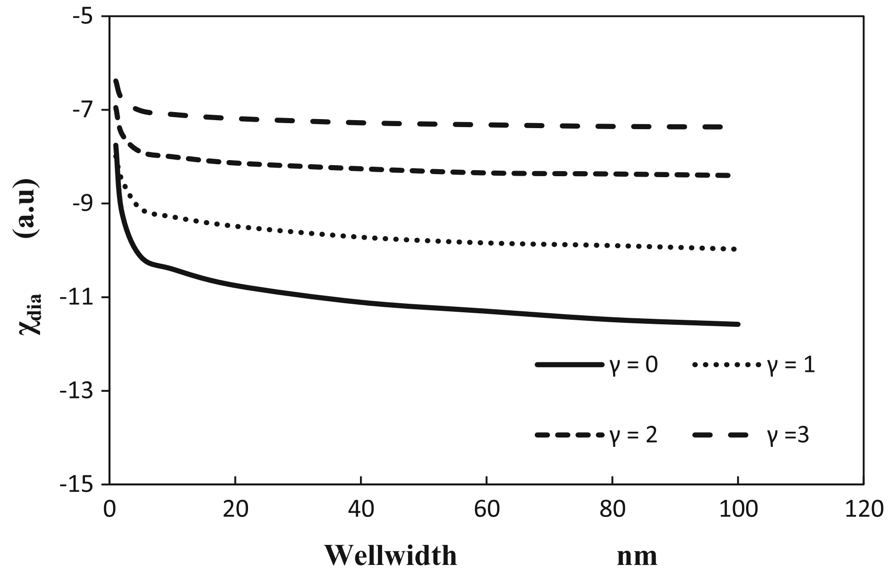

Fig. 10 Variation of the diamagnetic susceptibility of hh-exciton in NTQW formed by ZnO/$Zn_{0.7}Mg_{0.3}O$ as a function of wellwidth L for different magnetic fields

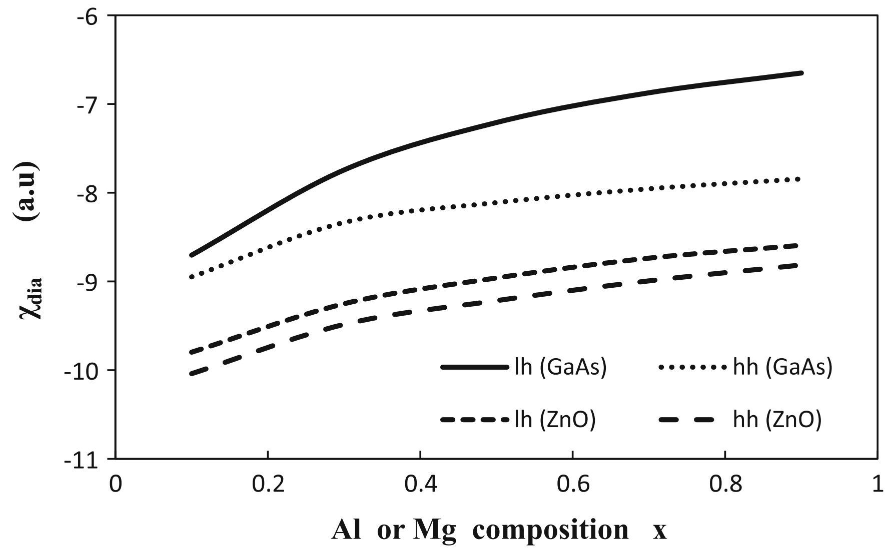

Fig. 11 Variation of the diamagnetic susceptibility of lh-exciton and hh-exciton in NTQW formed by GaAs/$Ga_{1-x}Al_xAs$ and ZnO/$Zn_{1-x}Mg_xO$ as a function of x for $\gamma = 1$

diamagnetic susceptibility of exciton in ZnO/$Zn_{1-x}Mg_xO$ NTQW. However, in future our calculation may support the experimental work.

4. Conclusions

We have studied the diamagnetic susceptibility and binding energy of lh-exciton and hh-exciton in NTQW formed by GaAs/GaAlAs and ZnO/ZnMgO as a function of wellwidth and Al/Mg composition. The diamagnetic susceptibility and the binding energy increases when the applied magnetic field increases. Excitons in ZnO/ZnMgO quantum well have larger binding energy than in GaAs/GaAlAs quantum well which leads to higher stability of the exciton in this quantum well and enhancement of the performance of ZnO based excitonic devices. Diamagnetic susceptibility is larger in ZnO/ZnMgO quantum well than in GaAs/GaAlAs quantum well, which implies ZnO to be more promising for magnetic field applications.

Acknowledgments The authors thank the University Grants Commission (UGC), New Delhi, India for the financial support through Major Research Project [No. F. 42-836/2013 (SR) dated 22.03.2013] and the authorities of Jayaraj Annapackiam College for Women (Autonomous), Periyakulam, Theni District, Tamilnadu, India for the encouragements.

References

[1] S Mosleni-Tabrizi *Eigenstate Calculations for Multidimensional Nanostructures: Quantum Wells, Wires and Dots* (Germany: VDM Verlag Dr. Muller Aktiengesellschaft & Co.KG) (2008)

[2] N H Lu, P M Hui and T M Hsu *Solid State Commun*. **78** 145 (1991)

[3] B Gerlach, J Wusthoff, M O Dzero and M A Smondyrev *Phys. Rev. B* **58** 10568 (1998)

[4] E M Lopes et al *J. Lumin.* **144** 98 (2013)

[5] G J Zhao, X X Liang and S L Ban *Int. J. Mod. Phys. B* **21** 2735 (2007)

[6] N Raigoza, C A Duque, E Reyes-Gomez and L F Oliveira *Phys. B* **367** 267 (2005)

[7] A Tabata, J B B Olivera, E C F da Silva, T E Lamas, C A Duarte and G M Gusev *J. Phys.: Conf. Ser.* **210** 012052 (2010)

[8] M Tomasz and M Rusin *J. Phys.: Condens. Matter* **12** 575 (2000)

[9] F Kyrychenko and J Kossut *Acta Phys. Polon. A* **94** 406 (1998)

[10] G Z Jiang and C Z Wen *Phys. Rev. B* **502** 689 (1994)

[11] M Arulmozhi and A Anitha *Superlatt. Microstruct.* **75** 222 (2014)

[12] S K Sputz and A C Gossard *Phys. Rev. B* **38** 3553 (1988)

[13] M Arulmozhi and S Balasubramanian *Phys. Rev. B* **51** 2592 (1995)

[14] H D Sun et al *J. Appl. Phys.* **91** 1993 (2002)

[15] T Gruber, C Kirchner, R Kling, F Reuss and A Waag *Appl. Phys. Lett.* **84** 5359 (2004)

[16] G Coli and K K Bajaj *Appl. Phys. Lett.* **78** 2861 (2001)

[17] K Zhao, G Chen, B S Li and A Shen *Appl. Phys. Lett.* **104** 212104-1 (2014)

[18] V M Edelshtein *Sov. Phys. JETP* **50** 384 (1979)

[19] P Nithiananthi and K Jayakumar *Solid State Commun.* **137** 427 (2006)

[20] E Kilicarslan, S Sakiroglu, E Kasapoglu, H Sari and I Sokmen *Superlatt. Microstruct.* **48** 305 (2010)

[21] P M Mathews and K Venkatesan *A Text Book of Quantum Mechanics* (New Delhi: Tata McGraw-hill) 2nd ed. (2014)

[22] M Arulmozhi and S Balasubramanian *Phys. Scr.* **54** 651 (1996)

[23] A Anitha and M Arulmozhi *Int. J. ChemTech Res.* **7** 1438 (2015)

ChemTech

International Journal of ChemTech Research
CODEN (USA): IJCRGG ISSN: 0974-4290
Vol.9, No.03 pp 308-315, 2016

A Comparative Study on the Properties Of ZnO And ZnS Nanoparticles

Panchavarnam D., Menaka S., Anitha A. and *Arulmozhi M.

Department of Physics, Jayaraj Annapackiam College for Women (Autonomous) Periyakulam – 625 601, Theni District, Tamil Nadu, India

Abstract: ZnO and ZnS nanoparticles are synthesized by a simple precipitation method by varying the growth temperature. These nanoparticles are characterized by X-ray Diffraction (XRD), Ultraviolet-Visible Spectroscopy (UV-Vis), Fourier Transform Infrared Spectroscopy (FTIR) and Scanning Electron Microscopy (SEM). In addition, the conductivity of the synthesized ZnO and ZnS nanoparticles are measured for different concentrations. The average particle size of the as-prepared ZnO and ZnS nanoparticles is determined by XRD in the range of 30 - 50 nm and 40 - 60 nm respectively with hexagonal form. The functional groups were confirmed by FTIR. SEM images confirm the nanocrystalline nature of the particles. The optical band gaps of ZnO and ZnS particles are calculated from the UV-Vis spectra in the range of 4.5- 4.6 eV and 5.2 - 5.4 eV respectively. The conductivity of the prepared samples increases with the growth temperature as well as the concentration. The results of the as-prepared ZnO and ZnS nanoparticles are compared with each other and with those reported in literature.
Keywords: XRD, UV-Vis, FTIR, SEM, Conductivity.

1. Introduction

Zinc oxide (ZnO) nanoparticles have much attention due to their novel optical and electronic properties for applications in various fields such as solar cells [1-3], gas sensors [4], optical devices such as LED, laser and thin film transistor and piezoelectric devices [5]. Zinc sulphide (ZnS)-based nanostructured materials are potentially important due to the large band gap**.** Because of the unique electronic properties, ZnS nanoparticles can be used in light-emitting diodes [6], cathode-ray tubes [7], photocatalysis [8], biosensors [9] and thin film electroluminescent displays [10]**.** ZnO and ZnS semiconductors have wide band gap of 3.37 eV and 3.8 eV respectively at room temperature and large exciton binding energy which leads to stable excitation even at room temperature. ZnO nanoparticles are prepared by several methods such as hydrothermal method, sol-gel method and simple precipitation method [11-13]. ZnS nanoparticles are synthesised by wet-chemical synthesis route, co-precipitation method and simple precipitation method [14-16].

In the present work, ZnO and ZnS nanoparticles are synthesized by cost effective simple precipitation method with different growth temperatures. The optical properties of the synthesized samples were investigated by Ultra Violet Visible Spectroscopy (UV-Vis) and Fourier Transform Infrared Spectrometry (FTIR). Structural properties were analysed by X-Ray Diffraction (XRD) and Scanning Electron Microscopy (SEM). The conductivity of the samples is measured for different concentrations.

2. Experimental Procedure

2.1 Preparation of ZnO nanoparticles

ZnO nanoparticles are synthesized by simple precipitation method. The aqueous solutions of Zinc sulphate and Sodium hydroxide are slowly added drop wise under vigorous stirring. The stirring was continued for 5 hours and precipitation is observed. The obtained precipitate is filtered and washed thoroughly with deionised water. Then the precipitate is dried in hot air oven at 100°C, 150°C and 200°C and ground to make fine powder using agate mortar.

2.2 Preparation of ZnS nanoparticles

ZnS nanoparticles are synthesized by mixing Zinc chloride and Sodium sulphide. 1:1 ratio of Sodium sulphide and Zinc chloride are separately dissolved in distilled water and stirred constantly for one hour at 100^0C separately. After allowing them to cool to room temperature, Zinc chloride is added drop wise to Sodium sulphide with constant stirring. This is maintained at 100^0C and stirred constantly for one hour, which resulted in formation of ZnS nanocolloid. The nanoparticles are collected by centrifugation at 2000 rpm for 15 minutes and extracted with distilled water. The precipitate is washed with distilled water and the sample is dried with different temperature such as 100^0C, 150^0C and 200^0C. The fine ZnS nanopowder is obtained by grinding the powdered sample to its finer form.

All steps of synthesis are carried out in distilled water for its inherent advantage of being simple and environment friendly.

All the chemicals used in all the methods of synthesis are of analytical reagent grade.

3. Results and Discussion

3.1 XRD studies

XRD patterns of the ZnO nanoparticles for various growth temperatures are shown in Fig. 1 for a 2θ range of 20^o-70^o. All diffraction peaks are well indexed with hexagonal structure of ZnO reported in JCPDS File Card No. 89-0510. No impurity peaks are observed which shows the high purity of ZnO. Fig. 2 displays the XRD patterns of ZnS nanoparticles which confirm the presence of pure hexagonal structure of ZnS from the JCPDS File Card No. 74-5018 for various growth temperatures. The mean grain size of the particles is calculated using the Debye-Scherrer equation,

$$D = 0.89\lambda/\beta\cos\theta \qquad (1)$$

where λ is the wavelength of (Cu K_α) X-rays, β is the full width at half maximum (FWHM) and θ is the angle of half diffraction.

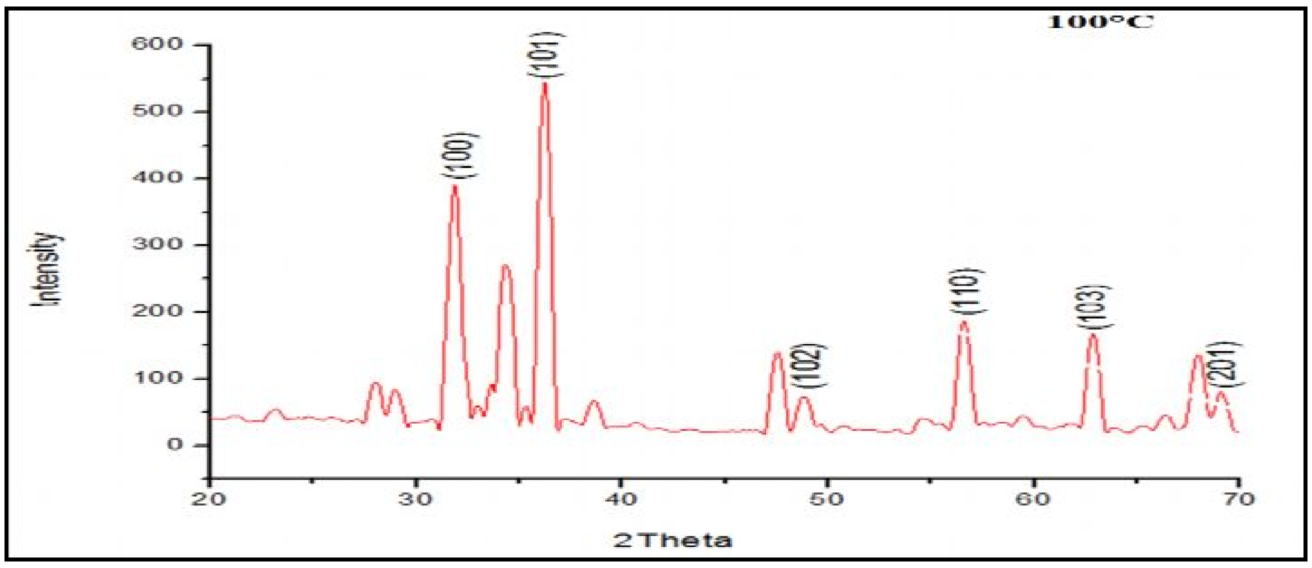

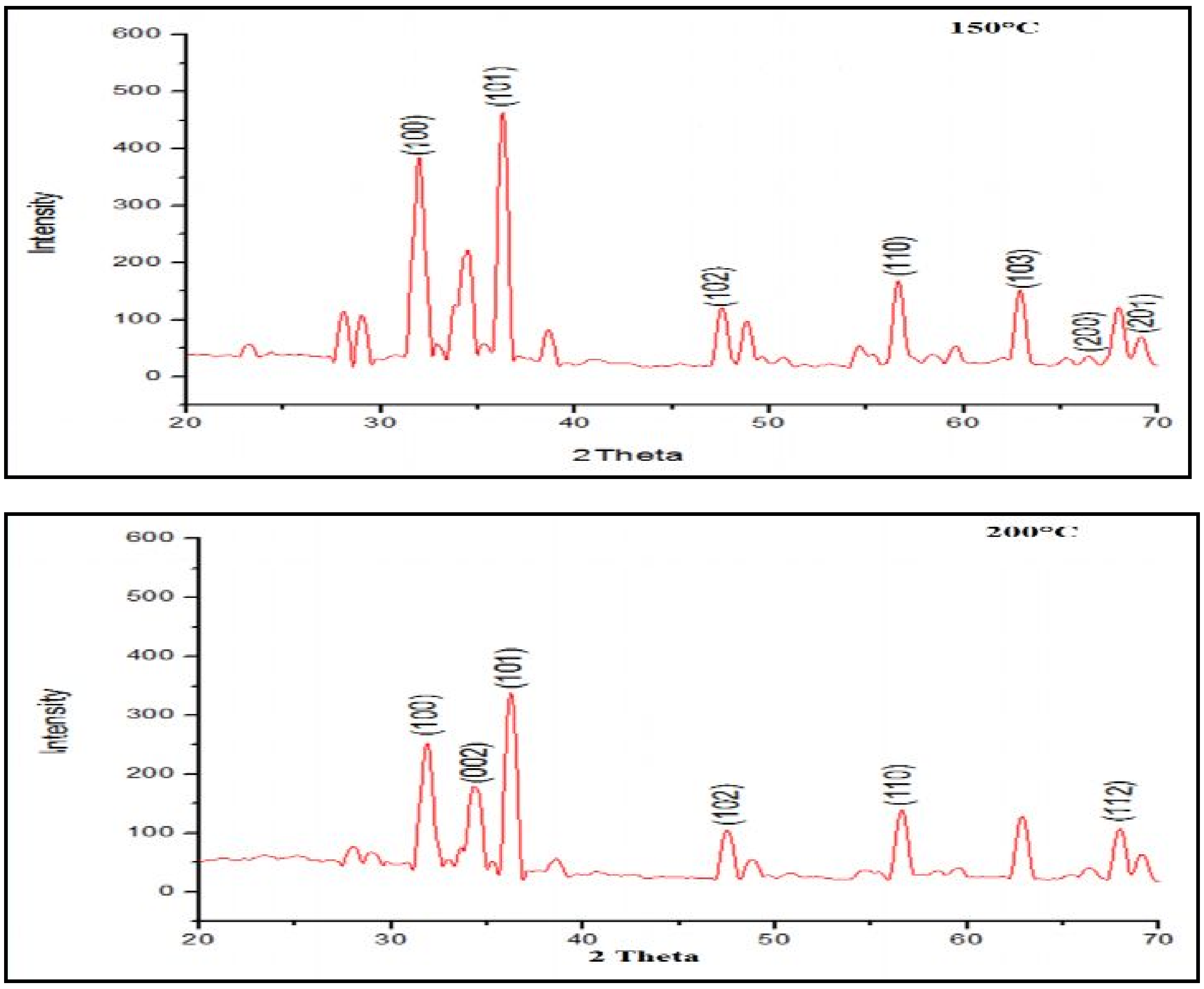

Fig. 1 XRD patterns of ZnO nanoparticles for various growth temperatures

The grain size of the ZnO nanoparticles are calculated in the range of 36 - 46 nm while ZnS nanoparticles are in the range of 49 - 56 nm. The grain size decreases when growth temperature increases for both ZnO and ZnS nanoparticles which is in contradiction to the results of Aneesh et al [11]. ZnO nanoparticles are smaller in size than the ZnS nanoparticles.

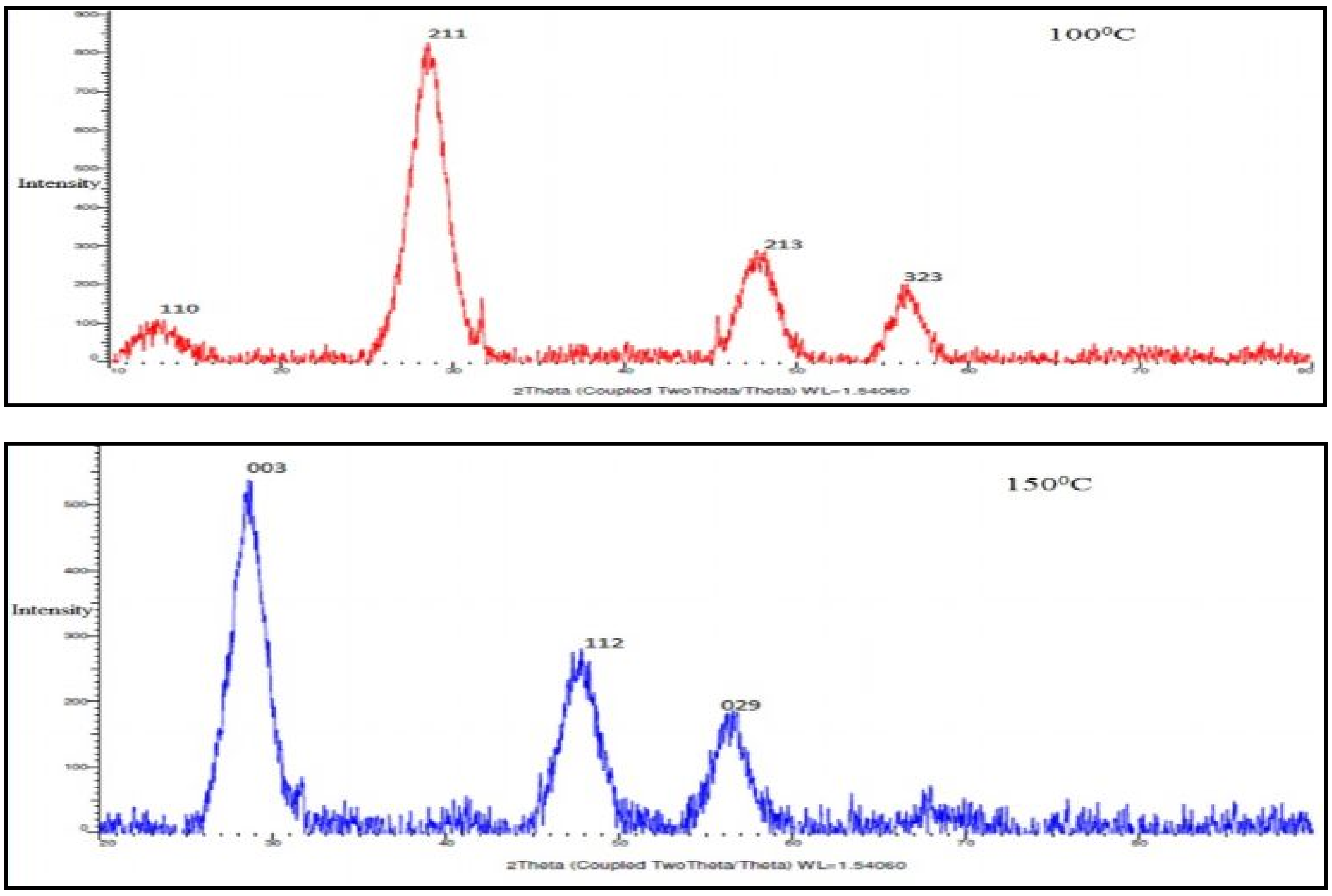

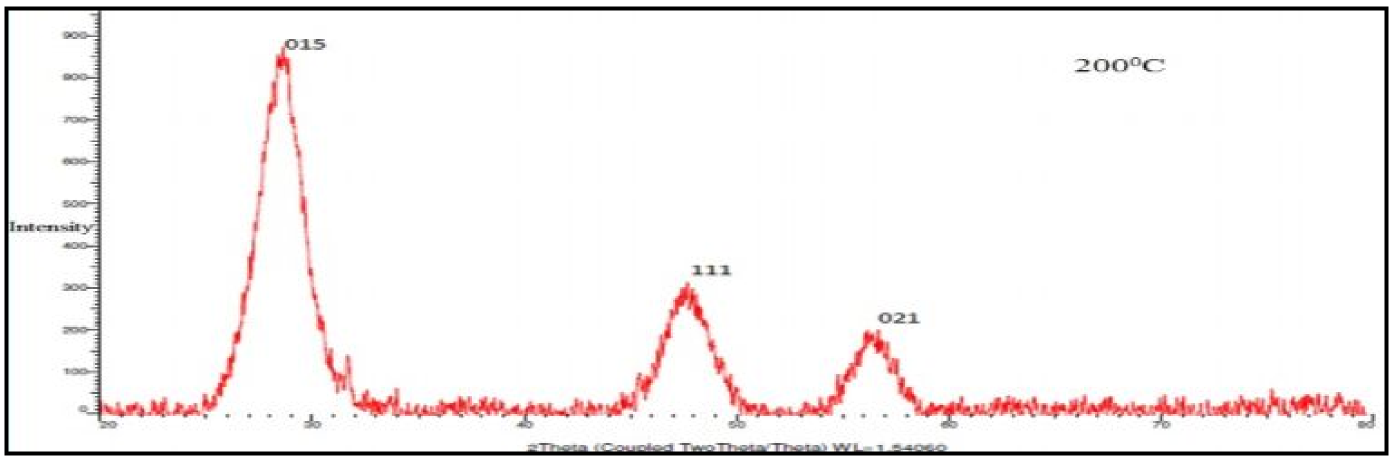

Fig. 2 XRD patterns of ZnS nanoparticles for various growth temperatures

3.2 UV-Visible absorption studies

Fig. 3 presents the UV-Visible absorption spectra of ZnS nanoparticles for various growth temperatures. The absorption peaks are observed at 344 nm, 343 nm and 342 nm for growth temperatures 100^0C, 150^0C and 200^0C respectively. A systematic blue shift is observed in the absorption peak with the increase in the growth temperature which implies an increase in the band gap, ie., 4.5 - 4.6 eV.

Fig. 4 exhibits the absorption spectra of ZnO nanoparticles and the absorption peaks are found at 272 nm, 274 nm and 269 nm respectively for growth temperatures 100^0C, 150^0C and 200^0C, which are large blue shift from the bulk absorption at 315nm [15]. The optical energy gaps for the ZnO samples are calculated to be in the range 5.2 - 5.4 eV. Hence ZnO nanoparticles show larger blue shift than ZnS nanoparticles which agrees with XRD results.

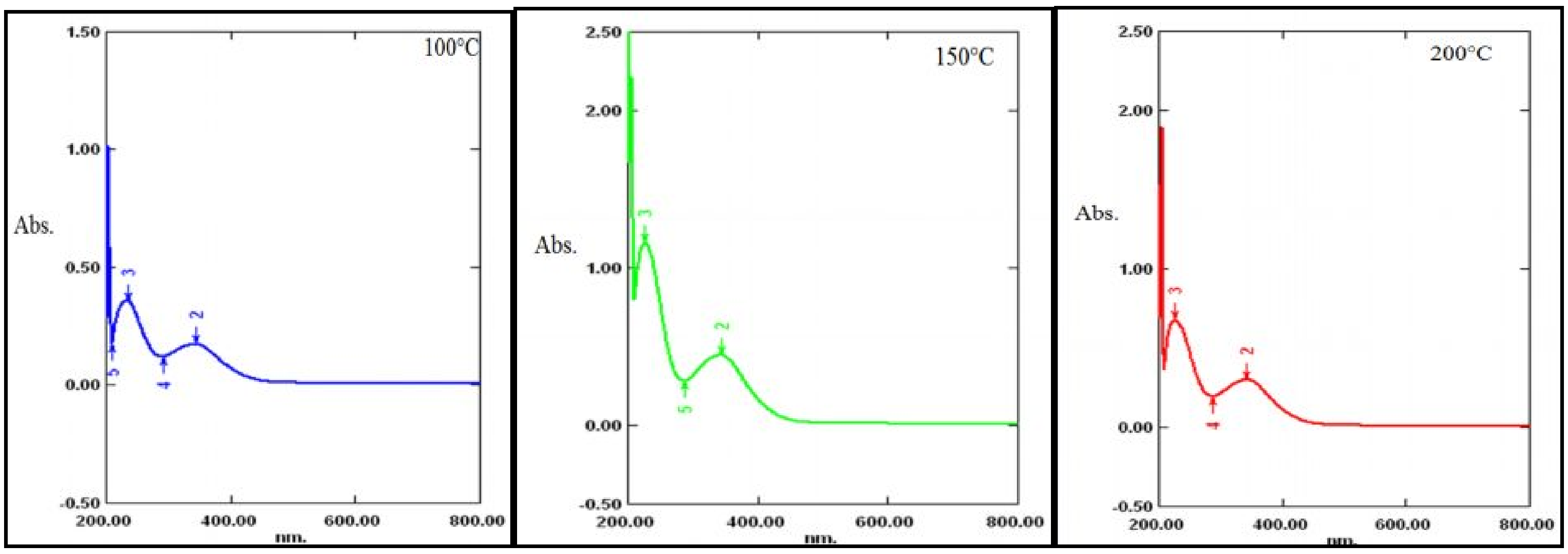

Fig. 3 UV-Visible absorption spectra of ZnS nanoparticles for various growth temperatures

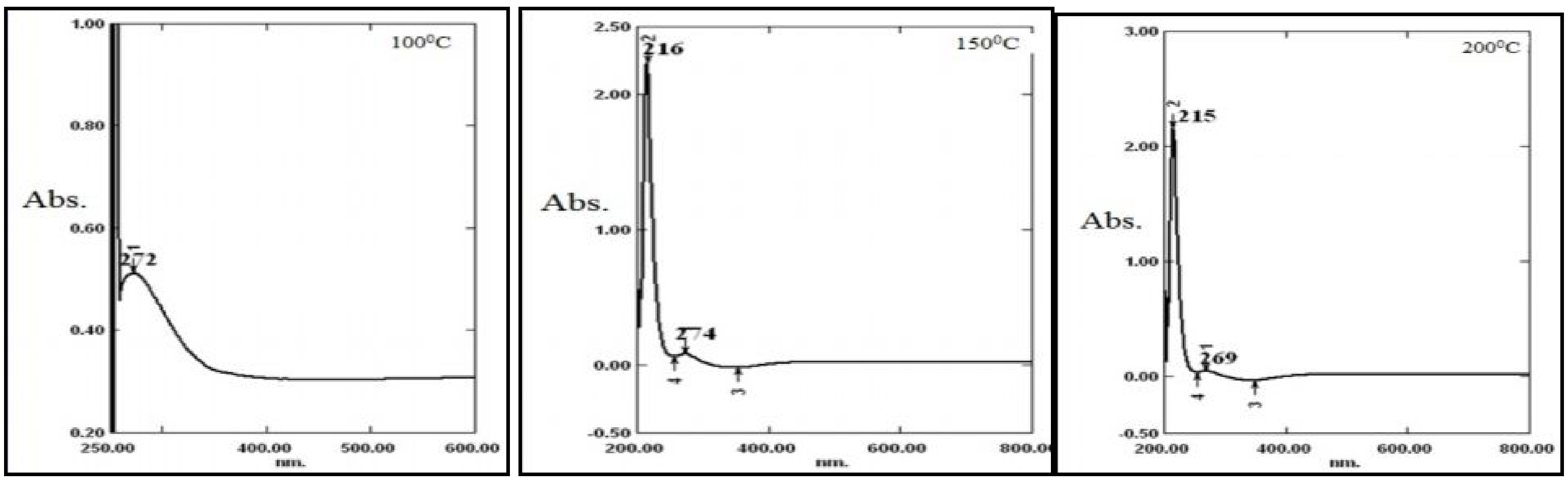

Fig. 4 UV-Visible absorption spectra of ZnO nanoparticles for various growth temperatures

3.3 FTIR studies

Fig. 5 provides the FT-IR spectra of ZnO nanoparticles for various growth temperatures. It is observed that the O-H stretching mode is represented by the absorption band at 3504.66 cm^{-1}, 3506.59 cm^{-1} and 3506.59 cm^{-1} for various growth temperatures 100^{0}C, 150^{0}C and 200^{0}C respectively. Similarly C-O stretching mode is represented by 1122 cm^{-1}, 1118 cm^{-1}and 1120 cm^{-1}.

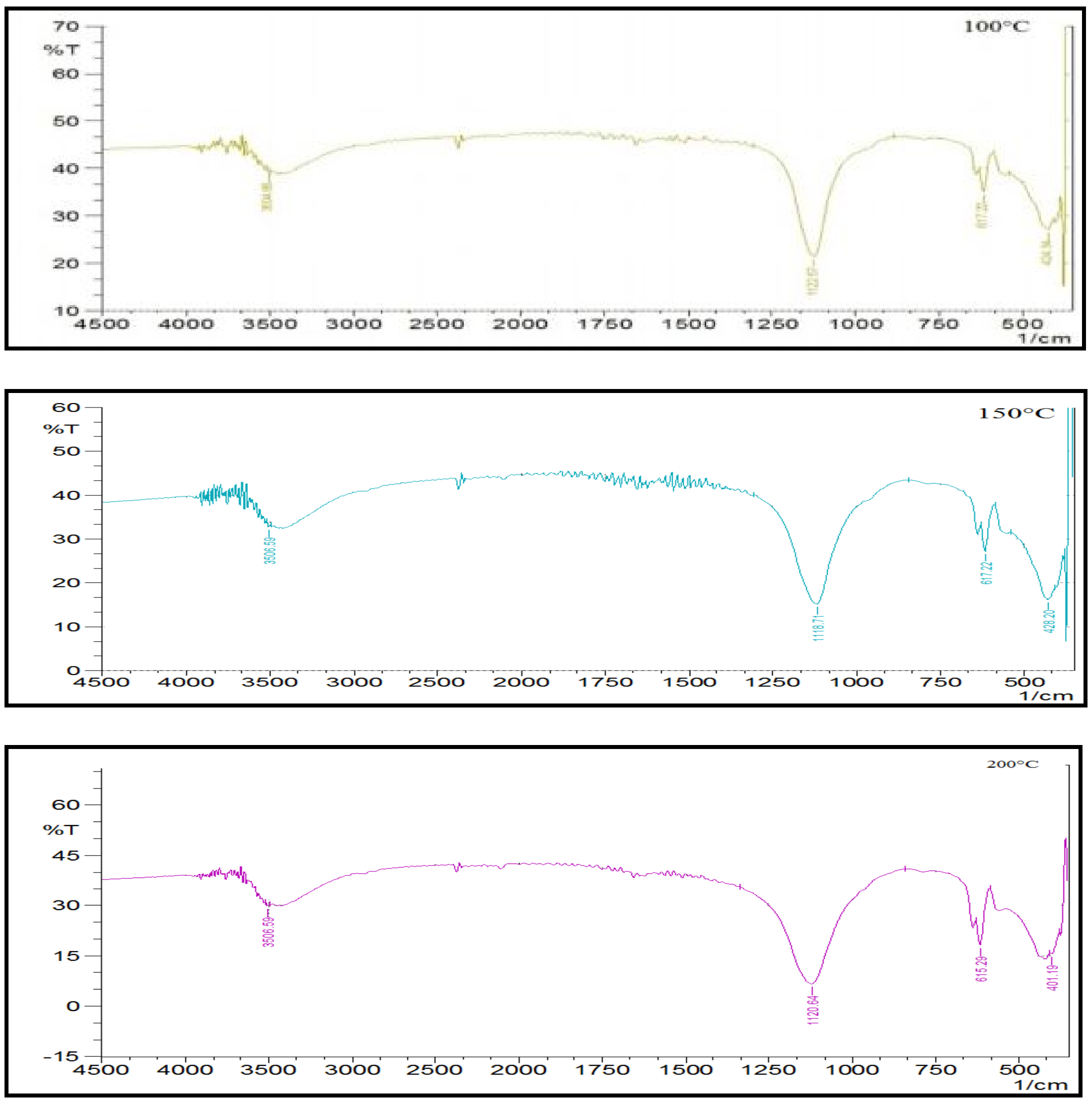

Fig. 5 FTIR Spectra of ZnO nanoparticles with various growth temperatures

The absorption bands at 617 cm^{-1}, 616 cm^{-1} and 615 cm^{-1} belong to C-Br stretching and those at 424 cm^{-1}, 428 cm^{-1} and 401 cm^{-1} for various growth temperatures 100^{0}C, 150^{0}C and 200^{0}C respectively are related to Zn-O stretching.

Fig. 6 presents the FT-IR spectra of ZnS nanoparticles for various growth temperatures. It is observed that the O-H stretching mode is represented by the absorption band at 3404.36 cm^{-1}, 3408.22 cm^{-1} and 3396.64 cm^{-1} for various growth temperatures 100^{0}C, 150^{0}C and 200^{0}C respectively. 1620.2 cm^{-1}, 1614.2 cm^{-1} and 1606.7 cm^{-1}absorption bands belong to O-H bending mode. Zn-S stretching is represented by absorption bands at 402 cm^{-1}, 403cm^{-1} and 443 cm^{-1}.

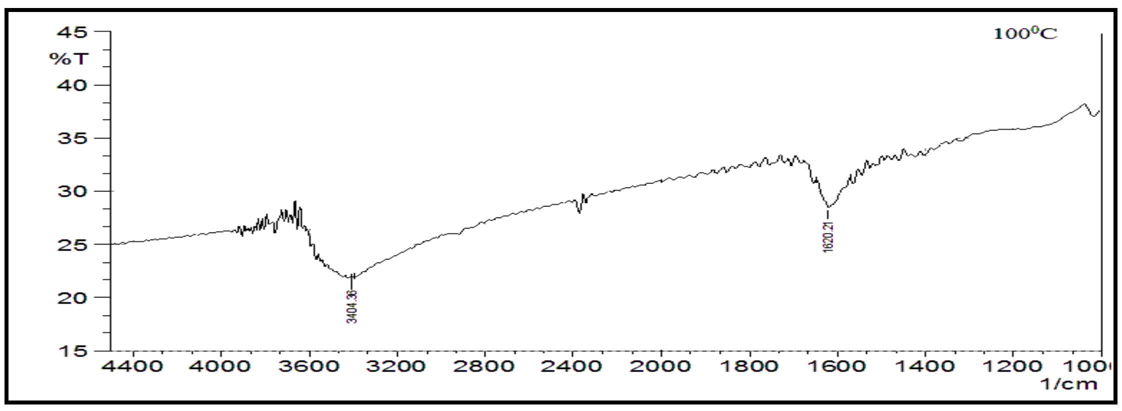

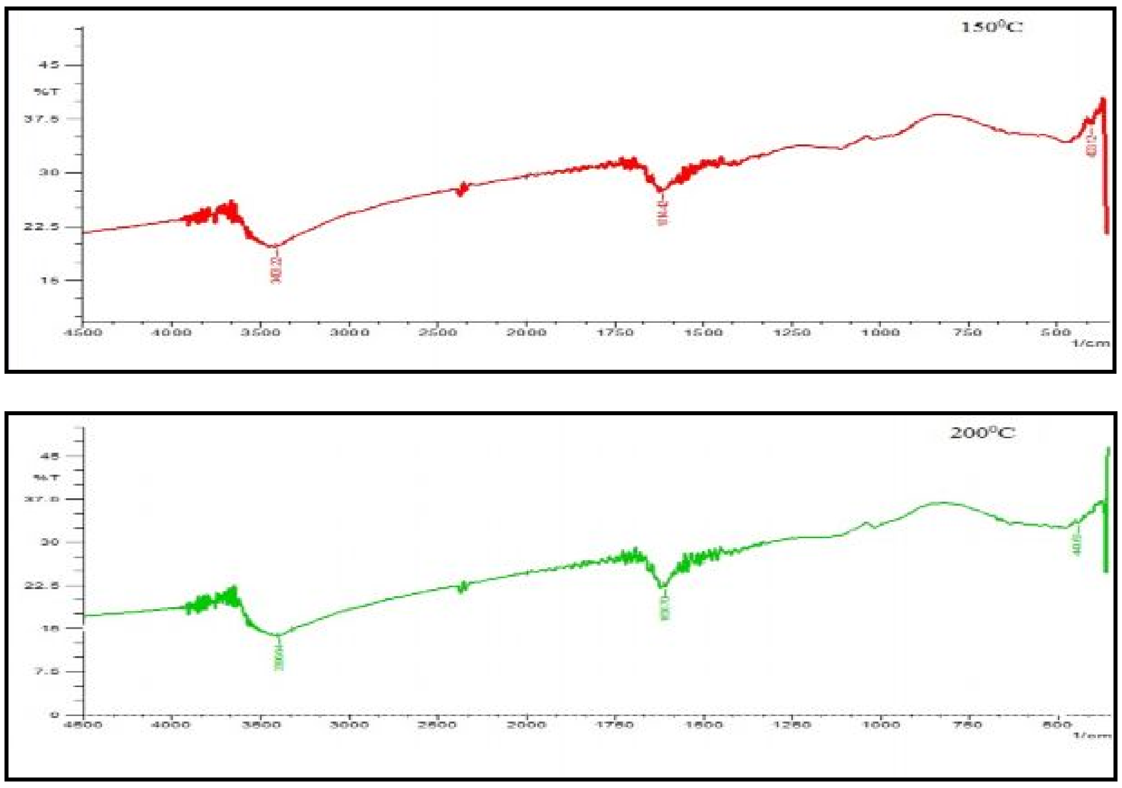

Fig. 6 FTIR Spectra of ZnS nanoparticles with various growth temperatures

3.4 SEM studies

Fig. 7 and 8 display the SEM images of ZnO and ZnS nanoparticles for various growth temperatures respectively. It can be seen from Fig. 7 that the morphology of the ZnO nanoparticles prepared at the growth temperatures 100^{0}C and 200^{0}C is spherical but for 150^{0}C, it is found to be sheets. From Fig. 8, it is observed that the morphology of the ZnS nanoparticles is cluster structure for the growth temperatures 100^{0}C and 150^{0}C. For 200^{0}C, the morphology of the ZnS nanoparticles is found to be the cluster of sheets.

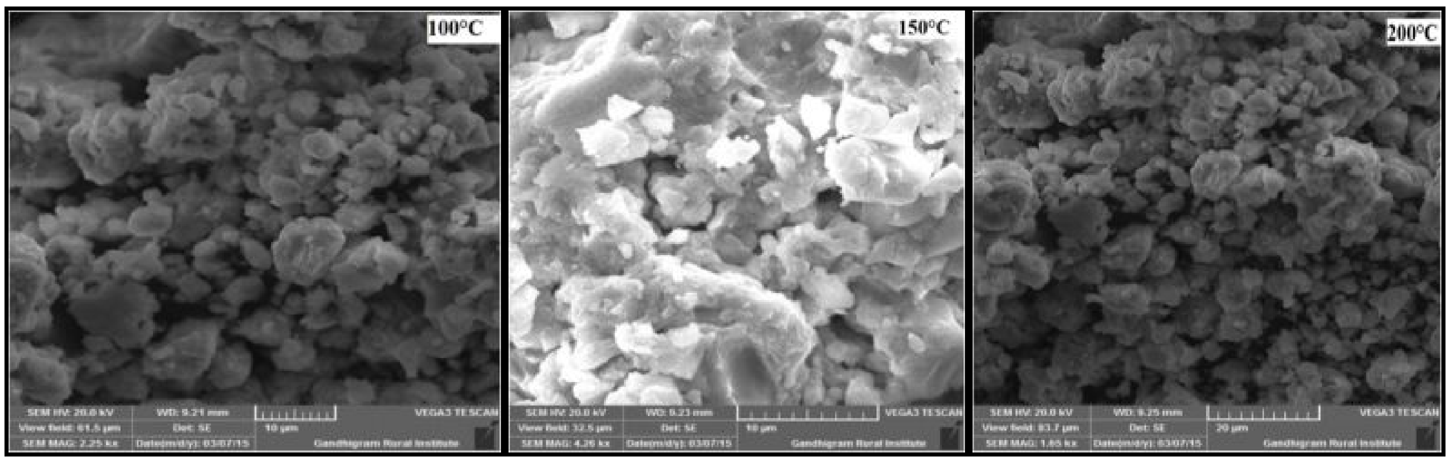

Fig. 7: SEM images of ZnO nanoparticles for various growth temperatures

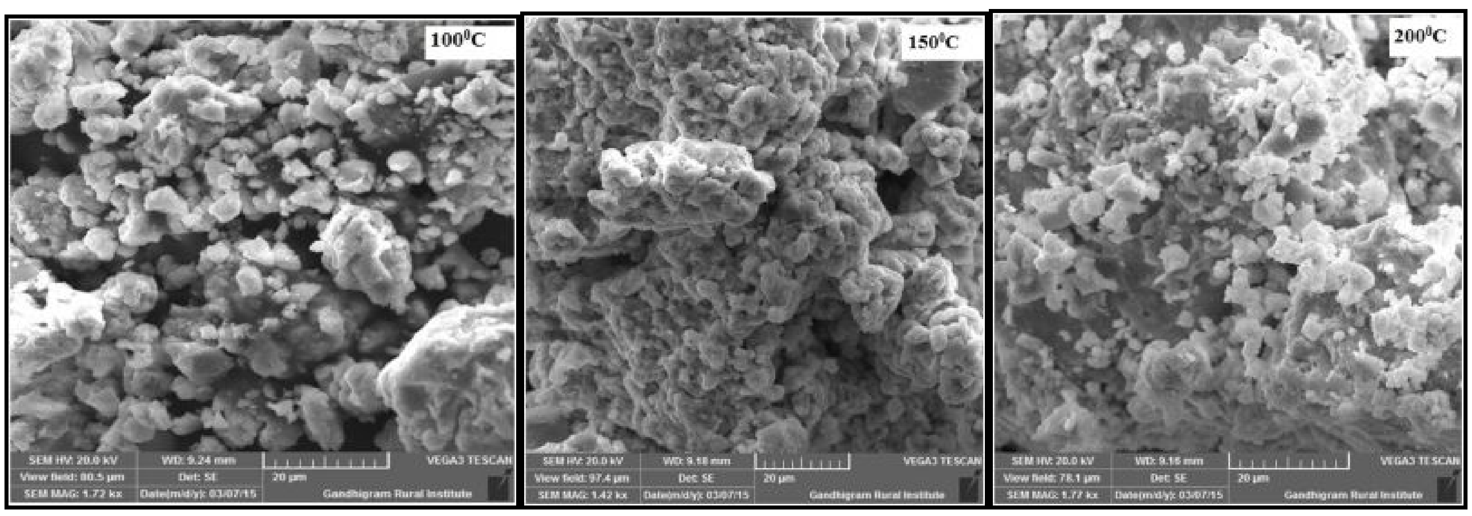

Fig. 8 SEM images of ZnS nanoparticles for various growth temperatures

3.5 Conductivity studies

ZnO and ZnS nanoparticles are dissolved in HCl at various concentrations and the conductivity is measured using a digital conductivity meter.

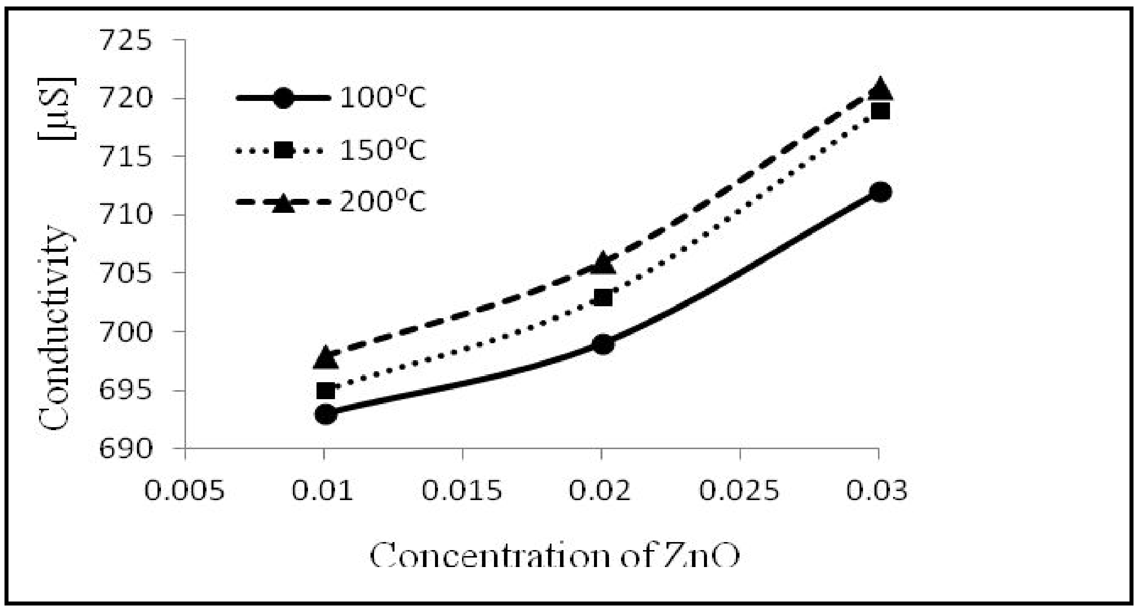

Fig. 9 Variation of conductivity of ZnO nanoparticles as a function of concentration for various growth temperatures

Fig. 9 and 10 show the variation of conductivity with the growth temperatures of ZnO and ZnS nanoparticles respectively. As expected, the conductivity increases with the growth temperature as well as concentration for both nanoparticles. Moreover, ZnO nanoparticles are found to be more conducting than ZnS nanoparticles.

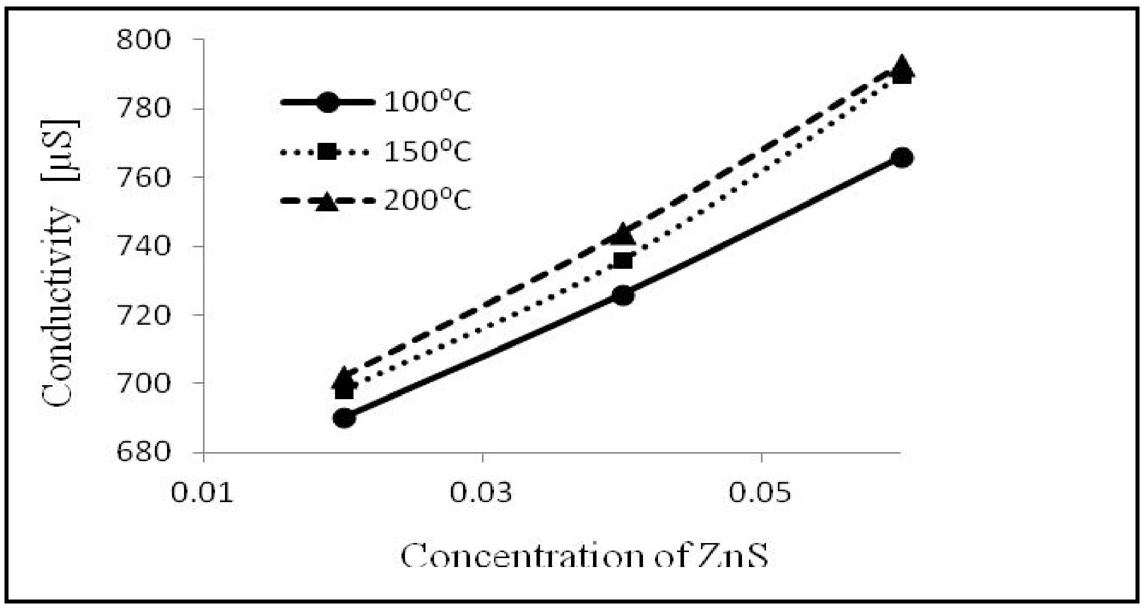

Fig. 10 Variation of conductivity of ZnS nanoparticles as a function of concentration for various growth temperatures

4. Conclusion

ZnO and ZnS nanoparticles are successfully synthesized by simple precipitation method with various growth temperatures. The XRD patterns clearly indicate that ZnO and ZnS nanoparticles prepared with various growth temperatures have hexagonal structure, but the size of the particles vary with growth temperature. The band gaps are calculated from the UV-Visible absorption spectra for each sample. The functional groups are analysed by FTIR spectra. SEM images show that the ZnO nanoparticles have the morphology of spherical for 100^0C and 200^0C, sheets for 150^0C. The morphology of ZnS nanoparticles is cluster structure for the growth temperatures 100^0C and 150^0C, cluster of sheets for 200^0C. The conductivity of both ZnO and ZnS nanoparticles increases with the growth temperatures as well as concentration. Comparing the characterization studies, it is found that ZnO nanoparticles are more application oriented (ie., more suitable for optoelectronic devices) than ZnS nanoparticles.

Acknowledgements

The authors thank the University Grants Commission (UGC), New Delhi, India for the financial support through Major Research Project (No. F. 42-836/2013 (SR) dated 22.03.2013) and the authorities of Jayaraj Annapackiam College for Women (Autonomous), Periyakulam, Theni District, Tamilnadu, India for the encouragements.

References

1. J. Han, F. Fan, C. Xu, S. Lin, M. Wei, X. Duan and Z. L. Wang, ZnO nanotube-based dye sensitized solar cell and its application in self-powered devices, Nanotechnology, 2010, 21, 405203.
2. S. Agrawal, R. Rane and S. Mukherjee, ZnO thinfilm deposition for TCO application in solar cell, 2013 doi: 10.1155/2013/718692
3. R. R. Thankalekshmi, S. Dixit and A. C. Rastogi, Doping sensitive optical scattering in zinc oxide nanostructured films for solar cells, Adv. Mat. Lett., 2013, 4, 9.
4. X. L. Cheng, H. Zhao, L. H. Huo, S. Gao and J. G. Zhao, ZnO nanoparticulate thin film: preparation, characterization and gas-sensing properties, Sens. Actuat. B Chem., 2004, 102, 248.
5. U. Ozgur, D. Hofstetter and H. Morko, Proceedings of the IEEE, ZnO devices and applications: A review of current status and future prospects, 2010, 98, 1255.
6. P. Thiagarajan, M. Kottaisamy and M. S. Ramachandra Rao, SrS:Ce/ZnS:Mn – A diband phosphor for near-UV and blue- LED converted white light emitting diodes, J. Luminescence, 2009, 129, 991.
7. M. Bredol and J. Merikhi, J. Mater, Sci., ZnS precipitation: morphology control, 1998, 33, 471.
8. H. R. Pouretedal, A. Norozi, M. H. Keshavarz and A. Semnani, Nanoparticles of zinc sulfide doped with manganese, nickel and copper as nanophotocatalyst in the degradation of organic dyes, J. Hazard Mater., 2009, 162, 674.
9. E. Mohagheghpour, M. Rabiee, F. Moztarzadeh, M. Tahriri, M. Jafarbeglou, D. Bizari and H. Eslami, Controllable synthesis, characterization and optical properties of ZnS:Mn nanoparticles as a novel biosensor, Mater. Sci. Eng. C., 2009, 29, 1842.
10. K. Hirabayashi and H. Kozawaguchi, ZnS: Mn electroluminescent device prepared by metal-organic chemical vapor deposition, Jpn. J. Appl. Phys., 1986, 25, 711.
11. P. M. Aneesh, K. A. Vanaja and M. K. Jayaraj, Synthesis of ZnO nanoparticles by hydrothermal method, Proceedings of SPIE, 2007, 6639, 66390J-1.
12. T. V. Kolekar, H. M. Yadav, S. S. Bandgar and P. Y. Deshmukh, Synthesis by sol-gel method and characterization of ZnO nanoparticles, Indian streams of research journal, 2011, 1, 1.
13. S. Sivakumar, P. Venkateswarlu, V. R. Rao and N. Rao, Synthesis, Charaterization and optical properties of zinc oxide nanoparticles, International Nano letters, 2013, 3, 1.
14. A. I. Cadis, E. J. Popovici, E. Bica, I. Perhaita, L. Barbu Tudoran, E. Indrea and L. Silaghi Dumitresch, Synthesis of Maganese doped Zinc sulphide nanocrystalline powders by wet chemical synthesis route, Digest Journal of Nanomaterials and Biostructures, 2011, 6, 1479.
15. B. Bodo, R. Singha and S. C. Das, Structural and optical properties of chemically synthesized ZnS Nanostructures, International Journal of Applied Physics and Mathematics, 2012, 2, 287.
16. S. Sasi Florence and Rita John, Synthesis and structure studies of ZnS semiconducting nanoparticles, Proceedings of ICMSRN, 2008, 131.

*****

ChemTech

International Journal of ChemTech Research
CODEN (USA): IJCRGG, ISSN: 0974-4290, ISSN(Online):2455-9555
Vol.9, No.08 pp 298-304, 2016

Effect of Temperature on Exciton Binding Energy in ZnSe/ $Zn_{1-x}Mg_xSe$ Quantum Well with Poschl-Teller Potential

P.Sathiyajothi, A.Anitha and M. Arulmozhi*

Department of Physics, Jayaraj Annapackiam College for Women (Autonomous) Periyakulam-625601, Theni District, Tamil Nadu, India.

Abstract : Exciton binding energies with temperature in a quantum well with Poschl-Teller Potential formed by $ZnSe/Zn_{1-x}Mg_xSe$ are calculated theoretically. Using the temperature dependent value of the effective mass and barrier height, the sub-band energies of the electron, heavy hole and light hole are calculated by variational method. Binding Energy of light hole exciton and heavy hole exciton are calculated as a function of the wellwidth for different temperatures. We have obtained the result that the binding energy of exciton decreases with enhancing the temperature and increases with reducing the wellwidth upto 12 nm for heavy hole exciton and 10 nm for light hole exciton, beyond this wellwidth the exciton binding energy decreases.
Keywords : Quantum well, Exciton, Binding energy, Poschl-Teller Potential, Temperature.

Introduction

In the last two decades, the low dimensional semiconducting systems have received much attention due to their potential application in optoelectronic devices such as displays[1], light emitting diodes[2], solar cells[3] and photovoltaic devices[4]. Elabsy[5] displays the variation of the binding energy of shallow donor in $GaAs/Ga_{1-x}Al_xAs$ superlattice with respect to temperature. Abraham and John Peter[6] have studied the exciton binding energy, interband emission energy and nonlinear optical properties in ZnMgSe quantum well with the effect of dielectric constant mismatch. Cingolani *et al.*[7] have investigated the excitonic states in $Zn_{1-x}Cd_xSe/ZnSe$ as a function of wellwidth and composition of Cd experimentally. Krystek *et al*[8] have reported the variation of energy and broadening parameter of the fundamental bandgap of ZnSe with different temperatures in the range 27 K to 370 K. Stachow *et al.*[9] have showed that the energy gap of CdMnTe epilayers depends upon the temperature. Several authors[10-11] have studied the effect of hydrostatic pressure on the binding energy of donor and acceptor in GaAs/GaAlAs quantum wells. Morales *et al*[12] have made theoretical studies on simultaneous effect of hydrostatic stress and electric field on donor binding energy in GaAs/GaAlAs. Arulmozhi[13] has studied the influence of temperature and pressure on the binding energy of hydrogenic donor in parabolic quantum well. Tevosyan *et al*[14] have computed the energy levels and direct interband absorption in a spherical quantum dot with Poschl-Teller potential. Mora-Ramos *et al*[15] have calculated the exciton binding energy in a cylindrical quantum dot with Poschl-Teller potential profile variationally. Effect of magnetic field on exciton binding energy in near triangular quantum well has been studied by Anitha and Arulmozhi[16]. II-VI semiconductors are extensively studied at nanoscale experimentally without doping[17-19], with doping[20-22] and with external perturbations[23, 24]. The purpose of the present work is to report the effect of temperature on binding energy of light and heavy hole exciton in quantum well with Poschl-Teller confining potential profile composed of $ZnSe/Zn_{1-x}Mg_xSe$ as a function of wellwidth.

Theory

The Hamiltonian of an exciton in effective mass approximation is given by[25]

$$\mathcal{H} = -\left[\frac{1}{\rho}\frac{\partial}{\partial\rho}\rho\frac{\partial}{\partial\rho}+\frac{1}{\rho^2}\frac{\partial^2}{\partial\varphi^2}\right]-\frac{\mu_{hi}^*}{m_e^*}\frac{\partial^2}{\partial z_e^2}-\frac{\mu_{hi}^*}{m_{hi}^*}\frac{\partial^2}{\partial z_h^2}+V(z_e)+V(z_h)-\frac{2}{r} \quad (1)$$

The subscripts h and e represent the hole and electron respectively. μ_{hi}^* is the reduced effective mass of the heavy hole (i = h) or light hole (i = l) and the electron, $r = \sqrt{\rho^2 + |z_e - z_h|^2}$. The reduced effective mass of the exciton is

$$\frac{1}{\mu_{hi}^*} = \frac{1}{m_e^*} + \frac{1}{m_{hi}^*} \quad (2)$$

The potential profile for the electron and hole in Poschl-Teller potential[15] are given by

$$V(z_i) = \begin{cases} V_0\dfrac{\mu_i\eta^2}{m^*_i}\left(\dfrac{\chi(\chi-1)}{sin^2(\eta z_i)}+\dfrac{\lambda(\lambda-1)}{cos^2(\eta z_i)}\right) & |z_i| < \dfrac{L}{2} \\ V_0 & |z_i| > \dfrac{L}{2} \end{cases} \quad (3)$$

where, V_0 is the barrier height, which depends on the composition x of Mg, $\eta = \frac{\pi}{2L}$.. The numerical values of χ and λ are chosen to be 1.0001. Since χ and λ are chosen to be same, a symmetric Poschl-Teller potential profile is considered. The trial wave function of the exciton in the Poschl-Teller potential[15] is taken to be

$$\Psi(\rho,\rho_e,\rho_h,z_e,z_h) = \Upsilon(\rho_e,\rho_h,z_e,z_h)e^{-\alpha\rho-\beta(z_e-z_h)^2} \quad (4)$$

where, $\Upsilon(\rho_e,\rho_h,z_e,z_h) = F(\rho_e)F(\rho_h)g(z_e)g(z_h)$ and $\rho = |\rho_e - \rho_h|$. Substituting the available values from Ref.15, the final trial wave function

$$\Psi = \begin{cases} NAe^{(-\alpha_e\rho-\beta_e(z_e-z_h)^2}e^{(-ar)} & -L/2 < z_e, z_h < L/2 \\ N_1 e^{(-\beta_e|z_e|)}e^{(-\beta_h|z_h|)}e^{(-ar)} & \end{cases} \quad (5)$$

where $A = J_0(\Theta_0\rho_e)J_0(\Theta_0\rho_h)\sin\left[\frac{\pi z_e}{2L}\right]^{\chi}\cos\left[\frac{\pi z_e}{2L}\right]^{\lambda} * \sin\left[\frac{\pi z_h}{2L}\right]^{\chi}\cos\left[\frac{\pi z_h}{2L}\right]^{\lambda}$. α_i, β_i and α are variational parameters, J_0 is the Bessel function of zeroth order with θ_0=2.40483 (Ref.15), N is the normalization constant. The continuity conditions at z_e = L/2 and z_h = L/2 relates the normalization constant N and N_1. We have computed expectation value of Hamiltonian as a function of the variational parameters using the Hamiltonian in (1) and the trial wave function in (5).

The binding energy of exciton is then given by

$$E_B = E_e + E_h - \langle\mathcal{H}\rangle_{min} \quad (6)$$

where, E_e and E_h are the ground state energies of electron and hole in bare quantum well respectively obtained variationally. $\langle\mathcal{H}\rangle_{min}$ is the minimized value of $\langle\mathcal{H}\rangle$ with respect to the variational parameters. By applying external temperature to the system, the band gap of the material changes, as[7]

$$E_g(T) = E_g(0) - \frac{\alpha T^2}{T+\beta} \quad (7)$$

where $E_g(0)$ is the energygap at T=0, α and β are Varshni coefficients, respectively.

The variation of effective mass, dielectric constant, barrier height according to the temperature is determined[12] by

$$\frac{1}{m*(T)} = 1 + E_p\left(\frac{2}{E_g(T)} + \frac{1}{E_g(T)+\Delta_0}\right) \quad (8)$$

In this equation E_p is an energy related to the momentum matrix element, Δ_0 is the spin-orbit splitting and $E_g(T)$ is the temperature dependence of the energy gap.

The variation of the barrier height with temperature is calculated by

$$V_0(T) = Q_c \Delta E_g(x, T) \quad (9)$$

Conduction band offset parameter Q_c is 0.70 eV and bandgap difference between quantum well and barrier layer material as a function of temperature and Mg concentration is given by

$$\Delta E_1 g\ (x, T) = \Delta E_1 g\ (x) + TC(x\ ) \quad (10)$$

Variation of dielectric constant with temperature is expressed as

$$\epsilon(T) = \epsilon(0)(1 + C(x)T) \quad (11)$$

The numerical values for this calculation is taken from the references (Ref. 6, 8).

Results and discussion

Table 1 represents the physical parameters of ZnSe, taken from references[6, 8, 27]. The difference of total band gap between $Zn_{1-x}Mg_xSe$ and ZnSe is determined[5] by the equation

$$\Delta E_g = 0.87x + 0.37x^2\ eV$$

The conduction band and valence band discontinuity is taken to be 70% and 30% of this band gap difference respectively.

Table 1: Physical parameters of ZnSe

Physical parameters	Absolute values
Mass of Electron (m_e)	0.16 m_0
Mass of heavy hole (m_h)	0.6 m_0
Mass of light hole (m_l)	0.145 m_0
Dielectric Constant (ϵ)	8.8
Spin-Orbit splitting (Δ_0)	0.43 eV
Energy gap at 0 K ($E_g(0)$)	2.8 eV
Varshni co-efficient (α)	7.3x10^{-4} eV/^{0}K
Varshni co-efficient (β)	295^{0}K
Linear temperature co-efficient (C)	1.71x10^{-4} K^{-1}

where m_0 is the free electron mass.

Fig.1 shows that the variation of binding energy of heavy hole exciton as a function of well width L for different temperatures T for a barrier height corresponding to the Mg composition x = 0.3. When L is reduced, the binding energy increases. If the L is reduced further, they reach a maximum value and then start to decrease rapidly. The peak value of binding energy is observed at L = 12 nm, for all values of T.

The behavior of binding energy of light hole exciton as a function wellwidth L for different temperatures is shown in Fig. 2. The peak value of binding energy is observed at L = 10 nm, for all values of T. It is also noted that the binding energy of heavy hole exciton is more than that of the light hole exciton. So the hh-exciton is more bound than the lh-exciton, which is due to $m_{hh}^* > m_{lh}^*$. In both cases, the decrease in wellwidth produces a spreading of the wave function, which causes a lowering in the binding energy. The contribution of confinement is dominant for smaller wellwidth and make the electron unbound, and tunnels through the barrier. This behavior is similar to those reported in Ref. 15 for a quantum dot of same profile. But a decrease in binding energy for narrow wells is observed in quantum wells.

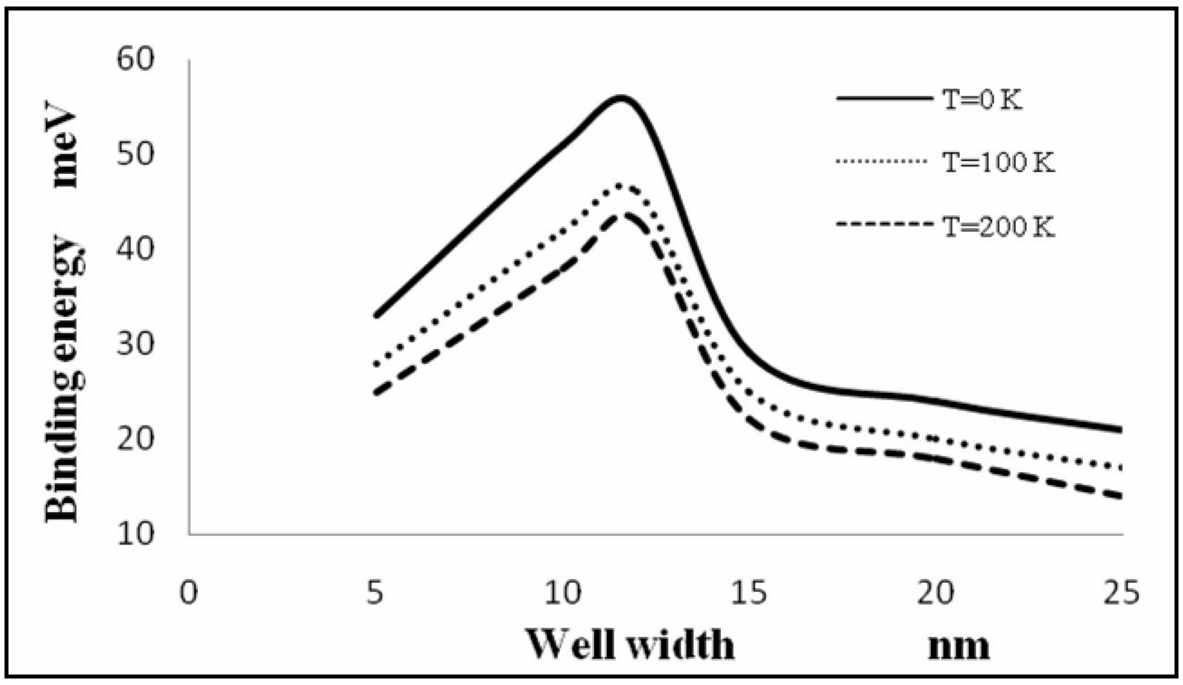

Fig.1. Variation of the binding energy of hh-exciton as a function of wellwidth for different temperatures

Fig.3 shows that the variation of binding energy of heavy hole exciton as a function of temperature for different wellwidths, for a barrier height corresponding to the Mg composition x = 0.3. As temperature increases, the binding energy decreases[4].

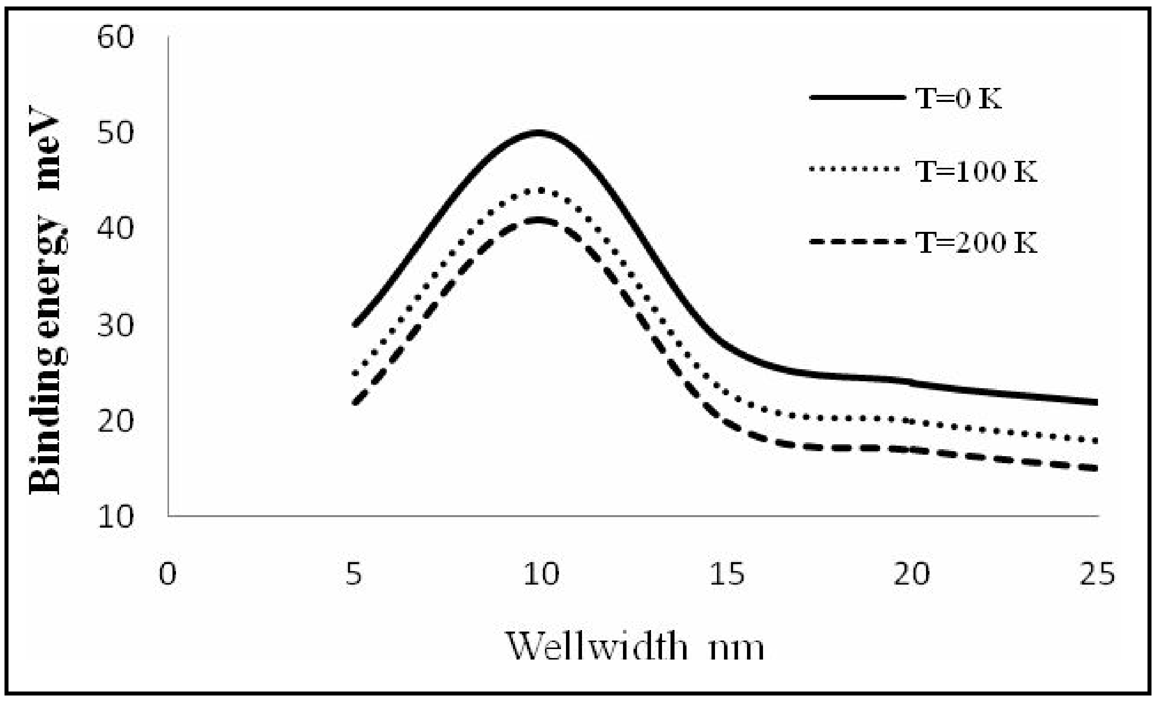

Fig.2. Variation of the binding energy of lh-exciton as a function of wellwidth for different temperatures

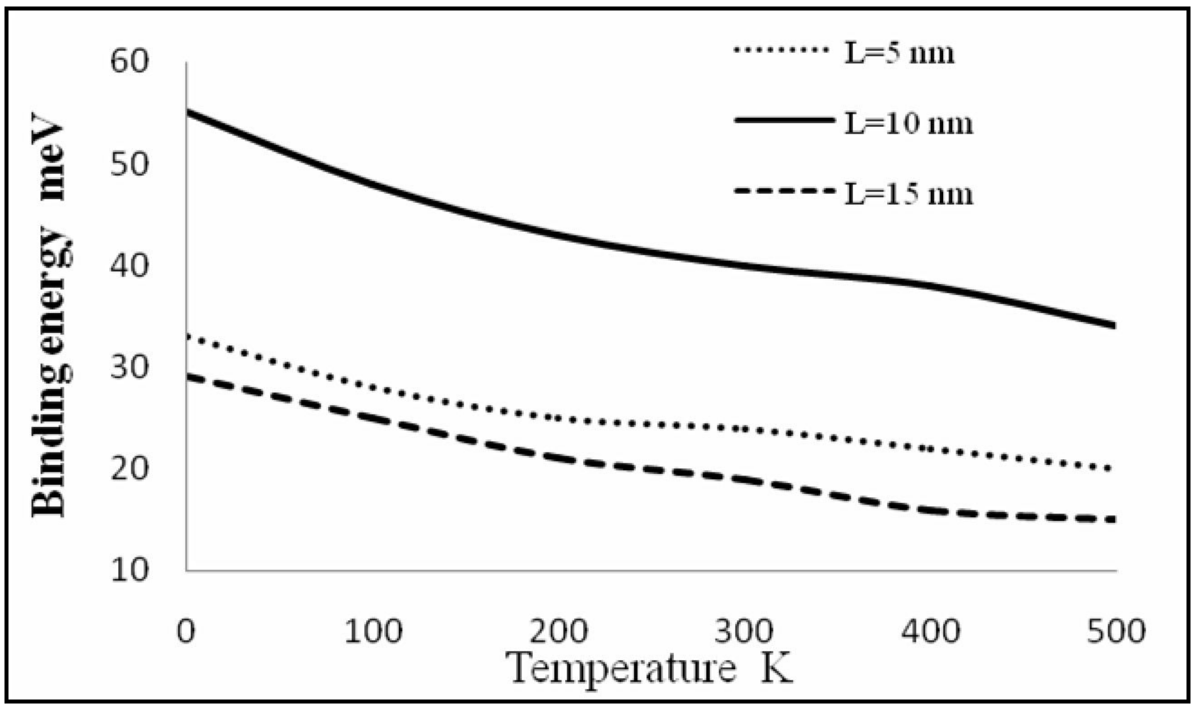

Fig.3. Variation of the binding energy of hh-exciton as a function of temperature for different wellwidths

The behavior of binding energy of light hole exciton as a function of temperature for different wellwidths is shown in Fig. 4. For a given quantum well thickness, there is a decrease in the binding energy of the exciton, when the temperature is increased, because increasing the temperature, decreases the values of both the effective mass and the barrier height.

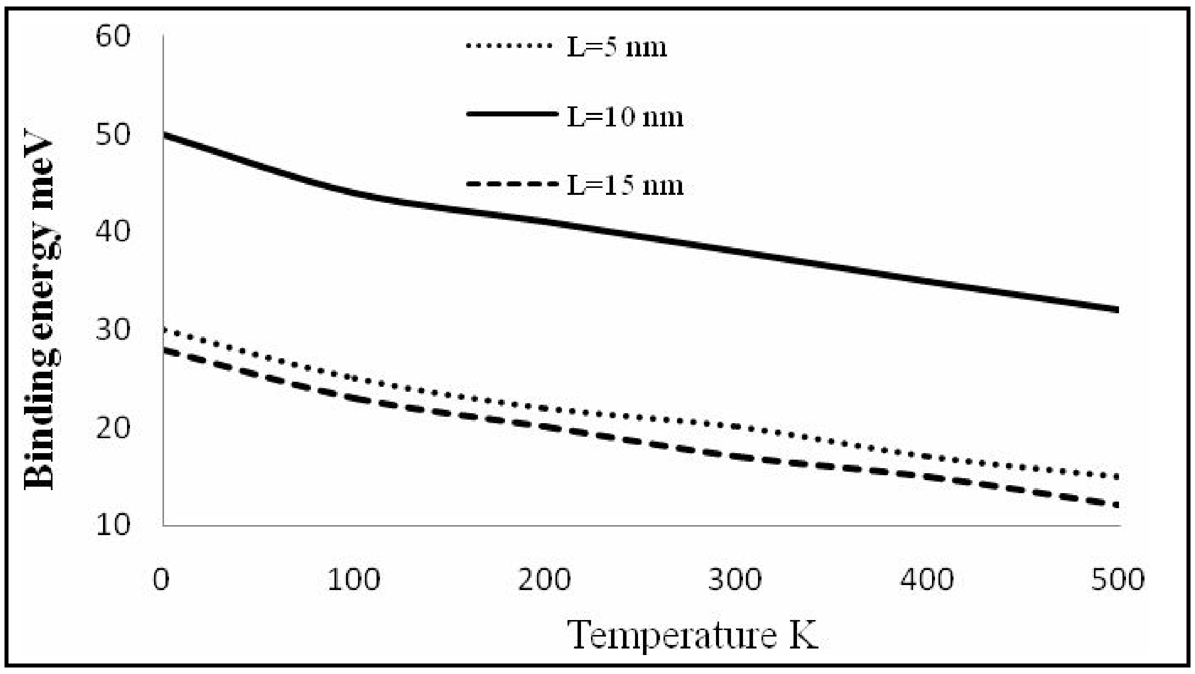

Fig.4. Variation of the binding energy of lh-exciton as a function of temperature for different wellwidths

Conclusions

Binding energies of hh-exciton and lh-exciton in the presence of temperature in a quantum well with Poschl-Teller potential are calculated variationally. A maximum value of binding energy occurs at a critical well width (12 nm for hh-exciton and 10 nm for lh-exciton), same for all values of temperature. For a fixed wellwidth, the binding energy decreases as temperature increases. For same wellwidth and temperature, the binding energy of hh-exciton is more than that of lh-exciton.

Acknowledgements

The authors thank the University Grants Commission (UGC), New Delhi, India for the financial support through Major Research Project (No. F. 42-836/2013 (SR) dated 22.03.2013) and the authorities of Jayaraj Annapackiam College for Women (Autonomous), Periyakulam, Theni District, Tamilnadu, India for the encouragements.

References

1. Colvin V. L., Schlamp M .C. and Alivisatos A. P., Light-Emitting-Diodes made from cadmium Selenide Nano crystals and a semiconducting polymers, Nature, 1994, 370 354-357.
2. Tessler N., Medvedev V., Kazes M., Kan S. and Banin U., Efficient near infrared polymer nanocrystal light emitting diodes, Science, 2002, 295, 1506-1508.
3. Gal D., Hodes G., Hariskos D., Braunger D. and Schock H.W., Size-quantized CdS films in thin film $CuInS_2$ solar cells, Applied physics letters, 1998, 73, 3135-3137.
4. Thirumavalavan S., Mani K. and Sagadevan S., Nanostructured Semiconductor Thinfilms and Its Applications: An Overview, International Journal of ChemTech Research, 2015, 8, 554-558.
5. Elabsy A. M., Temperature dependence of shallow donor states in GaAs-$Al_xGa_{1-x}As$ compositional superlattice, Physica scripta, 1992, 46, 473-475.
6. Mark J. A. H. and Peter A. J., Dielectric confinement on exciton binding energy and nonlinear optical properties in a strained $Zn_{1-xin}Mg_{xin}Se$ /$Zn_{1-xout}Mg_{xout}Se$ quantum well, Journal of semiconductor, 2012, 33, 092001-1-092001-7.
7. Chingolani R., Prete P., Greco D., Giugno P. V., Lomascolo M., Rinaldi R. and Calcagnile L., Exciton Spectroscopy in $Zn_{1-x}Cd_xSe$/ZnSe quantum wells, Phy.Rev B, 1995, 51, 5176-5183.
8. Krystek W., Malikova L., Pollak F. H., Tamargo M. C., Dal N., Zeng L. and cavus A., Contactless Electro reflectance study of temperature dependence of fundamental bandgap of ZnSe, ACTA PHYSICA POLONICA A, 1995, 88, 1013-1017.
9. Stachow A., Khoi W. M., Twardowski A., Karczewski G., Janik E., Wojtowicz T. and Kossut J., Temperature dependence of energy gap of highly concentrated $Cd_{1-x}Mn_xTe$ $(0.6 < x < 1.0)$ epilayers, ACTA PHYSICA POLONICA A, 1995, 88, 913-916.
10. Lopez S. Y., Porras-Montenegro N. and Duque C. A., Binding energy and density of shallow impurity states in GaAs-(Ga,Al)As quantum wells: effect of an applied hydrostatic stress, Semicond. Sci. Technol, 2003, 18, 718-722.
11. Lefebvre P., Gil B. and Mathieu H., Effect of hydrostatic pressure on GaAs-GaAlAs microstructures, Phy.Rev. B., 1987, 35, 5630.
12. Morales A. L., Montes A., Lopez S. Y. and Duque C. A., Simultaneous effects of hydrostatic stress and an electric field on donors in GaAs-(Ga,Al)As quantum well, J. Phys: Condens. Matter, 2002, 14, 987-995.
13. Arulmozhi M., Donor binding energies in nano quantum wells with external perturbations, OJP, 2012, 4, 7-15.
14. Tevosyan H. K. H., Hayrapetyan D. B., Dvoyan K. G. and Kazayan E. M., Direct interband light absorption in a spherical quantum dot with the modified poschl-teller potential, world scientific, 2012, 15, 204-210.
15. Mora-Ramos M. E., Barseghyan M. G. and Duque C. A., Excitons in a cylindrical GaAs Poschl Teller quantumdot, Phys. Status Solidi B, 2001, 248, 1412-1419.
16. Anitha A. and Arulmozhi M., Magnetic field effects on the exciton binding energy in a near triangular quantum well, International Journal of ChemTech Research, 2015, 7, 1438-1444.
17. Rukade D., Dalvi T., Saitavdekar J., Jha A., Mahadkar A., Kulkarni N. and Bhattacharyya V., Influence of annealing on the characteristics of nanostructure ZnSe thin films, International Journal of ChemTech Research, 2015, 7, 963-966.
18. Manjulavalli T. E. and Kannan A. G., Structural and optical properties of ZnS thin films prepared by chemical bath deposition method, International Journal of ChemTech Research, 2015, 8, 396-402.
19. Vanaja A. and Rao K. S., Influence of Precursors on Structural and Optical Properties of ZnO Nanopowders Synthesized in Hydrolysis medium, International Journal of ChemTech Research, 2016, 9, 691-698.
20. Malarkodi P. and Kannan J. C., Structural and optical properties of $Zn_xCd_{1-x}O$ nanoparticles, International Journal of ChemTech Research, 2015, 8, 522-529.
21. Mahmud Abba Ibrahim, Annie Sujatha R., Mani Rahulan K. and Pandian C., Structural and Optical characteristics of Graphene nanoplatelets doped with Zinc Sulphide, International Journal of ChemTech Research, 2015, 7, 1162-1166.
22. Malarkodi P. and Kannan J.C., Microwave assisted Synthesis and Characterization of Cu^{2+} doped ZnO Nano particles, International Journal of PharmTech Research, 2016, 9, 393-399.

23. Sugapriya S., Lakshmi S. and Senthilkumaran C. K., Effect on Annealing Temperature on Zno Nanoparticles, International Journal of ChemTech Research, 2015, 8, 297-302.
24. Saravanakumar M., Agilan S. and Muthukumarasamy N., Effect of Annealing Temperature on Characterization of ZnO thin films by sol-gel method, International Journal of ChemTech Research, 2014, 6, 2941-2945.
25. Arulmozhi M. and Balasubramanian S., Binding energy of hydrogenic donor and of a Wannier exciton in the $|z|^{2/3}$ quantum well, Phy. Rev. B, 1995, 51, 2592.
26. Adachi S., Optical properties of Crystalline and Amorphous semiconductor materials and its fundamental principles, Springer science, 1999.
27. Rajakarunayake Y., Miles R. H., Wu G. Y. and McGill T. C., Band offset of the ZnSe-ZnTe superlattices: A fit to photoluminescence data by k.p. theory, J. Vac. Sci. Technol. B, 1988, 6, 1354-1359.

*****

Indian Journal of Science and Technology, *Vol 9(40), DOI: 10.17485/ijst/2016/v9i40/92696, October 2016*
ISSN (Print) : 0974-6846
ISSN (Online) : 0974-5645

A Comparative Analysis of the Properties of Zinc Oxide (ZnO) Nanoparticles Synthesized by Hydrothermal and Sol-Gel Methods

S. Preethi, A. Anitha and M. Arulmozhi*

Department of Physics, Jayaraj Annapackiam College for Women (Autonomous), Periyakulam – 625601, Theni, Tamil Nadu, India; preethivinikrish@gmail.com, anitha.jayarani@gmail.com, arulpkm@yahoo.co.in

Abstract

Objective: To study the structural, optical and conductivity properties of ZnO nanoparticles synthesized by two different methods such as hydrothermal and sol-gel methods. **Methods/Analysis:** ZnO is synthesized at various temperatures 100°C, 150°C and 200°C using hydrothermal method with oxalic acid and zinc acetate and using sol-gel method with sodium hydroxide, zinc chloride and zinc nitrate. **Findings:** For both methods, the average crystal size determined by X-ray Diffraction **(**XRD) is noted to be in the range 20–30 nm. The pattern confirmed the composition, crystallinity and the synthesized products are ZnO with high purity and the hexagonal phase. The absorption peak of ZnO nanoparticles has a blue-shift compared with that of the bulk. In hydrothermal method, the band gap is large (i.e) from 4.4–4.9 eV and in the sol-gel method 3.5–3.9 eV. ZnO nanoparticles synthesized by both methods exhibit similar luminescence. Scanning Electron Microscopy (SEM) pictures reveal the morphology as near-spherical prismatic nano particles for hydrothermal method and as nanoflakes for sol-gel method. The Energy Dispersive X-ray Spectroscopy (EDAX) analysis confirms the presence of ZnO only and no other element. The conductivity decreases with the growth temperature as well as the concentration of the ZnO samples by sol-gel method. In contrast, the conductivity of the sample prepared by hydrothermal method, increases with the growth temperature but decreases with the concentration. **Novelty:** In addition, conductivity of the synthesized ZnO nanoparticles is measured for various concentrations of ZnO. The results of both the methods are compared with each other and with those reported in the literature.

Keywords: Conductivity, EDAX, PL, SEM, XRD, ZnO

1. Introduction

Zinc Oxide (ZnO) is a material with multifunctional and salient properties such as high photostability, low dielectric constant, high chemical stability, high electrochemical coupling co-efficient and broad range of radiation absorption. In typical wurtzite hexagonal structure, ZnO crystallizes with the arrangement of Oxygen atoms in hexagonally closed structure, while the distorted tetrahedron structure is occupied by Zinc atoms. It has a wide band gap of 3.37 eV and large exciton binding energy of 60 meV even at room temperature. It provides the greatest assortments of very rich variety of structures among all known materials. ZnO is one of the extensively studied semiconductor materials because of its interest as a fundamental study and also its applied aspects such as, luminescence, electronics, optoelectronics, photocatalysis, varistors, solar energy conversion, laser technology, medicine, transparent UV protection films and chemical sensors.

Optical and surface morphological properties of ZnO nanomaterials synthesized by hydrothermal method have been investigated[1]. The use of the sol-gel synthesis for the production of ZnO nanopowders has been proposed and the structure and morphology have been investigated with respect to the type of precursor, temperature of synthesis and dripping time[2]. The effects of reaction temperatures,

**Author for correspondence*

the precursors concentration and growth time on the properties of ZnO nanopowders synthesized by hydrothermal method have been invesigated[3]. The morphology, crystallite size and optical properties of ZnO nanopowders synthesized by simple precipitation method were investigated. They also correlated the optical properties with morphology and crystallite size[4]. ZnO nanoparticles were synthesized by wet chemical method, based on cyclohexylamine, in aqueous and ethanolic media and tested for the photogradation of cyanide ions[5].

A quick process for preparation of ZnO nanoparticles with the use of microwave irradiation and the advantages in yield and reaction time were reported[6]. ZnO nanoparticles were synthesized using wet chemical method at room temperature and characterized[7]. The growth mechanism and modeling of ZnO nanopowders have been presented[8]. The characterization of ZnO nanoparticles synthesized by sol-gel method using zinc acetate as a precursor, acetic acid as the complexing agent and triton X-100 as a surfactant has been studied[9]. One pot synthesis of ZnO nanoparticles via Chemical and Green method using aqueous leaf extract of Corriandrum Sativum have been reported[10]. The influence of the reaction conditions and sintering on the properties of ZnO nanoparticles synthesized by sol-gel process assisted by Polyvinyl Alcohol (PVA) have been investigated[11]. Reviews of the growth, properties and applications of ZnO nanoparticles have been presented[12, 13]. The structural and optical properties of nanocrystalline ZnO powders controlled by the effect of PVP concentration in sol-gel method has been studied[14]. The influence of cobalt doping on optical properties of ZnO nanoparticles synthesized by simple solution method has been analysed[15]. The effect of Al doping on the properties of ZnO nanoparticles fabricated by Sol-gel method has been studied[16].

In the present work, hydrothermal and sol–gel methods are used to prepare ZnO nanoparticles. The optical properties, particle size, conductivity and crystallinity of the synthesized ZnO nanopowders are investigated. The results of the two methods are compared with each other and with those reported in the literature.

2. Experimental Procedure: Synthesis of ZnO Nanoparticles

2.1 Hydrothermal Method

Aqueous solution of Oxalic acid and Zinc acetate dihydrate, under hydrothermal condition, are used. Oxalic acid with 0.1M molarity is taken in a beaker. Zinc acetate dihydrate ($Zn(CH_3COO)_2.2H_2O$) solution with 0.1M molarity is mixed with the oxalic acid and this mixture is left for stirring for 6 hours. A white precipitate is formed. Impurities are removed by filtering and washing with acetone and de-ionized water. It is then dried with various temperatures such as 100°C, 150°C and 200°C for 2 hours.

2.2 Sol-gel Method

Zinc nitrate ($Zn(NO_3)_2$), Zinc chloride ($ZnCl_2$) and Sodium hydroxide (NaOH) are used as precursors. 1.0M molarity of NaOH is prepared with distilled water and continuously stirred at a desired reaction temperature, 50°C. After obtaining the desired temperature, a solution of $ZnCl_2$ 0.5M and another of $Zn(NO_3)_2$ are slowly added (dripping for 26 min) under constant stirring for 2 hours. A colourless precipitate of ZnO is formed and then the colour of the precipitate changes to white. The solution was agitated for a period of two hours, maintaining the desired temperature. The gel formed was filtered, washed with de-ionized water several times and dried for various temperatures such as 100°C, 150°C and 200°C.

All the chemicals used in all the methods of synthesis are of analytical reagent grade.

3. Results and Discussion: Characterization Studies

3.1 Structural Studies – X-ray Diffraction (XRD) Analysis

XRD patterns of the grown ZnO samples are recorded with the intensity data over a 2θ range of 20°-80°. Figure 1 shows the XRD patterns of ZnO nanoparticles prepared by 1. hydrothermal method and 2. sol-gel method at different annealing temperatures.

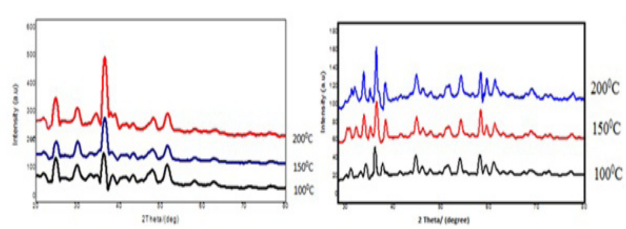

(a) (b)

Figure 1. XRD patterns of ZnO nanoparticles prepared by **(a)** hydrothermal method and **(b)** sol-gel method at different annealing temperatures.

It is observed that,

- The nature of ZnO is good crystalline which is confirmed by the sharp and intense diffraction peaks and they agree with the reported Joint Committee on Powder Diffraction Standards (JCPDS) data.
- The particles have a hexagonal phase with Wurtzite structure with hexagonally closed pack lattice of oxygen atoms and half the tetrahedral sites of zinc atoms[11].
- No characteristic peaks other than ZnO are observed which confirms that the synthesized products are of high purity.
- The intensity of the diffraction peaks increases and becomes sharper with increase in temperature, implying that the crystalline structure tends to have more integrity.
- A definite line broadening of the diffraction peaks is an indication that the synthesized ZnO materials are in nanometer range.

  The size (D) of the particles is calculated from the XRD line broadening measurement by Debye Scherrer's formula,

$$D = \frac{0.89\lambda}{\beta cos\theta} \quad (1)$$

- where λ is the wavelength of (Cu K_α) X-rays, θ is the half diffraction angle and β is the Full Width at Half Maximum (FWHM).

The particle morphology of the ZnO nanoparticles is greatly influenced by the reaction temperature. In both synthesis methods, there is a decrease in crystallite size when temperature increases and the decrease in hydrothermal method is steeper than in sol-gel method. The crystallite size is same in both methods at 150^{0}C. FWHM increases with the reaction temperature but the size of the ZnO nanoparticles decreases with it, which may be due to the following reasons. 1. different crystallographic planes have different growth rates and 2. the quantum confinement effects, which is also confirmed by the Ultraviolet-Visible (UV-Vis) Absorption Studies. This behaviour is in contrast to that observed by Aneesh et al[3], where the FWHM decreases and the crystallite size increases.

3.2 Morphological Studies - Scanning Electron Microscopy (SEM)

Figure 2 shows the morphology of the samples observed in SEM. These images confirm the formation of ZnO nano powders. The morphology is analysed for various temperatures such as 100^{0}C, 150^{0}C and 200^{0}C. SEM pictures reveal the morphology as near-spherical prismatic nanoparticles for hydrothermal method and as nanoflakes for sol-gel method.

3.3 Dispersion Studies – Energy Dispersive X-ray Spectroscopy (EDAX)

EDAX spectra are shown in Figure 3 for the ZnO nanoparticles prepared by 1. hydrothermal method and 2. sol-gel method. Element with large concentration in the sample can be noted from the EDAX spectrum, as the one with highest peak. EDAX reveals the presence of required elemental composition of both Zinc (Zn) and Oxygen (O) in the samples.

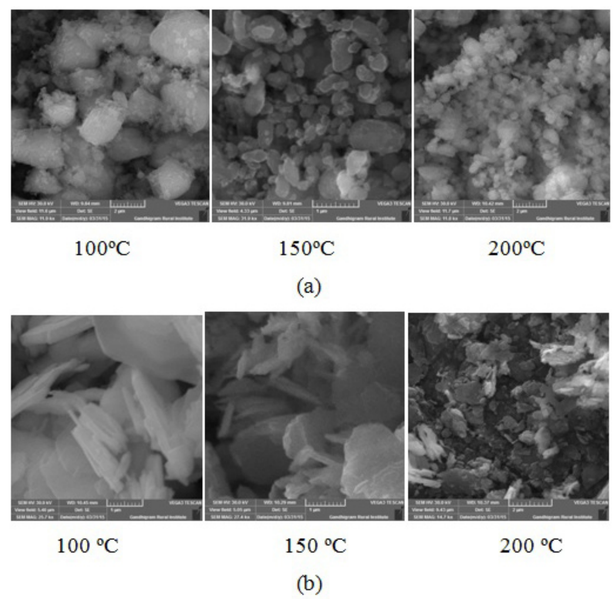

Figure 2. SEM images of ZnO nanoparticles prepared by **(a)** hydrothermal method and **(b)** sol-gel method.

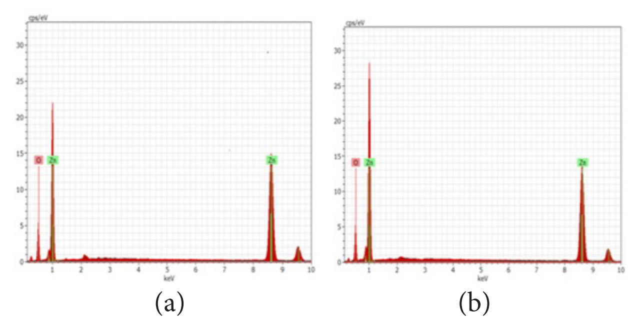

Figure 3. EDAX spectrum of ZnO nanoparticles prepared by **(a)** hydrothermal method and **(b)** sol-gel method.

3.4 Optical Studies -Ultraviolet-Visible (UV-Vis) Absorption Studies

Figure 4 depicts the spectra of optical absorption in ZnO nanoparticles prepared by 1. hydrothermal method and 2. sol-gel method annealed at various temperatures, 100^0C, 150^0C and 200^0C. UV-Vis absorption of ZnO nanoparticles was recorded in the wavelength range of 200 – 800 nm.

ZnO has a band gap of 3.37 eV and hence a peak in the absorption spectra[7] is expected to occur at ≈ 358 nm. Exciton binding energy in ZnO ≈ 60 meV and hence shows unique features of exciton absorption.

It is observed that,

- The absorbance increases with temperature, and hence, there should be a decrease in band gap.
- Hydrothermal method shows a widened shoulder peaks at 252, 265 and 277 nm implying the absorption spectra with a strong blue shift. This indicates that the exciton in ZnO has a Bohr radius larger than the size of the ZnO nanopowders. These results are in good agreement with those of Oladiran and Olabisi[7].
- Strong excitonic absorption peaks at 311, 318 and 330 nm in sol-gel method confirm the lower particle size of ZnO[1] and the photosensitivity of the sample in the UV region[2].
- No emission peaks are observed indicating the absence of free exciton recombination via a collision process of exciton-exciton and oxygen interstice.

The band gap energies are calculated by extrapolating the straight line portion of the plot of modified Kubelka-Munk function $(\alpha h\nu)^2$ against photon energy[4] ($h\nu$), as shown in Figure 5.

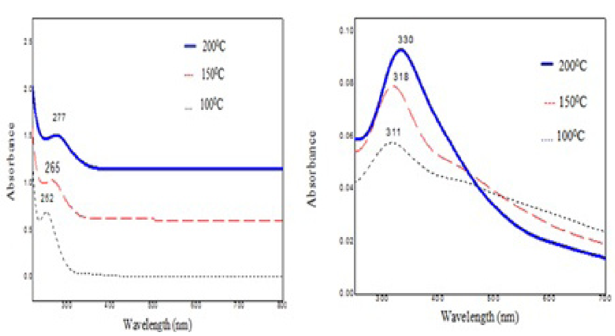

(a) (b)

Figure 4. UV-Vis absorption spectra of ZnO nanoparticles by **(a)** hydrothermal method and **(b)** sol-gel method at different annealing temperatures

The UV cut-off provides the value of band gap in the range 4.4 to 4.9 eV in hydrothermal method and 3.5 to 3.9 eV in sol-gel method higher than that of bulk ZnO of 3.37 eV. Hydrothermal method shows larger blue shift than sol-gel method. This blue shift, (the absorption maximum shifted to lower wavelengths), is due to quantum confinement effects[3] that led to the decrease in the particle size smaller than the exciton Bohr radius for ZnO and the radiative recombination of photo-generated holes with singularly ionized oxygen vacancies[17, 18].

3.5 Photoluminescence (PL) Emission Studies

Both physical and applied aspects of ZnO nanoparticles can be well understood from the luminescence studies of them. Figure 6 depicts the photoluminescence spectrum of ZnO nanoparticles synthesized by 1. hydrothermal and

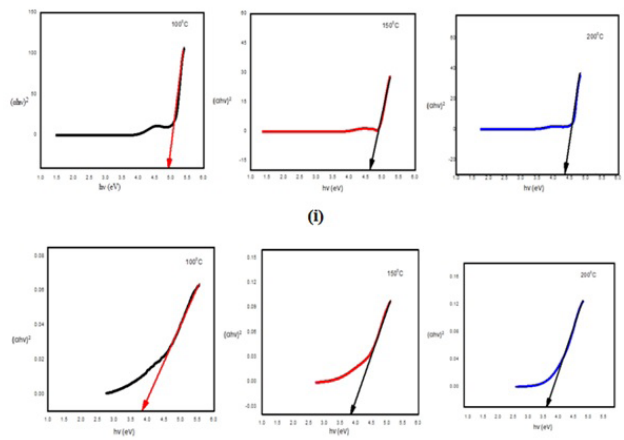

Figure 5. UV band gap measurement for **(i)** hydrothermal method and **(ii)** sol-gel method at different annealing temperatures.

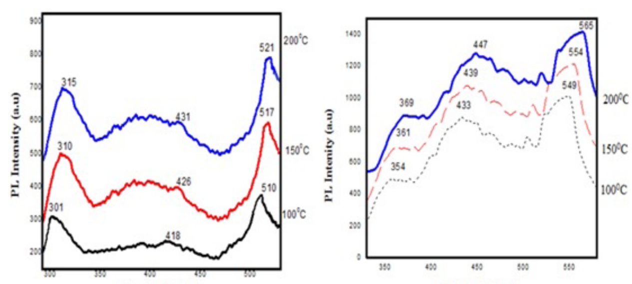

(a) (b)

Figure 6. PL spectrum of the ZnO nanoparticles prepared by **(a)** hydrothermal method and **(b)** sol-gel method with different annealing temperatures.

2. sol-gel methods. It is observed that ZnO nanoparticles synthesized by both the methods exhibit similar luminescence.

- Strong emission peaks centred at 301, 306 and 312 nm for hydrothermal method and 354, 361 and 368 nm for sol-gel method are observed. The blue shift in the bandgap of ZnO nanoparticles is confirmed by these excitation peaks which correspond to the transition from band to band[3].
- Blue emission peaks observed at 418, 426 and 431 nm for hydrothermal method and 433, 439 and 447 nm for sol-gel method are the artifacts arising due to the improper alignment of the measurement set-up or the inappropriate choice of components in a PL system.
- Photo-generated holes recombine radiatively with electrons created by specific defect in the surface or subsurface which are of singly ionized charge state[1, 6]. A transition occurs between oxygen vacancy of single charge and hole which is photo-excited or defects which are Zn interstitial related[3]. Green-yellow emission peaks observed at 510, 517 and 521 nm for hydrothermal method and 549, 554 and 565 nm for sol-gel method are due to either of these two effects.

3.6 Conductivity Studies

Figure 7 depicts the conductivity of ZnO synthesized by hydrothermal and sol-gel methods for various temperatures and concentrations. The conductivity decreases, when the growth temperature as well as the concentration of the prepared ZnO samples by sol gel method increases. In contrast, the conductivity of the sample prepared by hydrothermal method increases as the growth temperature increases, but decreases as the concentration increases.

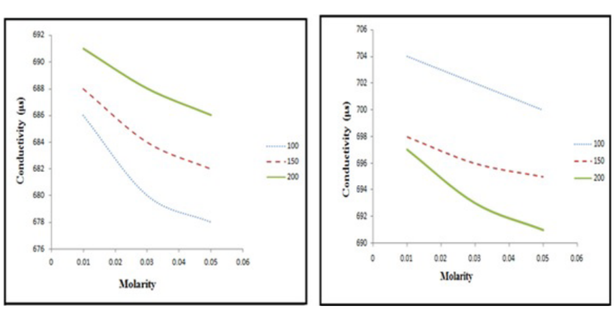

(a) (b)

Figure 7. Conductivity of the ZnO samples prepared by **(a)** hydrothermal method and **(b)** sol-gel method.

4. Conclusion

ZnO nanopowders are synthesized by hydrothermal and sol-gel methods at different temperatures such as 100^0C, 150^0C and 200^0C for 2hrs. In both the methods, the mean crystal size, calculated from XRD pattern, is found to be in the range 20-30 nm. The pattern confirmed the composition, crystallinity and the synthesized products are ZnO with high purity and the hexagonal phase. Crystallite size decreases as temperature increases. The peak in absorption spectra of the prepared ZnO nanoparticles shows a blue-shift comparatively larger than the bulk. When the temperature increases, the absorbance also increases and the band gap decreases. In hydrothermal method, the band gap is large (i.e) from 4.4-4.9 eV and hence it has large applications in solar field. ZnO nanoparticles synthesized by both the methods exhibit similar luminescence. SEM pictures reveal the morphology as near-spherical prismatic nanoparticles for hydrothermal method and as nanoflakes for sol-gel method. The EDAX analysis confirms the presence of ZnO only and no other elements is present. The maximum peak is obtained for Zinc. In both hydrothermal as well as sol-gel methods, a pure ZnO occurrence is obtained. The conductivity decreases with the growth temperature as well as the concentration of the ZnO samples by sol gel method. In contrast the conductivity of the sample prepared by hydrothermal method increases as the growth temperature increases, but decreases as the concentration increases.

5. Acknowledgement

The financial support of the University Grants Commission, New Delhi, India through Major Research Project (No. F. 42-836/2013 (SR) dated 22.03.2013) and the encouragements of the authorities of Jayaraj Annapackiam College for Women (Autonomous), Periyakulam, Theni District, Tamil Nadu, India are gratefully acknowledged.

6. References

1. Sridevi D, Rajendran KV. Synthesis and optical characteristics of ZnO nanocrystals. Bulletin of Materials Science. 2009; 32(2):165–8.
2. Savi BM, Rodrigues L, Bernardin AM. Synthesis of ZnO nanoparticles by sol-gel processing. Qualicer '12. 2012. p. 1–8.
3. Aneesh PM, Vanaja KA, Jayaraj MK, Synthesis of ZnO nanoparticles by hydrothermal method. Proceedings of SPIE, India. 2007; 66390J:1–9.

4. Sivakumar S, Venkateswarlu P, Rao VR,Rao GN. Synthesis, characterization and optical properties of zinc oxide nanoparticles. International Nano Letters. 2013; 3(30):1–6.
5. Bagabas A, Alshammari A, Aboud MF, Kosslick H. Room-temperature synthesis of Zinc Oxide nanoparticles in different media and their application in cyanide photodegradation. Nanoscale Research Letters. 2013; 8:516.
6. Ha TT, Canh TD, Tuyen NV. A quick process for synthesis of ZnO nanoparticles with the aid of microwave irradiation. ISRN Nanotechnology. 2013; Article ID 497873:1–7.
7. Oladiran AA, Olabisi IA. Synthesis and Characterization of ZnO nanoparticles with Zinc Chloride as Zinc source. Asian Journal of Natural and Applied Sciences. 2:41.
8. Hale PS, Maddox LM, Shapter JG, Voelcker NH, Ford MJ, Waclawik ER. 2005, Growth Kinetics and Modeling of ZnO nanoparticles. Journal of Chemical Education. 2013; 82:775.
9. Kolekar TV, Yadav HM, Bandgar SS, Deshmukh PY. Synthesis by Sol-gel Method and characterization of ZnO nanoparticles. Indian Streams Research Journal. 2011; 1:1.
10. Gnanasangeetha D, Sarala Thambavani D. One pot synthesis of ZnO nanoparticles via Chemical and Green method. Research Journal of Material Sciences. 2013; 1:1.
11. Kundu TK., Karak N, Barik P, Saha S. Optical properties of ZnO nanoparticles prepared by Chemical method using Polyvinyl Alcohol (PVA) as capping agent. International Journal of Soft Computing and Engineering. 2011; 1:19.
12. Vaseem M, Umar A, Hahn YB. ZnO nanoparticles: Growth, properties and applications. Metal Oxide Nanostructures and Their Applications, 2010; 5:1–36.
13. Radzimska AK, Jesionowski T. Zinc Oxide – From synthesis to application: A review. Materials. 2014; 7:2833.
14. Suwanboon S. Structural and optical properties of nanocrystalline ZnO powder from Sol-Gel Method. ScienceAsia. 2008; 34:31.
15. Thangeeswari T, George AT, Arun Kumar A. Optical properties and FTIR studies of cobalt doped ZnO nanoparticles by simple solution method. Indian Journal of Science and Technology. 2016; 9(1).
16. Vanaja A, Ramaraju GV, Rao KS. Structural and optical investigation of Al doped ZnO nanoparticles synthesized by sol-gel process. Indian Journal of Science and Technology. 2016; 9(12).
17. Xu CL, Qin DH, Li H, Guo Y, Xu T, Li HL. Low temperature growth and optical properties of radial ZnO nanowires. Materials Letters. 2004; 58:3976.
18. Vanheusden K, Warren WL, Seager CH, Tallant DR, Voigt JA, Gnade BE. Mechanisms behind Green Photoluminescence in ZnO phosphor powders. Journal of Applied Physics. 1996; 79:7983.

International Journal of Modern Physics B
Vol. 31, No. 8 (2017) 1750050 (13 pages)

DOI:

Simultaneous effects of pressure and temperature on excitons in Pöschl–Teller quantum well

A. Anitha* and M. Arulmozhi†

Department of Physics,
Jayaraj Annapackiam College for Women (Autonomous),
Periyakulam - 625601, Theni District, Tamil Nadu, India
**anitha.jayarani@gmail.com*
†arulpkm@yahoo.co.in

Received 13 July 2016
Revised 18 October 2016
Accepted 2 November 2016
Published 9 January 2017

Binding energies of the heavy hole and light hole exciton in a quantum well with Pöschl–Teller (PT) potential composed of GaAs have been studied variationally within effective mass approximation. The effects of pressure and temperature on exciton binding energy are analyzed individually and also simultaneously for symmetric and asymmetric configuration of the well. The results show that exciton binding energy (i) decreases as the well width increases, (ii) increases with pressure and (iii) decreases with temperature. Simultaneous effects of these perturbations lead to more binding of the exciton. The results are compared with the existing literature.

Keywords: Exciton; temperature; pressure; Pöschl–Teller quantum well; binding energy.

PACS numbers: 73.21.Fg, 71.55.Eq, 71.35.-y

1. Introduction

Studies on low dimensional semiconductor systems with quantum confinement are paid much attention due to their effective applications in electronic and optoelectronic devices. Most of the investigations are carried out with III–V semiconductor heterostructures, mainly with GaAs/GaAlAs. Because of the optical properties, GaAs/GaAlAs structures have become more important in the field of device fabrication. Theoretical investigations on hydrogenic donor and exciton in quantum semiconductor nanostructures play an important role to understand the electrical, magnetic and optical properties of the nanostructures.[1–6] Confinement of excitons

†Corresponding author.

in semiconductor nanostructures are exploited in the design of novel optoelectronic devices. Various authors have theoretically and experimentally studied the exciton binding energy in cylindrical quantum dot,[7] parabolic quantum wire,[8] spherical quantum dot,[9] triangular quantum well,[10] rectangular quantum well[11,12] and coupled double quantum well.[13]

Band structure and the properties of semiconductor materials can be controlled and altered by the application of pressure and temperature. Hence, an understanding of the effects of pressure and temperature on excitonic binding energy in a quantum well may be useful in the design and preparation of a new generation of efficient semiconductor devices like heterostructure lasers, QLEDs, white light sources, etc.

Raigoza *et al.*[14] have calculated theoretically the effects of hydrostatic pressure and electric field on exciton states in GaAs–GaAlAs quantum well. The combined influences of temperature and hydrostatic pressure on exciton binding energy in a GaAs spherical quantum dot have been investigated by Jeice and Wilson.[9] Effects of temperature and pressure on exciton binding energy in a cylindrical GaAs quantum dot have been studied by Elmeshad *et al.*[7] Moussaouy *et al.*[15] have investigated the temperature and pressure effects on exciton–phonon coupled states in semiconductor quantum dot composed of GaAs–GaAlAs.

Due to the evolution of growth techniques of low dimensional structures, it is possible to alter distinct conduction and valence band potential energy to make different potential profiles of various dimensions. Pöschl–Teller (PT) potential is one among the novel confining potential profiles.[16] An important feature of PT potential is that the degree of asymmetry of the potential is tunable which yields nonlinear optical properties[17,18] such as third-order absorption co-efficient, second-order susceptibility and optical rectification associated with inter-subband optical transitions. By adjusting the characteristic parameters of the potential, there can be a switchover from symmetric to asymmetric configuration.

Studies on such a potential are receiving much attention in the past two decades due to their specific applications like photo detector operations. Barseghyan *et al.*[19] have studied the simultaneous effects of pressure and temperature on the binding energy of a hydrogenic donor impurity in PT quantum well and also investigated the combined effects of pressure, electric and magnetic fields on donor binding energy in InAs PT quantum ring.[20] Mora-Ramos *et al.*[21] have investigated the exciton binding energy in a cylindrical PT GaAs quantum dot. The influence of temperature on exciton binding energy in ZnSe–ZnMgSe PT quantum well has been investigated by Sathiyajothi *et al.*[22] The effects of hydrostatic pressure and temperature on exciton binding energy in a cylindrical quantum dot have been studied by Mora-Ramos *et al.*[23] Optical properties of cylindrical and spherical quantum dots with symmetric or modified PT potential have been studied by Hayrapetyan *et al.*[24,25]

In the present paper, we have investigated the combined effects of pressure and temperature on light hole (lh) and heavy hole (hh) exciton binding energy in PT quantum well formed by GaAs as a function of well width for different symmetric and asymmetric configurations of the quantum well. We have used variational method to compute the binding energy of exciton.

2. Theoretical Framework

2.1. *Hamiltonian and wavefunction of exciton*

The Hamiltonian of an exciton in a quantum well with PT potential composed of GaAs is given in effective-mass approximation and in dimensionless variables as

$$\mathcal{H} = -\left[\frac{1}{\rho}\frac{\partial}{\partial\rho}\rho\frac{\partial}{\partial\rho} + \frac{1}{\rho^2}\frac{\partial^2}{\partial\varphi^2}\right] - \frac{\mu_{ih}^*}{m_e^*}\frac{\partial^2}{\partial z_e^2} - \frac{\mu_{ih}^*}{m_{ih}^*}\frac{\partial^2}{\partial z_h^2} + V(z_e) + V(z_h) - \frac{2}{r}, \quad (1)$$

where $r = \sqrt{\rho^2 + |z_e - z_h|^2}$ and μ_{ih}^* is the reduced mass of hh- $(i = h)$ exciton or lh- $(i = l)$ exciton given by

$$\frac{1}{\mu_{ih}^*} = \frac{1}{m_e^*} + \frac{1}{m_{ih}^*}. \quad (2)$$

m_e^* and m_{ih}^* are the effective masses of electron and hole, respectively. The effective Bohr radius $(a^* = \hbar^2\varepsilon_0/\mu_{ih}^* e^2)$ and the effective Rydberg $(R^* = \mu_{ih}^* e^4/2\hbar^2\varepsilon_0^2)$ are used as the units of length and energy, respectively.

The PT potential for electron $(j = e)$ and hole $(j = ih)$ in quantum well is given by,[20]

$$V_{\mathrm{PT}}(z_j) = \frac{\mu_{ih}^*\eta^2}{m_j^*}\left[\frac{\chi(\chi-1)}{\sin^2\eta z_j} + \frac{\lambda(\lambda-1)}{\cos^2\eta z_j}\right]. \quad (3)$$

χ and λ are the parameters which characterize the asymmetry of the potential. The potential is perfectly symmetric when $\chi = \lambda$. $\eta = \frac{\pi}{2L}$ and L is the well width of the quantum well.

Figure 1 shows the different shapes of the PT potential quantum well with three different asymmetry cases. (a) When $\chi = \lambda = 1.5$, the shape of the quantum well is perfectly symmetric named as modified PT potential.[24,25] The shape of the quantum well is deviated from the symmetric well and becomes asymmetric, when (b) $\chi = 1.5$ and $\lambda = 5$ and (c) $\chi = 1.5$ and $\lambda = 8$.

Since an accurate solution of the Schrödinger equation for the Hamiltonian of Eq. (1) is not possible, a variational method is adopted. The trial wavefunction for

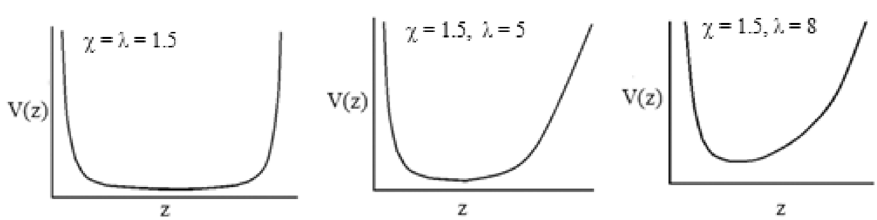

(a) (b) (c)

Fig. 1. PT quantum well according to the asymmetric parameters χ and λ.

excitons within the PT quantum well is taken to be of the form,[20]

$$\Psi = N \sin^{\chi} \eta z_e \cos^{\lambda} \eta z_e \sin^{\chi} \eta z_{ih} \cos^{\lambda} \eta z_{ih} e^{-ar}, \tag{4}$$

where 'N' is normalization constant and 'a' is variational parameter. The expectation value of Hamiltonian $\langle \mathcal{H} \rangle$ with respect to the variational parameter is calculated using the expression

$$\langle \mathcal{H} \rangle = \frac{\int \Psi^* \mathcal{H} \Psi d\tau}{\int \Psi^* \Psi d\tau}. \tag{5}$$

The binding energy of exciton in the PT quantum well is then given by

$$E_B = E_e + E_{ih} - \langle \mathcal{H} \rangle_{\min}, \tag{6}$$

where E_e and E_{ih} are the ground state energies of electron and hole in bare quantum well, respectively, obtained variationally. $\langle \mathcal{H} \rangle_{\min}$ is the minimized value of $\langle \mathcal{H} \rangle$ with respect to the variational parameter a.

2.2. *Effect of temperature and hydrostatic pressure*

The application of temperature and hydrostatic pressure alter the energy gap, effective masses of electron and hole, dielectric constant and well width. Variations of these variables with respect to the applied hydrostatic pressure in kbar and temperature in K are as given below.

The variation of effective-mass of electron in conduction band of GaAs as a function of pressure and temperature is given by the expression[3]

$$m_e^*(P,T) = \frac{m_0}{1 + E_m \left\{ \frac{2}{E_g^{\Gamma}(P,T)} + \frac{1}{E_g^{\Gamma}(P,T) + \triangle_o} \right\}}, \tag{7}$$

where m_0 is free electron mass, $E_m = 7.51$ eV is energy related to the momentum matrix element, $\Delta_o = 0.341$ eV is spin–orbit splitting and $E_g^{\Gamma}(P,T)$ is the energy gap of the GaAs quantum well which depends on both pressure and temperature given by[3]

$$E_g^{\Gamma}(P,T) = E_g^{\Gamma}(0,T) + bP + cP^2, \tag{8}$$

where $b = 1.26 \times 10^{-2}$ eV bar^{-1} and $c = 3.77 \times 10^{-5}$ eV bar^{-2}. $E_g^{\Gamma}(0,T)$ is the energy gap of GaAs as a function of temperature without pressure given by[3]

$$E_g^{\Gamma}(0,T) = 1.519 - \frac{5.405T^2 \times 10^{-4}}{T + 204}. \tag{9}$$

The valence band effective-mass as a function of temperature and pressure is calculated using the expression[26]

$$m_{ih}^*(P,T) = [m_{ih}^* + x_1 P + x_2 P^2] \frac{E_g^{\Gamma}(0,T)}{1.519}, \tag{10}$$

where $x_1 = -0.1 \times 10^{-3}$ kbar^{-1} and $x_2 = 5.56 \times 10^{-6}$ kbar^{-2} are the pressure coefficients.

The variation of dielectric constant as a function of temperature and pressure is given as,[3]

$$\varepsilon_0(PT) = \begin{cases} 12.74e^{-1.73\times10^{-2}P}e^{9.4\times10^{-5}}(T-75.6), & T \le 200\ \text{K}, \\ 13.18e^{-1.73\times10^{-2}P}e^{20.4\times10^{-5}}(T-300), & T > 200\ \text{K}. \end{cases} \tag{11}$$

Since the temperature dependence of well width is not available in the literature, variation of well width with pressure alone is considered. The expression for well width as a function of pressure is given by[7]

$$L(P) = L - L(S_{11} + 2S_{12})P, \tag{12}$$

where $S_{11} = 1.16 \times 10^{-3}$ kbar^{-1} and $S_{12} = -3.7 \times 10^{-4}$ kbar^{-1} are the elastic constants of GaAs.

3. Results and Discussion

The material parameters for GaAs[27] used in the calculations are, (i) effective masses of hh, $m^*_{\text{hh}} = 0.34\ m_0$, lh, $m^*_{\text{lh}} = 0.094\ m_0$ and electron, $m^*_e = 0.0665\ m_0$; (ii) reduced masses of lh-exciton, $\mu^*_{\text{lh}} = 0.05562\ m_0$ and hh-exciton, $\mu^*_{\text{hh}} = 0.03895\ m_0$ where m_0 is the free electron mass; (iii) dielectric constant $\varepsilon_0 = 13.2$.

Figure 2 shows the variation of lh-exciton binding energy as a function of well width without applied pressure and temperature for different values of asymmetric parameters χ and λ, which define the shape of PT quantum well. We have calculated the exciton binding energy as a function of well width for four different cases (i) $\chi = \lambda = 1.5$, (ii) $\chi = \lambda = 3$, (iii) $\chi = 1.5$, $\lambda = 3$ and (iv) $\chi = 1.5$, $\lambda = 5$. It is observed that when the well width reduces, the binding energy of lh-exciton increases for all the four cases. The wavefunction of exciton squeezed together in the well, due to the confinement, leads to more binding. This behavior is analogous

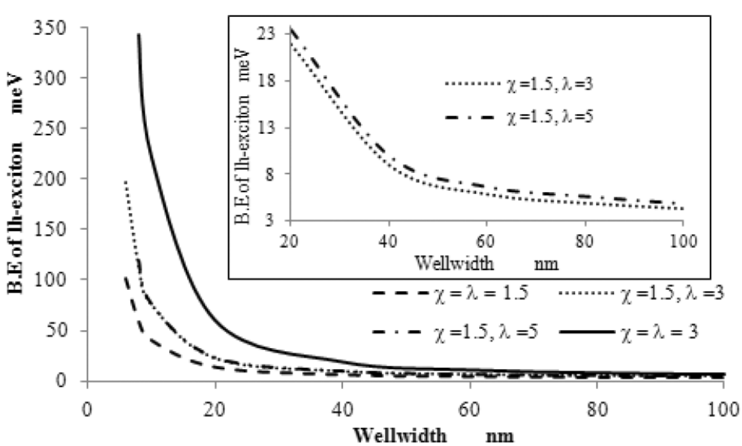

Fig. 2. Binding energy of lh-exciton as a function of well width for different asymmetry parameters.

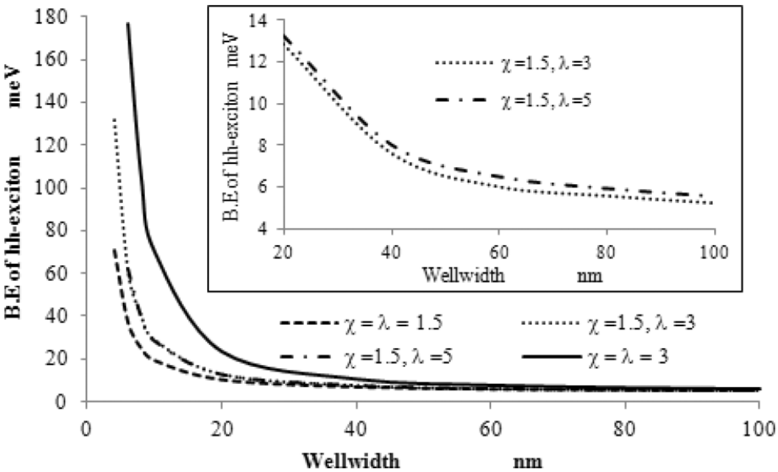

Fig. 3. Binding energy of hh-exciton as a function of well width for different asymmetry parameters.

to the results of Mora-Ramos *et al.*[23] It is also noted that the lh-exciton binding energies increases as the parameters χ and λ increase for zero pressure and zero temperature. As λ increases, keeping χ as a constant, the lh-exciton binding energy increases. But the amount of increase, i.e., the increment decreases as λ increases which is clearly seen from the closeness of curves (iii) and (iv). This behavior may be due to the increase of tendency of the wavefunction to spread out of the well, as λ increases.

In Fig. 3, we show the variation of hh-exciton binding energy in PT quantum well as a function of well width for different combinations of asymmetry parameters without applied pressure and temperature. As in the case of lh-exciton, the hh-exciton binding energy also increases when the well width reduces. It is also observed that the behavior of the hh-exciton binding energy with respect to the asymmetric parameter is same as in case of lh-exciton, but the value of the hh-exciton binding energy is smaller than that of lh-exciton.[10,12]

Figure 4 depicts the variation of lh-exciton binding energy as a function of pressure for different well widths without applied temperature and the value of asymmetry parameters are chosen as $\chi = \lambda = 1.5$ which means that the quantum well is perfectly symmetric. It is observed that for well width $L = 20$ nm, the binding energy of lh-exciton increases with pressure applied to the quantum well. Another significant result from the plot is that the lh-exciton binding energy increases with pressure up to 30 kbar and for well widths such as $L = 6$, 8 and 10 nm, further increase of pressure leads to less binding. This behavior is similar to those observed for a donor by Morales *et al.*[28] This may be due to the penetration of lh-exciton wavefunction through the barrier with small well width under large pressure. So the choice of the pressure level for a particular well width must be given importance during the fabrication of devices.

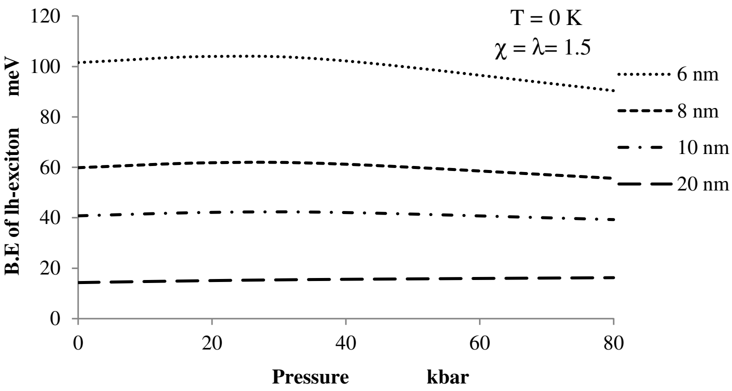

Fig. 4. Binding energy of lh-exciton as a function of pressure for different well widths.

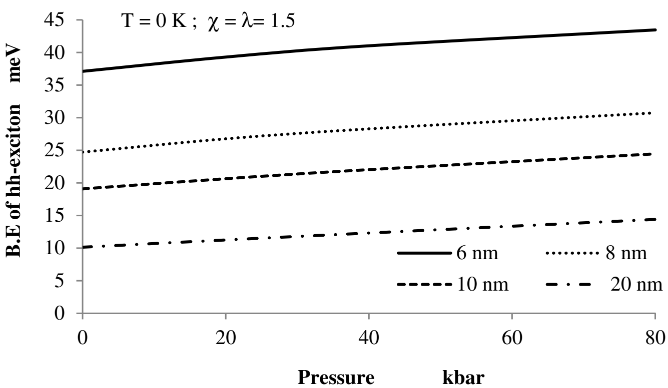

Fig. 5. Binding energy of hh-exciton as a function of pressure for different well widths.

Figure 5 displays hh-exciton binding energy as a function of pressure for different well widths for $T = 0$ K. The asymmetry parameters are considered as $\chi = \lambda = 1.5$. It is noted that the hh-exciton binding energy increases with pressure (up to 80 kbar) for all well widths.[7] This behavior is not similar to that of lh-exciton case presented in Fig. 4. Since the effective-mass of the hh-exciton is greater than that of lh-exciton, the wavefunction of hh-exciton, though compressed together, does not penetrate through the barrier even up to the pressure of 80 kbar.

The results depicted in Figs. 6 and 7 are similar to those in the case of Figs. 4 and 5, respectively, but the PT potential is deformed asymmetrically in the later case by choosing the values of asymmetry parameters as $\chi = 1.5$ and $\lambda = 3$. Comparing Figs. 4 and 6, it is observed that the variation of lh-exciton binding energy with respect to pressure and well width for asymmetric PT quantum well with $\chi = 1.5$ and $\lambda = 3$ is same as in the case of symmetric configuration $\chi = \lambda = 1.5$. However, for all the values of pressure and well width the binding energy in asymmetric case is larger than that in symmetric case ($\chi = \lambda = 1.5$). Similarly, it

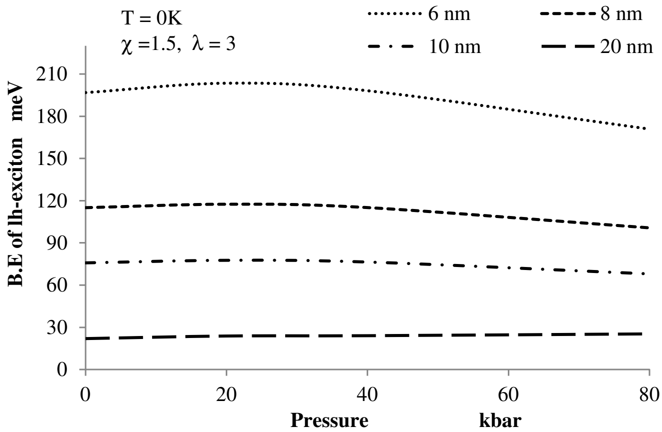

Fig. 6. Binding energy of lh-exciton as a function of pressure for different well widths with $\chi = 1.5$ and $\lambda = 3$.

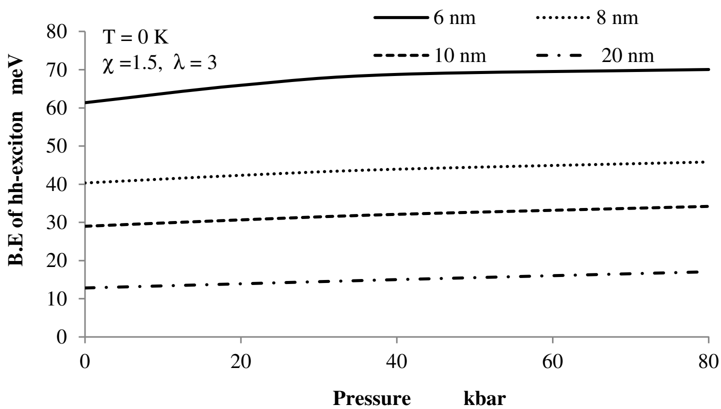

Fig. 7. Binding energy of hh-exciton as a function of pressure for different well widths with $\chi = 1.5$ and $\lambda = 3$.

can be seen from Figs. 5 and 7, the hh-exciton binding energy in symmetric case is smaller than that in asymmetric case $\chi = 1.5$ and $\lambda = 3$.

The variation of lh-exciton and hh-exciton binding energy in GaAs PT quantum well as a function of temperature without applied pressure is presented in Figs. 8 and 9. The PT quantum well is considered as perfectly symmetric with $\chi = \lambda = 1.5$. In both the cases, it is observed that the binding energy decreases with temperature for large well widths $L = 10$, 20 and 80 nm. This behavior agrees with those for a quantum dot reported by Mora-Ramos *et al.*[23] The reason is that the effective mass of the electron and hole diminishes with increase of temperature. Hence the reduced mass of the electron–hole pair also decreases. But for small well widths, the binding energy remains constant when the temperature increases. This may be due to the competitive effects of temperature and confinement.

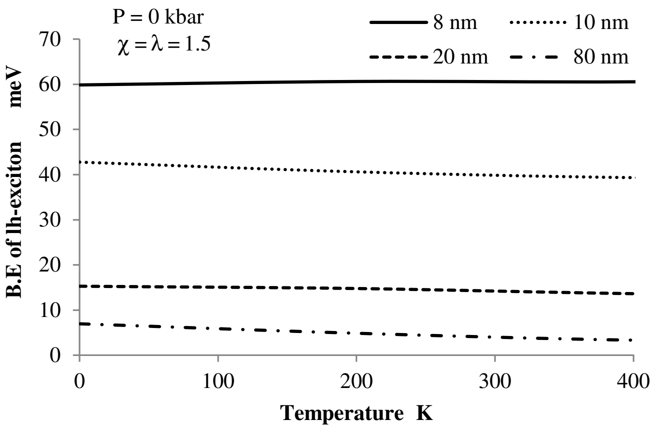

Fig. 8. Binding energy of lh-exciton as a function of temperature for different well widths.

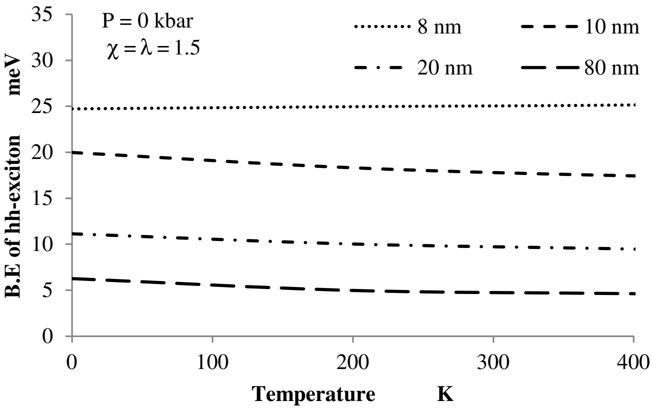

Fig. 9. Binding energy of hh-exciton as a function of temperature for different well widths.

The variation of binding energy of lh-exciton and hh-exciton as a function of temperature for various well widths with asymmetry effect ($\chi = 1.5$, $\lambda = 3$) is shown in Figs. 10 and 11, respectively. It is observed that, the binding energy of lh-exciton and hh-exciton in asymmetric ($\chi = 1.5$, $\lambda = 3$) PT well is larger than that in symmetric ($\chi = \lambda = 1.5$) PT well. It can be seen from Figs. 8 and 10 that the lh-exciton binding energy in asymmetric case increases with temperature for $L = 8$, 10 and 20 nm and decreases with temperature for $L = 80$ nm. This result is quite different from the symmetric case, where the binding energy of lh-exciton increases with temperature for $L = 8$ nm and decreases with temperature for $L = 10, 20$ and 80 nm. This is a consequence of the fact that increase of λ decreases the spatial distance between the electron and hole as depicted in Fig. 1 and the localization of electron and hole states increases in quantum well; hence the coulomb interaction is strengthened which leads to the increase of the exciton binding energy.

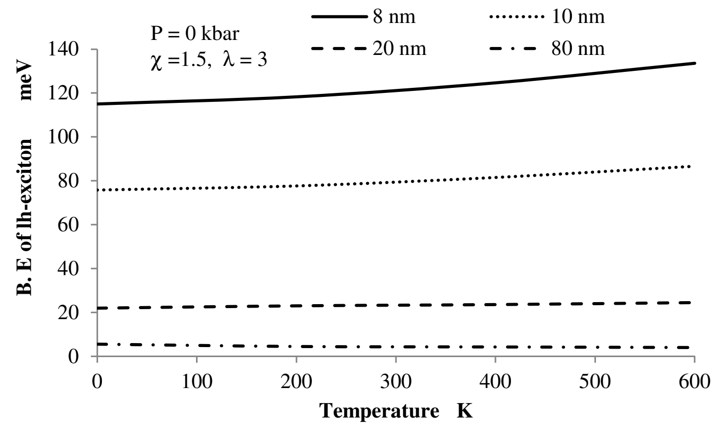

Fig. 10. Binding energy of lh-exciton as a function of temperature for different well widths with $\chi = 1.5$ and $\lambda = 3$.

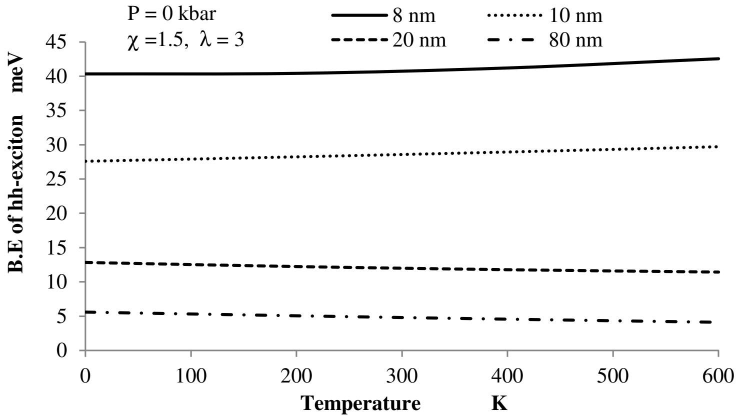

Fig. 11. Binding energy of hh-exciton as a function of temperature for different well widths with $\chi = 1.5$ and $\lambda = 3$.

Comparing Figs. 9 and 11, the hh-exciton binding energy, in symmetric case, increases with respect to temperature for $L = 8$ nm and decreases with temperature for $L = 10, 20$ and 80 nm. But in the case of asymmetric well, the lh-exciton binding energy increases with temperature for well widths $L = 8$ and 10 nm and decreases for $L = 20$ and 80 nm.

The combined effects of asymmetry, temperature and pressure on lh-exciton binding energy in PT quantum well is shown in Fig. 12 for $L = 10$ nm and $T = 200$ K. It shows that the binding energy increases with pressure up to 30 kbar, beyond that it starts to decrease for all asymmetric cases. It is observed that the binding energy decreases when the value of λ increases with χ kept as a constant. It is also noted that the simultaneous effects of temperature, pressure and asymmetry on lh-exciton leads to increased binding.

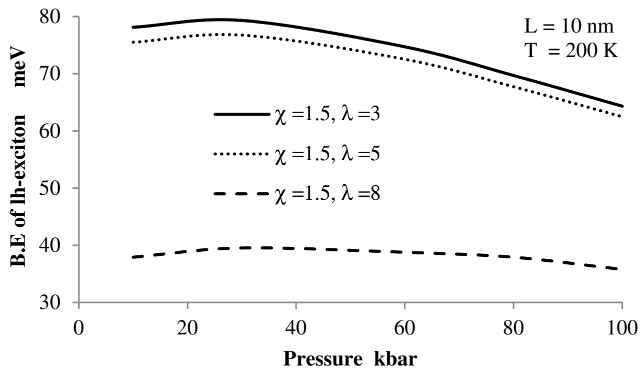

Fig. 12. Binding energy of lh-exciton as a function of pressure for different asymmetric shape of the quantum well with $L = 10$ nm and $T = 200$ K.

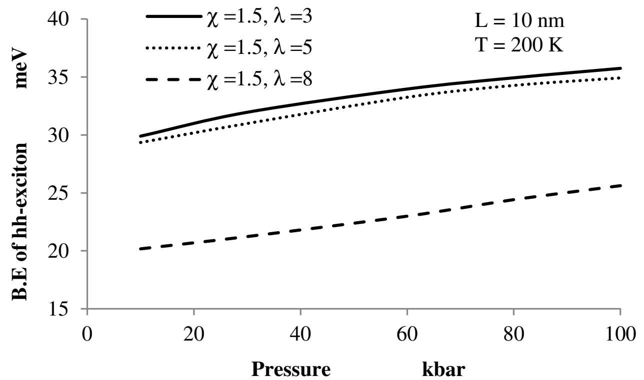

Fig. 13. Binding energy of hh-exciton as a function of pressure for different asymmetric shape of the quantum well with $L = 10$ nm and $T = 200$ K.

Figure 13 presents the results of hh-exciton binding energy as a function of pressure with $L = 10$ nm and $T = 200$ K. The asymmetric PT pattern was chosen with constant $\chi = 1.5$ and three different values of $\lambda = 3, 5$ and 8. It can be seen that, for all asymmetry configurations the binding energy increases with pressure. It is also important to note that, the hh-exciton binding energy decreases when asymmetry parameter λ increases. The hh-exciton binding energy decreases to a large extent when the value of λ goes beyond five. As in the case of lh-exciton, the simultaneous application of pressure, temperature and asymmetry pattern leads to more binding for hh-exciton also.

4. Conclusion

We have investigated the hh- and lh-exciton binding energy under the effects of pressure, temperature and asymmetry pattern of the PT quantum well composed of GaAs as a function of well width by variational method. The following points are noted: (i) increase in the degree of asymmetry of the PT quantum well increases the binding energy of both excitons, (ii) both in symmetric and asymmetric cases, for $L \leq 20$ nm, lh-exciton binding energy increases with pressure up to 30 kbar and decreases for further increase in pressure. But for $L > 20$ nm, it increases with pressure continuously, (iii) hh-exciton binding energy increases with pressure for all well widths (noted up to 80 kbar), (iv) in the asymmetric case, for $L \leq$ ($>$)20 nm, lh-exciton binding energy increases (decreases) with temperature. But in the symmetric case, the same behavior is observed for $L \leq 8$ nm, (v) similar behavior is observed for hh-exciton binding energy also, in asymmetric case for $L \leq 10$ nm and in symmetric case for $L \leq 8$ nm and (vi) simultaneous effects of pressure, temperature and asymmetry pattern of PT quantum well lead to increased binding of both excitons. The values of pressure and temperature in semiconductor materials for the potential device applications must be properly chosen and our calculations give an idea of the choice of these values which will be surely useful in the preparation of semiconductor devices. However, choice of the wavefunction with two variational parameters as in Mora-Ramos *et al.*[21,23] may give still improved results for the exciton binding energy.

Acknowledgments

The authors thank the University Grants Commission (UGC), New Delhi, India for the financial support through Major Research Project (Grant No. F. 42-836/2013 (SR) dated 22.03.2013) and the authorities of Jayaraj Annapackiam College for Women (Autonomous), Periyakulam, Theni District, Tamil Nadu, India for the encouragements.

References

1. P. Baser, I. Altuntas and S. Elagoz, *Superlattices Microstruct.* **92**, 210 (2016).
2. M. R. Fulla, Y. A. Suaza and J. H. Marin, *Phys. Status Solidi* **252**, 678 (2015).
3. H. D. Karki, S. Elagoz and P. Baser, *Superlattices. Microstruct.* **48**, 298 (2010).
4. K. Sivalertporn, *Phys. Lett. A* **380**, 1990 (2016).
5. A. Anitha and M. Arulmozhi, *Int. J. ChemTech Res.* **7**, 1438 (2015).
6. R. Macedo *et al.*, *J. Phys.: Condens. Matter* **25**, 485501-1 (2013).
7. N. Elmeshad, H. Abdelhamid and H. Hassanein, *Chin. J. Phys.* **47**, 92 (2009).
8. S. Wu, *Physica B* **406**, 4634 (2011).
9. A. R. Jeice and K. S. J. Wilson, *e-J. Surf. Sci. Nanotech.* **12**, 358 (2014).
10. G. Z. Jiang and C. Z. Wen, *Phys. Rev. B* **50**, 2689 (1994).
11. N. H. Lu, P. M. Hui and T. M. Hsu, *Solid State Commun.* **78**, 145 (1991).
12. B. Gerlach *et al.*, *Phys. Rev. B* **58**, 10568 (1998).
13. E. M. Lopes *et al.*, *J. Lumin.* **144**, 98 (2013).
14. N. Raigoza *et al.*, *Physica B* **367**, 267 (2005).
15. A. El Moussaouy *et al.*, *Superlattices Microstruct.* **73**, 22 (2014).
16. J. Radovanovic *et al.*, *Phys. Lett. A* **269**, 179 (2000).
17. H. Yildirim and M. Tomak, *Phys. Rev. B* **72**, 115340-1 (2005).
18. O. Aytekin, S. Turgut and M. Tomak, *Physica E* **44**, 1612 (2012).
19. M. G. Barseghyan *et al.*, *Physica E* **42**, 1618 (2010).

20. M. G. Barseghyan *et al.*, *Superlattices Microstruct.* **51**, 119 (2012).
21. M. E. Mora-Ramos, M. G. Barseghyan and C. A. Duque, *Phys. Status Solidi B* **248**, 1412 (2011).
22. P. Sathiyajothi, A. Anitha and M. Arulmozhi, *Int. J. ChemTech Res.* **9**, 298 (2016).
23. M. E. Mora-Ramos, M. G. Barseghyan and C. A. Duque, *Physica E* **43**, 338 (2010).
24. D. B. Hayrapetyan, E. M. Kazaryan and H. Kh. Tevosyan, *Physica E* **46**, 274 (2012).
25. D. B. Hayrapetyan, E. M. Kazaryan and H. Kh. Tevosyan, *Superlattices Microstruct.* **64**, 204 (2013).
26. S. Adachi, *Properties of Group-IV, III–V and II–VI Semiconductor* (John Wiley & Sons Ltd, England, 2005).
27. M. Arulmozhi and S. Balasubramanian, *Phys. Rev. B* **51**, 2592 (1995).
28. A. L. Morales *et al.*, *J. Phys.: Condens. Matter* **14**, 987 (2002).

11. MECHANICAL AND THERMAL PROPERTIES OF NANOSTRUCTURED MATERIALS – A THEORETICAL STUDY

S. Preethi[1], A. Anitha[2] and M. Arulmozhi[3]

[1]*II M.Sc., Department of Physics, Jayaraj Annapackiam College for Women (Autonomous), Periyakulam-625 601, Theni District, Tamil Nadu, India.*

[2]*Research scholar, Department of Physics, Jayaraj Annapackiam College for Women (Autonomous), Periyakulam-625 601, Theni District, Tamil Nadu, India.*

[3]*Associate Professor, Department of Physics, Jayaraj Annapackiam College for Women (Autonomous), Periyakulam-625 601, Theni District, Tamil Nadu, India. arulpkm@yahoo.co.in*

ABSTRACT

Nanostructured materials exhibit more fascinating properties in the range of 1-100nm distinct from those of bulk materials. The properties of these materials are, hence, dependent on the grain size. In the present study, thermal property such as melting point, mechanical properties such as yield strength of the nanomaterials are calculated as a function of grain size for various dimensions such as quantum well, quantum wire and quantum dot. The above properties are theoretically studied and discussed in this paper. The studies show new results which call for further research and are in close agreement with the available experimental data.

Keywords: melting point, yield strength, grain size, quantum well, quantum wire, quantum dot.

1. INTRODUCTION

During the last few years, nanostructured materials have received extensive attention due to their unique physical, chemical, electrical, optical and mechanical properties [1]. The quantum nanostructures have a great potential for application in infrared detectors, quantum dot lasers, superconductivity, solar cells, single electron transistor and quantum computers.

The conduction electron in nanostructures can be partially delocalized, depending on the shape and the dimensions of the structure. One limiting case is a quantum dot in which they are totally confined, and the other limiting case is a bulk material, in which they are all delocalized. The intermediate case are a quantum wire, which is long in one dimension and very small in its transverse direction; and a quantum well, which is a flat plate nanosized in thickness and much more larger in length and width. The quantum wire exhibits electron confinement in two dimensions and delocalization in one dimension, and the quantum well reverse these characteristics [2]. The grain size is known to have a strong influence on many *material* properties.

The purpose of the present paper is to report the results on the properties like melting point, yield strength of quantum nanostructures for various grain sizes. These properties are theoretically calculated and compared for nanostructured materials of various dimensions and with the available experimental data.

MODEL AND FORMULATION

1 Melting Point

Melting point of a solid is the temperature at which it changes state from solid to uid at atmospheric pressure. At the melting point, the solid and liquid phase exists in uilibrium. The melting temperature of a bulk material is not dependent on its size. wever as the dimensions of a material decrease towards the atomic scale, the melting nperature scales with the material dimensions. The melting point of atomic clusters and noparticles can be understood by scaling the cohesive energy to the melting temperature. nda et al [3] derived an empirical relation for the size dependent melting temperature of noparticles (T_m) in terms of bulk melting temperature (T_{mb}) as,

$$T_m = T_{mb} - \frac{6v_0\gamma}{0} \cdot 0005736d \qquad (1)$$

$$\frac{T_m}{T_{mb}} = 1 - \frac{\beta}{d}$$

ere v_0 is the molar volume, d is the diameter of the particle and γ represents the fficient of surface energy of the material. Here the particle shape is assumed to be erical. For a nanomaterial with general shape, the size dependent melting temperature, general, can be written as

$$T_m = T_{mb}\left\{1 - \frac{\beta}{zd}\right\} \qquad (2)$$

ere z = 1, 3/2, and 3 for quantum dot, quantum wire and quantum well respectively. In (2), d represents the diameter in case of dots and wires, whereas it represents the ckness in case of wells [4].

Yield Strength

Yield strength or yield point of a material is defined, in engineering and materials nce, as the stress at which a material begins to deform plastically. Prior to the yield point, material will deform elastically and will return to its original shape, when the applied ss is removed. Once the yield point is passed, some fraction of the deformation will be manent and non-reversible [5].

Yield strength of a conventional grain-sized material is related to the grain size by Hall - Petch equation [2],

$$\sigma = \sigma_0 + K\,(d)^{-1/2} \qquad (3)$$

ere σ_0 is the stress required to move dislocations, K is a material constant, d is the grain . Equation (1) applies to alloys in which only grain boundaries act as dislocation sources ield and where the motion of dislocation is not impeded between the grain boundaries [6]. ng the concept reported by Nanda et al. [4], equation (3) is rewritten (replacing d by zd)

$$\sigma = \sigma_0 + K\,(zd)^{-1/2} \qquad (4)$$

ere z = 1, 3/2, and 3 for quantum dot, quantum wire and quantum well respectively.

RESULTS AND DISCUSSION

Using the equations (2), (4), (6) and (8), thermal property like melting point, hanical properties like yield strength and strain rate, and optical property like refractive index of nanostructured materials are calculated as a function of grain size for various dimensions.

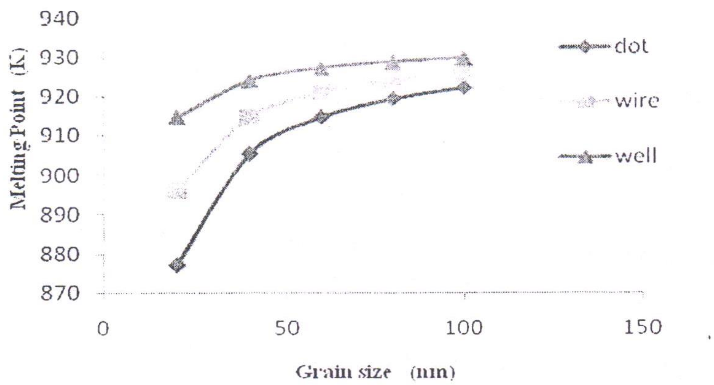

Figure 1. Variation of melting point with Grain size for Aluminium

Figure 1 shows the behavior of melting point with grain size for quantum well, quantum wire and quantum dot. For Aluminium, T_{mb} = 933.25 K, γ = 1.146 J/m^2 at 298K, v_o = 10.0 x 10^{-6}m^3, β = 1.2nm [4]. As the grain size decreases, the melting point of the material also decreases. Changes in melting point occur because nanoscale materials have a much larger surface-to-volume than bulk materials, drastically altering their thermodynamic and thermal properties. There is a sudden decrease in the melting point at a critical grain size ≈ 40nm. Beyond the grain size of 60 nm, the melting point is nearly a constant.

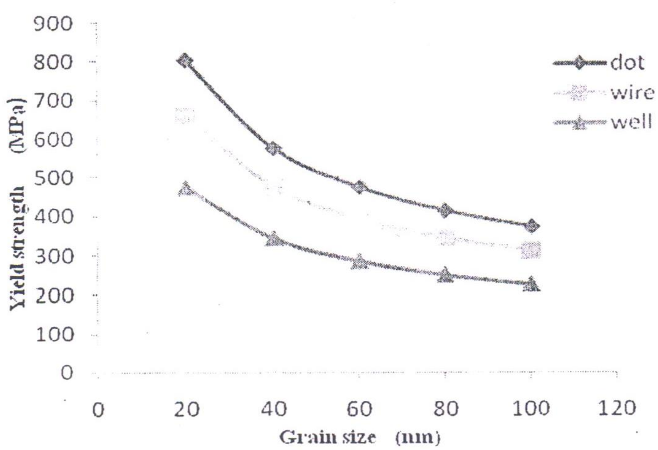

Figure 2. Variation of yield strength with Grain size for Copper

Figure 2 shows the yield strength of Copper in various dimensions like quantum well, quantum wire and quantum dot as a function of grain size. For Copper, σ_o= 25MPa, k = 0.11MPa m$^{1/2}$ [8]. When the grain size decreases, yield strength increases due to the increase in grain boundaries, blocking dislocation movement. There is a significant decrease in the slope for small grain sizes. The yield strength plateaus below a critical grain size

(≈ 60nm). The yield strength of quantum wire is more than that of quantum well, and less than that of quantum dot.

4. CONCLUSIONS

We have presented the behavior of yield strength and melting point of the nanostructured materials of various dimensions as a function of the grain size. The theoretical results agree well with the experimental data available in the literature and confirm the influence of grain size on various important properties of materials.

REFERENCES

[1] V. Tellkamp and E. Lavernia (1999) Nanostructured materials, 12, 249.

[2] Charles P. Poole and Jr., Frank J. Owens (2006) Introduction to Nanotechnology, John Wiley & Sons, New Delhi.

[3] K.K. Nanda, S. N. Sahu and S. N. Behera (2002) Phys. Rev. A, 66, 013208

[4] K. Sadaiyandi (2009) Material Chemistry and Physics, 115, 703–706.

[5] Information retrieved from http://en.wikipedia.org/wiki/Yield_(engineering).

[6] J.W. Martin (1998) Precipitation Hardening: Theory and application, 2nd edition, Oxford.

[7] A.H. Chokshi, A. Rosen, J. Karch and H. Gleiter (1989) Scripta Materialia, 23, 1679–84.

[8] Smith, William F. and Hashemi, Javad (2006) Foundations of Materials Science and Engineering, 4th edition, McGraw-Hill.

Proceedings of the UGC sponsored National Workshop on Research Practices in Mathematics and Computer Science (RPMCS – 2015)

MATHEMATICAL MODELLING OF NOVEL POTENTIAL PROFILES AND ASSOCIATED ENERGY LEVELS BY VARIATIONAL METHOD

A. Anitha[1] and M. Arulmozhi[2]

Department of Physics, Jayaraj Annapackiam College for Women (Autonomous), Periyakulam – 625 601, Tamil Nadu, India

ABSTRACT

Variational method is one of the approximation methods used in quantum mechanics mainly to study the ground state energy of a system. We have considered the quantum well composed by GaAs/$Ga_{1-x}Al_xAs$ with novel potential profiles such as Rosen-Morse potential, Poschl-Teller potential and Woods-Saxon potential. The ground state energy of electron, light hole and heavy hole states are calculated as a function of wellwidth and barrier height. The results of these potential profiles are compared.

Keywords: Variational method, Potential profile, Wellwidth, Barrier height

1. Introduction

The variational method can be used for the approximate determination of the lowest or ground state energy level of a system, when there is no closely related method that is capable of exact solution. It consists in evaluating the integrals with trial wave function Ψ that depends on a number of parameters and varying these parameters until the expectation value of the energy is a minimum [1].

The ground state energy of a Hydrogen molecule and a Helium atom have been determined by variational method and these values are in good agreement with the experimental value [2, 3]. Arup Banerjee *et al.* have calculated the energies for ground state and some excited states of confined helium atom by employing Rayleigh-Ritz variational method [4].

In this paper, we present a mathematical model for the novel potentials such as Rosen-Morse potential (RM), Poschl-Teller potential (PT) and Woods-Saxon potential (WS) composed of GaAs/GaAlAs and a numerical calculation of ground state energy of electron, heavy hole and light hole as a function of wellwidth using the variational method.

2. Theory

The Hamiltonian of the electron, heavy hole or light hole in bare quantum well formed by GaAs/$Ga_{1-x}Al_xAs$ in the effective mass approximation as [5],

$$\mathcal{H} = -\frac{d^2}{dz^2} + V(z) \tag{1}$$

The Potential profiles for electron and hole in Woods-Saxon, Rosen-Morse and Poschl-Teller Potential well are, respectively, of the form [6],

$$V_{WS}(z) = \begin{cases} -\frac{V_0 e^{-2az}}{1+e^{-2az}} & -\frac{L}{2} < z < \frac{L}{2} \\ V_0 & Otherwise \end{cases} \tag{2}$$

$$V_{RM}(z) = \begin{cases} -\frac{4V_1 e^{-2az}}{(1+e^{-2az})^2} + \frac{V_2(1-e^{-2az})}{1+e^{-2az}} & -\frac{L}{2} < z < \frac{L}{2} \\ V_0 & Otherwise \end{cases} \tag{3}$$

$$V_{PT}(z) = \begin{cases} -\frac{4V_1 e^{-2az}}{(1+e^{-2az})^2} & -\frac{L}{2} < z < \frac{L}{2} \\ V_0 & Otherwise \end{cases} \tag{4}$$

where, a = 0.01 defines the range of depth of the well. V_0, V_1 and V_2 are barrier heights.

The trial wave functions for the ground state of the electron, heavy hole and light hole are described respectively as,

$$\Psi_e = \begin{cases} N\ e^{-\alpha_e^2 z_e^2} & |z| < L/2 \\ N_1\ e^{-\beta_e |z_e|} & |z| > L/2 \end{cases} \tag{5}$$

$$\Psi_{ih} = \begin{cases} N\ e^{-\alpha_{ih}^2 z_{ih}^2} & |z| < L/2 \\ N_1\ e^{-\beta_{ih} |z_{ih}|} & |z| > L/2 \end{cases} \tag{6}$$

where α and β are variational parameters. The subscripts i = h and l stands for heavy hole and light hole respectively. The continuity conditions at z_e = L/2 and z_h = L/2 relates the normalization constants N and N_1. The expectation value of Hamiltonian $\langle\mathcal{H}\rangle$ is evaluated as a function of the variational parameters using the Hamiltonian in Eq.(1) and the trial wave function in Eq.(5) and (6) as,

$$\langle\mathcal{H}\rangle = \frac{\int \Psi^* \mathcal{H}\, \Psi\, d\tau}{\int \Psi^*\, \Psi\, d\tau} \tag{7}$$

The value of $\langle\mathcal{H}\rangle$ is minimized with respect to the variational parameters α and β. This gives the ground state energy of electron, light hole and heavy hole in GaAs/GaAlAs.

3. Results and Discussion

All the material parameters used in our calculations such as effective masses of heavy hole (hh), light hole (lh) and electron; dielectric constant for GaAs are given in Table 1.

Table 1: Material parameters used in the calculations

Parameters	GaAs [7]
m_e^*	$0.0665\ m_0$
m_{hh}^*	$0.34\ m_0$
m_{lh}^*	$0.094\ m_0$
ε_0	13.2

where m_0 is the free electron mass.

The total bandgap difference ΔE_g between GaAs and $Ga_{1-x}Al_xAs$ is calculated as [7],

$$\Delta E_g = 1.155x + 0.37x^2\ eV \tag{8}$$

where x is the concentration of aluminium. The barrier height V_0 or the conduction band discontinuity is taken to be $0.65\ \Delta E_g$ for GaAs/ GaAlAs [7].

We have performed the calculations for different potential wells and various values of wellwidth L. In each case the minimization of $\langle \mathcal{H} \rangle$ with respect to the variational parameters is carried out using the software Mathcad 14. Table 2, shows the ground state energy of electron, heavy hole and light hole in various potentials such as Wood-Saxon, Poschl-Teller and Rose-Morsen Potential as a function of wellwidth.

Table 2: Ground state energies of electron, light hole and heavy hole in different novel potential as a function of wellwidth 'L'

It is observed that,

1. For all potential profiles, the ground state energies E_0 decrease with increase of the wellwidth, as expected.
2. $E_0(WS) < E_0(PT) < E_0(RM)$
3. $E_0(electron) < E_0(lh) < E_0(hh)$
4. The ground state lies closer in Pochl-teller and Rosen-Morse potentials.
5. The energy levels of the heavy hole in Pochl-Teller potential and Rosen-Morse potential are limited up to -99.48 meV at 80 nm and -97.97 meV at 50 nm respectively.

L	Ground state energies (meV)								
nm	Woods-Saxon Potential			Poschl-Teller Potential			Rosen-Morse Potential		
	E_e	E_{lh}	E_{hh}	E_e	E_{lh}	E_{hh}	E_e	E_{lh}	E_{hh}
10	-123.14	-66.24	-65.65	-199.99	-99.99	-99.98	-199.76	-99.83	-99.37
20	-122.84	-66.01	-64.84	-199.99	-99.99	-99.92	-199.51	-99.65	-98.74
30	-122.55	-65.79	-64.04	-199.98	-99.98	-99.82	-199.27	-99.48	-98.21
40	-122.26	-65.58	-63.23	-199.97	-99.97	-99.70	-199.03	-99.31	-98.0
50	-121.96	-65.39	-62.43	-199.96	-99.96	-99.58	-198.8	-99.14	-97.97
60	-121.67	-65.12	-61.63	-199.94	-99.94	-99.51	-198.59	-98.99	-97.97
70	-121.37	-64.9	-60.83	-199.92	-99.92	-99.49	-198.42	-98.86	97.97
80	-121.08	-64.67	-60.03	-199.90	-99.90	-99.48	-198.29	-98.77	-97.97
90	-120.79	-64.45	-59.24	-199.88	-99.88	-99.48	-198.22	-98.73	-97.97
100	-120.49	-64.23	-58.45	-199.85	-99.85	-99.48	-198.19	-98.71	-97.97

4. Conclusion

We have presented a mathematical model for novel potential profiles such as Rosen-Morse potential, Poschl-Teller potential and Woods-Saxon potential formed by GaAs/GaAlAs and its associated energy levels of electron, heavy hole and light hole are determined for various wellwidths using variational method. A comparative study on the ground state energies in these potential profiles is also presented.

Acknowledgements

The authors thank the University Grants Commission (UGC), New Delhi, India for the financial support through Major Research Project (No. F. 42-836/2013 (SR) dated 22.03.2013) and the authorities of Jayaraj Annapackiam College for Women (Autonomous), Periyakulam, Theni District, Tamil Nadu, India for the encouragements.

References

[1]. Leonard I. Schiff, "Quantum Mechanics", 4th Edition, McGraw Hill Education (India) Private Limited, New Delhi, 2014.

[2]. P. M. Mathews and K. Venkatesan, "A Text Book of Quantum Mechanics", 2nd Edition, McGraw Hill Education (India) Private Limited, New Delhi, 2014.

[3]. G. Aruldhas, "Quantum Mechanics", 2nd Edition, PHI Learning Private Limited, New Delhi, 2013.

[4]. http://www.arxiv.org/abs/physics/0601152v1

[5]. M. Arulmozhi and S. Balasubramanian, Phys. Rev. B., 51 (1995) 2592.

[6]. A. N. Ikot, A. D. Antia, I. O. Akpan, and O. A. Awoga, Revista Mexicana de Fisica, 59 (2013) 46.

[7]. M. Arulmozhi and S. Balasubramanian, Physica Scripta., 54 (1996) 651.

SUBBAND ENERGIES OF ELECTRON, HEAVY HOLE AND LIGHT HOLE IN SURFACE QUANTUM WELL WITH APPLIED ELECTRIC FIELD

A. Anitha and M. Arulmozhi*
Department of Physics, Jayaraj Annapackiam College for Women (Autonomous)
Periyakulam-625601, Theni District, Tamil Nadu, India.
*Corresponding author: arulpkm@yahoo.co.in

ABSTRACT

Quantum nanostructure with surface quantum well (SQW) shows novel behaviour of optical properties and hence it has many opto-electronic device applications. In the present work, we consider the SQW composed of vacuum/InSb/$In_{1-x}Ga_xSb$ with electric field applied along growth direction. We have performed a calculation of the subband energy of electron, heavy hole and light hole as a function of wellwidth and barrier height for various strength of electric field. When the electric field perturbation is applied, there is an increase in electron subband energy and decrease in heavy hole and light hole subband energies. These studies are further extended to optical studies of the exciton.

Keywords: Subband energy, Electric field, SQW, Electron, Light hole, Heavy hole.

1. INTRODUCTION

Much attention has been paid recently to the response of exciton in a low dimensional semiconductor system to an applied electric field due to the potential applications in high speed optoelectronic devices. It is possible to fabricate the quantum well with advanced semiconductor growth techniques such as molecular-beam epitaxy, chemical lithography and etching for various potential shapes [1].

The behaviour of hydrogenic donor and exciton in Parabolic Quantum Well (PQW) formed by $GaAs/Ga_{1-x}Al_xAs$ have been studied quantitatively [2 - 4]. Kyrychenko et al. have determined the influence of magnetic field on exciton binding energy in PQW composed of diluted magnetic semiconductors by variational method [5]. The effect of electric field, hydrostatic stress and temperature on donor and exciton states in a quantum well of $GaAs/Ga_{1-}$

$_x$Al$_x$As have been investigated extensively [6-10]. Many authors have investigated the effect of confinement in ZnO quantum well on the exciton binding energies experimentally for ZnO/ZnMgO quantum well [11 -13]. Abraham Hudson Mark et al. have calculated the exciton binding energy in $Zn_{1-x}Mg_xSe$/ZnSe quantum well for various Mg composition, taking into the account of dielectric confinement [14]. The influence of the height and thickness of the inter - well barrier on the excitonic binding energy in GaAs/$Ga_{1-x}Al_xAs$ single and coupled double quantum well has been determined theoretically as well as experimentally [15]. Exciton binding energy in a Surface Quantum Well composed of Vacuum/ GaAs/$Ga_{1-x}Al_xAs$ has been calculated as a function of wellwidth including the effect of non-parabolicity and image charges [16].

In this paper, an effort is made to investigate the behaviour of electron, light hole and heavy hole in Surface Quantum Well (SQW) formed by Vacuum/InSb/$In_{1-x}Ga_xSb$ with applied electric field along the growth direction. We have calculated the Subband energies of electron, light hole and heavy hole as a function of wellwidth for different electric fields. The results are compared with the available experimental data and also with the results for various potential profiles.

2. THEORY

The Hamiltonian for electron and hole in SQW formed by Vacuum/ InSb/$In_{1-x}Ga_xSb$ with an applied electric field F along the growth direction is given in the effective mass approximation as,

$$\mathcal{H} = \mathcal{H}_i + \mathcal{H}_F \tag{1}$$

$$\mathcal{H}_i = \frac{-\hbar^2}{2m_i{}^*}\frac{d^2}{dz_i{}^2} + V(z_i) \tag{2}$$

$$\mathcal{H}_F = eFz_i \tag{3}$$

The effective Bohr radius a^* ($a^* = \hbar^2\varepsilon_0/ m_i^* e^2$) and the effective Rydberg R^* ($R^* = m_i^* e^4/2\hbar^2\varepsilon_0{}^2$) are used as the units of length and energy respectively. η is dimensionless measure of the electric field defined as $\eta = \frac{eFa^*}{R^*}$. i= e or hh or lh. The e, hh and lh stand for electron, heavy hole and light hole respectively.

The potential profile for the electron and hole in SQW [16] are given by

$$V(z_i) = \begin{cases} \infty & z_i < 0 \\ 0 & 0 < z_i < L \\ V_{0i} & z_i > L \end{cases} \tag{4}$$

where V_{0i} is the barrier height, which depends on the composition x of impurity.

The trial wave function of the electron and hole in the SQW is taken to be of the form [16]

$$\Psi_i = \begin{cases} 0 & z_i < 0 \\ A\, sin\alpha_i z_i & 0 < z_i < L \\ B\ e^{-\beta_i z_i} & z_i > L \end{cases} \tag{6}$$

Where, A and B are the normalization constants. B is related to A through the continuity of ψ at $z_i = L$ as $B = A\, e^{\beta_i L} sin\alpha_i L$. The α's and β's are given by

$$\alpha_i = \sqrt{\frac{2m_i E_i}{\hbar^2}} \text{ and } \beta_i = \sqrt{\frac{2m_i(V_{0i} - E_i)}{\hbar^2}} \tag{7}$$

where E_i is the well state energy of electron or hole. In order to get the E_i, the transcendental equation to be solved for the quantum well states is obtained by matching the wavefunction given in Eq. (6) and its first derivative at $z_i = L$, which is true when the effective mass mismatch between InSb and $In_{1-x}Ga_xSb$ is neglected. One gets after simplification and substitution for α_i and β_i,

$$\pm\left(\frac{E_i}{V_{0i}}\right)^{1/2} = \sin(\sqrt{E_i}L) \tag{8}$$

Component of the energy of the electron or hole by applied electric field can be determined as

$$E_{Fi} = \langle \psi_i^* | H_F | \psi_i \rangle \tag{9}$$

The subband energy of the electron, light hole and heavy hole can be determined by

$$E_{Ti} = E_i + E_{Fi} \tag{10}$$

3. RESULT AND DISCUSSION

All the material parameters used in our calculations such as effective masses of heavy hole, light hole and electron; dielectric constant for InSb are given in table 1.

The total bandgap difference between InSb and $In_{1-x}Ga_xSb$ is calculated from the equation [17],

$$\Delta E_g = 0.139x + 0.415x^2\ eV \tag{11}$$

Table 1: Material parameters used in the calculations

Parameters	**InSb** [17]
m_e^*	0.0145 m_0
m_{hh}^*	0.44 m_0
m_{lh}^*	0.016 m_0
ε_0	17.7

Where m_0 is the free electron mass.

The barrier height V_0 or the conduction band discontinuity is taken to be 0.7 ΔE_g for the material vacuum/InSb/InGaSb quantum well. We have not considered the effect due to the effective mass mismatch, conduction band nonparabolicity and dielectric constant mismatch, because it is expected to be small.

Figure 1 shows the variation of subband energy of electron as a function of wellwidth for different electric fields. From the figure it is observed that, when the wellwidth of the quantum well increased, the subband energy of the electron found to be increased. The increasing of the electric field leads to more subband energy.

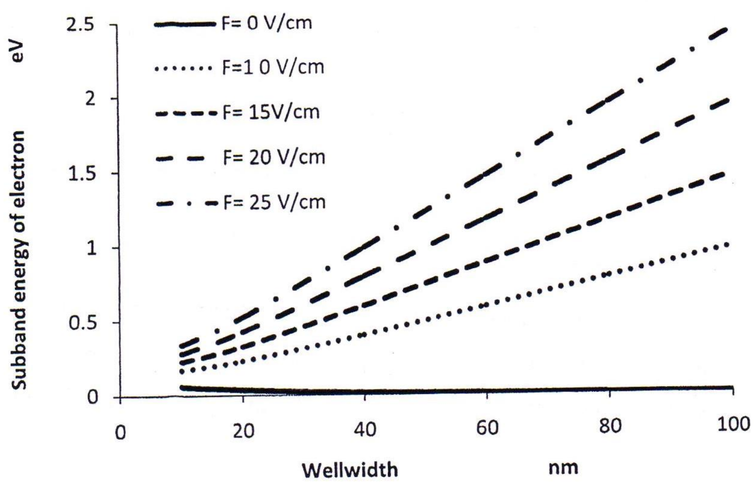

Fig 1: Variation of subband energy of electron as a function of wellwidth for different electric fields.

Figure 2 display the variation of subband energy of light hole as a function of wellwidth for various electric fields applied to the nanostructure. If the wellwidth L is reduced, the subband energies slowly decrease until they reach a minimum at certain value of L as well as applied electric fields. As L is reduced further, the subband energies start to increase. The minimum subband energies are observed at 80 nm for all electric fields.

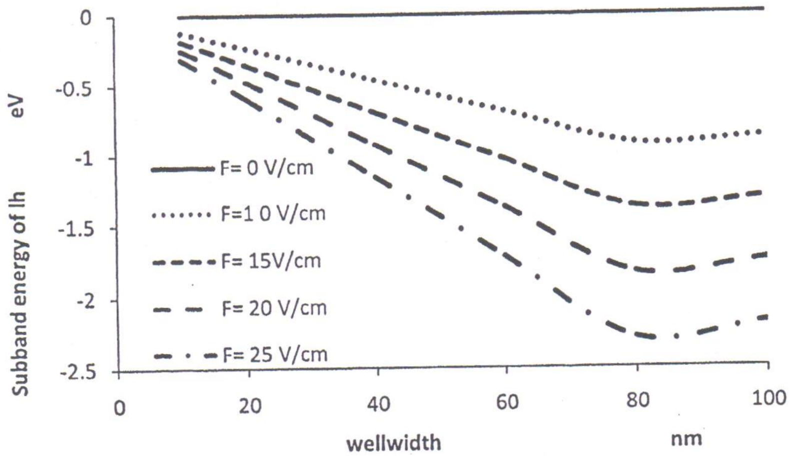

Fig 2: Variation of subband energy of light hole as a function of wellwidth for different electric fields.

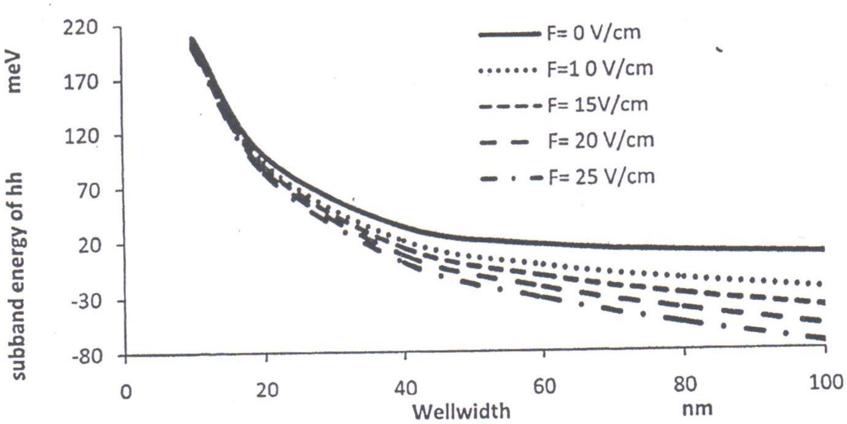

Fig 3: Variation of subband energy of heavy hole as a function of wellwidth for different electric fields.

The behaviour of the subband energies of heavy hole as a function of wellwidth as well as electric field is shown in figure 3. The decreasing of wellwidth and increasing of electric field lead to less subband energy.

4. SUMMARY

We have studied the Subband energy of electron, hh and lh in SQW formed by InSb/InGaSb as a function of wellwidth. The important result is that the subband energy of electron is increased when the applied electric field is increased. But it decreased for heavy hole and light hole. These results can be extended further for the study of optical properties of exciton.

ACKNOWLEDGEMENTS

The authors thank the University Grants Commission (UGC), New Delhi, India for the financial support through Major Research Project (No. F. 42-836/2013 (SR) dated 22.03.2013) and the authorities of Jayaraj Annapackiam College for Women (Autonomous), Periyakulam, Theni District, Tamilnadu, India for the encouragements.

REFERENCE

[1]. Sanam Mosleni-Tabrizi, "Eigenstate calculations for multidimensional nanostructures: Quantum wells, wires and Dots", VDM Verlag Dr. Muller Aktiengesellschaft & Co.KG, Germany, 2008.

[2]. A.Tabata, J.B.B. Olivera, E.C.F. da Silva, T.E. Lamas, C.A. Duarte and G. M. Gusev, J. Physics: Conference series, 2010, 210, 012052.

[3]. Tomasz M. Rusin, J. Phys.: Condens. Matter, 2000, 12, 575.

[4]. El-Meshad. N., Hassanien. H. M. and Hassan. H. H., FIZIKA A (Zagreb), 2001, 1, 13.

[5]. Kyrychenko. F. and Kossut. J., ACTA PHYSICA POLONICA A. 1998, 94, 406.

[6]. A.L. Morales, A. Montes, S.Y. Lopez and C.A. Duque, J. Phys.:Condens. Matter, 2002, 14, 987.

[7]. Raigoza. N., Duque. C. A., Reyes-Gomez. E. and Oliveira. L. F., Physica B: Physics of Condensed Matter, 2005, 367, 267.

[8]. Zhao. G. J, Liang. X. X and Ban. S. L., International Journal of Modern Physics B, 2007, 21, 2735.

[9]. S.Y. Lopez, N. Porras-Montenegro and C.A. Duque, Semicond. Sci. Technol. 2003, 18, 718.

[10]. P.J Klar, H. Grunning, W. Heimrodt, J. Koch, W. Stolz, P.M.A. Vicente, A.M. Kamal saadi, A. Lindsay and E.P.O'Reilly, Phys. stat. sol. (b), 2001, 223, 163.

[11]. H.D. Sun, T. Makino, Y. Segawa, M. Kawasaki, A. Ohtomo, K. Tamura and H. Koinuma, J. Appl. Phys., 2007, 91, 1993.

[12]. C. H. Chia, T. Makino, K. Tamura, Y. Sagawa, M. Kawasaki, A. Ohtomo and H. Koinuma, J. Appl. Phys., 2003, 82, 1848.

[13]. Th. Gruber, C. Kirchner, R. Kling, F. Reuss and A. Waag, Appl. Phys. Lett., 2004, 84, 5359.

[14]. J. Abraham Huson mark and A. John peter, J. Semicond., 2012, 33, 092001-1.

[15]. E.M. Lopes, D.F. Cesar, F. Franchello, J.L. Duarte, I.F.L. Dias, E. Laureto, D.C. Elias, M.V.M. Pereira, P.S.S. Guimaraes, and A.A. Quivy, Journal of Luminescence, 2013, 144, 98.

[16]. Anitha. A. and Arulmozhi. M., Superlattices and Microstructures, 2014, 75, 222.

[17]. M. Razeghi, The MOCVD challenge volume 2: A survey of GaInAsP-GaAs for photonic and electronic device applications, (1995), pp.2, IOP Publishing L

Copies of the Certificates for Paper Presentations in Seminars/Conferences/ Workshops

International Conference on NANO ELECTRONIC SCIENCE & TECHNOLOGY

PG & Research Department of Electronics

Sri Vasavi College (Self Finance Wing)

Erode, Tamilnadu, India.

Certificate

ICNEST 2014

This is to certify that Mr./Ms./Dr.

M. Arulmozhi

Jayaraj Annapackiam College for Women (Autonomous)

Chaired / Participated / Presented a paper titled

Theoretical Investigations on the Properties of

Quantum Nanostructures dependent on Density of States

at the International Conference on Nano Electronic Science & Technology (*ICNEST-2014*)

organised by Post Graduate & Research Department of Electronics,

Sri Vasavi College (Self Finance Wing), Erode

On 14th and 15th February 2014

Dr.J.Deenathayalan
Convenor

SRI VASAVI COLLEGE ERODE (Self Finance Wing)

Prof. V. Sivakumar
Director

International Conference on NANO ELECTRONIC SCIENCE & TECHNOLOGY

PG & Research Department of Electronics

Sri Vasavi College (Self Finance Wing)

Erode, Tamilnadu, India.

Certificate

ICNEST 2014

This is to certify that Mr./Ms./Dr.

A. Anitha

Jayaraj Annapackiam College for Women (Autonomous)

Chaired / Participated / Presented a paper titled

Theoretical Investigations on the Properties of

Quantum Nanostructures dependent on Density of States

at the International Conference on Nano Electronic Science & Technology (ICNEST-2014)

organised by Post Graduate & Research Department of Electronics,

Sri Vasavi College (Self Finance Wing), Erode

On 14th and 15th February 2014

Dr.J.Deenathayalan
Convenor

SRI VASAVI COLLEGE ERODE (Self Finance Wing)

V. Sivakumar
Prof. V. Sivakumar
Director

3rd International Conference on Nanoscience and Nanotechnology (ICONN 2015)

SRM UNIVERSITY (Under section 3 of UGC Act 1956)

SRM University

Kattankulathur - 603 203

ICONN 2015

Certificate

This is to certify that Mr. /Ms. /Dr. Mrs. M. Arulmozhi *has* **Participated/Presented a Paper** *entitled* Magnetic field Effects on the Exciton Binding Energy in A Near triangular Quantum well *in International Conference on Nanoscience and Nanotechnology (ICONN 2015) organized by Department of Physics and Nanotechnology, SRM University during 04 - 06 February 2015 in association with Shizuoka University, Japan and Institute of Geological and Nuclear Sciences, New Zealand, Co-sponsored by Science & Engineering Research Board (DST-SERB), Defence Research & Development Organization (DRDO) and Department of Biotechnology (DBT), Government of India.*

Convenor - ICONN 2015

Director (E &T)

Shizuoka University, Japan

GNS - New Zeland

The Institution of Engineering and Technology

सत्यमेव जयते Govt. of India

Department of Biotechnology Govt. of India

3rd International Conference on Nanoscience and Nanotechnology (ICONN 2015)

SRM UNIVERSITY
(Under section 3 of UGC Act 1956)

SRM University
Kattankulathur - 603 203

ICONN 2015

Certificate

This is to certify that Mr. /Ms. /Dr. A.Anitha *has* **Participated/Presented a Paper** *entitled* Magnetic Field Effects On The Exciton Binding Energy In A Near Triangular Quantum Well *in International Conference on Nanoscience and Nanotechnology (ICONN 2015) organized by Department of Physics and Nanotechnology, SRM University during 04 - 06 February 2015 in association with Shizuoka University, Japan and Institute of Geological and Nuclear Sciences, New Zealand, Co-sponsored by Science & Engineering Research Board (DST-SERB), Defence Research & Development Organization (DRDO) and Department of Biotechnology (DBT), Government of India.*

Convenor - ICONN 2015

Director (E &T)

Shizuoka University, Japan

GNS - New Zeland

IET The Institution of Engineering and Technology

सत्यमेव जयते Govt. of India

Department of Biotechnology Govt. of India

JAYARAJ ANNAPACKIAM COLLEGE FOR WOMEN (AUTONOMOUS)

(A Unit of the Sisters of St. Anne, Tiruchirapalli)

Accredited with 'A' Grade (3rd cycle) by NAAC

PERIYAKULAM - 625 601, THENI DISTRICT, TAMIL NADU

RESEARCH CENTRE OF MATHEMATICS

UGC sponsored National Workshop on

RESEARCH PRACTICES IN MATHEMATICS AND COMPUTER SCIENCE

CERTIFICATE

This is to certify that Mr. / Ms. / Dr. M. Arulmozhi, Asso. Prof ~~of~~ of Physics of J. A College, Periyakulam participated and presented a paper entitled Mathematical Modelling of Novel Potential profile and associated energy levels by Variational Method in the UGC sponsored National Workshop on **RESEARCH PRACTICES IN MATHEMATICS AND COMPUTER SCIENCE** organized by the Research Centre of Mathematics, Jayaraj Annapackiam College for Women (Autonomous), Periyakulam on 3rd & 4th August, 2015.

S.M.W. **Dr. S. M. SAROJA THEERDUS KALAVATHY**
S. Athisaya Ponmani **Dr. S. ATHISAYA PONMANI**
ORGANIZING SECRETARIES

Mrs. G. AMALARUBY
CONVENOR & HEAD

Rev. Sr. Dr. T. NIRMALA
PRINCIPAL

JAYARAJ ANNAPACKIAM COLLEGE FOR WOMEN (AUTONOMOUS)

(A Unit of the Sisters of St. Anne, Tiruchirapalli)

Accredited with 'A' Grade (3rd cycle) by NAAC

PERIYAKULAM - 625 601, THENI DISTRICT, TAMIL NADU

SERVE WITH LOVE

JAC

PERIYAKULAM

RESEARCH CENTRE OF MATHEMATICS

UGC sponsored National Workshop on

RESEARCH PRACTICES IN MATHEMATICS AND COMPUTER SCIENCE

CERTIFICATE

This is to certify that Mr. / Ms. / Dr. A. Anitha, of J. A. College, Periyakulam participated and presented a paper entitled Mathematical Modelling of Novel Potential Profile and associated energy levels by Variational Method in the UGC sponsored National Workshop on **RESEARCH PRACTICES IN MATHEMATICS AND COMPUTER SCIENCE** organized by the Research Centre of Mathematics, Jayaraj Annapackiam College for Women (Autonomous), Periyakulam on 3rd & 4th August, 2015.

S. M. W

Dr. S. M. SAROJA THEERDUS KALAVATHY

S. Athisaya Ponmani

Dr. S. ATHISAYA PONMANI

ORGANIZING SECRETARIES

Mrs. G. AMALARUBY

CONVENOR & HEAD

R. Nirmala

Rev. Sr. Dr. T. NIRMALA

PRINCIPAL

Arul Anandar College (Autonomous)

(Re-accredited by NAAC with 'A' Grade with a CGPA of 3.66)
Karumathur, Madurai - 625 514
www.aactni.edu.in

PG & Research Department of Physics

State Level Seminar on
EXPANDING FRONTIERS IN MATERIAL SCIENCE

Certificate of Appreciation

This is to certify that Dr. / ~~Mr.~~ / ~~Ms.~~ M. ARULMOZHI, Associate Prof. Jeyaraj Annapackiam College for Women has ~~participated~~ / presented a paper on Simultaneous effects of Pressure, Temperature and Magnetic fields on subband energy in near Triangular Quantum Well (Oral / ~~Poster~~) in the State Level Seminar on

EXPANDING FRONTIERS IN MATERIAL SCIENCE

held on 15th December 2015 at Arul Anandar College (Antonomous), Karumathur - 625 514, Madurai District, Tamil Nadu.

Dr. S. Valanarasu	Dr. I. Kulandaisamy	Rev. Dr. S. Basil Xavier S.J.
Convener	Head of the Dept.	Principal

Arul Anandar College (Autonomous)

(Re-accredited by NAAC with 'A' Grade with a CGPA of 3.66)
Karumathur, Madurai - 625 514
www.aactni.edu.in

PG & Research Department of Physics

State Level Seminar on
EXPANDING FRONTIERS IN MATERIAL SCIENCE

Certificate of Appreciation

This is to certify that ~~Dr.~~ / ~~Mr.~~ / Ms. A. Anitha, J. A. College for Women, Periyakulam has ~~participated~~ / presented a paper on Simultaneous effect of Temprature, pressure and magnetic field on subband energy on NTQW (Oral / ~~Poster~~) in the State Level Seminar on

EXPANDING FRONTIERS IN MATERIAL SCIENCE

held on 15th December 2015 at Arul Anandar College (Antonomous), Karumathur - 625 514, Madurai District, Tamil Nadu.

Dr. S. Valanarasu	Dr. I. Kulandaisamy	Rev. Dr. S. Basil Xavier S.J.
Convener	Head of the Dept.	Principal

RESEARCH CENTRE OF PHYSICS

JAYARAJ ANNAPACKIAM COLLEGE FOR WOMEN (AUTONOMOUS)

Accredited with 'A' Grade in 3rd Cycle by NAAC

(Affiliated to Mother Teresa Women's University, Kodaikanal)

PERIYAKULAM - 625 601, THENI DISTRICT, TAMIL NADU

CERTIFICATE

This is to certify that ~~Mr. / Ms.~~ / Dr. M. ARUL MOZHI, ASSOCIATE PROFESSOR has participated / presented a paper in the UGC sponsored National Conference on "**RECENT TRENDS IN PHYSICS & MATERIALS RESEARCH**" on 4th & 5th February 2016 at Jayaraj Annapackiam College for Women (Autonomous), Periyakulam.

Paper Title : SUBBAND ENERGIES OF ELECTRON, HEAVY HOLE AND LIGHT HOLE IN SURFACE QUANTUM WELL WITH APPLIED ELECTRIC FIELD.

R. Mary Mathelane		R Nirmala
Dr. Mrs. R. Mary Mathelane	Rev. Sr. Dr. S. Jesurani	Rev. Sr. Dr. T. Nirmala
Head	Convenor & Controller of Examinations	Principal

RESEARCH CENTRE OF PHYSICS

JAYARAJ ANNAPACKIAM COLLEGE FOR WOMEN (AUTONOMOUS)

Accredited with 'A' Grade in 3rd Cycle by NAAC

(Affiliated to Mother Teresa Women's University, Kodaikanal)

PERIYAKULAM - 625 601, THENI DISTRICT, TAMIL NADU

CERTIFICATE

This is to certify that ~~Mr.~~ / Ms. / ~~Dr.~~ A. ANITHA Research Scholar Jayaraj Annapackiam College for Women (Autonomous) Periyakulam has participated / presented a paper in the UGC sponsored National Conference on "**RECENT TRENDS IN PHYSICS & MATERIALS RESEARCH**" on 4th & 5th February 2016 at Jayaraj Annapackiam College for Women (Autonomous), Periyakulam.

Paper Title : Subband Energies of Electron, Heavy hole and Light hole in Surface Quantum Well with applied Electric Field

R. Mary Mathelane

Dr. Mrs. R. Mary Mathelane
Head

Rev. Sr. Dr. S. Jesurani
Convenor & Controller of Examinations

R. Nirmala

Rev. Sr. Dr. T. Nirmala
Principal

Since 1951

PG and Research Department of Physics

JAMAL MOHAMED COLLEGE (Autonomous)

College with Potential for Excellence
Accredited with 'A' Grade by NAAC – CGPA 3.6 out of 4.0
(Affiliated to Bharathidasan University)
TIRUCHIRAPPALLI- 620 020

ज्ञान-विज्ञान विमुक्तये

INTERNATIONAL CONFERENCE ON

ICRTMSA 2016

Recent Trends in Materials Science and Applications

(ICRTMSA - 2016)
(Under UGC Autonomous Grant)

Certificate

This is to certify that ~~Mr./Ms.~~/Dr. M. ARULMOZHI, Associate professor of Physics J. A. college for women (Autonomous) presented a paper in the field of condensed Matter Physics participated in the **International Conference on Recent Trends in Materials Science and Applications (ICRTMSA - 2016)**, organized by the PG and Research Department of Physics, Jamal Mohamed College (Autonomous), Tiruchirappalli on 29th February 2016.

Paper title: Exciton binding energy in Surface Quantum Well under Electric field

J. Ebenezar		
Dr. J. EBENEZAR	**Dr. M JAMAL MOHAMED JAFFAR**	**Dr. S. MOHAMED SALIQUE**
Organizing Secretary and Convener	Co-ordinator	Principal

PG and Research Department of Physics

JAMAL MOHAMED COLLEGE (Autonomous)

College with Potential for Excellence
Accredited with 'A' Grade by NAAC – CGPA 3.6 out of 4.0
(Affiliated to Bharathidasan University)
TIRUCHIRAPPALLI- 620 020

Since 1951

ज्ञान-विज्ञान विमुक्तये

INTERNATIONAL CONFERENCE ON

ICRTMSA 2016

Recent Trends in Materials Science and Applications

(ICRTMSA - 2016)
(Under UGC Autonomous Grant)

Certificate

This is to certify that Mr./Ms./Dr. ANITHA

Department of Physics, Jayaraj Annapackiam College for Women (Autonomous), Theni.

presented a paper entitled Exciton Binding Energy in Surface Quantum Well under Electric Field

in the **International Conference on Recent Trends in Materials Science and Applications (ICRTMSA - 2016)**, *organized by the PG and Research Department of Physics, Jamal Mohamed College (Autonomous), Tiruchirappalli on 29th February 2016.*

J. Ebenezar
Dr. J. EBENEZAR
Organizing Secretary and Convener

Dr. M JAMAL MOHAMED JAFFAR
Co-ordinator

Dr. S. MOHAMED SALIQUE
Principal

SRIGURU INSTITUTE OF TECHNOLOGY

Near Saravanampatti, Coimbatore-641110

(Approved by Aicte, New Delhi, Affliated to Anna University, Chennai)

INTERNATIONAL CONFERENCE
ON
Innovations in science and Technology
(ICIST 2016)

This is to Certify that Dr./~~Prof.~~/~~Mr.~~/~~Ms.~~ M. ARULMOZHI, ASSO. PROF of JAYARAJ ANNAPACKIAM COLLEGE FOR WOMEN has presented a paper entitled EFFECT OF TEMPERATURE ON EXCITON BINDING ENERGY IN $ZnSe/Zn_{1-x}Mg_xSe$ QUANTUM WELL WITH POSCHL-TELLER POTENTIAL in the International Conference on "INNOVATIONS IN SCIENCE & TECHNOLOGY" (ICIST'16) during 31st March & 1st April 2016.

CONVENER

PRINCIPAL

SRIGURU INSTITUTE OF TECHNOLOGY

Near Saravanampatti, Coimbatore-641110

(Approved by Aicte, New Delhi, Affliated to Anna University, Chennai)

INTERNATIONAL CONFERENCE
ON
Innovations in science and Technology
(ICIST 2016)

This is to Certify that ~~Dr.~~/~~Prof.~~/~~Mr.~~/Ms. A. ANITHA, RESEARCH SCHOLAR

of JAYARAJ ANNAPACKIAM COLLEGE FOR WOMEN has presented a paper

entitled EFFECT OF TEMPERATURE ON EXCITON BINDING ENERGY IN $ZnSe/Zn_{1-x}Mg_xSe$ QUANTUM WELL WITH POSCHL-TELLER POTENTIAL in the International Conference on "INNOVATIONS IN SCIENCE & TECHNOLOGY" (ICIST'16) during 31^{st} March & 1^{st} April 2016.

CONVENER

PRINCIPAL

MANDATE FORM

MANDATE FORM

ELECTRONIC CLEARING SERVICE (CREDIT CLEARING) REAL TIME GROSS SETTLEMENT (RTGS) FACILITY FOR RECEIVING PAYMENTS

A. DETAIL OF ACCOUUONT HOLDER

NAME OF THE ACCOUUONT HOLDER	:	Principal
COMPLETE CONTACT ADDRESS	:	Jayaraj Annapackiam College for Women, (Autonomous) Thamaraikulam, Periyakulam (P.O) Theni Dist. 625 601
TELEPHONE NUMBER/FAX/E-MAIL	:	Phone No. 04546 : 231482/04546231482/principal@annejac.com

B. BANK ACCOUNT DETAILS:

BANK NAME	:	INDIAN OVERSEAS BANK
BRANCH NAME WITH COMPLETE ADDRESS, TELEPHONE NUMBER AND E-MAIL	:	Tamaraikulam, Jayaraj Annapackiam College for Women, (Autonomous) Thamaraikulam, Periyakulam (P.O) Theni Dist. 625 601 04546-233759/ tkulambr@madsco.iobnet.co.in
WHETHER THE BRANCH IS RTGS ENABLED? IF YES THAN WHAT IS THE BRANCH **IFSC CODE**	:	YES, IFSC CODE: IOBA0001789
IS THE BRANCH ALSO NEFT ENABLED?	:	Yes
TYPE OF BANK AACCOUNT (SB/CURRENT/CASH CREDIT)		SB A/C
COMPLETE BANK ACCOUNT NUMBER (LATEST)	:	178901000000003
MICR CODE OF BANK	:	625020107
UNIQUE CODE OF PFMS		FST/COLLEGE-245

I hereby declare that the particulars given above are correct and complete. If the transaction is delayed or not effected at all for reasons of incomplete or incorrect information. I would not hold the used institution responsible. I have read the option invitation letter and agree to discharge responsibility expected to me a participant under the scheme.

Date:27.03.2017

R Nirmala ……………………………………
(Signature of Head of the Institution)

Principal
Jayaraj Annapackiam College
for Women (Autonomous)
Periyakulam - 625 601.
Theni District.

Certified that the particulars furnished above are correct as per our records.

कृते इण्डियन ओवरसीज़ बैंक
For Indian Overseas Bank

Bank's Stamp

INDIAN OVERSEAS BANK ★ THAMARAIKULAM ★ THENI DT.

……………………………………
(Signature of Bank Manager)
प्रबंधक Manager
तामरइकुळम THAMARAIKULAM

Date: 28/3/2017

1. Please attach a photocopy of cheque along with the verification obtain from the bank.
2. In case you bank branch is presently not RTGS enabled branch, please submit the information again in the above proforma to the department at earliest.

इण्डियन ओवरसीज़ बैंक
Indian Overseas Bank

TAMARAIKULAM BRANCH(1789)
Jayaraj Annapackiam College for Women
Campus, J.A.College Road, Periyakulam - 625 601.

VALID FOR THREE MONTHS FROM THE DATE OF INST

D D M M Y Y Y

या धारक को OR BEAR

RUPEES

अदा करें ₹

178901000000003

IFS Code : IOBA0001789

IOB

कृते इण्डियन ओवरसीज़ बैंक
For Indian Overseas Bank

प्रबंधक Manager
तामरैकुलम THAMARAIKULAM

INDIAN OVERSEAS BANK ★ THAMARAIKULAM-625605 ★

Please sign above

275948 625020107 13